The influence of the stomach pacemaker on brain and behavior : methods and experiments in humans

Nicolai Wolpert

PSL
UNIVERSITÉ PARIS

THÈSE DE DOCTORAT
DE L'UNIVERSITÉ PSL

Préparée au Laboratoire de Neurosciences Cognitives et Computationnelles (LNC^2), UMR 960, DEC, ENS, Inserm

The influence of the stomach pacemaker on brain and behavior: methods and experiments in humans

Soutenue par
Nicolai WOLPERT
Le 18 juin 2021

Ecole doctorale n° 158
Cerveau, Cognition, Comportement

Spécialité
Sciences Cognitives, neurosciences, psychologie

Composition du jury :

Niko, BUSCH Prof. Dr., WWU Münster	*Président, Rapporteur*
Adriano, TORT Dr., Federal University of Rio Grande do Norte	*Rapporteur*
Laura, DUGUÉ Dr., Université Paris Descartes	*Examinatrice*
GAEBLER, Michael Dr., Max-Planck-Institut Leipzig	*Examinateur*
Catherine, TALLON-BAUDRY Dr., Ecole Normale Supérieure – PSL University	*Directrice de thèse*

ENS | PSL

Acknowlegements

I would like to start by expressing my deepest thanks to Catherine; it has been a great honor for me to work with her and do my thesis under her supervision. When I started as an intern in 2014, I had no idea how much I would enjoy this work, and how much this journey would change my life. With her curiosity, wisdom, rigor, and thoroughness, she has truly been an inspiration for me. Over the almost six years I worked with her, Catherine has trained me in critical thinking, attention to detail, organization – in short, all the tools important for becoming a researcher. She has also been very supportive, especially with regard to the difficult times during the last year of my thesis.

I also want to thank the members of the jury who do me the honor of reading this manuscript and dedicate some of their precious time.

This work has been so enjoyable not least because of all the great colleagues that make the lab such a great working environment. I would like to thank all the former and current members of my team (in roughly chronological order): Mariana, Ignacio, Craig, Samuel, Victor, Kayeon, Diego, David, Damiano, Clémence, Max, Stephen, Anne, Cooper, Juliette, Tahnée, Janina and Constance. Thanks to the veteran gastronauts Stephen and Ignacio, who helped me become familiar with the magic of the gut and advised me in my projects. Special thanks to Ignacio, with whom I closely collaborated and exchanged so many inspiring ideas, and whose enthusiasm and energy brought so many good vibes to the lab. Thank you Clémence and Juliette who not only helped me in data acquisition, but also brought to the experiments a lot of fun. A big thanks to Anne Buot for her invaluable help and technical support. I am also grateful for Marion's dedicated mentoring and career advice. I also want to thank all the other amazing researchers and students of the LNC2 who made the lab such a pleasant place. Overall, having worked among so many smart and talented people has truly been an honor. You have been more than colleagues for me, and I will think back with joy to the after-work beers, lunchtime conversations and breaks in the ENS garden. Special thanks to Laura and Marine for their kind and efficient administrative support. Also thanks to the ENS canteen, who continuously supplied me with delicious French desserts I was looking forward to every morning.

I would also like to thank the members of the MEG platform which has been so fundamental to this work – Nathalie, Denis and Laurent. A special thanks to Christophe Gitton for his invaluable technical assistance during MEG recordings, and for making the data acquisition so fun and amusing.

I am also grateful to all the friends outside the immediate academic environment who supported me throughout the time of my thesis. Thank you Zuma for helping me become installed in Paris and making me discover so many aspects of Parisian culture. Thanks to all the international friends I made in Paris with whom I have shared (and will create more) precious memories. Coming from a small village I would have never imagined making so many awesome friends from all parts of the world. My deepest thanks go to Natasha. Sharing my life with you is the greatest gift every day, and it has kept me on my feet especially during the dark months of confinement.

Finally, I would like to thank my mother, who always supported and believed in me in my journey from the primary school of my village to the PhD in Paris, and without whom I would not have become who I am today. What I accomplished is also a fruit of your efforts over all those years. Thanks to Nils, I could not imagine a closer and more caring brother. I will also always keep in memory my grandmother, who passed away just before I started the thesis and who was so proud that I was doing a PhD. I wish you would be here now to see me finish it.

Danke

Table of contents

Abbreviatons

ACC	**A**nterior **C**ingulate **C**ortex
BMI	**B**ody **M**ass **I**ndex
BOLD	**B**lood **O**xygenation **L**evel **D**ependent
CNS	**C**entral **N**ervous **S**ystem
DMN	**D**efault **M**ode **N**etwork
DMV	**D**orsal **M**otor Nucleus of the **V**agus
DRG	**D**orsal **R**oot **G**anglion
ECG	**E**lectro**c**ardio**g**raphy
EEG	**E**lectro**e**ncephalo**g**raphy
EGG	**E**lectro**g**astro**g**ram
ENS	**E**nteric **N**ervous **S**ystem
EOG	**E**lectro**o**culo**g**ram
FFT	**F**ast **F**ourier **T**ransform
fMRI	**F**unctional **M**agnetic **R**esonance **I**maging
GI	**G**astro**i**ntestinal
HRV	**H**eart **R**ate **V**ariability
HRV-LF	**L**ow **F**requency **H**eart **R**ate **V**ariability
HRV-HF	**H**igh **F**requency **H**eart **R**ate **V**ariability
ICA	**I**ndependent **C**omponent **A**nalysis
ICCs	**I**nterstitial **C**ells of **C**ajal
IML	**I**nter**m**edio**l**ateral Cell Column
ISF	**I**nfra**s**low **F**luctuations
LC	**L**ocus **C**oeuruleus
MI	**M**odulation **I**ndex
MT	**M**edial **T**emporal Area
NTS	**N**ucleus **T**ractus **S**olitarius
PAC	**P**hase-**A**mplitude **C**oupling
PET	**P**ositron **E**mission **T**omography
PBN	**P**ara**b**rachial **N**ucleus
POS	**P**hase **O**pposition **S**um

PPC	**P**airwise **P**hase-**C**onsistency
REM	**R**apid **E**ye **M**ovement Sleep
RN	**R**aphe **N**ucleus
RSN	**R**esting **S**tate **N**etwork
SI	Primary Somatosensory Cortex
SII	Secondary Somatorsensory Cortex
STAI	**S**tate-**T**rait **A**nxiety **I**nventory
V1	Primary Visual Cortex
vmPFC	**V**entro**m**edial **P**re**f**rontal **C**ortex
VPM	**V**entro**p**osterior **M**edial Nucleus
VPL	**V**entro**p**osterior **L**ateral Nucleus

Foreword

It has long been recognized that visceral signals play an important role for understanding brain and behavior, with theories linking the brain's registering of visceral input with emotions, self and consciousness (Christoff et al., 2011; Craig, 2002; Critchley and Harrison, 2013). However, while many studies have investigated the functional role of brain-visceral interactions by focusing on the heart or respiratory system, empirical studies investigating the electrical activity of the gastrointestinal system remain scarce. Gastrointestinal organs such as the stomach generate their own intrinsic activity which is constantly sent to the brain, reaching a broad network of subcortical and cortical regions through multiple pathways (Azzalini et al., 2019). More specifically, the stomach produces a slow rhythmic pattern of electrical activity (~0.05 Hz) that sets the pace for gastric contractions during digestion, but this rhythm is generated at all times, even during fasting. The gastric rhythm can be measured noninvasively by the Electrogastrogram (EGG). Previous work has shown that an extended network of brain regions is coupled to the phase of the gastric rhythm at rest (Rebollo et al., 2018). Moreover, gastric phase modulates the amplitude of the brain alpha rhythm (Richter et al., 2017), a rhythm that indexes arousal and cortical excitability and underlies fluctuations in perceptual performance (Jensen and Mazaheri, 2010; Mathewson et al., 2011).

The goal of this thesis was to study the coupling of the gastric rhythm with the amplitude of cortical alpha oscillations and its functional consequences for behavior. The hypothesis of my PhD was that there is a slow fluctuation in cortical excitability driven by the gastric rhythm that has an impact on fluctuations in perception. In order to tackle this question, there were two methodological challenges. The first was to obtain good quality EGG recordings in healthy human participants. So far, this recording method has mostly been used in the clinical literature, with a lack of standardized recording and analysis procedures to extract a regular gastric rhythm. The aim of my first project therefore was to improve the standardization of this method and to develop a preprocessing and analysis procedure (article I, Wolpert, Rebollo & Tallon-Baudry, Psychophysiology, 2020). The second methodological challenge was to quantify the statistical relationship between the gastric phase and behavioral outcome. With a simulation approach, I evaluated different statistical tests and procedures for estimating coupling between the phase of an oscillation and behavioral events, to answer how such a link could be optimally detected (article II, Wolpert & Tallon-Baudry, NeuroImage, in press).

In order to test the hypothesis that the phase of the gastric rhythm is coupled to brain alpha oscillations and thereby influences fluctuations in perception, we designed an experiment to target fluctuations in perceptual performance, and simultaneously measured the gastric rhythm and Magnetoencephalography (MEG) in 30 healthy human participants. We analyzed whether the probability to perceive the near-threshold target stimulus was modulated by the gastric rhythm by testing whether hits and misses cluster at different potions of the gastric phase. However, we found no effect of gastric phase on hits vs. misses. In a more exploratory analysis, we found that gastric phase significantly

modulated alpha power in a large cluster spanning parieto-occipital and more anterior regions, showing for the first time that gastric phase modulates alpha power also when participants are actively engaged in a task. We then correlated the strength of coupling in the cluster with individual performance across task blocks, to assess whether individual gastric-alpha coupling explains interindividual variability in performance. However, no link with hit rate or reaction time was found. The methodology and results of this experimental work will be presented in chapter 8.

During my thesis, I also had the opportunity to contribute to an article (appendix, Rebollo, Wolpert & Tallon-Baudry, Current Opinion in Biomedical Engineering, 2021) reviewing current knowledge on gastric-brain coupling and future avenues for testing hypotheses about gastric-brain functions.

Before presenting the methodology and experimental work, I will review the anatomy of the stomach and its intrinsic nervous system, as well as its intrinsic pacemaker activity which can be measured by the EGG (chapter 1). In chapter 2, I will describe the potential anatomical pathways relaying gastric signals to the central nervous system, and focus on the subcortical and cortical structures receiving gastric afferents. In chapter 3, I review the work demonstrating that the gastric rhythm influences spontaneous brain dynamics, and notably modulates brain alpha power. Finally, in order to reveal the potential behavioral consequences of this influence, I describe the functional role of spontaneous cortical activity, with a focus on the alpha rhythm and its influence on visual perception (chapter 4).

1. Anatomy and physiology of the stomach

1.1. Overview of the gastrointestinal tract

The gastrointestinal (GI) tract is the body's largest and most vulnerable surface to the outside world (Furness et al., 2013). Its function is to digest and absorb ingested food. The GI tract is a long tubular muscle separated by muscular sphincters and includes the oral cavity, esophagus, stomach, small and large intestines and the rectum (Figure 1). Each of these organs serves different functions: In the mouth food is chewed and mixed with saliva, while the esophagus conveys solids and liquids to the stomach using peristaltic waves. The stomach stores food, mixes it with secretions and grinds it into particles that can be emptied into the duodenum, the first section of the small intestine, where most of the nutrients and minerals are absorbed. Liquids become absorbed in the large intestine (colon), where remaining waste material is stored and expelled as feces.

A peculiarity of the GI system is that it its functioning is controlled by an intrinsic nervous system, the **enteric nervous system**, which can be seen as a third branch of the autonomic nervous system, next to the sympathetic and parasympathetic system. Digestive function is also regulated by extrinsic innervations: First, signals from the upper GI tract are sent to the 10^{th} cranial nerve, the **vagus nerve**, which in turn sends descending projections controlling GI functioning. These vagal pathways form an important part of the **parasympathetic** system. Second, visceral information is projected to neurons in the spinal cord, which in turn have descending projections to the GI tract. These spinal pathways are part of the **sympathetic** system. In addition to intrinsic and extrinsic innervation, the stomach and other organs of the GI tract contain a specialized type of cell, called the **Interstitial Cells of Cajal**, which act as electrical pacemaker for the contraction of smooth muscles and are at the interface between the enteric and the rest of the autonomic nervous system.

In the following, I will focus on the stomach, beginning with its general anatomy and a description of the layers of the gut wall and their innervations. I will then describe how stomach rhythmicity is achieved through pacemaker activity. Next, I will review in more detail how gut functioning is regulated by the autonomic and enteric nervous system. In the final section, I will describe how the stomach electrical activity can be measured non-invasively.

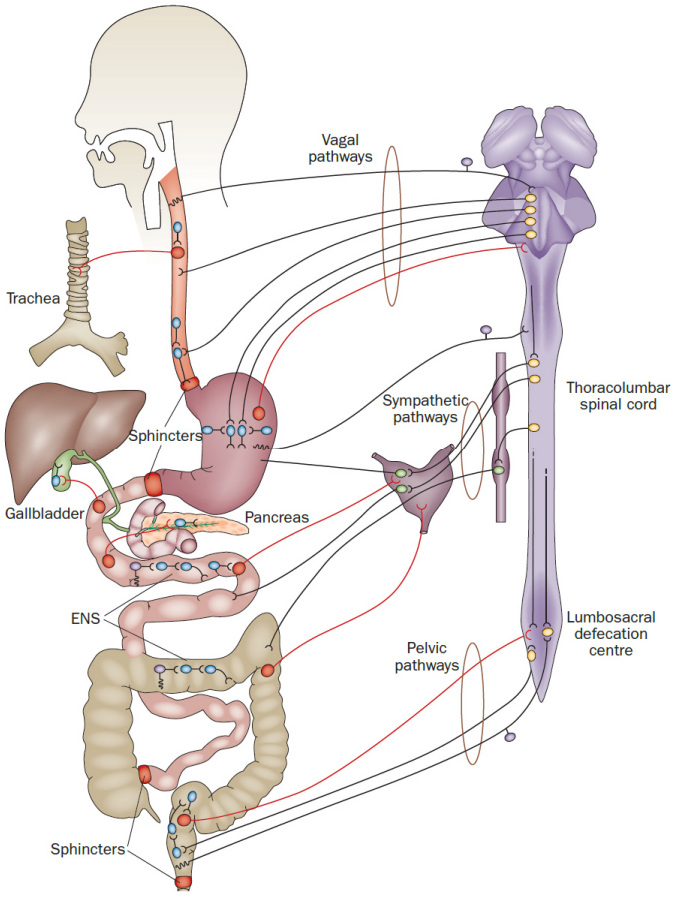

***Figure 1**: The gastrointestinal tract and its innervation. The gastrointestinal tract consists of different organs separated by sphincters. The enteric nervous system contains motoneurons and interneurons (blue), sensory neurons (purple), as well as neurons (red) that project directly to the central nervous system (yellow). The GI tract sends sensory information to and is innervated by the central nervous system through vagal (parasympathetic) and spinal (sympathetic) pathways. (Note that the pelvic pathway was recently suggested to be part of the sympathetic nervous system (Espinosa-Medina et al., 2016)). From Furness, 2012.*

1.2. The stomach and its innervation

The stomach is a crescent-shaped hollow organ in the upper part of the abdomen, between the left dome of the diaphragm and the transverse colon (Fritsch and Kühnel, 2008). Its exact shape and position varies from human to human and as a function of extension due to the ingestion of food. It consists of the following parts (Figure 2A): The *cardia* is the funnel-shaped entrance to the stomach where contents from the esophagus enter the stomach. The *fundus* is the highest point of the stomach and in upright position contains swallowed air. The body or *corpus* makes up the largest part of the stomach, which is continuous into the (pyloric) *antrum*. Finally, a muscle ring called the *pylorus* empties content into the duodenum. The stomach is classically divided into a proximal and a distal part (Cannon, 1898), divided by the lesser and greater curvature. The proximal part consists of the fundus and upper third of the corpus, while the distal part consists of the rest of the corpus, the antrum and the pylorus. While the proximal region acts as a reservoir and generates pressure to drive liquid emptying, the distal part is responsible for the trituration and grinding of solids (Kelly, 1980; Rayner et al., 2012).

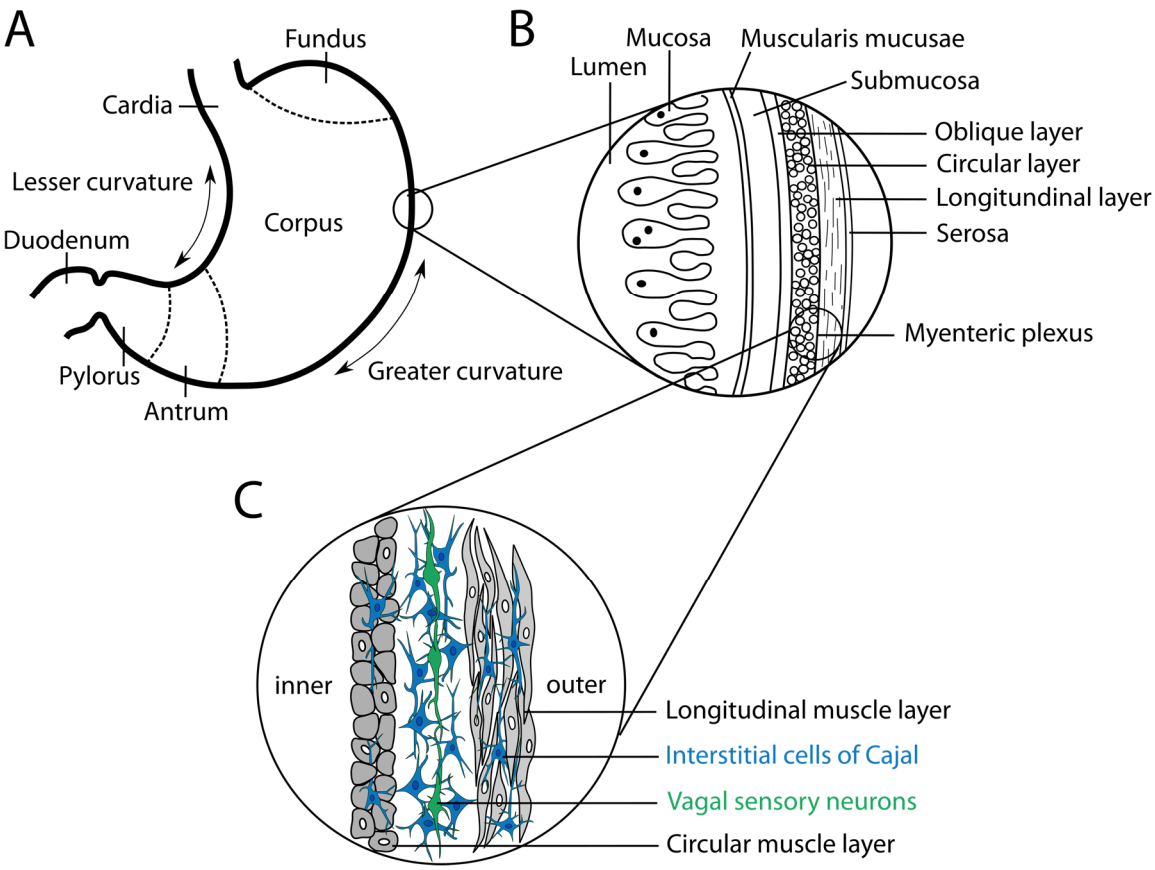

***Figure 2**: Stomach anatomy, the stomach wall and its innervation. **A**: Anatomical regions of the stomach, with the main division into fundus, corpus and antrum. **B**: The different layers of the gastric wall. **C**: The Interstitial Cells of Cajal (ICC, blue) are the generators of the gastric rhythm. They lay in the stomach wall, between and within the circular and longitudinal muscle layers. The electrical activity of the pacemaker is passed through the entire ICC network and is also passively conducted into coupled muscle cells. ICCs make synapse-like contact with vagal sensory neurons (Powley et al., 2008), presented in green, that can detect mechanical changes in smooth muscles. Adapted from Koch & Stern, 2004.*

As the rest of the intestinal canal, the wall of the stomach consists of the *mucosa*, *submucosa*, smooth muscle layers (*muscularis externa*), a thin subserosal layer and the *serosa* (Figure 2B). The mucosa is the innermost layer which surrounds the gastric lumen (the space inside the gut), which is formed by a layer of epithelial tissue and an underlying thin layer of smooth muscles (*muscularis mucosae*) (Figure 3). It functions as a barrier to protect the stomach from acid and enzymes produced for digestion, and senses the rich milieu inside the lumen. It is highly folded, which allows the stomach to extend, and consists of millions of fingerlike protrusions called *villi* and indentations called *gastric pits* or *crypts*. Connected to these pits are the gastric glands, which produce digestive enzymes and digestive acidic juice, as well as secretions protecting the stomach itself from the highly acidic environment. Below this is the submucosa, attaching the gastric mucosa to the muscular layers. The

smooth muscles consists of three muscular layers controlling gut peristalsis: a longitudinal and a circular muscle layer, as well as an additional oblique layer inside the circular layer, which is specific to the stomach and which allows more refined control of motility patterns (Birmingham, 1898; Christensen and Torres, 1975; Fritsch and Kühnel, 2008).

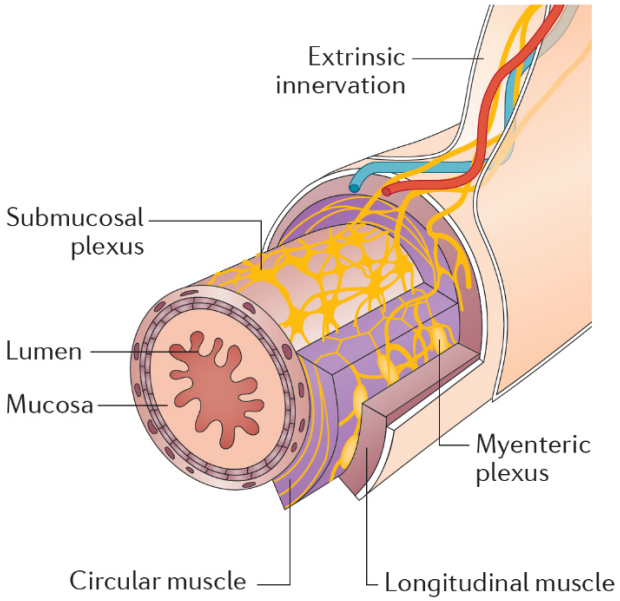

***Figure 3**: The layers of the intestinal wall and its innervation. The inner layer, surrounding the lumen, is the mucosa, which forms filaments (vili) and indentations (gastric pits). Gut peristalsis is controlled by the circular and longitudinal muscle layer. The myenteric plexus is located between the circular and longitudinal muscle layers, and the submucosal plexus between the circular muscle layer and the mucosa. From Rao and Gershon, 2016.*

The muscularis externa contains the myenteric (Auerbach's) plexus, a network of ganglia forming part of the enteric nervous system and which run throughout the entire GI tract, in between the circular and longitudinal muscle layer (Shahrestani and Das, 2020). The intestines contain an additional submucosal plexus which is involved in sensing and absorbing luminal contents (Brehmer et al., 2010). The myenteric plexus carries sympathetic and parasympathetic fibers to the smooth muscle layers and contains the bodies of enteric motor neurons controlling digestive motility. These neurons are linked to smooth muscle cells through the so-called **Interstitial Cells of Cajal** (**ICCs** – Figure 2C). These special cells, which themselves have neuron-like properties (Klüppel et al., 1998), not only mediate neural signals but also act as the intrinsic pacemakers that generate and propagate slow pacemaker currents that form the basis of the gastric rhythm (more in section 1.3). ICCs additionally act as transducers of inputs from motor neurons and stretch receptors (Hirst and Edwards, 2006; Sanders et al., 2006, 2014).

The myenteric plexus also includes mechanically and chemically sensitive receptors which provide afferent input to interneurons in the enteric nervous system. Two types of mechanoreceptive vagal sensory neurons (Figure 2C) have been characterized (Powley and Phillips, 2011): *intramuscular arrays* and *intraganglionic laminar endings*. Intramuscular arrays are mostly distributed in major sphincters of the gut and in the stomach wall (Wang and Powley, 2000), where they are grouped in arborized structures running along the smooth muscles (like ICCs). They make synapse-like contact

with ICCs, smooth muscles and enteric neurons (Powley et al., 2008). Functionally, they operate as stretch detectors reporting the stretch of length of muscle in the gut wall, similar to muscle spindle organs (Powley and Phillips, 2011). In contrast, intraganglionic laminar endings are distributed homogenously throughout the GI tract, with denser concentrations of endings in the gastric corpus (Wang and Powley, 2000), and act as tension receptors (Berthoud and Neuhuber, 2000; Powley et al., 2016).

1.3. Pacemaker activity and stomach rhythmicity

The entire GI tract generates its **own electrical rhythmicity** through ICCs, which can also be found in the kidney, bladder, urinary and reproductive tract, where their function is less clear (Sanders et al., 2014). There are two types of ICCs: Myenteric ICCs, located between the circular and longitudinal muscle layer, and intramuscular ICCs, located within the muscular layers. Intramuscular ICCs are also involved in the transduction of inputs from enteric motor neurons (Hirst and Edwards, 2006; Sanders et al., 2006, 2014). ICCs spontaneously depolarize and repolarize through calcium currents and thereby generate a **slow rhythm with a peak frequency of ~0.05 Hz in humans** (1 cycle every 20 seconds), called the **gastric rhythm**. By forming gap junctions with other ICCs and adjacent smooth muscle cells, ICCs conduct the slow waves through the ICC network as well as to electrically coupled smooth muscle cells. This pacemaker activity is autonomous: ICCs keep generating the gastric rhythm even when completely disconnected from the CNS (Suzuki et al., 1986). It is also continuous, as it is generated at all times, even in the absence of contractions (Bozler, 1945). During fasting (also called the *preprandial* period), ICCs depolarize smooth muscles close to the threshold for generating contractions. During digestion (also called the *postprandial* period), the additional input from excitatory enteric motor neurons and vagal efferent neurons triggers contractions of smooth muscles (Chang et al., 2003; Sanders et al., 2014). The pacesetter potentials are thus much stronger during digestion than fasting, which is expressed in higher amplitude in cutaneous recordings (Koch and Stern, 2004). Despite the ICCs' autonomous activity, proper stomach functioning is also dependent on input from the central nervous system. In support of this notion, vagotomy results in reduced gastric contractions (Andrews et al., 1980). It also follows that the phase of the gastric rhythm is mostly driven by ICCs, while the amplitude is a combination of currents generated in ICCs, enteric motor neurons and smooth muscles.

In serosal recordings, the gastric rhythm is observed as sharp potentials (Figure 4). Two types of activity can be observed (Sanmiguel et al., 1998). *Electrical control activity reflects* periodic depolarization of smooth muscle cells and can occur in the absence of contractions. *Electrical response activity* comes in the form of plateau potentials or spikes/ripples superimposed on the electrical control activity and is associated with contractions. In contrast, in cutaneous recordings, the slow wave is visible as a smooth sinusoidal shape, which is due to the filtering and integrating properties of the abdominal

wall and the superposition of slow waves generated simultaneously at many sites (Koch and Stern, 2004).

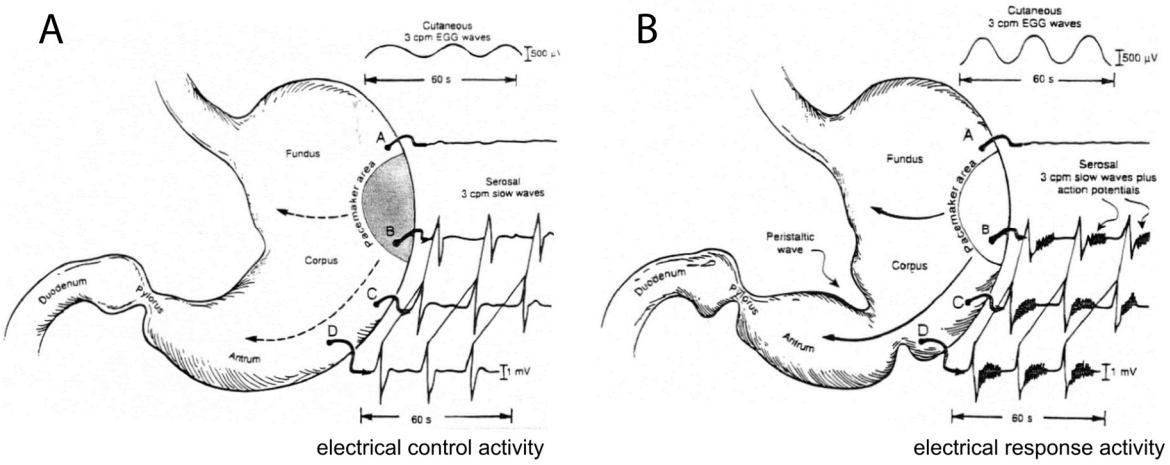

Figure 4*: Slow wave propagation.* ***A****: Stomach during fasting. With serosal electrodes, the gastric rhythm is observed as sharp potentials ("electrical control activity") originating from the pacemaker area and propagating in a proximal to distal gradient. In cutaneous electrodes (top), the gastric rhythm appears in sinusoidal shape with a cycle length around 3 cycles per minute (cpm), i.e., ~20 seconds.* ***B****: Stomach in the postprandial (fed) state. During muscular contractions, ripples become superimposed on the slow waves in serosal recordings, resulting in what is called "electrical response activity". The amplitude of the cutaneous 3 cpm waves is increased. From Koch and Stern, 2004.*

It has long been assumed that the stomach contains a "dominant pacemaker" area, in the greater curvature of the mid/upper corpus, entraining slow waves at other sites (Hinder and Kelly, 1977; Kelly et al., 1969; Koch and Stern, 2004; O'Grady et al., 2010; Riezzo et al., 2013). Accordingly, ICCs at the pacemaker region generate regular discharges of slow waves, thereby depolarizing the ICC network, which causes an active spread of slow waves in a proximal to distal direction. The rapid circumferential conduction of slow waves triggers rings of contractions migrating along the stomach (Koch and Stern, 2004). Moreover, the propagation of rings of pacesetter potentials occurs with a frequency gradient, with a high velocity and amplitude at the pacemaker region, slower velocity and lower amplitude in the lower corpus, and a transition back to faster and larger slow waves in the antrum (Hinder and Kelly, 1977; Kelly et al., 1969; Koch and Stern, 2004; O'Grady et al., 2010; Riezzo et al., 2013). Note though that the existence of both a dominant pacemaker and a frequency gradient has been questioned by a few authors (Rhee et al., 2011; Sanders, 2019).

1.4. Gut regulation by the autonomic and enteric nervous system

The GI tract differs from the other peripheral organs in that it has its own intrinsic nervous system, the **enteric nervous system** (**ENS**) (Furness et al., 2014). Due to its high degree of anatomical complexity and functional autonomy, it is sometimes called the "second brain". It regulates and coordinates the many complex tasks of the GI system, including GI motility, secretory mechanisms, sensory processes, mucosal maintenance, immunological defense, local blood flow and interactions with gut microbiota (Rao and Gershon, 2016). It consists in a complex network of neurons organized in thousands of small ganglia, with the majority located in the myenteric and submucosal plexus. This network is organized in microcircuits, with interneurons and intrinsic primary afferent neurons. The ENS in humans contains between 200 and 600 million neurons (Furness et al., 2014), which is more neurons than all other peripheral ganglia together, and the millions of enteric sensory neurons outnumber the vagal and spinal afferents even when taken together (Grundy, 2002). Enteric sensory neurons (also called intrinsic primary afferent neurons, Figure 5, middle) located in the gut mucosa are sensitive to changes in chemical contents of the gut lumen, movements of the mucosa and contractions of intestinal muscles. They respond to these signals to initiate local reflexes on motility, secretion and blood flow. Different types of enteric motoneurons control muscle movements, secretions, and vasodilation. They receive excitatory inputs from descending interneurons and act directly on smooth muscles and indirectly via the ICC network. All of these neurons make the ENS capable to function autonomously, controlling GI behavior independently of input from the brain or spinal cord (Bayliss and Starling, 1899; Furness et al., 2014; Gershon, 2010). Nevertheless, spinal and vagal innervations play an important a role in GI regulation, each including ascending sensory and descending motor innervations.

The main afferent pathway from the abdominal cavity to the brain is the **vagus pathway**, as part of the parasympathetic system (Figure 5, left). It provides sensory and motor innervation for the upper GI tract (from esophagus to the upper colon) (Forsythe et al., 2014) and carries tonic information not only about the GI tract but also the heart, lungs and liver to the brain. In the GI tract, the mechanical and chemical state of the gut is sensed by different types of vagal afferent nerve endings, intraganglionic laminar endings and intramuscular arrays. Their signals help to regulate functions such as control of appetite and satiety, gastric volume, contractile activity and acid secretion (Forsythe et al., 2014).

The GI innervation by sympathetic neurons emerges from cell bodies of **spinal afferent neurons** located in dorsal root ganglia in the thoracolumbar segments of the spinal cord (Figure 5, right). Spinal afferent endings encode the contraction and distension of the gut wall, and provide nociceptive information (Brookes et al., 2013). A high proportion of afferent endings is also located around arterioles in the gut wall.

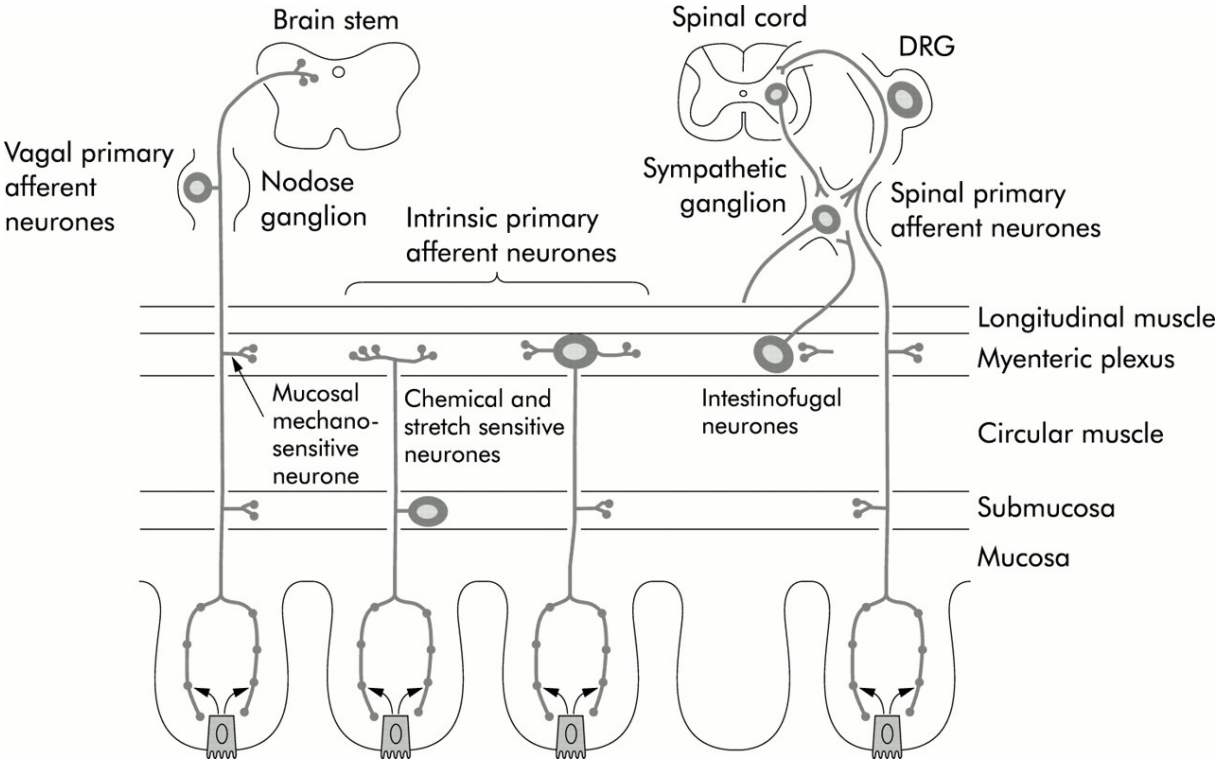

Figure 5*: Schema of enteric sensory neurons and vagal and spinal innervation with ascending projections. Left: Vagal primary afferent neurons terminating in the submucosa and myenteric plexus carry information about the mechanical and chemical state of the gut to the nodose ganglion and from there to the brain stem. Middle: Intrinsic innervation by enteric sensory neurons (intrinsic primary afferent neurons) senses chemical and stretch related information to initiate local reflexes. Right: The cell bodies of spinal afferent neurons are located in the dorsal root ganglion (DRG) and terminate in the mucosa and myenteric plexus to sense the contractile state of the stomach, as well as nociceptive information. From the dorsal root ganglion, they project to several laminae of the spinal cord. From Grundy, 2002.*

The vagal and spinal branch also carry descending signals from the brain and spinal cord to the stomach. Classically, the spinal sympathetic pathway has been associated with initiating “fight or flight” responses, while the parasympathetic system has been more associated with “rest and digest” responses (Cannon, 1930), although this is a gross simplification. Of note, around 80% of the vagal fibers are afferent, indicating that the brain is more of a listener than sender of vagal information (Agostoni et al., 1957). In contrast to the parasympathetic system, the ratio between sympathetic efferents and afferents is closer to 50:50 (Foley, 1948; Leek, 1972). The interaction and relative contributions of these different systems still remains to be completely understood. The more detailed descending influences of vagal and spinal centers will be reviewed in section 2.2.

In sum, even though the GI tract contains its own nervous system that functions autonomously to a high extent, it does not work as a closed system. Vagal and spinal routes continuously carry sensory information about the mechanical and chemical state of the gut to the brain and spinal cord, which in turn send descending commands to regulate GI functioning.

1.5. Measuring the gastric rhythm: electrogastrography

The gastric rhythm can be measured noninvasively by means of cutaneous electrodes placed on the abdomen, recording a signal called the **electrogastrogram** (**EGG**) (Figure 6A). An example of a raw trace where the gastric rhythm is visible to the naked eye is shown in Figure 6B. The gastric cycle appears as waves of around 20 seconds duration, with respiratory and cardiac cycles superimposed. The power spectrum of EGG recordings in healthy human participants exhibits a peak around 0.05 Hz or three cycles per minute, i.e. one cycle every 20 seconds (Figure 6C), which is distinct from the spectral signatures of respiration and the cardiac rhythm (Figure 6D).

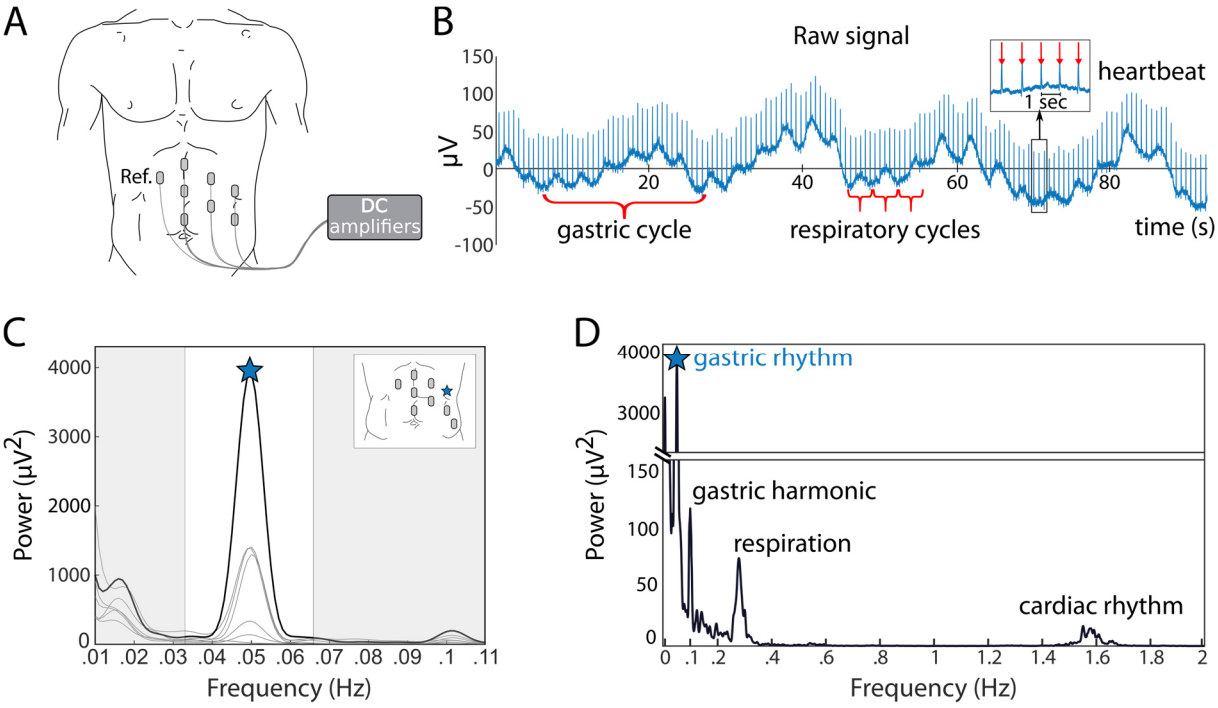

***Figure 6**: The electrogastrogram. **A**: Example recording setup from the group with cutaneous electrodes places on the left abdomen, with seven active electrodes, one reference and one ground electrode (over the right shoulder in an MEG setup – not visualized here). **B**: Example of a raw time course in one channel. The gastric rhythm is visible as slow waves around 20 seconds, superimposed by the much faster respiratory (around 3-5 seconds) and cardiac cycles (around 1 second). **C**: Power spectrum of each of the seven recording electrodes. A clear peak is visible around 0.05 Hz. Peak*

frequency is indicated by a star on the channel with the highest power (black line). ***D****: Power spectrum for the larger frequency range, where the spectral signatures of the respiratory (around 0.3 Hz) and cardiac rhythms (around 1.5 Hz) are visible. From Wolpert et al., 2020.*

EGG signals can be described by several parameters. First, the peak frequency in healthy human participants varies between 0.033 and 0.066 Hz (or 2-4 cycles per minute), which is labeled the *normogastric* frequency range (Yin and Chen, 2013) (Note however that the definition of the frequency range varies depending on authors (Chang, 2005; Parkman et al., 2003).) The frequency of the cutaneous EGG is a reflection of the gastric basal rhythm, as confirmed by simultaneous invasive and cutaneous EGG recordings (Brown et al., 1975; Chen et al., 1994; Coleski and Hasler, 2004; Familoni et al., 1987; Hamilton et al., 1986; Lin et al., 2000; Mintchev et al., 1993). The amplitude of the cutaneous EGG is more difficult to relate to gastric physiology. Generally, it likely reflects a combination of both ICCs and smooth muscle contractions. The relative contribution of the two is hard to disentangle since the signature of smooth muscle contractions visible in invasive recordings, i.e. sharp ripples, are filtered out in cutaneous recordings (Verhagen et al., 1999). Moreover, how electrical signals of gastric origin are combined in surface recordings still remains to be fully resolved (Cheng et al., 2013; Du et al., 2010). The amplitude of the gastric rhythm notably depends on the fast vs. fed state of the participant, with increases in amplitude observed in healthy participants after the intake of a meal (Riezzo et al., 2013). As an approximation, one can consider that in the fed state the amplitude is more driven by the smooth muscle contractions that accompany digestion, while in the fasted state, the surface EGG corresponds more closely to ICC activity, even though still some contractions may occur (O'Grady et al., 2010; Sanders et al., 2014).

The EGG has been first described in the 1920s (Alvarez, 1922; Tumpeer and Blitsten, 1926), with rekindled interest linked to computerized analysis in the 1990s (Koch and Stern, 2004). As an attractive method also due to its cheap and non-invasive nature, it has since mostly been used to characterize gastric motility problems and been related to different clinical conditions. For example, faster EGG rhythms (tachygastria) are observed in patients with nausea (Geldof et al., 1989) or depression (Ruhland et al., 2008). Additionally, pioneering psychophysiological studies have tried to relate changes in EGG amplitude and frequency to stress, emotions and some cognitive tasks, albeit with often mixed or inconsistent results (Baldaro et al., 1990, 1996, 2001; Davis et al., 1969; Ercolani et al., 1982, 1989; Holzl et al., 1979; Lin et al., 2007; Riezzo et al., 1996; Vianna et al., 2006; Walker and Sandman, 1977).

A challenge for electrogastrography is that in contrast to other methods such as electroencephalography or electrocardiography, clear and standardized recording and analysis procedures are lacking. Especially, this method has so far mostly been used to quantify abnormalities,

while less attention has been paid to healthy participants. This lack of standardization makes the comparison between studies difficult and may explain at least partly the discrepancies between psychophysiological studies. For example, there is a large variability in the number and placement of electrodes used, raising the question which electrode setting is optimal to detect the gastric rhythm. Moreover, while for methods such as electroencephalography (EEG), standard procedures are available to detect artifacted data segments, there is no consensus on what represents a "clean" recording in EGG. **One of the aims for my thesis was therefore to improve the standardization by formulating guidelines on recording the EGG in healthy participants, and to develop a semi-automatic analysis pipeline for identifying a regular gastric rhythm.**

2. Ascending and descending pathways of gut signals

The aim of this thesis is to investigate the role of the gastric rhythm for brain and behavior. For this, knowing the anatomical pathways and cortical and subcortical structures receiving gastric input is essential. In this chapter, I will first review the ascending vagal and spinal pathway and then present in more detail the nuclei with descending control. I will then focus on the different visceral centers receiving visceral afferents, going from neuromodulatory centers and subcortical structures to higher cortical levels. As a note of caution, much about the anatomical pathways between stomach and brain is still to be determined. The anatomical projections described here are mostly drawn from anatomical tracing and electrophysiological studies in mice, rats, cats and monkeys. While an argument can be made that visceral pathways are probably ancient and conserved through evolution, differences between species have been reported (Bishop, 1932; Pritchard et al., 2000; Shipley and Sanders, 1982). Moreover, there are only very few stomach-specific anatomical tracing studies in animals. Finally, determining the organ-specific projections, or the relative contributions of the vagal and spinal input, becomes more difficult the higher the level. Despite these limitations, anatomy suggests that gastric input reaches a wide array of subcortical and cortical structures that are in charge of homeostasis, i.e. the sensing and regulation of the internal milieu, but also are involved in function such as arousal, emotion, decision making, perception, memory and reward.

2.1. The vagal and spinal ascending pathway

An overview of the ascending pathways and central projections of visceral signals can be found in Figure 7. Visceral inputs reach the brain via vagal and spinal pathways (Figure 7A). Vagal afferent fibers with cell bodies in the nodose ganglion terminate in the **nucleus tractus solitarius** (**NTS**), located dorsally within the caudal medulla oblongata and containing several subnuclei. The NTS is a major site of convergence of inputs from many homeostatic systems within the body (Critchley and Harrison, 2013), and there is evidence that it has a loose viscerotopic organization (Altschuler et al., 1989). NTS has long been considered a pure sensory relay center, but it is now clear that it plays a key role in many integrative processes. It is here that most GI reflexes are initiated, due to projections to the dorsal nucleus of the vagus, the efferent motor branch of the parasympathetic system. Next, spinal visceral afferents project to the dorsal horns of the spinal cord, with the spino-thalamic tract projecting mostly to the thalamus without passing through brainstem relays, with some additional projections to the parabrachial nucleus.

The **parabrachial nucleus** is an oval-shaped group of neurons at the junction of the pons and midbrain, containing several subnuclei (Pritchard et al., 2000; Saper, 2002). It is here that vagal inputs from the NTS and spinal inputs from the spinothalamic pathway converge. It is involved in taste processing and taste aversion learning (Pritchard et al., 2000), and it also mediates a “liking” response to pleasurable stimuli like food (Berridge and Kringelbach, 2015). A further function is fluid homeostasis (Pritchard et al., 2000), and it is a relay station in pain pathways (Ren and Dubner, 2008),

responding to noxious stimuli (Palmiter, 2018; Pritchard et al., 2000). It also plays a role in wakefulness and arousal (Fuller et al., 2011). Parabrachial neurons transmit taste, temperature, respiratory signals, satiety, thirst, salt-appetite and glucose level signals (Palmiter, 2018). It is likely that the parabrachial nucleus is involved in GI motility, although no direct evidence for this is available (Gillis et al., 2011).

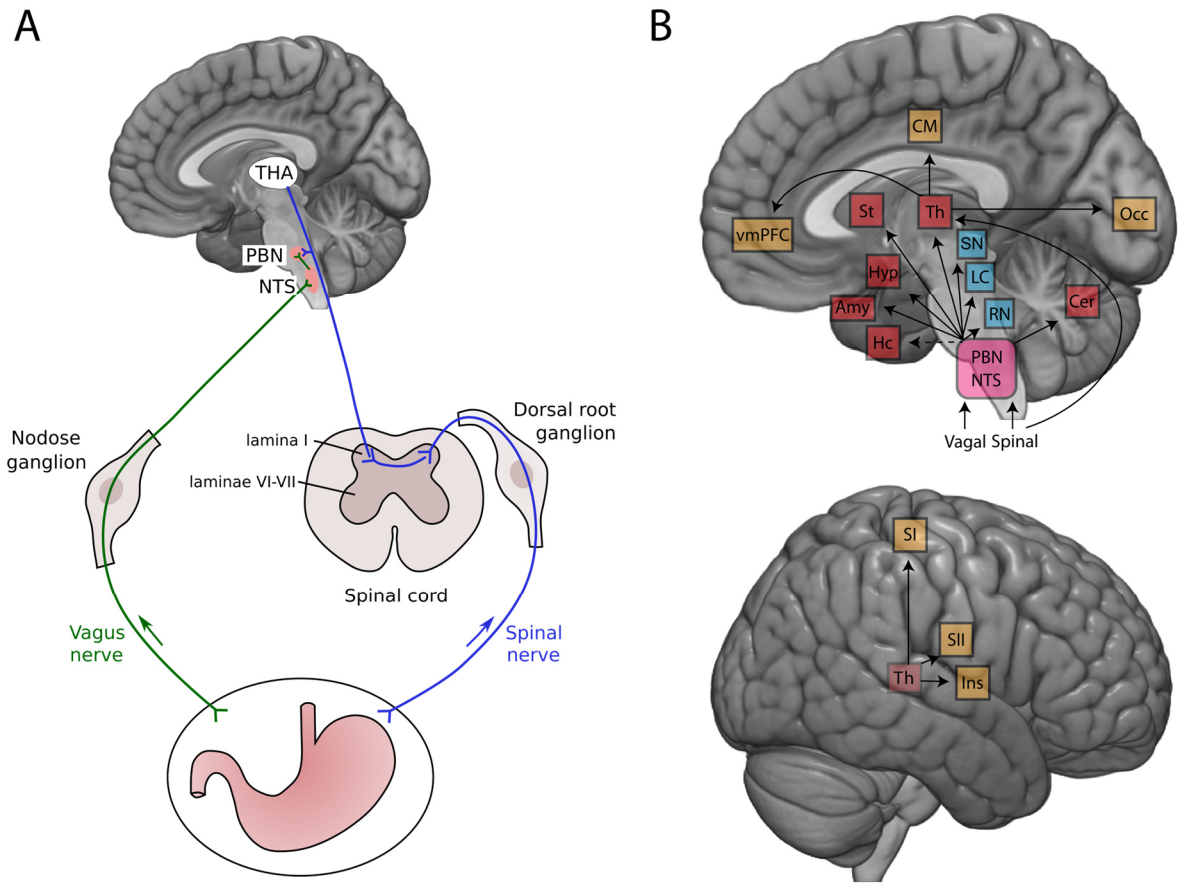

***Figure 7**: **A**: Schematic representation of the vagal (green) and spinal (blue) ascending pathway. Vagal neurons innervating the gut travel to the nodose ganglion and project to the nucleus of the solitary tract (NTS) and from there to the parabrachial nucleus (PBN). Spinal afferent inputs with cell bodies in the dorsal root ganglia enter the spinal cord at the lamina I and synapse mainly onto neurons in laminae I, VI and VII of the spinal cord. From there they project to the thalamus (THA) bypassing the brainstem, with some additional projections to the PBN. Own figure, inspired by Chavan et al., 2017. **B**: Overview of projection sites of vagal and spinal afferents from the gastrointestinal tract. Visceral afferents target the major relays in the brainstem (purple), the nucleus of the solitary tract (NTS) and parabrachial nucleus. PBN projects to neuromodulation nuclei (blue), including the raphe nucleus (RN), locus coeruleus (LC) and substantia nigra (SN). The NTS and PBN also project to subcortical structures (red). The spinothalamic route goes to the thalamus (Th), which in turn projects to cortical regions (yellow). Abbreviations: Amy, amygdala; Cer, cerebellum; CM, cingulate motor regions; Hc, hippocampus; Hyp, hypothalamus; Ins, insula; LC, locus coeruleus; NTS, nucleus of the solitary tract; PBN, parabrachial nucleus; RN, raphe nucleus; SI, primary somatosensory; SII, secondary somatosensory; SN, substantia*

nigra; St, striatum; Th, thalamus; vmPFC, ventromedial prefrontal cortex. Modified from Azzalini et al., 2019.

From the parabrachial nucleus, vagal and spinal projections target the main **neuromodulatory centers**, including the serotonergic dorsal raphe nucleus, the noradrenergic locus coeruleus and the dopaminergic substantia nigra and ventral tegmental area (Figure 7B, blue). The parabrachial nucleus also connects the viscera with **subcortical structures** involved in autonomic regulation, including the striatum, hypothalamus, amygdala, hippocampus and cerebellum (Figure 7B, red), and parabrachial outputs also target a set of **thalamic nuclei**. Next, the spinothalamic pathway reaches the thalamus without passing through brainstem relays. From the thalamus, numerous **cortical areas** receive direct visceral inputs, including the primary and somatosensory cortex, insula, ventro-medial prefrontal cortex, cingulate motor regions and the occipital cortex (Figure 7B, yellow).

2.2. Descending vagal and spinal projections

2.2.1. Vagal control by the dorsal motor nucleus of the vagus

GI functioning is regulated by both vagal/parasympathetic and spinal/sympathetic centers. The parasympathetic motor supply of the stomach is provided by the **dorsal motor nucleus of the vagus** (**DMV**) and the **nucleus ambiguus** (Furness et al., 2014). Some parts of the stomach receive parasympathetic innervation from the DMV and additionally the nucleus ambiguus (e.g. the cardia), while others receive innervation only from the DMV (e.g. the antrum and pylorus) (Gillis et al., 2011). The functional relevance of these differences is unclear but probably related to the different functions of the stomach regions.

The DMV is the most important center for **parasympathetic control of gastric activity**. It is a paired structure in the dorsal caudal medulla adjacent to the central canal, area postrema and the nucleus of the solitary tract (Travagli et al., 2006). Its majority of nerves are cholinergic. The DMV is mainly involved in modulations of gastric contractions, control of gastric acid secretion, gastric accommodation and relaxation. Besides the stomach, it also innervates the esophagus, pancreas, kidney and small intestine (Hornby and Wade, 2011). It is not rigidly viscerotopically organized, but in medio-lateral columns spanning its rostro-caudal extent (Travagli et al., 2006). It is also segregated by functions, with descending vagal pathways responsible for gastric contractions vs. relaxations being localized in different DMV regions. Moreover, it contains a site-specific organization, with different DMV regions innervating different parts of the stomach (Okumura and Namiki, 1990). DMV receives input from the nucleus of the solitary tract, which plays a major role in shaping the vagal efferent output.

Tracing studies in rats (Berthoud, 1996; Berthoud et al., 1991; Holst et al., 1997; Kressel et al., 1994; Zheng and Berthoud, 2000) and the guinea pig (Schemann and Grundy, 1992) showed that the stomach receives a particularly dense innervation from the DMV, with at least two thirds or up to 100% of enteric neurons receiving input from pre-enteric vagal neurons. In comparison, the esophagus and small intestine seem to receive much less input (Holst et al., 1997; Neuhuber et al., 1998). Moreover, it has been found that the DMV neurons that innervate different parts of the stomach (as well as other organs) have different morphologies, which are associated with different response properties (Fogel et al., 1996). DMV neurons make excitatory synapses onto enteric motor neurons in the myenteric plexus of the stomach (Travagli et al., 2006). In cats, these projections have been found to have **both an excitatory and inhibitory effect on ICCs and smooth muscles**, depending on the DMV region (Pagani et al., 1985). These influences seem to be selective to the GI tract since they were not accompanied by changes in heart rate or arterial pressure. After vagotomy, gastric distension causes weaker phasic contractions in ferrets (Andrews and Scratcherd, 1980). Recently, it has been shown for the first time that the non-invasive stimulation of the vagus nerve in humans reduces gastric frequency (Teckentrup et al., 2020).

2.2.2.Sympathetic efferents – the interomediolateral cell column

Although the parasympathetic control is functionally dominant, there are also sympathetic descending visceral projections. The sympathetic efferent nuclei are located in the intermediolateral cell column, a columnar grouping of cells in the lateral horn of the spinal gray between the first thoracic spinal segment (T1) and the third lumbar segment (L3) (Furness, 2006; Powley, 2013 – Figure 8). The intermediolateral cell column displays a rostral-to-caudal viscerotopic organization and its neurons are mostly cholinergic. From there, they project to ganglia outside of the spine. There are two different ganglia receiving separate input from the intermediolateral cell column and projecting directly to the viscera (Gillis et al., 2011). The *paravertebral ganglia* run lateral and adjacent to the spinal cord from the neck to the sacrum (Figure 8). Their main functions are vasoconstriction and liquid balance. The *prevertebral ganglia* pass through the paravertebral ganglion without relays and are located in the thoracic wall. They are mainly involved in vasoconstriction, motility and secretion (Furness, 2006).

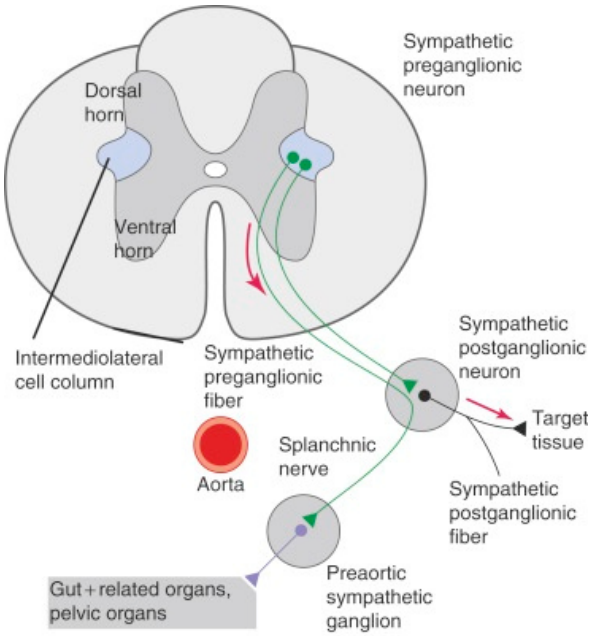

***Figure 8**: The intermediolateral cell column (IML) and its projections. Sympathetic preganglionic neurons are located in the different nuclei of the IML, located the lateral horn of the spinal gray. Form there they project to either paravertebral ganglia or prevertebral ganglia. Fibers going to the prevertebral ganglion pass through the paravertebral ganglion without relays. Ganglia directly project to the visceral targets. From Powley, 2013.*

Spinal neurons have different effects on GI motility: On the one hand, they can have a general inhibitory effect on gastric motility, which is based on inhibition of the excitatory vagal cholinergic input to the enteric plexus (Travagli et al., 2006). On the other hand, the spinal efferents can stimulate stomach contractions via serotonin (Sveshnikov et al., 2012). Accordingly, stimulation of the sympathetic centers of the spinal cord can either have a **stimulatory or inhibitory effect on stomach contractions** (Semba and Mizonishi, 1978; Smirnov and Lychkova, 2003; Tsuchiya et al., 1974). Other functions of spinal efferents include the constriction of muscular sphincters to regulate transit across GI organs (Furness, 2012) and control of liquid balance, including peptide secretion in the mucosa (Racké et al., 1996) and blood flow to different parts of the GI tract (Holzer, 2006).

2.3. Neuromodulatory centers

Through the parabrachial nucleus, visceral signals might reach the main neuromodulatory centers: The serotoninergic dorsal raphe nucleus, the noradrenergic locus coeruleus and the dopaminergic substantia nigra (Coizet et al., 2010; Pritchard et al., 2000; Saper and Loewy, 1980). Since these systems have important consequences for behavior, I will here briefly review their anatomy and functions.

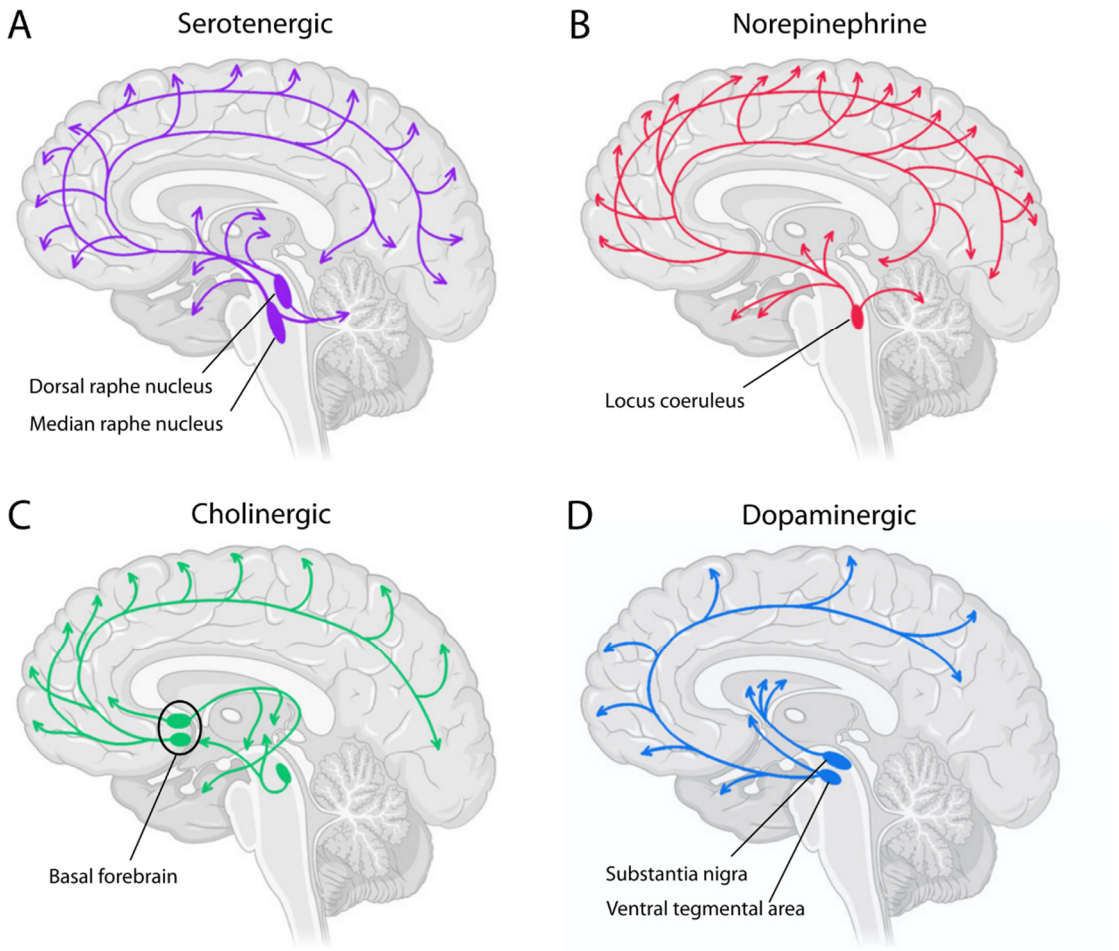

***Figure 9**: Overview of neuromodulatory pathways with their nuclei and projections to brain regions. Adapted from O'Callaghan et al., 2021.*

The **raphe nuclei** are embedded within the reticular formation, a region in the brainstem where grey and white matter mixes together (Figure 9A). The reticular formation consists of a network of specialized nuclei. The nucleus raphe magnus, dorsal and median nuclei represent the three largest raphe nuclei. While the nucleus raphe magnus is part of the analgesia system, the dorsal and median raphe nuclei provide the main source of **serotonin** to the brain (Hornung, 2003). The serotonergic system innervates the thalamus, striatum, amygdala, cerebellum and most cortical regions. It has effects on almost all CNS functions, including mood, anxiety, stress, aggression, feeding and cognition (Olivier, 2015). Notably, it plays a role in the sleep-wake cycle (Monti, 2010, 2011), with serotonin being necessary to obtain and maintain sleep, while promoting cortical responsiveness during waking (Portas et al., 2000).

The **locus coeruleus** (LC) is located in the pons (Figure 9B) and provides the major source of **norepinephrine** in the brain (Samuels and Szabadi, 2008). It has extensive projections to all brain regions except the basal ganglia, and also sends descending projections to the spinal cord and autonomic

nuclei, suppressing afferents from the spinothalamic tract. The norepinephrine system largely overlaps with the serotonin system, the two systems in fact depending on each other (Sara, 2009). Functionally, norepinephrine stimulates cortical and behavioral arousal, and modulates many other functions like attention, motivation, reward, learning, memory and decision making (Jones, 2020). For example, LC neurons are activated in response to many arousal-related contexts such as sleep-wake transitions (Carter et al., 2010), novel stimuli (Hervé-Minvielle and Sara, 1995), and shifts in perception (Aston-Jones and Cohen, 2005), which in turn are associated with changes in pupil diameter, suggesting a tight link between arousal, pupil and norepinephrine levels (Einhäuser et al., 2008; Kloosterman et al., 2015; Larsen and Waters, 2018). Norepinephrine has also a specific effect on sensory pathways, with an involvement in signal/background noise ratio, gating and sharpening of tuning to preferred stimuli (Sara, 2009). Moreover, the LC sends projections to the **cholinergic basal forebrain** (Figure 9C) (Berntson et al., 2003), which plays an important role in sustained attention (Bentley et al., 2003; Sarter et al., 2001). Although it is unclear if the cholinergic system receives also direct modulation by visceral signals, chemical stimulation of the parabrachial nucleus induces modulations in arousal through projections to the basal forebrain (Qiu et al., 2016).

There is evidence for visceral input to modulate LC activity, arousal and the sleep-wake cycle. For example, distension and electrical stimulation of the small intestine in cats induces sleep onset, EEG synchronization and increases slow wave duration (Juhász and Kukorelli, 1973; Kukorelli and Juhász, 1976, 1977). In rats, distention of the stomach, colon, rectum and bladder activates norepinephrine neurons in the locus coeruleus and hippocampus and thus increases arousal (Elam et al., 1986; Saito et al., 2002). The reason for these apparently contradictory findings between small intestine vs. stomach or colon distension are unknown. Moreover, links between visceral signals and arousal have also been demonstrated for the cardiovascular system, with stimulation or distention of the carotid sinus inducing sleep, increasing slow waves and reducing cortical activity in cats, dogs and monkeys (Bonvallet et al., 1954; Koch, 1932), mediated by reductions in LC activity (Persson and Svensson, 1981).

The **dopaminergic** pathways emanate from the **Substantia Nigra and the Ventral Tegmental Area** (Figure 9D) and send most dense innervations to the striatum, hypothalamus and prefrontal cortex (Alcaro et al., 2007). This system is associated with processes including rewarding stimuli, motivated behavior, maintenance of working memory and emotion regulation (Bissonette and Roesch, 2016; Cools, 2019; Palmiter, 2018). Recently, the role of gastric vagal afferents on the dopaminergic pathway and reward behavior has been strikingly demonstrated in mice (Han et al., 2018): Optogenetic activation of vagal sensory neurons specifically innervating the stomach activated the parabrachial nucleus and induced dopamine-release from the substantia nigra. During stimulation, rats exhibited self-stimulation and conditioned place and flavor preferences.

In conclusion, the central functions of neuromodulatory systems include the regulation of arousal and the sleep-wake cycle, as well as the maintenance of sustained attention and responsiveness during wakefulness. This suggests that over parabrachial projections, gastric input might have an influence on arousal. This aspect was of particular interest for my thesis, and I will come back to it later.

2.4. Regions involved in homeostasis and affective or food-related behavior

Input from the parabrachial nucleus and NTS reaches a number of subcortical regions from the limbic system and the cerebellum. These regions perform many different functions that could be broadly summarized to be related to homeostasis, affective regulation, as well as food-related behavior, often working in tight coordination.

The **hypothalamus** is a small structure consisting of a group of subnuclei ventral to the thalamus. It has an important role in homeostasis, involved in thermoregulation, control of blood pressure, energy maintenance, control of food intake, circadian rhythms, stress and reproduction (Blevins and Baskin, 2010; Saper et al., 2005). It also adjusts emotional behavior, especially defensive reactions to affective threat (Fuchs et al., 1985). It receives input from the NTS, parabrachial nucleus, retina, ventricles and regions from the limbic system (including amygdala, hippocampus, prefrontal and cingulate cortices) (Barbas et al., 2003; Blevins and Baskin, 2010; Ongür et al., 1998). In turn, the hypothalamus sends projections to the pituary gland (Ju et al., 1986), most regions of the limbic system as well as brainstem and spinal autonomic nuclei (Barbas et al., 2003). Notably, it projects to NTS and the dorsal motor nucleus of the vagus (Blessing et al., 1982; van der Kooy et al., 1984; Rogers et al., 1980). Stimulation of the paraventricular nucleus of the hypothalamus inhibits gastrointestinal motility (Sakaguchi and Ohtake, 1985), probably due to an activation of inhibitory vagal fibers in the dorsal motor nucleus of the vagus (Gillis et al., 2011).

The **amygdala** is an almond-shaped structure with at least 12 subnuclei located deep in the medial temporal lobe, and is part of the limbic system. It regulates behaviors associated with affective state, including fight or flight responses, social and reproductive behaviors, and controls acquisition, recall and consolidation of implicit emotional learning. The amygdala receives input from all senses and has bidirectional connections with the parabrachial nucleus, NTS and hypothalamus (Hardaway et al., 2019; McDougall et al., 2017; Palmiter, 2018; Saper, 2002, 2002). This circuitry has an important role for taste memory formation (Miranda et al., 2002), regulation of consumption and reward to highly palatable food (Hardaway et al., 2019), as well as conditioned taste aversion (Yamamoto et al., 1994).

The **hippocampus** is a bilateral curled structure in the medial temporal lobe, and part of the limbic system. It is associated with consolidation from short- to long-term memory and spatial navigation. It receives input from the NTS, not directly but via a multisynaptic pathway, probably over

relays in LC and medial septum (Castle et al., 2005). There is evidence that hormonal signaling from stomach to hippocampus affects food intake, memory and anxiety-like behavior (Carlini et al., 2004; Kanoski and Grill, 2017), and hippocampus responds to colorectal distension in rats (Saito et al., 2002). Recently, it was demonstrated that a vagal gut-brain pathway regulates non-food related, hippocampus dependent memory function, with vagotomy impairing episodic and spatial memory (Suarez et al., 2018).

2.5. Thalamus

I will now come back to the thalamus to review the precise nuclei receiving visceral input. The thalamus is the largest structure in the diencephalon and is composed of a bilateral collection of subnuclei. It is the cerebral "entrance portal" for most sensory input, regulating consciousness, sleep and alertness. The thalamus also constitutes a main viscerosensory relay with input from both a direct spinothalamic pathway and an NTS-spinal-parabrachial pathway. Spinal and vagal afferents are already combined in the parabrachial nucleus, and further convergence takes place in the thalamus.

Of the different subnuclei, some receive signals from specific organs (e.g. retina), while others receive input from multiple viscera and somatic inputs, and still others receive input from other cortical areas (Apkarian, 2007). The specific thalamic nuclei identified as receiving visceral input are mostly drawn from the pain literature (Coen et al., 2012). There are two main nuclei that together form the main relay for vagal and spinal viscerosensory information: the **ventroposterior medial nucleus** (VPM) and the **ventroposterior lateral nucleus** (VPL) (Craig, 2002; Critchley and Harrison, 2013). VPM receives vagal input from the NTS as well as vagal and spinal input from the parabrachial nucleus (Craig, 2002). It projects further to insula and primary somatosensory cortex, and displays a viscerotopic organization (Coen et al., 2012). VPL receives input from the spinothalamic pathway (Craig, 2002; Craig et al., 1994), and mostly projects to primary somatosensory cortex (Coen et al., 2012). In contrast to VPM, VPL does not have a viscerotopic organization, and most of its neurons respond to both visceral and cutaneous stimuli (Coen et al., 2012).

Surprisingly, massive input from the parabrachial nucleus has also been reported for the **lateral geniculate nucleus**, the thalamic relay station in the visual pathway (Erişir et al., 1997a; Uhlrich et al., 1988), even constituting half of the input for this nucleus (Erişir et al., 1997b). Guillery and Sherman, 2002, stated that "based on numbers, one might conclude that the lateral geniculate nucleus relayed information to the cortex from parabrachial inputs". Functionally, stimulation of the parabrachial nucleus has been shown to affect responses in the lateral geniculate nucleus to visual stimuli in cats (Lu et al., 1993). Parabrachial projections have also been mentioned for the auditory medial geniculate nucleus, but not analyzed in detail (Uhlrich et al., 1988). **The projections to the lateral geniculate nucleus, as an entrance to the visual pathway, are of particular relevance for my thesis, and I will come back to this aspect later.**

2.6. Cortical structures

In the following, I will review the anatomy and function of some of the most prominent cortical structures that are known to receive visceral projections. As mentioned above, there are still many unknowns concerning the ascending anatomical pathways for gastric signals, and this is especially true for the cortical projections. Distinguishing the contributions of specific organs becomes very difficult. One method to identify cortical regions responding to gastric sensations in humans is the artificial distension of the stomach by an inflatable balloon while performing PET or fMRI scans (Ladabaum et al., 2001, 2007; Lu et al., 2004; van Oudenhove et al., 2009, 2009; Wang et al., 2008). Such studies have also been performed for other organs such as the colon (Hamaguchi et al., 2004) or esophagus (Yang et al., 2006). Of note, this procedure is highly uncomfortable for the participant, although some studies try to control for different levels of pain or felt intensity (Ladabaum et al., 2001; Lu et al., 2004; van Oudenhove et al., 2009). Nevertheless, the results of these studies tend to converge with anatomical pathways described in animals. Another question relates to how visceral signals are organized in the cortex. While viscerotopy is found in some brainstem and thalamic nuclei as well as in the insula (Cechetto and Saper, 1987), it is not clear for all brain regions visceral signals are equally represented in this manner, and how visceral information is integrated with somatic information. Also note that the structures reviewed here represent a non-exhaustive list.

2.6.1. Insula

The insula is a pair of lobules located deep within the lateral sulcus. It is a richly connected hub, with interconnections with limbic, as well as visual, auditory, olfactory and somatosensory structures. In rodents and monkeys, the insula receives visceral afferents through different thalamic nuclei (Craig, 2002; Evrard, 2018, 2019): First, afferents from the ventroposterior medial nucleus of the thalamus reach the anterior dorsal and ventral insula. Additionally, a direct vagal pathway from the nucleus of the solitary tract to the insula was reported in macaque monkeys (Strigo and Craig, 2016). Next, afferents form the spinothalamic pathway are relayed to the ventromedial nucleus of the thalamus and reach dorsal posterior regions. Given these pathways exist in rodents and monkeys, they are likely to exist in humans as well.

In the rat, the insula displays a **viscerotopic organization** (Cechetto and Saper, 1987), with gastric and taste-receptive neurons located in the anterior dorsal and ventral regions, and cardiac and respiratory neurons located in posterior dorsal regions. In monkeys and humans, the posterior insula also contains motor representations of the face, arm and foot (Evrard, 2018, 2019; Glasser et al., 2016) (Figure 10).

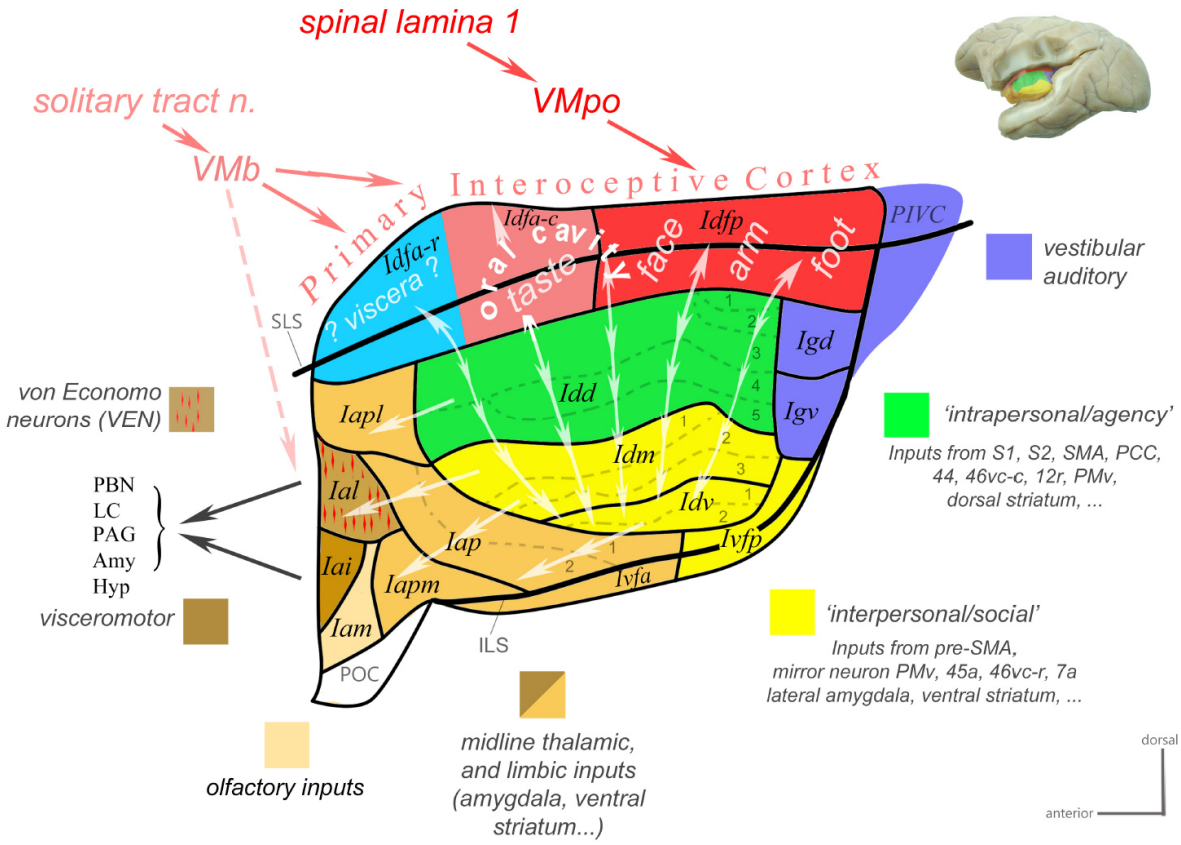

***Figure 10**: Map of the insula in macaque monkeys (Evrard, 2019). Color-coded flat map of the insula showing its possible functional organization. Vagal and spinal afferents from the nucleus of the solitary tract reach the insula via the ventromedial nucleus of the thalamus (VMb and VMpo, respectively). The insula displays a somatotopic organization, from posterior (foot-to-head, red) to mid (orofacial cavity, pink) to anterior (viscera, blue).*

The insula controls visceral activity through direct and indirect pathways, via connections to the parabrachial nucleus and periaqueductal gray (Evrard, 2019) as well as to the amygdala and cingulate cortex (Deen et al., 2011; Dum et al., 2016). A recent study injected a rabies virus into the rat stomach to identify cortical areas that influence parasympathetic and sympathetic control of the stomach (Levinthal and Strick, 2020). They found that parasympathetically activated neurons project from the rostral insula and medial prefrontal cortex to the stomach via a multisynaptic pathway, while sympathetic output to the stomach originated from a different network involving somatosensory and motor regions. The authors suggested that different aspects of regulation of stomach activity might be based on different cortical networks, with the insula being linked to interception and emotion, and the other network more involved in motor control. However, the precise role for the insula in gastric motility still needs to be established. Evidence for the role in motility in humans is provided by the finding that

stimulation of the insula generates both gastric sensations and motility changes (Penfield and Faulk, 1955).

The insula is hypothesized to be involved in a wide array of processes linked to interoception, emotional embodiment and subjective feeling states (Craig, 2002). As a major hub for visceral signals, it also participates in gustation, regulation of food intake and pain processing. Also since it contains a viscerotopic map, it has even been presented as "the" primary visceral cortex (Saper, 2002), although whether it represents the main entry point of visceral signals or only one of several is a matter of debate (Azzalini et al., 2019). However, it is not a pure visceral center, but many different cognitive, affective and regulatory functions converge in the insula (Chang et al., 2013; Nomi et al., 2018). It is also viewed as playing an important role in processing of salient stimuli, forming a "saliency network" with anterior cingulate cortex (Menon and Uddin, 2010). The insula has been divided into several subregions based on functional and cytoarchitectonic considerations, although precise divisions vary. For example (Deen et al., 2011), the mid-posterior insula, which is connected with primary and secondary somatomotor cortices, has been linked to sensorimotor processing, while the dorsal anterior insula, connected with frontal, anterior cingulate cortex and parietal regions, is involved in cognitive control. The ventral anterior insula is connected to limbic regions and mainly involved in affective processes, reward and saliency. It is unclear how these subdivisions relate to the function of the insula in visceral monitoring. In primates, visceral representations have been suspected to be located more in the anterior portion of the insula (Evrard, 2019, Figure 10). In humans, gastric and cardiac responses to disgust are linked to activations of the anterior insula (Harrison et al., 2010), and the right anterior insula is activated during gastric distension (Mayer et al., 2009). The anterior insula has also been prominently linked to *conscious* interoceptive awareness of visceral signals (Berntson and Khalsa, 2021; Critchley et al., 2004). Indeed, it is one of the few regions that co-varies with subjective reports. However, the anterior insula is activated by many different functions, and in particular these activations might be accounted for by the role of the anterior insula in saliency detection, which might actually be closely intertwined with its visceral role (Azzalini et al., 2019).

In sum, even though the insula seems to have an important role in the representation and control of visceral activity, many open questions remain. For example, the precise anatomical pathways for gastric-insula projections in humans remain to be determined. Moreover, it is unclear how the role of the insula in viscerosensation is integrated with other insular functions such as saliency, or how it relates to other cortical regions receiving gastric input.

2.6.2.Somatosensory cortex

The somatosensory cortices are involved in processing of somatic sensation, such as touch, proprioception, nociception, and temperature. They consist of the primary (SI) and secondary (SII) somatosensory cortex, located in the postcentral gyrus and parietal operculum respectively. As famously

observed by Penfield, SI represents different body parts (trunk, leg, arms, feet, …) in a homunculus-like manner, with different body districts being mapped in different regions of the cortex (Penfield and Boldrey, 1937).

The somatosensory and motor cortices receive input from the ventroposterior medial and ventroposterior lateral nucleus of the thalamus. Compared to somatic information, the visceral representations in the somatosensory cortex have received little attention. Studies in the 50's showed that SI and SII respond to spinal nerve stimulation in dogs, cats and rabbits (Amassian, 1951; Downman, 1951). Likewise, vagal stimulation has been found to elicit responses in SI in cats and rats, probably reflecting a mixture between somatic and visceral afferents (Ito, 2002; Ito and Craig, 2003). It has recently been demonstrated that SI and the motor cortex in rats possess a kidney representation in the trunk/feet area (Levinthal and Strick, 2012).

Recently, a study by Cao et al., 2019 stimulated the stomach specifically to investigate which cortical areas respond to gastric stimulation. They applied stimulation on the forestomach in rats (Figure 11A) in alternating periods of 30 seconds stimulation vs. rest. During stimulation periods, stimulation was delivered in ON/OFF patterns with a frequency of 0.2, 0.4 or 0.8 Hz. Simultaneously, they acquired single-echo and multi-echo fMRI which enabled them to detect fMRI activity at higher frequency beyond 0.2 Hz. They then applied independent component analysis to identify spatially independent functional networks where the temporal fluctuation of each network followed a response pattern at the same frequency as the gastric stimulation. As a result, the somatosensory cortex was robustly activated by stimulations at all three frequencies (Figure 11B). They went on to record local field potentials from the primary somatosensory cortex in five animals while applying the same gastric stimuli. Periodically modulated gastric stimuli induced periodically occurring transient neural responses in primary somatosensory cortex (Figure 11C).

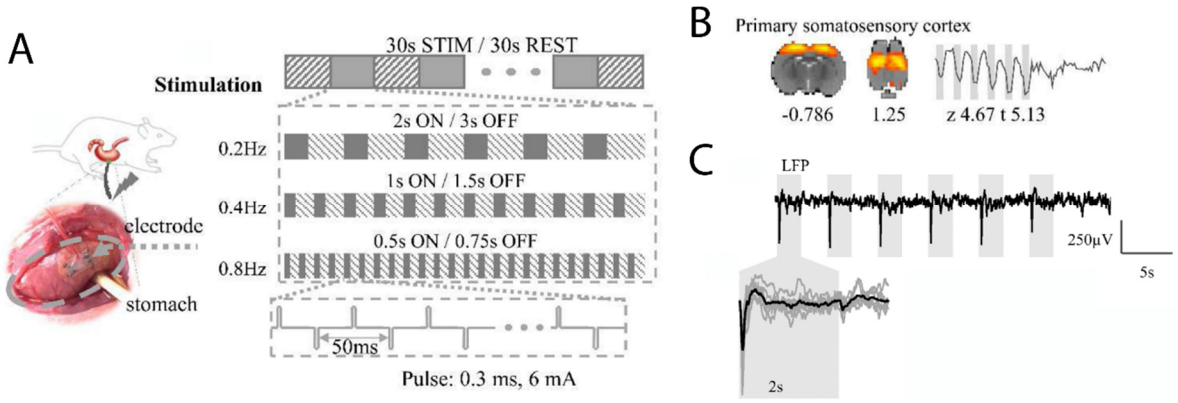

Figure 11*: Primary somatosensory cortex responds to gastric stimulation in rats (Cao et al., 2019).* ***A****: The authors stimulated the rat forestomach in alternating periods of 30 second stimulus vs. rest. Within stimulus periods, pulsed stimulation was applied in an ON/OFF sequence following a 0.2, 0.4 or 0.8 frequency.* ***B****: Average independent component time series for the primary somatosensory cortex and*

corresponding topography, for the example of a 0.2 Hz stimulation. fMRI BOLD responses were modulated by the frequency-specific gastric stimulation. ***C****: Local field potential responses at the somatosensory cortex site representing the forelimb. Gray backgrounds indicate the period of the stimulus ON period. The periodically modulated gastric stimuli induced periodically occurring transient neural responses in S1. The inset shows the evoked local field potential response during a single ON period, with gray curves representing the response for individual animals and the dark curve the grand average.*

It is highly likely that the somatosensory cortex receives intestinal inputs also in humans. For example, SI and SII are also among the regions responding to gastric distension in humans (Geeraerts et al., 2011; Van Oudenhove et al., 2008). The somatosensory cortex also shows heartbeat-evoked responses, suggesting a representation also for the heart (Azzalini et al., 2019; Kern et al., 2013).

Concerning descending influences, the recent study by Levinthal and Strick, 2020, using virus tracing in rat models, for the first time provided direct evidence that the primary somatosensory cortex, together with primary and secondary motor cortex, exerts descending control over sympathetic output to the stomach (Figure 12). Moreover, primary somatosensory cortex (as well as primary motor cortex) was found to contain a viscerotopic map of a stomach and kidney representation, embedded within the somatopic organization.

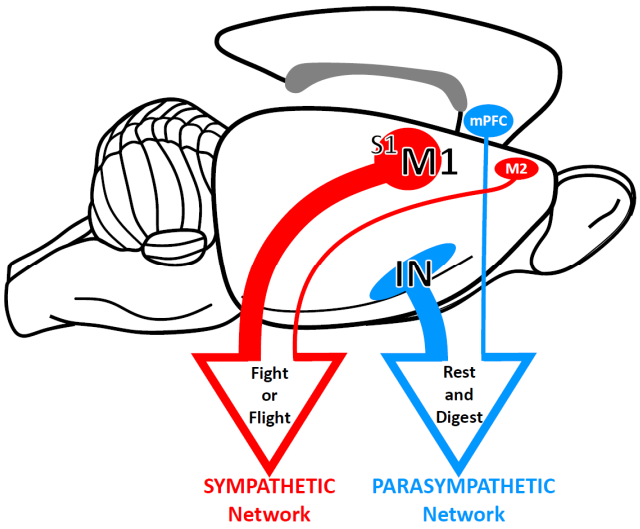

Figure 12*: Cortical regions for autonomic control of the stomach. Primary somatosensory cortex (S1), together with the primary (M1) and secondary motor cortex (M2) influence sympathetic (red) output to the stomach, while insula (IN) and medial prefrontal cortex (mPFC) influence parasympathetic control. From Levinthal and Strick, 2020.*

2.6.3. Cingulate motor regions

The cingulate motor regions reside within the cingulate sulcus in the medial wall. The cingulate cortex receives spinothalamic input in monkeys as has been suggested by anatomical tracing studies (Dum et al., 2009), and it also responds to gastric stimulation in rats (Cao et al., 2019).

First described in monkeys, the cingulate motor regions are involved in movement selection, preparation and execution (Dum and Strick, 1991; Hutchins et al., 1988). Recently, by asking human participants to move different body parts (eyes, tongue, hands and feets) during an fMRI scan, it has been demonstrated that they contain body maps representing different body parts (Amiez and Petrides, 2014). The cingulate motor regions receive input from limbic structures and the medial prefrontal cortex that represent motivation and internal state (Bates and Goldman-Rakic, 1993), and in turn project to SI and SII, other motor structures and the spinal cord (Dum and Strick, 1991; Morecraft and Van Hoesen, 1992). Additionally, together with other cortical motor structures, they influence the sympathetic adrenal medulla (Dum et al., 2016), a pair of glands located superior to the kidneys which has an important role in "fight or flight" or stress responses by releasing different products such as adrenaline or noradrenaline into the blood stream. The cingulate motor areas in the monkey project directly to the primary motor cortex, which influences sympathetic control over the stomach (Levinthal and Strick, 2020, Figure 12). It is still unresolved whether the cingulate motor regions contain a viscerotopic map, or how the representation of visceral signals relates to the organization into body maps.

2.6.4.Anterior cingulate and ventromedial prefrontal cortex

Two further cortical structures that receive visceral afferents and represent important control centers of autonomic function are the anterior cingulate cortex (ACC) and ventromedial prefrontal cortex (vmPFC).

The cingulate cortex is located in the medial wall of the cerebral hemispheres. The ACC receives input from the parabrachial nucleus stemming from the NTS and spinal cord, and in turn projects to visceral autonomic nuclei including the intermediolateral cell column and lateral hypothalamus (Vogt and Derbyshire, 2009). While the ACC is known to play a role in cardiac regulation, little is known whether and how it is related to control of gastric functioning. The ACC is among the regions activated by gastric distension in humans (Ladabaum et al., 2001). The vmPFC receives visceral information from the NTS-parabrachial pathway, hypothalamus and amygdala. It is an important center where input from different modalities (olfactory, guastatory/visceral, visual and somatic) are represented together, most likely with a role for feeding (Price, 1999). Like for the ACC, little is known how it processes specifically gastric information. van Oudenhove et al., 2009, reported vmPFC to be deactivated by gastric distension.

Apart from their role in autonomic control, ACC and vmPFC are both involved in affective processing. ACC has been linked to interoceptive visceral awareness, which is thought to underlie subjective experience of feelings (Critchley et al., 2004; Pollatos et al., 2007). vmPFC has been linked to emotions, decision-making and self-referential processes (Fossati et al., 2003; Paulus and Frank, 2003). It also forms part of a set of brain regions called the default mode network (see later section), which is involved in different functions related to the self (Qin and Northoff, 2011). Intriguing

interactions between the vmPFC's visceral and self-referential roles have been demonstrated in the group, with vmPFC responses to heartbeats predicting visual detection (Park et al., 2014), the self-relatedness of spontaneous thoughts (Babo-Rebelo et al., 2016a, 2016b) and preference-based decision making (Azzalini et al., 2020).

2.6.5. Occipital cortex

Given the massive input from the parabrachial nucleus reaching the lateral geniculate nucleus, the main thalamic relay station in the visual pathway (Erişir et al., 1997a, 1997b), it is tempting to speculate that visceral signals reach the visual cortex. Indeed, several results support to this possibility. For example, in cats, neurons in visual cortices are modulated by the rhythm of the small intestine during non-REM sleep (Pigarev et al., 2013). More recently, it has been demonstrated that the occipital cortex responds to stomach stimulation in rats (Cao et al., 2019, Figure 13A). The authors suggest two possible interpretations for the occipital activations. First, they might be linked to foraging or eating behaviors that involve multiple sensory modalities. Second, they might be driven by changes in cortical arousal, which might be based on the vagal and spinal afferents to the raphe nuclei and locus coeruleus complex.

In humans, the occipital area is also among the most reported regions activated by **gastric distension**. For instance, Ladabaum et al., 2001, found that distal stomach distension at high and painful stimulation intensities activates occipital cortex (Figure 13B), while Lu et al., 2004 applied gastric fundus distension and found that regions of the occipital cortex were activated at both non-painful and painful distension intensities. In contrast, van Oudenhove et al., 2009 found that gastric fundus distension (eliciting sensations that varied from weak to marked) *de*activated occipital regions (Figure 13C). The reason for this discrepancy is unknown. It might be that the inconsistent responses (i.e., activation vs. deactivation) are due to differences in the specific portions of the stomach targeted, as well as differences in stimulation strength or experimental settings. With regards to the functional interpretation of deactivations, Oudenhove et al. suggest that deactivations of sensory regions as the occipital cortex might reflect a shift from exteroceptive to interoceptive processing, prioritizing sensations from the viscera and filtering out resources from other sensory modalities to adjust for a potential internal threat. Potentially in line with that idea, the occipital cortex also shows decreased activation when participants pay attention to their heartbeats (Critchley et al., 2004).

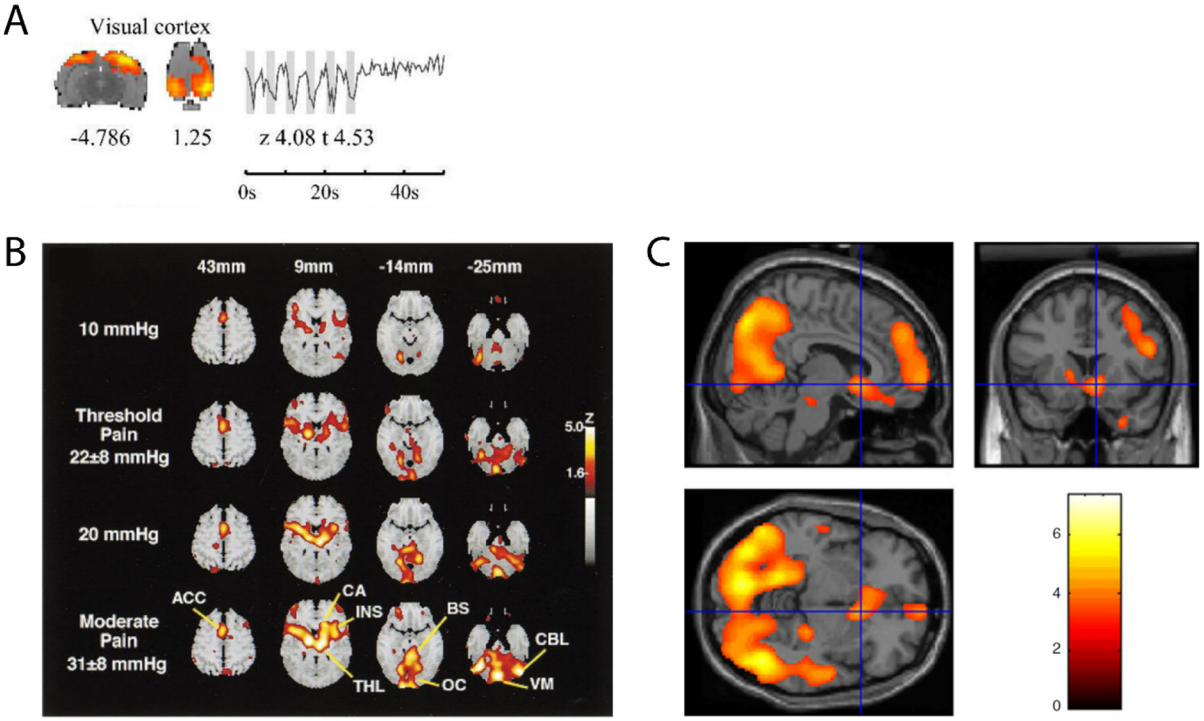

Figure 13*: The occipital cortex responds to stomach stimulation in rats and in humans.* ***A****: In the study of Cao et al., 2019 (cf. Figure 11), the visual cortex in rats is among the regions where BOLD responses are modulated by gastric stimulation (here at a frequency of 0.2 Hz).* ***B****: Ladabaum et al., 2001, applied distension of the distal stomach in humans, varying stomach distension from low (10 mmHg, top row) to higher, painful intensities (lower rows). At the higher distension activities, the occipital cortex was among the regions with significant activation.* ***C****: Regions with significant deactivations during (painful) gastric fundus distension in the study of Oudenhove et al., 2009.*

A recent study tried to identify neural responses to gastric sensations by applying a non-painful and minimally invasive form of gastric stimulation in humans (Mayeli et al., 2021). Participants swallowed a small vibrating capsule and were asked to attend to their stomach sensations while a sequence of stimulations was delivered. Vibrating stimulations induced evoked responses in midline parieto-occipital electrodes around 300-600 ms following vibration of the capsule. Although the authors did not identify the cerebral sources of this "gastric evoked potential", this study further supports the hypothesis that gastric sensation might be processed in posterior brain structures including occipital cortex. Recently, coupling was identified in humans between gastric phase and BOLD fluctuations or MEG power in the alpha band (Rebollo et al., 2018; Richter et al., 2017), which will be detailed in section 3.

In sum, even though direct anatomical evidence in humans is so far missing, there are multiple lines of evidence that support the surprising possibility that the occipital cortex receives

gastric input. Based on the parabrachial projection to neuromodulatory systems, one could speculate that the occipital activations reflect changes in arousal. This raises the compelling question why visual regions respond to gastric input. Could it be that visceral signals have an influence on processing of visual information?

2.7. Conclusion

In summary, despite the many unknowns, anatomy suggests that visceral signals reach a broad network of subcortical and cortical regions over multiple pathways. Some regions contain body maps, and for some of those (insula, somatosensory cortex) it is known that also internal organs are represented in a viscerotopic manner. The target areas support a variety of different functions including homeostasis, feeding behavior, affective behavior, control of gastric motility and conscious visceral interoception, and first studies provide evidence that gastric signals can have a role for non-food related cognition such as motivation, reward, decision making and memory (Han et al., 2018; Suarez et al., 2018). In addition, gastric signals might reach neuromodulatory centers that regulate many functions such as cortical and behavioral arousal. **Moreover, the surprising projections to the occipital cortex also raise the possibility that visceral input interacts with processing of sensory input from other modalities.**

So far, the many gaps in our understanding of the nature and roles of visceral input reaching the brain raises numerous questions: For example, how does the constant stream of gastrointestinal inputs to the brain interact with spontaneous brain activity? How can one probe non-invasively which regions interact with the gastric rhythm in humans? What is the functional role of the gastric input potentially reaching non-food related regions such as the occipital cortex?

3. The gastric rhythm constrains spontaneous brain dynamics in humans

Direct evidence for gastric input reaching the brain is so far scarce in humans. Studies have shown that numerous cortical areas respond to gastric distension, but these suffer from the limitation that gastric distension represents an artificial manipulation that is stressful and often painful for the participant. Moreover, it does not respond to the question how the gastric activity fluctuations interact with the dynamics of *resting* brain activity, in contrast to activity evoked by phasic stimulation. In this chapter, I will show that gastric activity acts as a pacemaker that shapes the organization of spontaneous cortical activity in humans.

Evidence that spontaneous brain activity is linked to intestinal signals comes from the study of Hashimoto et al., 2015. They simultaneously recorded fMRI and the electrical rhythm of the intestine in 18 fasted subjects during rest, using a technique called "electrointestinography", which is analogous to the electrogastrogram but covering lower locations. They correlated power fluctuations between intestinal signals (0.14-0.21 Hz) and the BOLD signal and found significant correlations in the right dorsal anterior insula, right middle insula and cerebellum. They also found correlations in a lower frequency band (0.008-0.05 Hz) which might include some signals from the stomach, but did not properly investigate the stomach-specific frequency band.

The first study to investigate coupling between spontaneous cortical activity and the stomach in humans was carried out in the team of Catherine Tallon-Baudry (Richter et al., 2017). An important organizing principle in the brain is phase-amplitude coupling, where the power of a faster oscillation varies with the phase of the slower oscillation (Figure 14). Here, they asked if this principle also exists across different bodily organs, i.e. whether the phase of the gastric rhythm influences the power of spontaneous cortical oscillations.

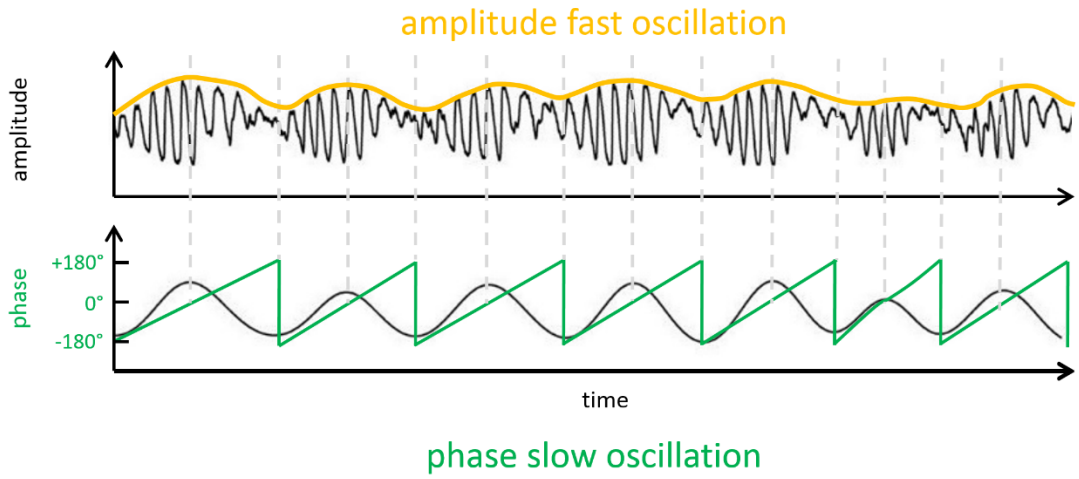

***Figure 14**: **Phase-amplitude-coupling**. Top row: A fast oscillation that varies in its amplitude (yellow line) over time. Bottom row: A slower oscillation, with its instantaneous phase in degrees, represented*

by the green line. The amplitude of the faster oscillation is higher at certain phases of the slower oscillation (in this case at 0°).

For this, they acquired simultaneous MEG and electrogastrogram recordings in seventeen healthy human participants at rest with eyes open. They applied a metric called Modulation Index (MI) to quantify the dependency of brain oscillatory power on gastric phase and compared obtained MI values with estimated chance level using a cluster-based procedure. Significant gastric-brain coupling in the alpha range at 10 and 11 Hz was observed in two bilateral parieto-occipital clusters with an extension over right fronto-temporal sensors (Figure 15A). In the significant clusters, gastric phase accounted for 8% of the variance of alpha amplitude. The modulation of alpha power by EGG phase came in different profiles between participants (Figure 15B), involving 1:1 but also higher coupling modes.

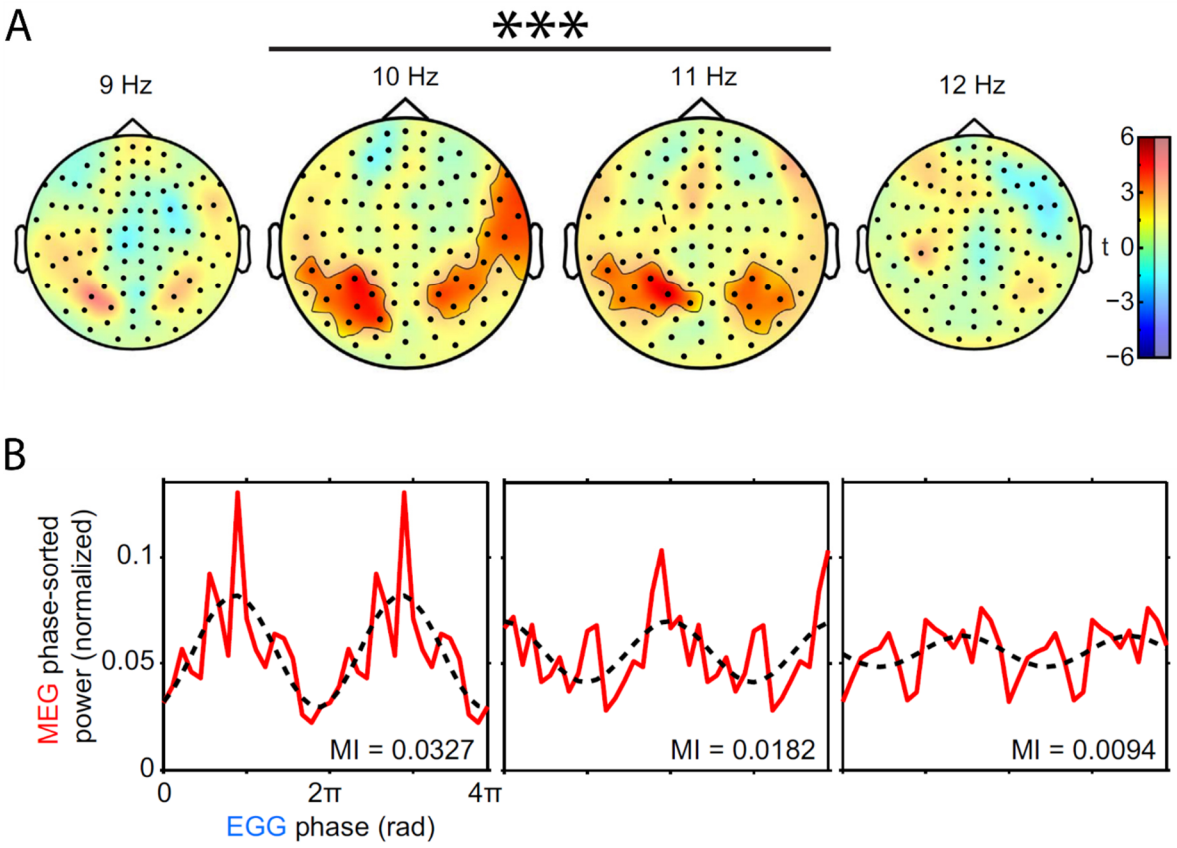

Figure 15*: The gastric slow wave is coupled with brain alpha oscillations.* ***A****: Statistical maps of gastric-alpha coupling at the MEG scalp level. Significant coupling occurred at 10 and 11 Hz, in the two clusters indicated by black outlines and saturated colors.* ***B****: Examples for profiles of phase-amplitude coupling, in the participant with the largest (left), median (middle) and the smallest (right) MI. The dashed black line is a cosine fit that emphasizes the coupling pattern between alpha power and gastric phase. Richter et al., 2017.*

The sources of these cluster were localized in the parieto-occipital sulcus and calcarine fissure, as well as in the right anterior insula (Figure 16A, B). By using transfer entropy, a measure of directionality of information transfer, they went on to show that this effect goes predominantly from the stomach to the brain (Figure 16C). **In sum, this study was the first to show that the slow rhythm of the stomach acts as an external pacemaker that influences the temporal structure of spontaneous brain dynamics. While these results seem intriguing, it is so far the only study investigating coupling between the stomach and brain oscillations, with data acquired during the resting state, leaving it open whether this coupling is specific to the resting state or also exists during active task performance. One aim for my thesis was to replicate the gastric-alpha coupling in an independent study, in both resting state and task recordings.**

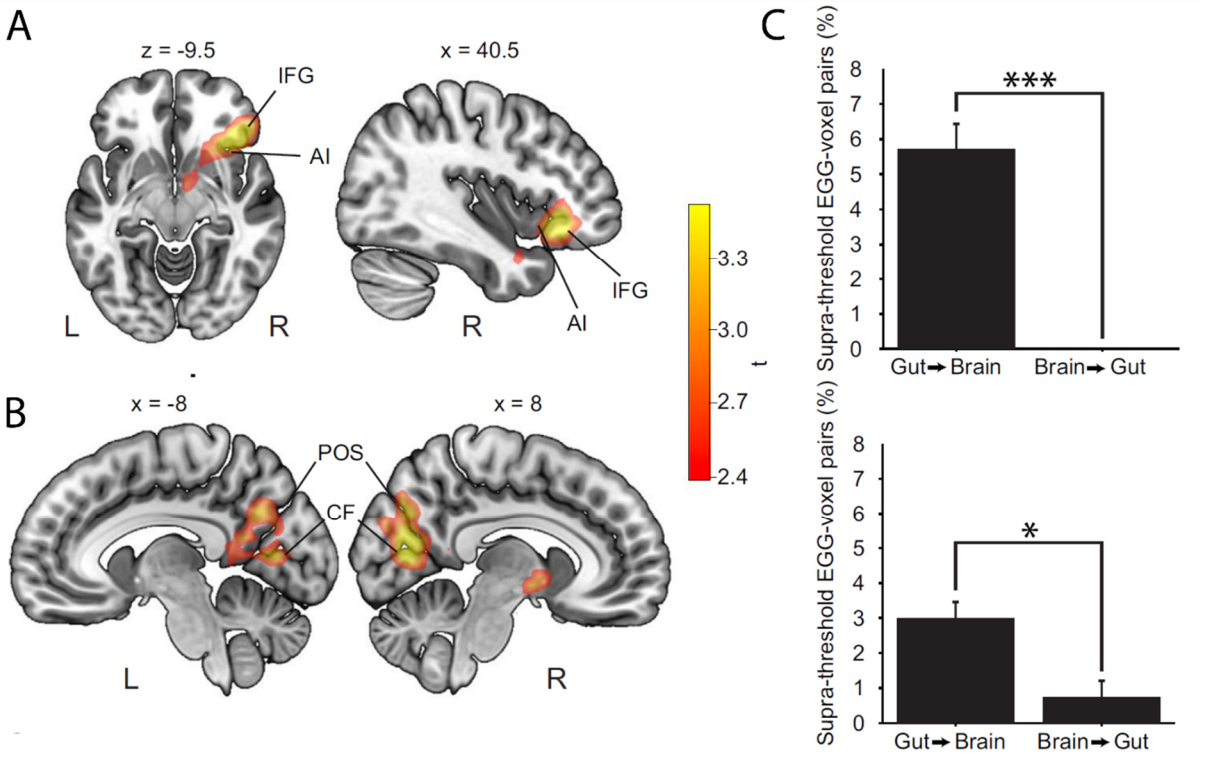

Figure 16*: Source localization and directionality of gastric-alpha coupling.* ***A****: An anterior cluster was centered on the right anterior insula (AI) and inferior frontal gyrus (IFG).* ***B****: A posterior cluster consist of the parieto-occipital sulcus (POS) and calcarine fissure (CF) bilaterally.* ***C****: Tranfer entropy of phase-amplitude coupling in the anterior (top) and posterior (bottom) cluster. The interaction between stomach brain is greater in the stomach-to-brain direction for both clusters. Richter et al., 2017.*

Next, an experiment carried out by my former colleague, Ignacio Rebollo, revealed that spontaneous BOLD activity in a network of brain regions is phase-synchronized to the gastric rhythm (Rebollo et al., 2018). They simultaneously recorded fMRI and EGG in 30 human participants at rest with eyes open. They then quantified the degree of phase synchrony between the EGG signal and BOLD time series filtered around gastric frequency. Regions with significant phase synchrony comprised the right primary somatosensory cortex, bilateral secondary somatosensory cortices, medial wall motor regions, extrastriate body area, posterior cingulate sulcus, dorsal precuneus, occipital cortex, retrosplenial cortex and superior parieto-occipital sulcus (Figure 17A). Further analyses revealed that different nodes of the gastric network were coupled to gastric phase with different phase delays of several seconds, indicating a precise temporal sequence of activations within each gastric cycle, which explains why this network could not previously be detected with standard correlation methods with instantaneous connectivity. There was no significant link with gender, body mass index or trait anxiety scores.

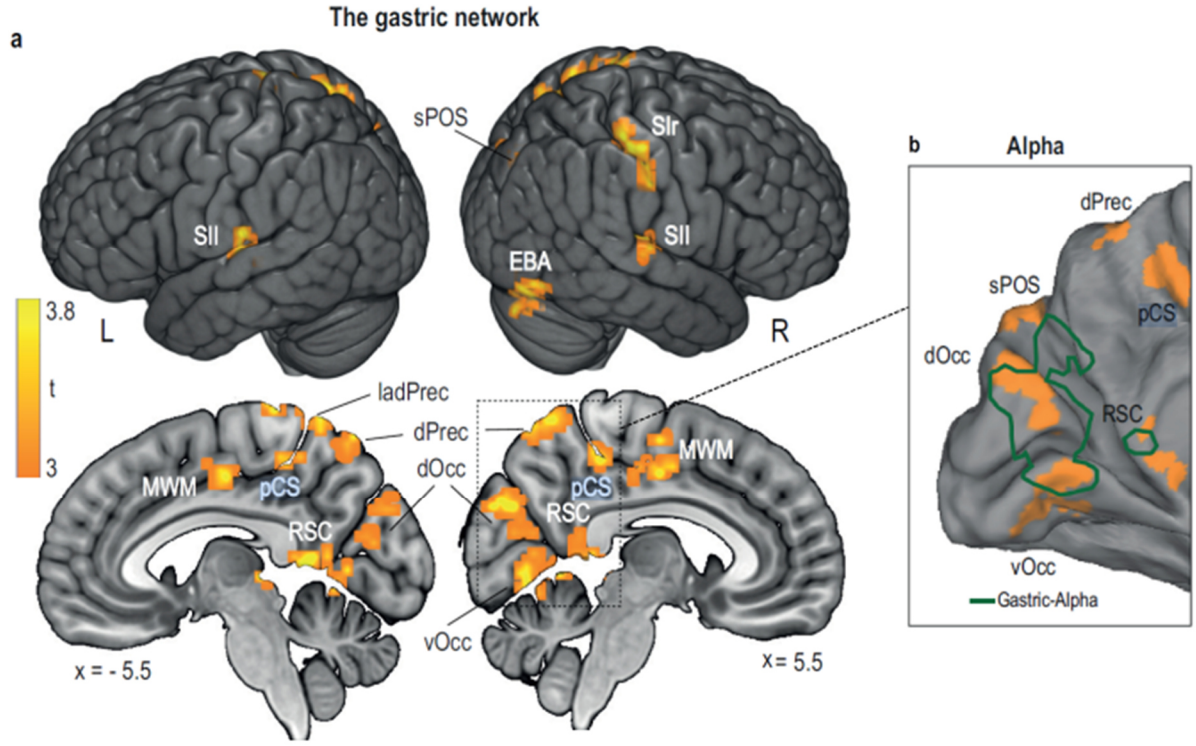

Figure 17: The gastric network identified by Rebollo et al., 2018. ***A****: Regions significantly phase synchronized to the gastric rhythm comprise right primary somatosensory cortex (SIr), bilateral secondary somatosensory cortex (SII), superior parieto-occipital sulcus (sPOS), extrastriate body area (EBA), medial wall motor regions (MWM), posterior cingulate sulcus (pCS), dorsal precuneus (dPrec), retrosplenial cortex (RSC), dorsal (dOCC) and ventral occipital cortex (vOcc).* ***B****: Gastric-BOLD coupling regions (orange) overlap with the cluster of gastric-alpha coupling found in Richter et al. (green outline).*

Functionally, the gastric network included regions containing body maps as well as regions playing a role in mapping the external space in bodily coordinates. However, coupling was also present in the parietal-occipital sulcus, where Richter et al., 2017 had found significant coupling with the MEG alpha rhythm (Figure 17B) and which is assumed to be the generator of the alpha rhythm. The gastric network also partially overlapped with autonomic networks. For example, 30% of the network was related to heart rate variability in high and low frequencies, which represent parasympathetic and a mixture of sympathetic and parasympathetic outputs, respectively. Further, 17% of the gastric network overlapped with regions correlating with pupil diameter. In sum, this study demonstrated that the synchronization of the gastric rhythm with the brain at rest forms a coherent network with delayed connectivity.

More recently, a study was undertaken in an independent group where concurrent resting state fMRI and EGG were acquired in a single participant in twenty-two sessions of 15 minutes over a span of seven weeks (Choe et al., 2021). The authors identified canonical resting state networks (RSNs) and computed phase locking between each RSN and gastric phase. They found that a cerebellar network, a dorsal somatosensory-motor network and the default mode network were significantly phase-locked with the gastric rhythm. The dorsal somatosensory-motor network included the primary somatosensory cortex and medial wall motor regions, two of the nodes reported by Rebollo et al., while the default mode network was centered on the precuneus, which was also a node of the gastric network reported by Rebollo et al. This study demonstrated the reproducibility of gastric brain-coupling within a single participant.

To conclude, these studies show that the gastric rhythm indeed constrains spontaneous fluctuations of brain activity, including in occipital regions, confirming studies using gastric distension or stimulation. This opens another question: What is the functional role of this coupling between the gastric rhythm and resting cortical activity?

4. The functional role of spontaneous brain fluctuations

In the previous chapter, I explained how the gastric rhythm modulates spontaneous fluctuations in brain activity, specifically the amplitude of occipital alpha oscillations. One of the central aims of my thesis is to investigate the potential functional consequences of this stomach-brain coupling. In the following, I will thus review the role of spontaneous brain activity, with a particular focus on alpha oscillations. We will see that behavioral performance in psychophysical tasks fluctuates on temporal time scales consistent with variability in endogenous brain activity. This makes slow fluctuations in performance an interesting candidate for a potential link with the gastric rhythm.

4.1. Spontaneous brain activity – more than noise

Spontaneous brain activity, or also called "ongoing", "endogenous" or "resting", is the neuronal activity generated in the absence of any external stimulation (Chaumon and Busch, 2014). It has long been treated as "noise" or baseline of brain activity (Anderson et al., 2000), against which task-related changes were contrasted, and interpreted as "activation" or "deactivation" (Laufs et al., 2003a). Brain energy consumption is huge, accounting for around 20% of the total body's energy expenditure. Spontaneous brain activity uses most of this energy, while task-related activity requires an additional energy of only 5% (Fox and Raichle, 2007; Raichle, 2009; Raichle et al., 2001). Fluctuations of brain activity have been observed in a wide range of temporal and spatial scales and methods, ranging from single neuron firing rate (Noda and Adey, 1970; Softky and Koch, 1993) or membrane potentials (Holcman and Tsodyks, 2006), through voltage sensitive dye imaging (Kenet et al., 2003) to electroencephalographic (EEG) recordings (Palva and Palva, 2012) and slow fluctuations in hemodynamic signals as measured by fMRI (Fox and Raichle, 2007). Spontaneous activity is indeed not random but highly structured. For example, spontaneous population activity in the primary visual cortex is organized in temporal-spatial patterns that resemble the orientation maps evoked during processing of sensory features (Arieli et al., 1996; Kenet et al., 2003). It thus seems that spontaneous cortical activity replays processes which are evoked during sensory input. It has been suggested that this replay represents an "internal memory of external causal dynamics" (Sadaghiani and Kleinschmidt, 2013) or statistically optimal representations of the environment (Berkes et al., 2011).

4.2. The spatial structure of spontaneous brain activity

An example for the functional consequences of spontaneous brain activity at a larger temporal-spatial scale comes from the study of Biswal et al., 1995. Using functional magnetic resonance imaging (fMRI), the authors identified regions that were activated during a finger-tapping task in humans. They then identified the voxels whose blood-oxygenation-level-dependent (BOLD) time series correlated with the seed region of the finger representation. Strikingly, they observed that the regions active during the motor task exhibited coherent fluctuations in spontaneous BOLD signals, forming a coherent network during rest. This was what would later be labeled the "somato-motor network". This landmark discovery paved the way for many subsequent studies of resting state fMRI that identified further

networks showing correlations of spontaneous activity, which are called “resting state networks” (for review, see Beckmann et al., 2005; Fox and Raichle, 2007).

Two widely distributed networks have been identified this way (Fox et al., 2005): The **default mode network** (DMN) and the task positive network. The DMN corresponds to set of brain regions that become deactivated during stimulation or goal-directed behavior, while showing elevated blood flow during rest (Greicius et al., 2003; Raichle et al., 2001; Shulman et al., 1997). It consists of a set of regions including the core ‘hubs’ posterior cingulate cortex and the temporoparietal junction. Functionally, the DMN has been associated with stimulus independent thoughts and introspective, self-referential processes (McGuire et al., 1996; Qin and Northoff, 2011). It has been especially linked with mindwandering, i.e., spontaneous thoughts not related to the current task (Christoff et al., 2009). It has also been found to be active in relation to imagining future scenarios or remembering the past (Addis et al., 2007), and when taking the perspective of others (Saxe and Kanwisher, 2003).

“Task positive network” is a collective term for regions or networks of regions that exhibit consistent activations during cognitively demanding tasks, including dorsal anterior cingulate cortex, dorsolateral and ventrolateral prefrontal cortex, intraparietal sulcus and lateral parietal cortex (Fox et al., 2005). The task positive regions have been shown to be anticorrelated to the DMN (Fox et al., 2005). They are variably divided into different subsystems, with the number of networks depending on the methods used and the definition depending on the theoretical framework of the authors. These subsystems include a cingulo-opercular network, which is involved in task set maintenance and tonic alertness (Dosenbach et al., 2006; Sadaghiani and D’Esposito, 2015), a fronto-parietal network, associated with more phasic aspects of attention (Dosenbach et al., 2007), a dorsal attention network, related to top-down orienting of attention (Fox et al., 2006), and a ventral attention network, linked with bottom-up orienting to salient stimuli (Fox et al., 2006).

In addition, several **sensory networks** have been identified, including a visual (Yeo et al., 2011) and auditory network (Cordes et al., 2000; Koyama et al., 2010).

In sum, spontaneous fluctuations in brain activity are organized in well-defined neural networks, which have functional significance (Romei et al., 2008).

4.3. Spontaneous activity in electrophysiological recordings

A lot of attention in the study of spontaneous brain activity has thus been drawn to the spatial organization of BOLD signal fluctuations into coherent networks. However, the limitation of measuring hemodynamic signals is that only permits the tracking of slow neural activity modulations, and not the neural dynamics at a faster time scale (Sadaghiani et al., 2010).

In electrophysiological recordings, spontaneous neural activity is characterized by **oscillations**, which are visible in both local field potentials measured from invasive electrodes, as well as in surface recordings (EEG, MEG) (Peelle and Davis, 2012). Oscillations reflect rhythmic changes in the degree of synchronization in a population of neurons (Varela et al., 2001), which in turn are associated with cyclical variations in neural excitability (Bartley and Bishop, 1932; Bishop, 1932; Buzsáki, 2006), in a wide range of temporal and spatial scales (Buzsáki and Draguhn, 2004). The raw EEG/MEG signal contains oscillations at many different frequencies, infraslow (< 1 Hz) rhythms coexisting with fast transient oscillations up to 500 Hz or greater, often in the same network. Frequency spectra of raw electrophysiological recordings reveal a $1/f^{\alpha}$ type power law distribution (i.e., the average power of oscillations is inversely proportional to their frequency), both in humans (Buzsáki and Draguhn, 2004; Linkenkaer-Hansen et al., 2001; Monto et al., 2008) and monkeys (Leopold et al., 2003) (Figure 18). However, also discrete peaks reflecting oscillatory activity in specific bands are visible, notably around 10 Hz (Sadaghiani et al., 2010). Oscillations are divided into canonical frequency bands, including delta (1-4 Hz), theta (4-8 Hz), alpha (8-12 Hz), beta (12-24 Hz) and gamma (24-80 Hz) (note though that the precise definition varies).

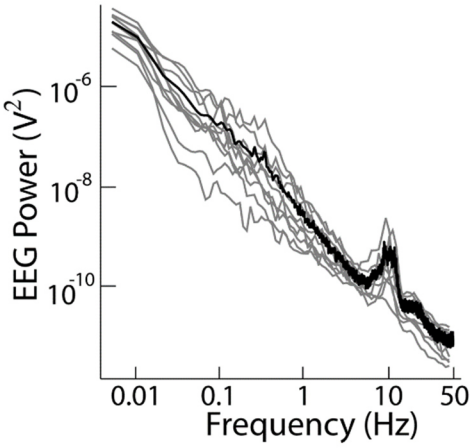

***Figure 18**: 1/f power spectrum in an electrophysiological recording. Plotted are the individual power spectra (grey) and the mean power spectrum (black) from an EEG channel in double-logarithmic coordinates. Power of oscillations is inversely proportional to their frequency. However, also a clear peak centered at 10 Hz is visible, reflecting the alpha rhythm (8-12 Hz). From Monto et al., 2008.*

Oscillations are characterized not only by their frequency, but also their phase and amplitude (Hanslmayr et al., 2011). The phase reflects the current position in the oscillatory cycle. As oscillations reflect the alternation between relatively depolarized vs. hyperpolarized states, phase has since long been assumed to index different moments of excitability (Bishop, 1932; Buzsáki and Draguhn, 2004; Klimesch et al., 2007; Lakatos et al., 2008), with the efficiency of the processing of an incoming stimulus depending on the moment of the oscillation when it arrives (Figure 19).

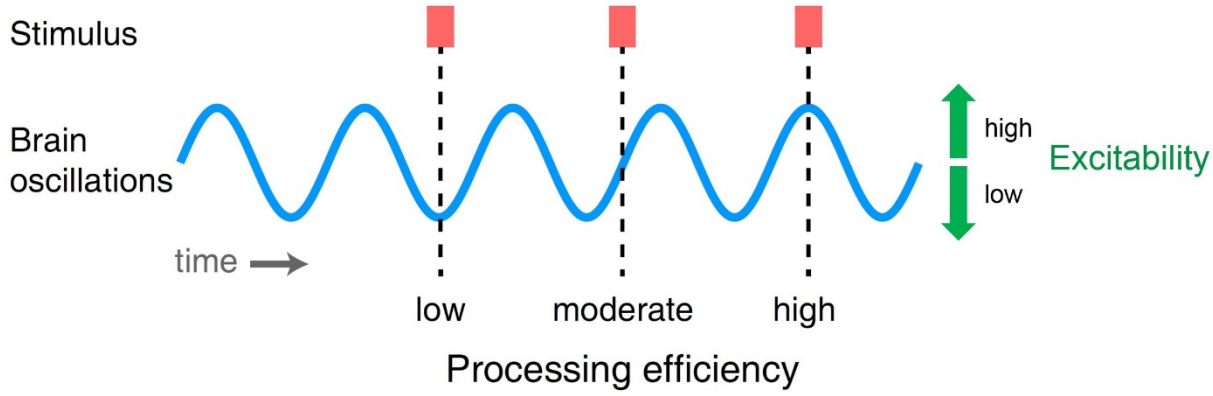

***Figure 19**: **Ongoing oscillatory activity reflects cortical excitability**. Stimuli (red squares) may arrive at different moments relative to an ongoing brain oscillation (blue). The phase (vertical dashed lines) of their arrival determines how efficiently sensory stimuli are processed. Adapted from Peelle and Davis, 2012.*

While phase reflects the temporally fine grained windows of excitability, fluctuations in amplitude, which is dependent on the total number of active neurons and the level of synchronization (Hanslmayr et al., 2011), occur on a much slower time scale. Growing evidence suggests that these slower fluctuations in amplitude may be the neurophysiological basis for the resting state networks observed in fMRI (Goldman et al., 2002; Laufs et al., 2003b, 2006; Moosmann et al., 2003).

Oscillations in different frequency bands have been linked to many perceptual and cognitive functions, a full review of which is outside the scope of this thesis (e.g., Fries, 2015; Linkenkaer-Hansen et al., 2004; Tallon-Baudry and Bertrand, 1999; Thut and Miniussi, 2009; Varela et al., 2001; Ward, 2003; Womelsdorf et al., 2006). Given that previous work from the group showed that the gastric rhythm is coupled to spontaneous alpha oscillations in the 10-11 Hz range, I will here focus on the role of the brain alpha rhythm.

4.3.1. The brain alpha rhythm

The alpha rhythm (8-12 Hz) is the dominant oscillation in the human brain. In electroencephalographic or magnetoencephalographic recordings at rest, it shows a waxing and waning in amplitude. It became was the first rhythm described in humans when Berger in the 1920s discovered it in the electroencephalographic trace (Berger, 1929). Alpha oscillations are distributed throughout the cortex (Lopes da Silva, 1991; for review see Palva and Palva, 2012), but the largest amplitude is observed in parietal-occipital areas (Johnson et al., 2010; Salmelin and Hari, 1994), with the source most likely being located in the parieto-occipital sulcus (Zhigalov and Jensen, 2020). Over the somatosensory

cortex, oscillations in the lower alpha frequency range are labeled the "mu rhythm" due to their different waveforms and functional properties (Tiihonen et al., 1989).

Functionally, the alpha rhythm is modulated by the level of attention paid to the visual environment, increasing with loss of attentional focus and being largest during eye closure (Mathewson et al., 2011). It typically decreases in sensory tasks compared to rest (Haegens et al., 2011), while increasing during internal tasks like mental arithmetic (Palva et al., 2005; Ray and Cole, 1985) or mental imagery (Cooper et al., 2003). For this reason, alpha has long been assumed to reflect **cortical idling**: EEG synchronization within the alpha band would reflect the deactivation of a cortical area which is not needed for processing sensory information or creating a motor output, and which would thus be in an idling state (Pfurtscheller et al., 1996). In this framework, alpha activity would thus index the *general* level of arousal (Mathewson et al., 2011). The idling hypothesis was challenged by studies reporting task-related increases in alpha. For example, alpha increases in retention tasks where subjects have to hold an item in mind and withhold their response until a probe is presented, and correlates positively with increasing working memory load (Busch and Herrmann, 2003; Cooper et al., 2003; Jensen et al., 2002, 2002; Schack and Klimesch, 2002). This suggests that alpha does not merely reflect an idling state but has an active role in perception and cognitive processes (Lange et al., 2014).

Several accounts proposed that increased alpha power reflects a **general inhibitory or attention mechanism** (Jensen and Mazaheri, 2010; Klimesch et al., 2007; Thut et al., 2006). Jensen and Mazaheri, 2010, in their "gating by inhibition hypothesis", suggested that alpha band oscillations reflect the routing of information from one task-relevant region to the other, while blocking information flow between regions not relevant for the task (Figure 20). Alpha power would thus modulate the excitability of task-relevant cortical regions, thereby "gating" which content reaches awareness. From this perspective, strong alpha activity during internal tasks does not reflect cortical idling but rather the active inhibition of sensory processing to avoid interference by distracting signals (Mathewson et al., 2010). Indeed, successful suppression of distractor stimuli, indexed by increased alpha power, predicts working memory performance (Sauseng et al., 2009). Alpha amplitude is also modulated by attention in a spatially selective way: In spatial cueing paradigms, alpha power typically decreases in the occipital cortex contralateral to the attended location while decreasing in the ipsilateral site processing the unattended location (Rihs et al., 2007; Worden et al., 2000), with the strength of this asymmetrical modulation being linked to performance (Kelly et al., 2009). Similarly, when a cue indicates whether an upcoming stimulus will be presented in the visual or auditory modality, alpha activity decreases in the region relevant for the modality-specific stimulus while increasing in the other (Mazaheri et al., 2014). From the view of the inhibition hypothesis, this attentional mechanism is seen as a suppression of task-irrelevant regions and de-inhibition of task-relevant areas (Klimesch et al., 2007; Palva and Palva, 2007).

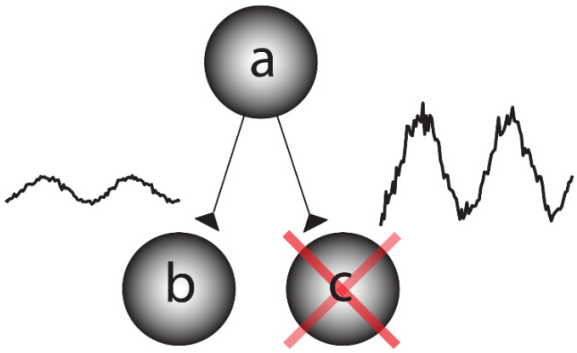

***Figure 20**: The gating by inhibition hypothesis. In this situation, information is supposed to be sent from node **a** to node **b** but not from node **a** to node **c**. According to the principle of gating by inhibition, node **c** is actively suppressed, reflected by large oscillations in the alpha band. This gates the information flow from **a** to **b** while functionally inhibiting node c. From Jensen and Mazaheri, 2010.*

Alpha amplitude does not only change during experimental manipulation like the direction of attentional focus, but also **fluctuates spontaneously** (Pfurtscheller, 1976). Indeed, the attentional modulation of alpha power is small compared to the spontaneous variations in alpha power (around 10% of baseline level – Palva and Palva, 2007). Moreover, Linkenkaer-Hansen et al., 2001, analyzing EEG and MEG recordings at rest, observed that the alpha amplitude envelope showed significant autocorrelations in multiple time scales up to more than 100 seconds.

The sources of these spontaneous fluctuations in alpha amplitude are not clear yet. One argument that has been proposed is that they arise from fundamental mechanisms intrinsic to the brain. For example, the scale-free dynamics have been argued to arise form self-organized neural network dynamics (Linkenkaer-Hansen et al., 2001). Spontaneous alpha amplitude changes might also be attributed to occasional drowsiness or levels of (in)attention (Romei et al., 2008). **However, as supported by Richter et al., 2017, and as an important idea for my thesis, the slow fluctuations of alpha activity might be partly driven by an *external* pacemaker, the gastric rhythm.**

4.4. Spontaneous neural activity is linked to behavioral variability and arousal

In the previous sections, I reviewed the spatial and temporal structure of spontaneous fluctuations in neural activity. We saw that spontaneous neural activity is highly organized, far from being random noise. In the next sections, I am going to review how these spontaneous dynamics are linked to task performance, particularly trial-to-trial variability in perception. I will specially focus on the alpha rhythm that is coupled to the gastric rhythm, in order to explore the potential functional consequences of the coupling. I will then describe that perceptual performance exhibits dynamics which are driven by infraslow fluctuations consistent with the frequency of the gastric rhythm. Finally, I will come back to arousal, a concept mentioned in the previous sections, to argue that it might represent an intriguing link between the fluctuations in performance, the brain alpha rhythm, and gastric input.

4.4.1.Spontaneous brain activity relates to behavioral variability

A central program for neuroscientific studies is to explain **perceptual variability**, which pertains to fluctuations in behavioral responses across repeated presentations of the same stimulus (Wyart and Tallon-Baudry, 2009). For example, in vision research, when an identical near-threshold stimulus is presented to a subject, it is sometimes perceived and sometimes not. Why is it that the percept changes despite identical physical input? To answer this question, studies classically focused on stimulus processing itself, i.e., by analyzing the task-evoked activity associated with detected vs. undetected targets (e.g., Cul et al., 2007; Fahrenfort et al., 2007; Sergent et al., 2005). However, there is mounting evidence that the brain's state *before* the presentation of a stimulus influences its perceptual outcome.

For example, several studies investigated the role of **ongoing hemodynamic signals in sensory regions**. Higher prestimulus BOLD activity in early visual areas (V1) predicts improved target detection (Ress et al., 2000; Schölvinck et al., 2012; Wohlschläger et al., 2016), while prestimulus BOLD activity in auditory cortex predicts auditory target detection (Sadaghiani et al., 2009). Moreover, ongoing BOLD fluctuations in motion-selective areas like MT predict motion perception (Hesselmann et al., 2008a, 2008b; Sapir et al., 2005), and fluctuations in face-selective areas during viewing of an ambiguous face/vase stimulus biases towards the face-percept (Hesselmann et al., 2008b). Additionally, perception of an upcoming stimulus has been linked to spontaneous activity in resting state networks such as the default mode and task positive network (Coste and Kleinschmidt, 2016; Hahn et al., 2007; Sadaghiani et al., 2009). There also exists a literature reporting differential activation of these networks during instable, error prone vs. stable periods of performance in prolonged tasks requiring sustained attention (Esterman et al., 2013, 2014; Fortenbaugh et al., 2018; Kucyi et al., 2017; Rosenberg et al., 2015).

Next, many studies have linked the conscious perception of subsequently presented stimuli to ongoing fluctuations in electrophysiological signals in different **frequency bands**. For example, prestimulus gamma power predicts visual awareness (Wyart and Tallon-Baudry, 2009) and response speed (Gonzalez Andino et al., 2005; Schoffelen et al., 2005; Womelsdorf et al., 2006), as well as the

percept of visual or auditory illusions (Kaiser et al., 2019; Lange et al., 2013). Furthermore, accumulated evidence suggests that the ongoing alpha rhythm has a strong influence in fluctuations of perception, which will be reviewed in the next section.

A study from the group (Park et al., 2014) showed that also spontaneous fluctuations in cortical response to visceral stimuli predicts visual detection. Using MEG, the authors found that neural responses to heartbeats before stimulus onset predicted the detection of a faint visual grating in the posterior right inferior parietal lobule and ventral anterior cingulate cortex. **This suggests that visceral input interacts with ongoing activity and affects behaviorally relevant cortical activations.**

4.4.2.Prestimulus alpha power modulates perception

Alpha oscillations dominate electrophysiological recordings, showing large endogenous fluctuations which are considered as an index of cortical excitability. This makes alpha oscillations a strong candidate for underlying fluctuations in performance. Importantly, these spontaneous fluctuations have been found to be modulated by the gastric rhythm (Richter et al., 2017), in occipital regions relevant for tasks of visual perception. To explore the potential functional consequences of the stomach-brain coupling, it is thus indispensable to review the role of alpha oscillations for perception.

In a pioneering study, Makeig and Inlow, 1993 ran an auditory detection experiment and computed the fraction of detected targets in moving time windows. They found that changes in performance were related to specific changes in the EEG power spectrum; especially, drops in hit rate were accompanied by increased in power of frequency bands in the alpha range. However, later studies showed that alpha power is not only related to performance on long time scales but also on a trial-by-trial level. Ergenoglu et al., 2004, presented participants with light pulses that were individually calibrated using a staircase procedure, such that participants would detect the stimulus in 50% of trials. They observed higher alpha power before nondetected compared to detected stimuli in parietal and occipital EEG channels. Alpha power has also been related to differences in performance between participants. Hanslmayr et al., 2005, 2007, ran visual discrimination tasks, in which subjects saw a masked target and had to respond which of the letters had been previously presented. They classified participants into “good” and “bad performers” by a median-split on the percentage of correct responses. The authors found that prestimulus alpha power was lower in good performers, while the opposite pattern was found in a memory task. Within participants, Dijk et al., 2008, found visual discrimination ability to decrease with an increase in prestimulus alpha power around the parieto-occipital sulcus. Next, Busch et al., 2009, found that prestimulus power in the wider 6-12 Hz range was lower in detected vs. undetected visual targets in the 800 ms preceding target onsets (Figure 21). Hit rate was 12% higher in the bin with lowest alpha power compared to the bin with highest alpha power. Mathewson et al., 2009, observed that prestimulus 10 Hz power at the posterior channel Pz was lower in hits than misses, reporting a 7% difference in hit rate between the bin with highest vs. lowest alpha power. This effect of

prestimulus alpha power on performance has since been frequently replicated (for a review, see Samaha et al., 2020).

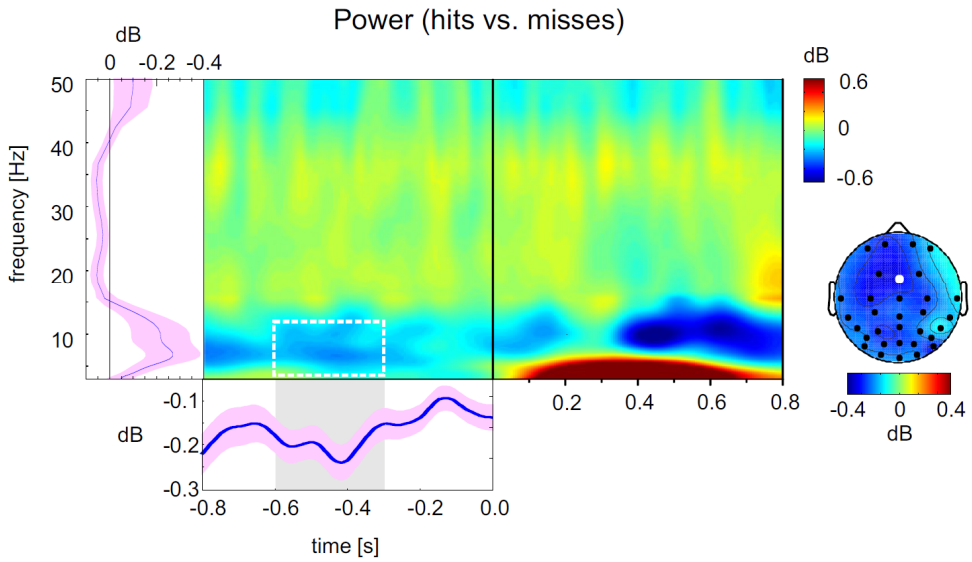

Figure 21*: Example for a study reporting a difference in prestimulus alpha power between hits and misses in a visual detection task (Busch et al., 2009). Spectral power across all EEG channels was significantly larger for misses than hits in a frequency range of 6-12 Hz in the 800 ms preceding target onsets (with the strongest effect in the -600 to -300 time window). Left inset: Mean power differences across time in the prestimulus window. Bottom inset: mean power difference in the 6-12 Hz frequency range. Topography right: distribution of 6-12 Hz power difference in the prestimulus window.*

Next, studies using transmagnetic stimulation found that stimulation specific to the alpha frequency interferes with target detection, suggesting a causal role of alpha oscillation in the forming of perceptual outcome (Dugué et al., 2011; Romei et al., 2010). Moreover, several studies showed that alpha power also predicts perceptual phenomena in the absence of veridical sensory input, including phosphenes (Dugué et al., 2011; Romei et al., 2008; Samaha et al., 2017a), tactile simultaneity (Lange et al., 2012) or double-flash illusions (Lange et al., 2013).

While many studies have replicated the negative link between prestimulus alpha power and visual detection, numerous studies also reported nonlinear, opposite, or even no relationships between alpha power and perception. For example, several studies found a U-shaped relationship between alpha power and detection of somatosensory stimuli (Ai and Ro, 2013; Zhang and Ding, 2010). Linkenkaer-Hansen et al., 2004 found that mu power over sensorimotor regions showed an inverted U-relationship with detection of tactile stimuli, while alpha power in parietal regions correlated positively with hit rate. Similarly, Babiloni et al., 2006, reported that prestimulus alpha power in the lower band (6-10 Hz) in frontal, parietal and occipital areas was stronger for seen than not seen masked visual stimuli. In contrast, prestimulus alpha power in the 10-12 Hz band did not differ for seen vs. unseen stimuli. Next, while

Hanslmayr et al., 2007 found that prestimulus alpha power different between "good vs. bad" perceivers, prestimulus alpha power did not predict hit rate *within* participants. Wyart and Tallon-Baudry, 2008 and Harris et al., 2018 found that alpha power contralateral to the validly cued location did not predict the perception of an upcoming visual stimulus. Also, in Park et al., 2014, prestimulus 8-12 Hz alpha power did not predict detection of a near-threshold visual stimulus. Whether those incongruent results can be explained by differences in the paradigms used, different analysis strategies or frequency ranges analyzed is an open question.

Furthermore, in recent years, numerous authors have proposed to refine the functional interpretation of alpha power. Numerous studies found that that alpha, instead of improving objective performance such as detection sensitivity or discrimination accuracy *per se*, decreased response criterion (Benwell et al., 2017, 2021; Iemi et al., 2017; Limbach and Corballis, 2016; Samaha et al., 2017b). For example, lower prestimulus alpha power not only leads to more hits but also false alarms (Limbach and Corballis, 2016). The effect of alpha power thus seems rather nonspecific, with associated higher excitability of the visual cortex boosting the representation of both target and noise. In experiments requiring target detection, this results in an increase of subjective awareness in both target-present and target-absent trials, thus leading to genuine but not necessarily correct impressions of seeing a target (Iemi and Busch, 2018).

In sum, many studies support the notion that the amplitude of alpha oscillations reflects the excitatory vs. inhibitory states of visual processing regions (Hanslmayr et al., 2011 - Figure 22). Through functional inhibition of irrelevant input, alpha activity increases the excitability of task relevant regions, increasing the probability to become aware of a visual stimulus (Van Diepen et al., 2019).

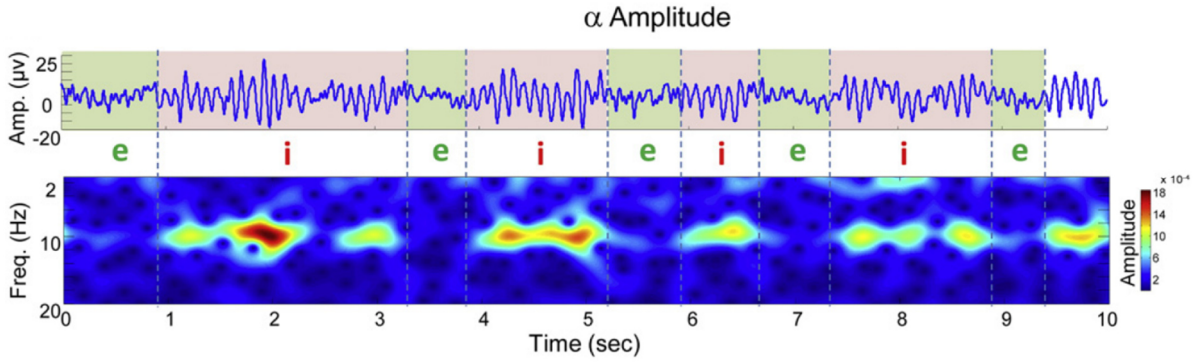

***Figure 22**: Alpha power reflects the excitability of visual regions. Top: Raw trace of an EEG for a parietal electrode. The alpha rhythm can be seen as a pattern of waxing and waning. Periods with low alpha amplitude (green) reflect excitatory states, while periods with high alpha amplitude (red) reflect inhibitory states. Bottom trace: Time-frequency presentation of amplitude. From Hanslmayr et al., 2011.*

The role of the amplitude of spontaneous alpha oscillations as an index of excitability influencing visual perception raises an exciting question: **If the gastric rhythm constrains the amplitude of the brain alpha rhythm, could it be that there exists a slow fluctuation in cortical excitability, driven by the gastric slow wave, that has an impact on fluctuations in perception?** If so, one should see a statistical relationship between the gastric phase and the probability to perceive a near-threshold target. **This raises the methodological question on how such a link could be optimally detected**, especially given that the relationship between alpha power and gastric phase can come in different profiles that vary between participants (see section 3; Figure 15B).

4.4.3. Infraslow fluctuations underlie periodicities in psychophysical performance

So far, I reviewed literature showing that spontaneous fluctuations in cortical activity, notably alpha power, modulate performance and account for a substantial variability in behavior between trials. In the following, I will focus onto another aspect of behavioral variability that may provide a further perspective on the link between the gastric rhythm with spontaneous neural activity and its potential behavioral consequences.

In near-threshold experiments, where an identical stimulus is presented to a subject (calibrated such that it is perceived in half of the trials and missed in the other half), a puzzling finding is that consecutive trials are not random and independent. Instead, behavioral outcomes are correlated such that the same outcomes tend to appear in clusters or "**streaks**" (Palva and Palva, 2012) – for example, subjects tend to detect a stimulus for a given period and then fail to detect it for a period of similar duration (Figure 22A). This dependency in psychophysical performance has been found in a number of early studies. Seashore and Kent, 1905, presented subjects auditory stimuli at threshold for perception and described nonrandom patterns in performance in the range from seconds to hours. Interest for serial dependence of perception then resurged in the 1950s. Verplanck et al., 1952, conducted a visual detection task and observed that trials showed significant serial correlation in their outcomes at different lags. Wertheimer, 1953, dynamically estimated subjects' thresholds for perception for visual and auditory targets during the course of an experiment. The author found that the thresholds time series were autocorrelated, with autocorrelation functions exhibiting similar patterns of fluctuations in threshold for the visual and auditory stimuli. From these results, he suspected the existence of a general "physiological rhythm" that affects multiple sensory systems at the same time. These findings have since been replicated and extended across diverse tasks and modalities, for perceptual decisions (Gilden and Wilson, 1995a; Makeig and Inlow, 1993), reaction time (Dehaene, 1993; Laming, 1968; Song et al., 2014; Van Orden et al., 2003), working memory (Gilden et al., 1995; Sinz and Stebel, 1970), perceptual judgments (Weiss et al., 1955) and skilled performance (Gilden and Wilson, 1995b). Interestingly, multiple studies found that the serial dependence of consecutive trials follows a $1/f$ power law distribution, exhibiting scale invariance just like electrophysiological time series (Gilden, 2001; Gilden et al., 1995; Kello et al., 2010; Van Orden et al., 2003; Wagenmakers et al., 2004).

A recent in-depth study on slow fluctuations in near-threshold perception has been done by Monto et al., 2008. In this experiment, participants had to detect somatosensory stimuli presented at random 1.5-4.5 second intervals, which were calibrated individually such that they were perceived in around 50% of the trials. The resulting time series of hits and misses exhibited "runs" of consecutive response outcomes of one type (Figure 23A). To statistically quantify if these runs occurred more often than expected by chance, the authors then compared the number of runs and run lengths to random data. They found that the number of runs was lower, and the duration of runs longer, in real compared to random data. This result indicates that behavioral outcomes do not alternate randomly but rather cluster in repeated responses of the same type. Specifically, the run probability decayed in a log-linear way as a function of run length, with runs of ~15-100 second duration occurring more frequently than would be expected by chance (Figure 23B). The authors then autocorrelated the time series of hits and misses and found significant autocorrelation for time lags up to ~170 seconds (Figure 23C). Finally, they quantified autocorrelations using detrended fluctuation analysis, a method to quantify long-range temporal correlations and power-law scaling in complex nonstationary time series. Across subjects, the response time series exhibited significant scale-free dynamics, the scaling exponent being higher for real data than for randomly created time series (Figure 23D). In sum, this experiment demonstrates that behavioral performance exhibits fluctuations at very slow time scales, with hit-miss cycles longer than 10 seconds.

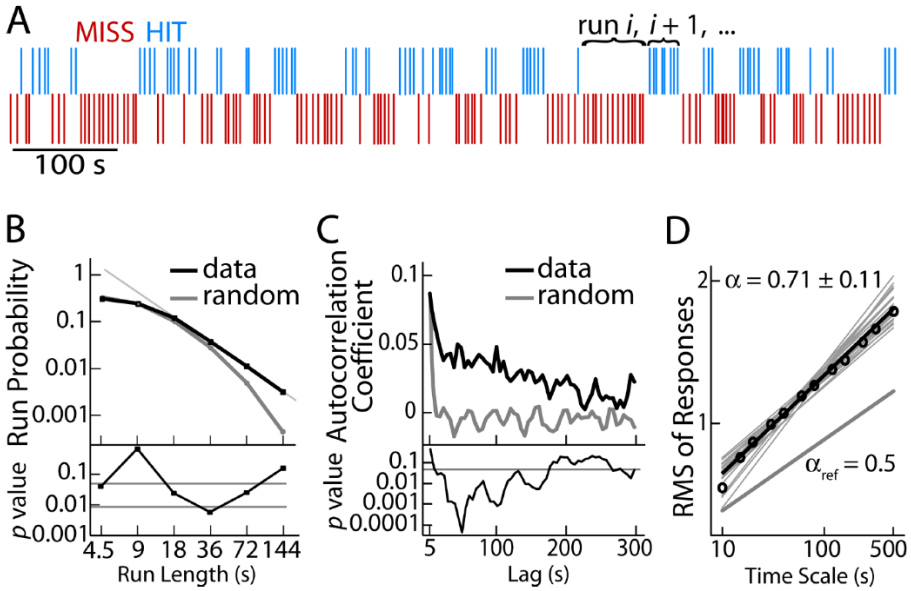

***Figure 23**: **A**: Time series of hits and misses to somatosensory stimuli in the experiment of Monto et al., 2008. Consecutive trials of one response type (hit or miss) are defined as "runs". **B**: Top: Probability of run length for real (black) vs. random (gray) data. Bottom: Associated p-values for each run length. Runs of lengths between ~15 and 100 seconds are more likely in real than random data. **C**: Autocorrelation coefficients for real (black) vs. random (gray) data. The response time series are*

significantly autocorrelated until ~170 seconds. ***D****: Scale-free dynamics of responses. The power law exponent of real response time series is significantly higher than for uncorrelated random data.*

Next, the authors sought to identify the neural correlates of these dynamics in performance. Here they were interested into the large-scale slow fluctuations in the range of 0.01 to 0.1 Hz, called infraslow fluctuations (ISFs). They extracted the instantaneous phase of ISFs and correlated it with occurrences of hits and misses. As a result, they found that hits and misses significantly clustered at different phases of infraslow fluctuations (Figure 24A, B). Moreover, they found that the amplitudes of higher frequency oscillations (1-40 Hz) were coupled with or 'nested' within the phase of infraslow fluctuations, with a very similar profile to the correlation of phase with the behavioral data (Figure 24C). These results suggest that infraslow fluctuations and their nested oscillations reflect variations in cortical excitability or state transitions that underlie fluctuations in behavioral performance.

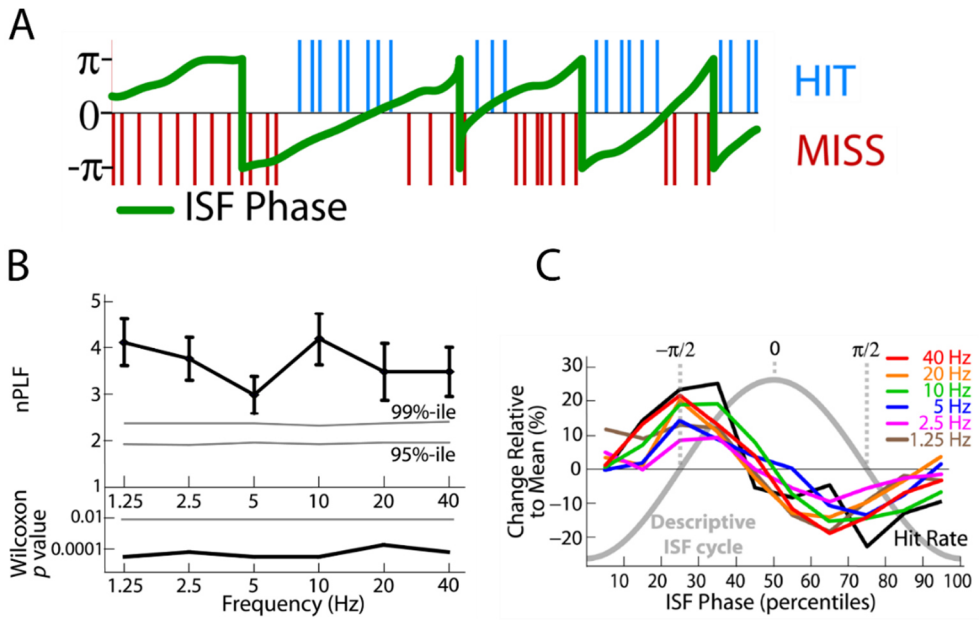

Figure 24*: **A**: Runs of hits and misses are phase-locked to neural infraslow fluctuations (ISF).* ***B****: Neural phase-locking (nPLF) to ISF phase for the amplitude of different frequencies, and associated p-vales. The amplitude of oscillations between 1 and 40 Hz are significantly locked to ISF phase.* ***C****: Correlation of 1-40 Hz oscillation amplitudes (colored lines) with the ISF phase is similar to that of the behavioral data (block line).*

The study of Monto et al. is interesting for my thesis since it represents an intriguing connection between alpha oscillations that are coupled to the gastric rhythm, fluctuations in performance, and very slow fluctuations in cortical excitability that are consistent in frequency with the gastric rhythm (~0.05 Hz).

4.4.4. The role of arousal

Studies investigating the link between spontaneous neural activity and behavior typically rely on experimental protocols that require alertness or responsiveness over prolonged periods, with alertness fluctuating over time. In the literature, this changing state of alertness/responsiveness is often referred to as *arousal*. We saw that on the neural level, arousal is reflected in alpha oscillations, with lower alpha power indexing higher arousal and vice versa. In this section, I will try to elucidate more in detail the meaning, correlates, and functional significance of arousal. In the end, I will argue that arousal might share a link with both behavioral variability and gastric input.

To start with a **conceptual clarification**, arousal is closely linked to other phenomena described in the literature, which are not always well defined and for which no commonly accepted taxonomy exists. Arousal can be defined as alertness or responsiveness to external stimuli (Azzalini et al., 2019; Berridge, 2008), as measured in both physiological or behavioral measures. It is also often used to refer to different sleep-wake states (Oken et al., 2006). Within waking states, it ranges between drowsiness and a hyperaroused state (Berridge, 2008). Next, *vigilance* or *sustained attention* are two often synonymously used concepts that refer to the ability to maintain attention on a task for a prolonged period of time (Davies and Parasuraman, 1982; Parasuraman et al., 1998). *Alertness* is used to refer to the motor responsiveness to external stimulation and differs from vigilance in that it does not involve perceptual sensitivity (Langner et al., 2012). In relation to arousal, it can be seen as a more specific component corresponding to the motor act of response, which is modulated by arousal. Finally, *mindwandering* refers to the engagement in cognition unrelated to the current demands of the external environment, involving thoughts, images and emotions not stemming from the immediate sensory input (Schooler et al., 2011; Smallwood and Andrews-Hanna, 2013). Note that despite the differences in definitions, these concepts have been operationalized very similarly, by changes in performance over an extended task.

Arousal has a wide range of **signatures**. On the bodily level, elevated arousal is associated with increased heart rate, blood pressure and skin conductance. On the neural level, it is characterized by an increase notably in alpha but also beta and gamma power, and it affects BOLD level in thalamus and widespread cortical regions (Olbrich et al., 2009), functional connectivity (Deco et al., 2014; Fox et al., 2005; Tagliazucchi and Laufs, 2014), visually evoked responses (Eason et al., 1969) and the signal-to-noise ratio or gain of neural responses (Aston-Jones and Cohen, 2005; Vinck et al., 2015). Behaviorally, it has a widespread role in functions such as perception, memory, learning and decision-making (Sara, 2009). Specifically, high arousal has been linked to faster reaction times (Eason et al., 1969; Langner et al., 2010), higher sensitivity and lower decision bias (de Gee et al., 2017). The relationship between performance and arousal has often been described by an inverted U-shape, with performance being optimal at intermediate levels of arousal (Aston-Jones and Cohen, 2005).

Arousal is regulated by the activation of the Ascending Reticular Arousal System, a set of nuclei in the brain stem including the noradrenergic locus coeruleus, dopaminergic ventral tegmental area and substantia nigra, the serotonergic dorsal and median raphe nucleus, and several thalamic nuclei. Mounting evidence points to the importance particularly of the locus coeruleus noradrenaline system as the physiological basis of arousal (Breton-Provencher and Sur, 2019; Rodenkirch et al., 2019; Sara, 2009). Noradrenergic locus coeruleus activity is reflected in pupil diameter both in phasic evoked responses (Alamia et al., 2019; Bradley et al., 2008) as well as in tonic fluctuations (Reimer et al., 2016), which can thus be used as an index to track brain arousal fluctuations. Indeed, pupil dynamics have been linked to many processes that involve manipulations of arousal. For example, the pupil dilates in response to new perceptual content (Einhäuser et al., 2008; Kloosterman et al., 2015) or unexpected events (Alamia et al., 2019), and small and large pupil diameters are linked to off-task focus and mindwandering (Konishi et al., 2017). Similar to task-performance, tonic pupil size has been shown to show a U-shaped relationship with arousal (de Gee et al., 2017; Konishi et al., 2017).

In sum, arousal is a strong modulator of cortical activity and behavioral state, and the behavioral variability seen in near-threshold experiments is in part a reflection of fluctuations in levels of arousal.

Intriguingly, the literature reviewed in this introduction allows to make several arguments that arousal might be linked to visceral signals or gastric input more specifically. First, anatomy suggests that gastric ascending signals might reach the parabrachial nucleus, which regulates arousal by projecting to the locus coeruleus and other neuromodulatory nuclei (see section 2.4.2). Although direct evidence for the role of gastric input to the locus coeruleus is missing, simulation of the colon or small intestine in rats/cats reportedly has effects on norepinephrine release and the sleep-wake cycle (Elam et al., 1986; Kukorelli and Juhász, 1977; Saito et al., 2002). Additionally, the cortical processing of heartbeats, measured as the heartbeat-evoked response, has been shown to be related to different arousal levels (Luft and Bhattacharya, 2015). Next, the occipital cortex responds to gastric stimulation in cats (Cao et al., 2019), and gastric distension in humans (Ladabaum et al., 2001; Lu et al., 2004), which, as has been speculated (Cao et al., 2019), could reflect changes in cortical arousal due to the gut-innervating vagal and spinal afferents projecting to neuromodulatory centers. Moreover, spontaneous BOLD activity in a wide network of brain regions in humans is phase-synchronized to the gastric rhythm at rest (Rebollo et al., 2018), and this network overlaps with brain regions correlating with pupil size or heart rate variability, pointing to a potential common link with arousal. Finally, the gastric rhythm modulates the amplitude of occipital alpha oscillations (Richter et al., 2017), a neural index of arousal. **Could it be that the gastric rhythm modulates arousal, which is then reflected in a modulation of cortical alpha power and visual perception?**

5. Questions for my PhD

The main goal of this thesis was to study the role of the coupling between the slow gastric rhythm and brain alpha oscillations for behavior. For this, I recorded simultaneously the EGG and MEG in over 30 participants while they were performing a visual perception experiment with stimuli at threshold. The main hypothesis was that the gastric rhythm drives slow fluctuations in cortical excitability, which modulate a perceiver's ability to detect the target (chapter 8). In order to test this hypothesis, there were two methodological challenges that had to be addressed: How to obtain good quality EGG recordings in human participants and to develop a principled preprocessing and analysis pipeline (chapter 6), and how to quantify the link between behavioral outcome and gastric phase (chapter 7).

6. Article I: Electrogastrography for psychophysiological research: Practical considerations, analysis pipeline, and normative data in a large sample

6.1. Introduction

Electrogastrography is the noninvasive measuring of the gastric rhythm by means of cutaneous electrodes placed on the abdomen, generating the signal called the electrogastrogram (EGG). In contrast to methods such as electroencephalography or electrocardiography, where practical guidelines are abundant, the EGG is lacking conventional standardized recording and analysis procedures. It has so far mostly been used in gastroenterology, where the aim is to quantify irregularities in the EGG signal in clinical conditions. Importantly, this differs from our purpose, which is to extract the regular gastric rhythm in healthy participants. Few pioneering studies in psychophysiology exist, which have attempted to relate changes in the EGG to stress, emotions and task performance (e.g., Chen et al., 2005; Harrison et al., 2010; Davis et al., 1969; Vianna et al., 2006), but produced mixed results, which might partly be attributed to the absence of rigorous and standardized procedures. Notably, there is typically no artifact rejection applied, and locations of the electrodes on the abdomen vary by authors, with mostly only one to three electrodes used, whose position has not been validated.

During my PhD, when wanting to record the gastric rhythm, we therefore faced numerous methodological questions. For example, where to place the electrodes to ideally detect the gastric rhythm? Moreover, when inspecting the EGG phase time series, we observed portions of signals that seemed "irregular", and stood in front of the difficult decision on whether include them or reject them as artifacts. While in the EEG, artifacts (movements, muscle, blinks) are well defined, in the EGG it is ambiguous whether a given signal represents an electronic artifact or physiological irregularity. Building on the nascent expertise in the group (Richter, Rebollo), we developed practical solutions to those questions, which often required a lot of testing and investigations. Moreover, the EGG recordings that I performed, together with the EGG recordings from other projects in the group, resulted in a large data set of >100 participants. This valuable data set allowed us to establish normative distributions of several EGG parameters, such as power, frequency, or gastric cycle duration, that in turn also helped us to define what represents a regular EGG, and to refine and validate our EGG analysis pipeline.

We also received requests from other researchers in neuroscience, who were interested in extracting the gastric rhythm and faced similar problems as us. We therefore felt that our experiences with this method would be valuable for the community and might contribute to a standardization of this method. It also seemed useful to capitalize on the large data set acquired and add to the literature our findings on distributions of EGG parameters in a healthy population, and their relation to demographical variables (BMI, gender, …). In order to target specifically the neuroscience audience, we also provided a literature review on potential anatomical pathways of gut-brain signaling and experimental findings in the cognitive neuroscience and psychophysiology literature, to underline the relevance of this technique. In sum, this project for us resulted in a preprocessing and analysis pipeline to extract the gastric rhythm,

and with our paper we hope to encourage the use of this method and potentially draw more interest in the potential of this technique to study brain-viscera interactions.

Received: 11 December 2019 | Revised: 12 March 2020 | Accepted: 14 April 2020

DOI: 10.1111/psyp.13599

ORIGINAL ARTICLE

PSYCHOPHYSIOLOGY SPR WILEY

Electrogastrography for psychophysiological research: Practical considerations, analysis pipeline, and normative data in a large sample

Nicolai Wolpert | **Ignacio Rebollo** | **Catherine Tallon-Baudry**

Laboratoire de Neurosciences Cognitives et Computationnelles, Ecole Normale Supérieure, PSL University, Paris, France

Correspondence
Nicolai Wolpert, Laboratoire de Neurosciences Cognitives & Computationnelles, École Normale Supérieure, 24 rue Lhomond, 75005 Paris, France.
Email: nicolaiwolpert@gmail.com

Funding information
This work was supported by funding from the European Research Council (ERC) under the European Union's Horizon 2020 research and innovation program (grant agreement No 670325, Advanced grant BRAVIUS) and by a senior fellowship of the Canadian Institute For Advanced Research (CIFAR) program in Brain, Mind and Consciousness to C.T.-B., as well as from ANR-17-EURE-0017.

Abstract

Electrogastrography (EGG) is the noninvasive electrophysiological technique used to record gastric electrical activity by means of cutaneous electrodes placed on the abdomen. EGG has been so far mostly used in clinical studies in gastroenterology, but it represents an attractive method to study brain-viscera interactions in psychophysiology. Compared to the literature on electrocardiography for instance, where practical recommendations and normative data are abundant, the literature on EGG in humans remains scarce. The aim of this article is threefold. First, we review the existing literature on the physiological basis of the EGG, pathways of brain-stomach interactions, and experimental findings in the cognitive neuroscience and psychophysiology literature. We then describe practical issues faced when recording the EGG in young healthy participants, from data acquisition to data analysis, and propose a semi-automated analysis pipeline together with associated MATLAB code. The analysis pipeline aims at identifying a regular rhythm that can be safely attributed to the stomach, through multiple steps. Finally, we apply these recording and analysis procedures in a large sample ($N = 117$) of healthy young adult male and female participants in a moderate (<5 hr) to prolonged (>10 hr) fasting state to establish the normative distribution of several EGG parameters. Our results are overall congruent with the clinical gastroenterology literature, but suggest using an electrode coverage extending to lower abdominal locations than current clinical guidelines. Our results indicate a marginal difference in EGG peak frequency between male and female participants, and that the gastric rhythm becomes more irregular after prolonged fasting.

KEYWORDS

electrogastrography, gastric rhythm, normative data, power and phase analysis, processing pipeline

1 | AN INTRODUCTION TO ELECTROGASTROGRAPHY

1.1 | The electrogastrogram and its usage

"Electrogastrography" refers to the monitoring technique of gastric myoelectrical activity from cutaneous electrodes placed on the abdomen (Figure 1a), which generates the electrogastrogram (EGG). The EGG has so far mostly been used for clinical purposes in gastroenterology (Koch & Stern, 2004; Parkman, Hasler, Barnett, & Eaker, 2003; Riezzo, Russo, & Indrio, 2013; Yin & Chen, 2013), but represents an interesting tool in psychophysiology (Stern, Koch, Levine, & Muth, 2007; Stern, Koch, Stewart, & Vasey, 1987). The EGG reflects the combination of the slow electrical gastric rhythm, constantly generated in the stomach wall, and of the more transient smooth muscle activity generating gastric peristaltic contractions. The main function of the stomach is to mix and grind food during digestion. The gastric rhythm sets the frequency of smooth muscle contractions and controls their propagation. The gastric rhythm is constantly generated in the stomach wall, even in the absence of muscular contraction (Bozler, 1945), or when the stomach is completely disconnected from the central nervous system (Suzuki, Prosser, & Dahms, 1986). Its normal frequency in healthy humans is around 0.05 Hz or three cycles per minute, that is, one cycle every 20 s. EGG frequency differs in other species (Mice: 2–5 cpm [Hou, Yin, Liu, Pasricha, & Chen, 2005]; Pigs: ~3.3 cpm [Květina et al., 2010; Varayil et al., 2009]; dogs: 4–6.5 cpm [Andreis et al., 2008; Mintchev, Otto, & Bowes, 1997]; macaque monkeys: ~3.6 cpm [Linsong, Huailin, Xitai, Xiaojin, & Pingan, 1989]).

The definition of normogastria, or normal frequency range of the gastric rhythm in humans, varies depending on authors (for review, Chang, 2005; Parkman et al., 2003). Along with a number of studies (e.g., Chen & McCallum, 1992; Chen, Zou, Lin, Ouyang, & Liang, 1999; Lin, 1999; Parkman, Harris, Miller, & Fisher, 1996; Parkman et al., 2003; Pfaffenbach, Adamek, Kuhn, & Wegener, 1995; Riezzo, Chiloiro, & Guerra, 1998) and guidelines (e.g., Yin & Chen, 2013), we adopted the 2–4 cpm cycles per minute (cpm) range. A narrower range has also been advocated (e.g., 2.5 to 3.6 cpm in

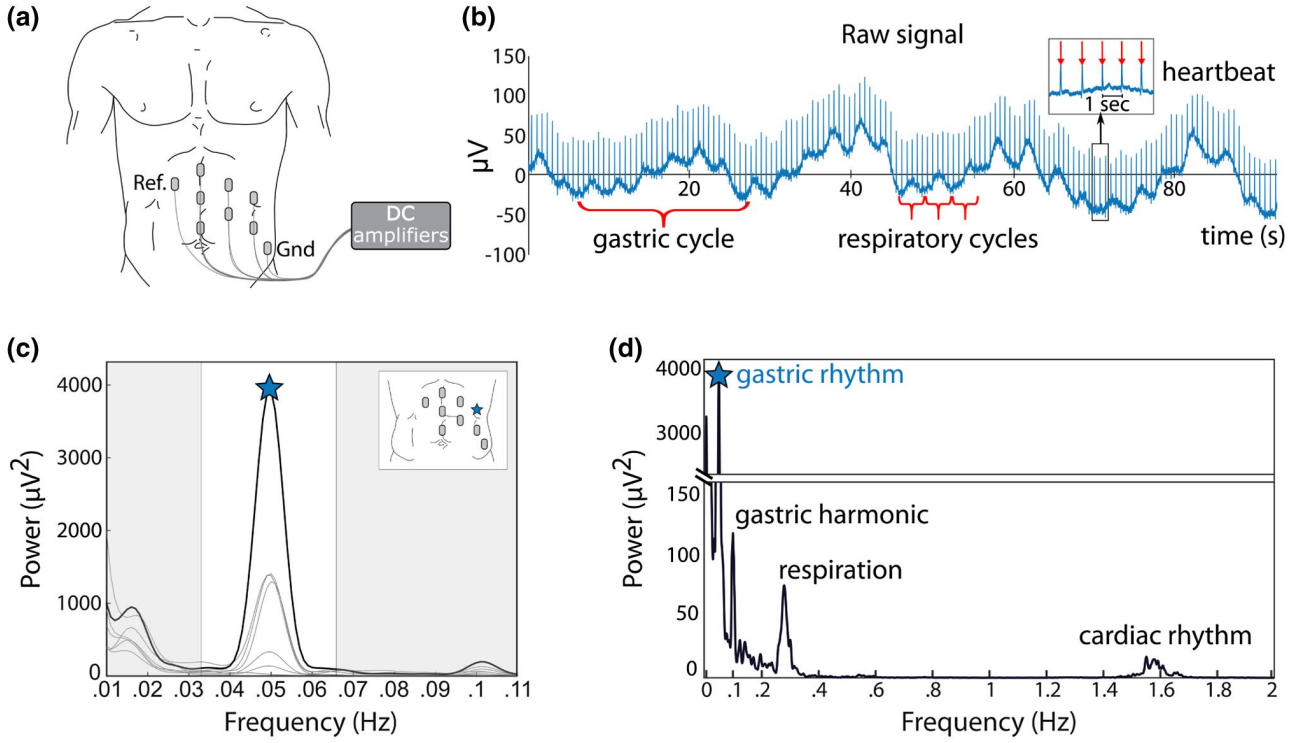

FIGURE 1 (a) Recording setup. Cutaneous electrodes are placed on the left abdomen of the participant in a grid-like arrangement and connected to DC amplifiers. Ref. and Gnd correspond to Reference and Ground, respectively. (b) Example of raw data in one participant, where the gastric rhythm is visible as cycles of ~20 s length. Respiratory cycles are much faster (typically 3 to 5 s length). Heartbeats appear as transients every ~0.8 s (inset). EGG amplitude in this participant is close the median value observed in 100 participants. (c) Power spectrum at each of the seven recording electrodes. Peak frequency is indicated by a star on the channel with the largest power (black line). The white area corresponds to the normal frequency range of the EGG, also known as normogastria (2 to 4 cpm or 0.033 to 0.066 Hz). Inset: Electrode layout with the location of the electrode displaying the largest spectral power marked with a blue star. (d) Spectral density over a wider frequency range at the selected channel, revealing the spectral signatures of the respiratory (~0.3 Hz) and cardiac rhythms (~1.5 Hz)

Koch & Stern, 2004), and a number of studies used ranges closer to this definition (e.g., Abell & Malagelada, 1988; Gianaros, Quigley, & Mordkoff, 2001; Homma et al., 1999; Koch, Bingaman, Tan, & Stern, 1998; Koch, Hong, & Xu, 2000; Meissner, Muth, & Herbert, 2011; Muth, Koch, Stern, & Thayer, 1999; Stern, Vasey, Senqi, & Koch, 1991; Vianna, Weinstock, Elliott, Summers, & Tranel, 2006).

An example of a raw signal obtained from cutaneous abdominal electrodes is shown in Figure 1b. In this good quality recording, the gastric rhythm is visible to the naked eye. In the same raw data, the faster rhythms of respiration (typically around 0.2–0.4 Hz) (Kaiho, Shimoyama, Nakajima, & Ochiai, 2000) and heartbeats (1–1.7 Hz) can be observed, superimposed on the gastric rhythm (Abell & Malagelada, 1988; Stern et al., 1987). The spectral analysis of the EGG reveals a sharp peak around 0.05 Hz (Figure 1c). The EGG spectral signature is markedly distinct from those of respiration and heart rate, that peak at much higher frequencies (Figure 1d). Note that a harmonic of the gastric rhythm can sometimes be observed (Figure 1d) when the EGG departs from a perfect sine wave (Verhagen, Van Schelven, Samsom, & Smout, 1999).

Historically, the EGG was independently discovered by Alvarez, 1922; Davis, Garafolo, & Kveim, 1959; Tumpeer & Blitsten, 1926. While this recording technique received little attention for decades, computerized analysis rekindled interest in the 1990s in the field of gastroenterology (Koch & Stern, 2004). EGG recording and analysis has been first and mostly performed in the clinical domain, where it represents an appealing method since it is noninvasive, cheap, and relatively easy to install and acquire. In gastroenterology, the EGG is typically acquired before and after a meal, called the pre- and postprandial period, respectively. The EGG amplitude normally increases in the postprandial period in healthy participants, while EGG frequency remains relatively unaffected (for review see Koch & Stern, 2004; Riezzo et al., 2013; Stern et al., 1987). Gastroenterologists have been interested in characterizing EGG abnormalities in patients by describing changes in power and frequency. For instance, postprandial increases in EGG amplitude are altered in gastric motility disorders (Cucchiara et al., 1997; Parkman & Orr, 2007) and Parkinson's disease (Kaneoke et al., 1995). Other studies analyzed changes in EGG frequency. The gastric rhythm tends to get faster (tachygastria) in patients with nausea (Geldof et al., 1989), depression (Ruhland et al., 2008), and schizophrenia (Peupelmann et al., 2009). Note that different approaches have been used to characterize departure from normogastria, either by analyzing the percentage distribution of EGG power in different frequency bands or by analyzing the shifts of EGG peak frequency over time (Stern et al., 2007). Here, we will focus on preprandial EGG recordings in healthy participants.

1.2 | The EGG in psychophysiology

The potential relevance of visceral signals for understanding brain and behavior has long been underlined for emotions (Cannon, 1927; Damasio, 1996; James, 1890; Lange, 1885), but also in a relationship with self and consciousness (Azzalini, Rebollo, & Tallon-Baudry, 2019; Christoff, Cosmelli, Legrand, & Thompson, 2011; Craig, 2002; Critchley & Harrison, 2013; Thompson & Varela, 2001), as well as in physical and mental health (Khalsa et al., 2018; Quadt, Critchley, & Garfinkel, 2018). Note that brain-viscera interplay ranges from the implicit nonconscious signaling of bodily afferents to the brain and/or automatic descending modulation of stomach activity by the brain to explicit or consciously accessible visceral perception (Azzalini et al., 2019; Quadt et al., 2018).

Despite the potential relevance of brain-viscera relationships, empirical studies investigating the electrical activity of the gastrointestinal system remain scarce and provided mixed results. Initial studies on shock/noise avoidance reported mixed results on EGG amplitude (Davis & Berry, 1963; Fedor & Russell, 1965; Stern, 1966, 1983; White, 1964). Different physical and psychological stressors were found to increase spectral power in the tachygastric range (Gianaros et al., 2001; Muth et al., 1999; for conflicting results see Riezzo, Porcelli, Guerra, & Giorgio, 1996; Stern et al., 1991), while the effects on amplitude have been mixed (Riezzo et al., 1996; Stern et al., 1991). In line with the results of stressors, videos evoking disgust were found to evoke tachygastria (Harrison, Gray, Gianaros, & Critchley, 2010) but this result was not replicated (Meissner et al., 2011). Emotions induced by movie clips (or music) most often do not alter the EGG frequency (Baldaro et al., 1996, 2001; Baldaro, Battacchi, Trombini, Palomba, & Stegagno, 1990; Chen, Xu, Wang, & Chen, 2005; Chen et al., 2008; Lin et al., 2007), while results on amplitude are inconsistent (Baldaro et al., 1996, 2001; Chen et al., 2005, 2008; Lin et al., 2007; Vianna et al., 2006). Several studies found increased mean EGG power during the performance of tasks of mental arithmetic (Davis, Berry, & Paden, 1969; Holzl, Schroder, & Kiefer, 1979; Riezzo et al., 1996; for conflicting null finding see Walker & Sandman, 1977), but other studies on mental arithmetic and puzzle-solving report fewer episodes of large amplitude gastric activity (Ercolani et al., 1982; Ercolani, Baldaro, & Trombini, 1989; Martin, Nicolov, Ormieres, Beloncle, & Murat, 1982). Different factors, like the type of task, or fed versus fasted state of participants, number of participants as well as interindividual variability (Riezzo et al., 1996) might account for discrepancies between different studies. The absence of standardized procedures in psychophysiology for recording and analyzing the EGG might play an additional role (but see e.g., Koch et al., 2000 for reproducibility in the water load test).

In addition to a potential modulation of EGG parameters by descending cognitive influences, ascending influences arising from the stomach were recently shown to influence brain dynamics at rest, with a modulation of the amplitude of the alpha rhythm by the phase of the EGG (Richter, Babo-Rebelo, Schwartz, & Tallon-Baudry, 2017) in the parieto-occipital region. fMRI data reveal that the brain at rest is coupled with the gastric rhythm in an extended cortical network (Rebollo, Devauchelle, Béranger, & Tallon-Baudry, 2018), including known viscero-sensitive regions such as primary and secondary somatosensory cortices, as well as the parieto-occipital region where gastric-alpha coupling was observed. Gastric-brain coupling thus appears to play a role in the large-scale organization of brain dynamics at rest. Although little employed so far, the EGG thus appears as an attractive method to study brain-viscera interactions.

1.3 | Physiological basis of the EGG

1.3.1 | Pacemaker cells and smooth muscles

The stomach mixes ingested food with secretions and grinds it into particles that can be emptied into the duodenum through the pylorus (Figure 2a). The stomach is classically divided into two parts (Koch & Stern, 2004). The proximal stomach consists of the fundus (upper curved part) and the corpus (or body, the main central part of the stomach), which acts as a reservoir and controls intragastric pressure (Tack, 2012). The distal stomach consists of the lower part of the corpus, the antrum, and the pylorus, and is responsible for the mixing, grinding, and emptying of solid food (Kelly, 1980; Rayner, Hebbard, & Horowitz, 2012). The gastrointestinal tract contains two muscular layers that control gut peristalsis: a thin outer longitudinal layer and a thick inner circular layer. Unlike the rest of the organs of the gastrointestinal tract, the stomach has an additional innermost oblique layer of smooth muscles, which allows more refined control of motility patterns (Birmingham, 1898; Christensen & Torres, 1975; Fritsch & Kühnel, 2008).

The stomach wall contains a distinctive type of cells, the Interstitial Cells of Cajal (ICCs), located between the circular and longitudinal muscular layer (myenteric Interstitial Cells of Cajal, ICC-MY) or within the muscular layers (intramuscular Interstitial Cells of Cajal, ICC-IM) (O'Grady, 2012; Sanders, Ward, & Koh, 2014) (Figure 2b). Although ICCs are not neurons (Klüppel, Huizinga, Malysz, & Bernstein, 1998), they display neuron-like properties. Both types of ICCs continuously and intrinsically generate and propagate slow pacemaker currents (for review see Huizinga & Chen, 2014), constituting the basis of the gastric rhythm (Hirst & Edwards, 2006; Sanders, Koh, & Ward, 2006; Sanders et al., 2014). During digestion, the gastric rhythm generated by ICCs triggers smooth muscle contraction with additional inputs from excitatory enteric motor neurons (Sanders et al., 2014) and vagal efferent neurons (Chang, Mashimo, & Goyal, 2003). In addition to their role in slow wave generation, ICC-IM is involved in the transduction of inputs from enteric motor neurons (Hirst & Edwards, 2006; Sanders et al., 2006, 2014). While ICCs control the pace of gastric contractions, enteric motor neurons and vagal efferent neurons regulate the amplitude of contractions. It follows that the frequency of the surface EGG is likely to be related to the intrinsic pacemaker activity of ICCs, while EGG amplitude is related to a combination of currents generated in ICCs, enteric motor neurons, and smooth muscles.

ICCs generate the gastric rhythm and actively propagate the slow waves through the ICC network as well as to

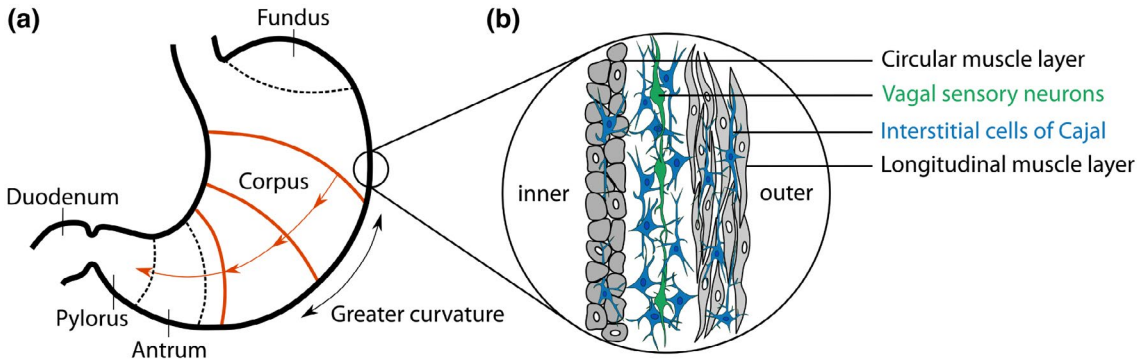

FIGURE 2 The stomach and the generation of the gastric slow rhythm. (a) Anatomical regions of the stomach, with the main divisions into fundus, corpus, and antrum. The gastric rhythm originates from the pacemaker region (orange) near the greater curvature of the mid/upper corpus. From here, it entrains other pacemaker cells, resulting in traveling rings of electrical wavefronts in the direction of the antrum (O'Grady et al., 2010). (b) The Interstitial Cells of Cajal (ICC, blue) are the generators of the gastric rhythm. They lay in the stomach wall, between and within the circular and longitudinal muscle layers. An additional thin oblique muscle layer located in the innermost part of the stomach, adjacent to the circular layer, is not represented here. The electrical activity of the pacemaker is passed through the entire ICC network and is also passively conducted into coupled muscle cells. ICCs make synapse-like contact with vagal sensory neurons (Powley et al., 2008), presented in green, in a structure known as *intramuscular arrays*, that can detect mechanical changes in smooth muscles. Adapted from Koch & Stern, 2004

electrically coupled smooth muscle cells. Rings of electrical wavefronts travel circumferentially in a proximal to distal gradient along the stomach (Koch & Stern, 2004), pushing food toward the pylorus when accompanied by muscular contractions. How wave propagation is orchestrated is not known with certainty. It has since long been assumed that the stomach contains a "dominant pacemaker" area in the greater curvature of the mid/upper corpus, entraining slow waves at other sites, possibly with a gradient in frequency (Hinder & Kelly, 1977; Kelly, Code, & Elveback, 1969; Koch & Stern, 2004; O'Grady et al., 2010; Riezzo et al., 2013).

1.3.2 | Relating cutaneous EGG to gastric physiology

Because the frequency of the gastric rhythm is determined by ICCs' intrinsic pacemaker activity, cutaneous EGG frequency directly reflects the frequency of the gastric basal rhythm, as revealed by simultaneous cutaneous EGG and invasive recordings in humans (Brown, Smallwood, Duthie, & Stoddard, 1975; Chen, Schirmer, & McCallum, 1994; Coleski & Hasler, 2004; Familoni, Kingma, & Bowes, 1987; Hamilton, Bellahsene, Reichelderfer, Webster, & Bass, 1986; Lin, Chen, Schirmer, & McCallum, 2000; Mintchev, Kingma, & Bowes, 1993).

The relative contribution of ICCs and smooth muscle contractions to cutaneous EGG amplitude is more difficult to estimate (Angeli et al., 2013; Bayguinov, Hennig, & Sanders, 2011; Hocke et al., 2009; O'Grady, 2012; Stern et al., 2007; Xing, Qian, & Chen, 2006), for two main reasons: First, the electrophysiological signature of smooth muscle contraction is filtered out in cutaneous EGG (Verhagen et al., 1999), and more generally how electrical signals of gastric origin are combined in surface recordings remains to be fully understood (Cheng, Du, & O'Grady, 2013; Du, O'Grady, Cheng, & Pullan, 2010). Second, the amplitude of the gastric rhythm is dependent on the fasting/fed state of the stomach. As a first approximation, one could consider that during digestion the EGG corresponds to a combination of muscle contractions and ICC intrinsic activity, whereas in the fasting state, the stomach is empty and surface EGG mostly corresponds to ICC activity (Smout, Van Der Schee, & Grashuis, 1980). This is the rationale underlying the clinical test comparing pre- and postprandial EGG amplitude. However, even when the stomach is resting as in moderate fasting, a few muscular contractions may occur (O'Grady et al., 2010; Sanders et al., 2014), and occasional intense muscular activity can be observed in prolonged (i.e., overnight) fasting (Koch & Stern, 2004).

Because ICCs are present all along the gastrointestinal tract, cutaneous electrodes might capture the myoelectrical activity of other organs of the GI tract, raising the question of the organ-specificity of the signal. The small intestine displays frequencies that are much higher than the stomach, usually above 0.16 Hz (Christensen, Schedl, & Clifton, 1966; Riezzo et al., 2013; Waldhausen, Shaffrey, Skenderis, Jones, & Schirmer, 1990). The frequency range of the colon is broader, ranging from 2 to 12 cycles per minute in humans (Erickson et al., 2019; Homma et al., 1995; Pezzolla, Riezzo, Maselli, & Giorgio, 1989; Riezzo, Pezzolla, Maselli, & Giorgio, 1994; Taylor, Duthie, Smallwood, & Linkens, 1975), that is, potentially overlapping in frequency with the gastric rhythm (Amaris, Sanmiguel, Sadowski, Bowes, & Mintchev, 2002; Erickson et al., 2019). Still, numerous studies found that the 3 cpm rhythm disappeared, or was largely reduced, following surgical removal of the stomach but not of the colon (Homma et al., 1995; Imai & Sakita, 2005; Kaiho et al., 2000; Pezzolla et al., 1989).

1.4 | Pathways of gut-brain signaling

There is evidence in the cognitive neuroscience literature that stress or emotions can alter cutaneous EGG frequency or amplitude (Baldaro et al., 1996; Gianaros et al., 2001; Lin et al., 2007; Muth et al., 1999; Stern et al., 1991; Vianna et al., 2006), indicating descending influences from brain to stomach, and that ascending influences, from stomach to brain, influence brain dynamics (Richter et al., 2017). What are the currently known anatomical pathways supporting those interactions? In this section, we present the mechanisms of sensory transduction of the gastric rhythm and ascending pathways up to cortical targets, followed by an overview of descending projections from brain to stomach. Note that much remains to be determined, from signal transduction (Umans & Liberles, 2018) to anatomo-functional pathways (Azzalini et al., 2019). Only very few stomach-specific anatomical tracing studies exist in animals (for a recent example in rodents see Han et al., 2018). Besides, it is tempting to extrapolate from anatomical tracing and/or electrophysiological studies in animals (rodents, cats and monkeys) to humans, on the assumption that visceral pathways are probably ancient and conserved through evolution. However, differences between species have been reported (Bishop, Malliani, & Thorén, 1983; Pritchard, Hamilton, & Norgren, 2000; Shipley & Sanders, 1982). The overall description presented in this section is drawn from studies in rodents, cats and monkeys, and some pathways may differ in humans.

1.4.1 | Detection of the gastric rhythm and mechanical changes in sensory neurons

The EGG reflects a combination of gastric smooth muscle contractions and of the gastric rhythm generated by ICCs. Both types of signals might be detected in the stomach by

sensory neurons. ICCs make direct synapse-like contact with vagal afferent neurons, also known as *intramuscular arrays* (Powley & Phillips, 2011; Powley et al., 2008). The gastric rhythm might thus be directly relayed to the brain through vagal afferent neurons, although this has not been directly tested. Experimental work has mostly been devoted to the signaling of gastric smooth muscle contractions. Multiple cell types, including ICCs, are grouped in arborized structures that run along the smooth muscle and act as mechanoreceptors across the gastrointestinal tract, with different sensitivity thresholds and adaptation profiles (Berthoud, Blackshaw, Brookes, & Grundy, 2004; Blackshaw, Brookes, Grundy, & Schemann, 2007; Umans & Liberles, 2018). Those mechanosensory structures continuously sense the contractile state of the stomach and can transmit changes in smooth muscles to the brainstem through vagal and spinal afferent fibers. It is worth underlining that in the vagus nerve, around 80% of the fibers are ascending, indicating the brain is probably more of a listener than a sender of vagal information (Agostoni, Chinnock, De Daly, & Murray, 1957). In contrast, the ratio between efferents and afferents in the spinal splanchnic nerve is closer to 50:50 (Foley, 1948; Leek, 1972).

1.4.2 | Vagal and spinal pathways relay gastric information to the brainstem, thalamus, and cortex

Vagal sensory neurons project to the nucleus of the solitary tract in the brainstem, an important relay center for visceral information, that is also involved in the initiation of gastric control reflexes (Azpiroz & Malagelada, 1990). The nucleus of the solitary tract displays a rough viscerotopic organization (Altschuler, Bao, Bieger, Hopkins, & Miselis, 1989), but with local overlap between inputs from the heart and the gastrointestinal tract (Paton & Kasparov, 2000). Visceral afferents are relayed to the parabrachial nucleus (Figure 3, right panel), which integrates vagal and spinal information and is the main relay of visceral information to subcortical and cortical structures (Hylden, Hayashi, Bennett, & Dubner, 1985; Norgren, 1978; Pritchard et al., 2000).

The nucleus of the solitary tract and parabrachial nucleus directly targets the main neuromodulatory centers (Figure 3): the serotoninergic dorsal raphe nucleus, the noradrenergic locus coeruleus, and the dopaminergic substantia nigra and ventral tegmental area (Coizet, Dommett, Klop, Redgrave, & Overton, 2010; Pritchard et al., 2000; Saper & Loewy, 1980). The functional relevance of gastric vagal signaling on the dopaminergic reward pathway has been recently elegantly demonstrated in mice (Han et al., 2018), where stimulation of the vagal sensory ganglion activated self-stimulation behavior, conditioned place preferences, and induced dopamine-release from substantia nigra. The parabrachial nucleus also targets the amygdala, the hypothalamus, and the striatum (Bester, Besson, & Bernard, 1997; Fulwiler & Saper, 1984; Saper, 2002).

Gastrointestinal inputs can reach the thalamus through parabrachial projections or direct spinothalamic pathways. Parabrachial outputs target the ventromedial, reticular, intralaminar, and ventroposterior thalamic nuclei (Coen, Hobson,

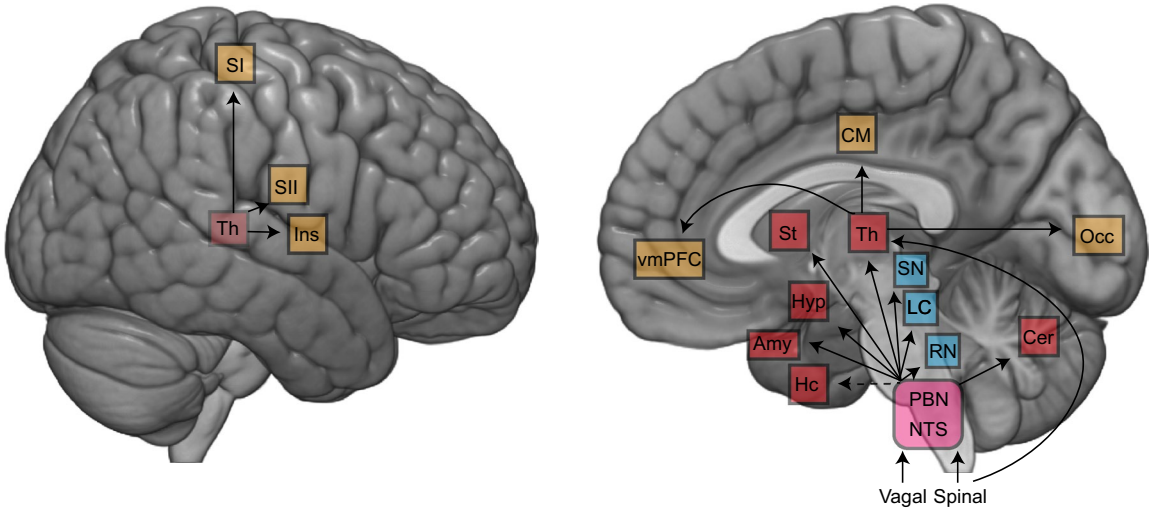

FIGURE 3 Projections of vagal and spinal afferents from the gastrointestinal tract to the brain. Afferents target brainstem nuclei (purple) including nucleus tractus solitarius (NTS) and parabrachial nucleus (PBN). The NTS and PBN in turn project to various subcortical structures, including the neuromodulatory structures (blue), as well as subcortical (red) and cortical (yellow) regions. Another spinal afferent pathway bypasses the brainstem and directly targets the thalamus. Abbreviations: Amy, amygdala; Cer, cerebellum; CM, cingulate motor regions; Hc, hippocampus; Hyp, hypothalamus; Ins, insula; LC, locus coeruleus; NTS, nucleus of the solitary tract; PBN, parabrachial nucleus; RN, raphe nucleus; SI, primary somatosensory; SII, secondary somatosensory; SN, substantia nigra; St, striatum; Th, thalamus; vmPFC, ventromedial prefrontal cortex. Modified from Azzalini et al., 2019

& Aziz, 2012). Spinal and vagal inputs are already combined in the parabrachial nucleus and further convergence takes place in the thalamus. Unexpectedly, the lateral geniculate nucleus, a visual thalamic relay, receives massive inputs from the parabrachial region (Erişir, Van Horn, & Sherman, 1997; Uhlrich, Cucchiaro, & Sherman, 1988), and parabrachial activation affects visual responses in the lateral geniculate nucleus (Lu, Guido, & Sherman, 1993; Uhlrich, Tamamaki, Murphy, & Sherman, 1995) and cortex (Munk, Roelfsema, König, Engel, & Singer, 1996).

From the thalamus, numerous cortical areas receive visceral inputs (Figure 3), including primary and secondary somatosensory cortex (Amassian, 1951; Downman, 1951), insula (Cechetto & Saper, 1987), ventromedial prefrontal cortex (Vogt & Derbyshire, 2009) and cingulate motor regions (Dum, Levinthal, & Strick, 2009). In rodents, viscerotopy is present in the ventrobasal nucleus of the thalamus and in the insula (Cechetto & Saper, 1987). Although it is known that in humans the somatosensory cortex is coupled with the stomach (Rebollo et al., 2018) and that it responds to heartbeats (Kern, Aertsen, Schulze-Bonhage, & Ball, 2013), whether the somatosensory cortex shows a viscerotopic organization, and how viscerotopy is integrated with somatotopy, has not between investigated since the 50's (Downman, 1951).

1.4.3 | Descending influences

As reviewed in Section 1.2, gastric amplitude and/or frequency can be modified by cognitive and emotional factors. Indeed, gastrointestinal functioning is regulated by both vagal (Hall, el-Sharkawy, & Diamant, 1986; Stern, Crawford, Stewart, Vasey, & Koch, 1989), or parasympathetic, and spinal, or sympathetic, centers. The main parasympathetic center is the dorsal motor nucleus of the vagus (Gillis, Quest, Pagani, & Norman, 1989), that has descending projections to smooth muscle cells as well as to Interstitial Cells of Cajal (Schemann & Grundy, 1992; Travagli, Hermann, Browning, & Rogers, 2006). The vagal innervation from the dorsal nucleus of the vagus modulates the amplitude of the gastric rhythm and can have either an activating or inhibiting effect (Andrews & Scratcherd, 1980; Pagani, Norman, Kasbekar, & Gillis, 1985; Travagli et al., 2006). The sympathetic efferent nuclei controlling the stomach are located in the intermediolateral cell column of the thoracic-lumbar spine, and project to prevertebral and paravertebral ganglia located outside the spine (Furness, 2006). In turn, spinal projections innervate enteric neurons, arterioles of the gut wall and striate muscles of sphincters to control vasoconstriction, liquid balance, secretion, blood flow, and motility (Furness, 2012; Holzer, 2006; Sveshnikov, Smirnov, Myasnikov, & Kuchuk, 2012). Sympathetic projections can induce either an inhibition or a stimulation of stomach contractions (Smirnov & Lychkova, 2003; Sveshnikov et al., 2012). Sympathetic projections are modulated by higher level structures, including parabrachial nucleus, nucleus of the solitary tract (Saper & Loewy, 1980), rostroventrolateral medulla (Deuchars & Lall, 2015), raphe nucleus (Morrison, Sved, & Passerin, 1999), locus coeruleus (Bruinstroop et al., 2012) as well as several hypothalamic nuclei (Deuchars & Lall, 2015).

1.4.4 | Brain-stomach coupling in humans

In humans, pioneering studies identified brain regions coupled with the stomach using gastric distension, induced by inserting and inflating a balloon in the stomach of participants, or, alternatively, by asking participants to drink a specific amount of liquid. Water ingestion can also be used to measure explicit gastric interoception, as recently proposed by van Dyck et al., 2016. Gastric distension activates somatomotor regions, insula, vmPFC and mid-cingulate, and deactivates occipital regions (Ladabaum et al., 2001; Lu et al., 2004; van Oudenhove et al., 2009; Vandenbergh et al., 2005; Wang et al., 2008). More recently, stomach-brain coupling was investigated during the resting state, without gastric stimulation. Rebollo et al., 2018, recorded the EGG in healthy participants during quiet rest, while simultaneously recording brain activity with functional magnetic resonance imaging. They then identified the regions where spontaneous fluctuations in the BOLD signal were phase-synchronized with the gastric rhythm. This revealed an extended network including primary and secondary somato-sensory cortices, mid-cingulate areas, and extended portions of the occipital lobe, indicating that gastric-brain coupling contributes to the large-scale organization of brain activity at rest.

2 | THE EGG: RECORDING, PREPROCESSING, AND DATA QUALITY ASSESSMENT

The aim of this section is to propose practical suggestions to record the EGG in the typical young and healthy population sampled in psychophysical research, as well as a semi-automatized procedure to assess data quality and to extract the gastric rhythm characteristics in terms of amplitude, frequency, and phase. The procedure aims at identifying the gastric rhythm, that is, a regular oscillation in the normogastric range (2–4 cpm). Such a signal can safely be attributed to the stomach, whereas artifacts are likely to disrupt the regularity of the rhythm. It follows that the procedure as it currently stands is not appropriate to investigate departure from normogastria. The procedure reported here is also not designed to analyze the spatial propagation of the gastric waves along the stomach, and we refer the interested reader to Angeli

et al., 2015; Bradshaw et al., 2016; Gharibans, Coleman, Mousa, & Kunkel, 2019; O'Grady et al., 2010, 2012.

2.1 | Recording apparatus

The EGG is recorded with standard cutaneous electrodes, similar to electrocardiogram electrodes, and standard skin preparation (e.g., slight abrasion of the skin for optimal skin-to-electrode interface contact). EGG amplitude lies typically between 50 and 500 microVolt, commensurate with electroencephalography (EEG). Standard EEG acquisition systems can thus adequately amplify EGG signals, but several additional conditions must be met, due to the very slow pace (~0.05 Hz) of the gastric rhythm. First, DC amplifiers are best suited to record the EGG since even a very low high-pass filter might distort the data. Most recent EEG acquisition systems have the large analog-digital conversion range required for DC recordings without amplifier saturation. Second, recordings have to be long enough to collect a sufficient number of gastric cycles. As a rule of thumb, one minute contains about three gastric cycles, and 15 min correspond to only 45 cycles. Note that it can be useful to acquire some extra data (about 40 s) before and after the period of interest to facilitate off-line filtering at the very low frequency of the gastric rhythm. Last, sources of very slow fluctuations in the recordings have to be minimized. In particular, hanging wires might swing around and induce slow drifts in the recordings and should thus be taped to a fixed support. Wrapping the wires in a shield can limit wire swinging as well as reduce electromagnetic artifacts. Because EGG frequency is around 0.05 Hz, sampling frequency could in principle be very low (below 1 Hz). However, a higher sampling frequency is required for proper artifact identification, in particular, participant's movements that are accompanied by muscle artifacts.

2.2 | Participants

2.2.1 | Participants' information and inclusion

Participants are informed early in the inclusion process of electrode location, which implies that their shirt is raised, their skin exposed between navel and sternum, and shaved if too hairy. Participants feeling uncomfortable with the procedure can thus withdraw at that early stage, and are informed that they can withdraw at any time later on. Participants might also feel more comfortable if the experimenter placing the electrodes is of the same gender as the participant. Last, participants are asked to avoid tight-fitting clothes that might potentially touch the electrodes and hence compromise recording quality.

Participants should obviously have no gastric or digestive disorder. Several medications might influence the EGG, including prokinetic anti-emetic agents, narcotic analgesics, anticholinergic drugs, and anti-inflammatory agents, as well as probiotics and prebiotics (Américo, Miranda, Corá, & Romeiro, 2009; Chiba et al., 2007; Indrio et al., 2009; Walldén, Lindberg, Sandin, Thörn, & Wattwil, 2008). Different recommendations exist in the gastroenterology literature with regards to the inclusion of participants taking these medications (Murakami et al., 2013; Riezzo et al., 2013; Yin & Chen, 2013). A practical solution for psychophysiological studies in healthy participants is to include only subjects without medication.

Another inclusion/exclusion criterion that might prove useful is the body mass index (BMI, Weight (kg)/ (Height (m))^2). Participants with a high BMI typically display a lower EGG amplitude (Riezzo, Pezzolla, & Giorgio, 1991; Simonian et al., 2004; Somarajan, Cassilly, Obioha, Richards, & Bradshaw, 2014), potentially because a thicker abdominal wall increases the distance between the electrical source and the recording electrodes and hence results in a lower amplitude recording (Liang & Chen, 1997; Obioha et al., 2016). In addition, people with high BMI show more activity outside the 2–4 cpm range (McCallum, Jones, Lin, Sarosiek, & Moncure, 2001; Simonian et al., 2004; Tolj, 2007), and in morbid conditions, altered gastric emptying (McCallum et al., 2001; Tosetti et al., 1996). In sum, it thus might prove advantageous to include only rather lean participants. In practice, we include subjects with a BMI comprised between 18 and 26. Note that the phase of the menstrual cycle might impact EGG frequency (Parkman et al., 1996; Tolj, 2007) and should thus be documented if the absolute EGG frequency is a parameter of interest.

Studies in gastroenterology focus on the typical EGG amplitude increase following food ingestion, reflecting muscle contractions and gastric motility and other parameters (Stern, Jokerst, Livine, & Koch, 2001; Stern et al., 1989). Another option for psychophysiology is to ask participants to fast for at least 2 hr preceding their appointment (i.e., about 3 hr before the actual beginning of the recording) to focus the analysis on the basal gastric rhythm in an almost empty stomach with little muscular contractions. Only about 10% of a solid meal remains in the stomach 2 to 3 hr after meal ingestion (Vasavid et al., 2014). In any case, the time elapsed since the last meal should be documented and taken into account in the experimental design. Note that details on the contents of pre-fast meal and feeling of hunger at the time of recordings are potentially relevant parameters but were not recorded in this data set.

2.2.2 | Participants' position

Most studies in gastroenterology record EGG with the patient in a lying position, which reduces voluntary movements,

although ambulatory EGG recordings are currently being developed (Gharibans et al., 2018). Another advantage of a lying position is that the electrodes rest on the abdominal surface and not in fatty folds (Koch & Stern, 2004). However, a good EGG can also be obtained in a sitting position, although the amplitude is typically a bit lower, most likely due to the distance of the stomach to the skin surface (Jonderko, Kasicka-Jonderko, & Blonska-Fajfrowska, 2005). In practice, we place the electrodes while subjects are in a standing or lying position, thus allowing easier access to anatomical landmarks. After electrodes are placed, we record from participants in a semi-reclined sitting position, as is customary for MEG or EEG recordings, and ask participants to avoid any voluntary movement. Movements induce large artifacts in the recording, and artifacted data segments should be identified and excluded from further analysis (Verhagen et al., 1999).

2.3 | Electrode placement

Unlike electrocardiography, electrode placement in electrogastrography is not standardized. The stomach is located in the upper left abdomen but the precise location with respect to external landmarks varies (Gharibans et al., 2019). Many clinical studies used between 2 and 4 electrodes. We initially used a 17 electrode grid (Richter et al., 2017), which proved too large, and after some trials and errors found that a grid of seven electrodes provided sufficient coverage to detect a good quality EGG in most participants. The coverage we propose is sufficient to detect a good quality signal in at least one recording location; if the aim of the study is to analyze the propagation of the gastric rhythm along the stomach, a higher density of electrodes and a wider coverage is recommended (Gharibans et al., 2019). Recording locations are illustrated in Figure 4a. The electrode location proposed here deviates from the electrode location reported in the clinical literature (see for instance the review of Riezzo et al., 2013) in that it covers lower portions of the abdomen. In clinical settings, electrodes are most often located in the vicinity of electrodes 2, 3, 5, and 7 in Figure 4 (Chen et al., 1999; Geldof et al., 1989; Koch & Stern, 2004; Mintchev et al., 1993; Parkman et al., 2003; Simonian et al., 2004).

In the proposed setup (Figure 4a) the first electrode (1) is placed 2 cm above the umbilicus. Electrodes 2 and 3 are placed above electrode 1 on the midline, at, respectively, one-third and two-thirds of the distance between electrode 1 and the xiphoid process. The locations of two other electrodes (6, 7) are determined by a vertical line crossing the midpoint of the left clavicle, and horizontally by the locations of electrodes 1 and 2. Note that the electrode 7 location might fall above the rib cage, in which case it is advisable to shift it toward the midline to improve the signal to noise ratio. Finally, electrodes 4 and 5 are placed in between the two columns

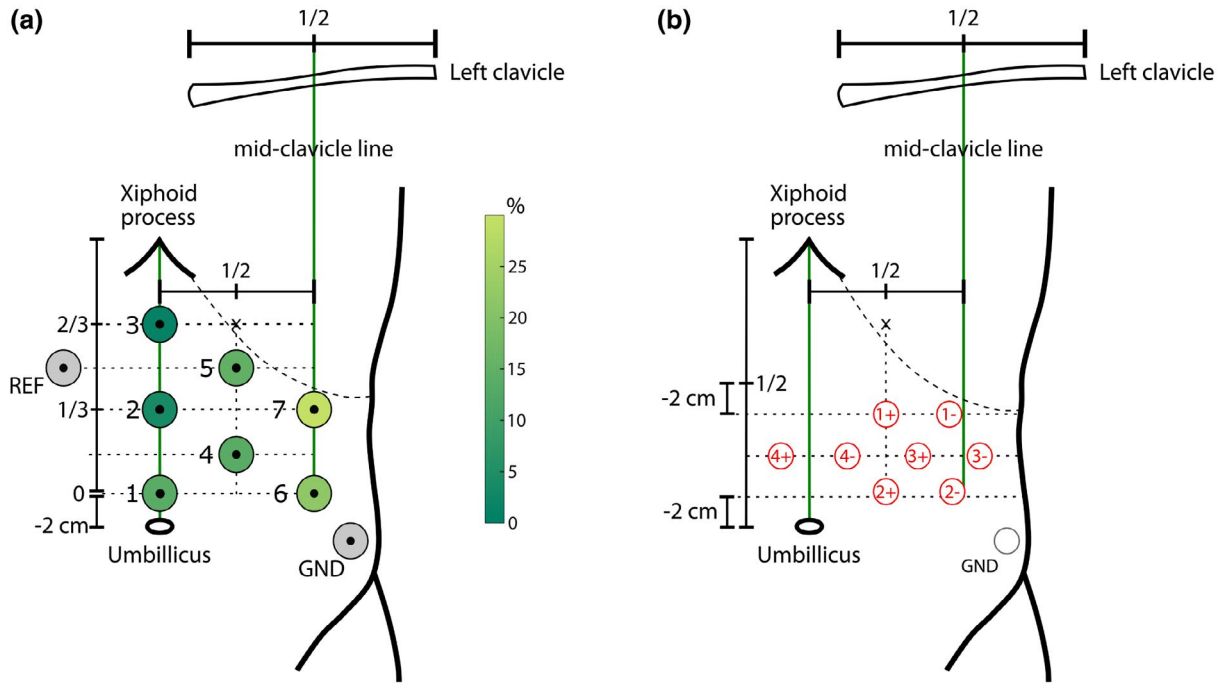

FIGURE 4 Localization of electrodes with respect to anatomical landmarks (umbillicus, xiphoid process, mid-clavicular line, and coastal margin). (a) Setup for a unipolar montage. The circle area and color code at each electrode location indicate how often this electrode was found to display the largest gastric rhythm, in a sample of 100 healthy participants with a good spectral signature of the gastric rhythm. (b) Setup for a bipolar montage, better suited for fMRI recordings. See text for detailed explanations. REF: Reference. GND: Ground

(1, 2, 3) and (4, 5), at the level of the vertical midpoint between electrodes 1 and 2 and electrodes 2 and 3. The reference electrode is placed symmetrically to electrode 5. Finally, the ground electrode is placed over the left abdomen, above the iliac crest. This setup can be combined with EEG and/or MEG recordings.

The EGG can also be recorded in an MRI environment, but it might require the use of bipolar electrodes to avoid amplifier saturation. We used the following scheme (Figure 4b; Rebollo et al., 2018): Four bipolar electrodes are placed in three rows over the abdomen, with the negative derivation placed 4 cm to the left of the positive one. The midpoint between the xiphoid process and umbilicus is identified, and the first electrode pair is set 2 cm below this area, with the negative derivation (1−) set at the point below the rib cage closest to the left mid-clavicular line. The second electrode pair (2+, 2−) is set 2 cm above the umbilicus and aligned with the first electrode pair. The positive derivation of the third pair (3+) is set in the center of the square formed by electrode pairs one and two. The positive derivation of the fourth electrode pair (4+) is centered on the line traversing the xiphoid process and umbilicus at the same level as the third electrode. The ground electrode is placed above the iliac crest (Figure 4b). Note that scanner artifacts are much faster than the gastric rhythm and can easily be filtered out, at least with a standard echo-planar imaging sequence and that the B0 magnetic field of the scanner does not affect EGG frequency (Rebollo et al., 2018).

2.4 | Power spectrum and channel selection

The first step in data analysis is to extract the gastric rhythm. We first present processing steps for a good quality recording and come back to noisy data and artifacts in section 2.6. Spectral power at each electrode is computed to identify the location with the largest activity in the normogastric 0.033–0.066 Hz (2–4 cpm) range and to determine the peak frequency of each participant. Several methods for spectral power estimation can be used. Here, we used a Fast Fourier Transform (FFT) as implemented in the Fieldtrip toolbox (Oostenveld, Fries, Maris, & Schoffelen, 2011) with a Hanning taper to reduce spectral leakage and control frequency smoothing. We provide the relevant code for spectral estimation and other analyses at https://github.com/niwolpert/EGG_Scripts (for computing the power spectrum, see function “compute_FFT_EGG”). As illustrated in Figure 1c, a good quality recording shows a distinctive spectral signature in the normogastric range, with a peak frequency similar at most, if not all, recording sites. The channel with the largest power at peak frequency is selected for further analysis. Note that the spectral signature of the EGG is clearly different from the spectral signatures of either respiration or heartbeats (Figure 1d), and that a harmonic at twice peak frequency might be observed. Peak frequency is usually fairly stable over a couple of hours but might vary over longer recording times (Lindberg, Iwarzon, & Hammarlund, 1996). Power and amplitude might also be extracted from the spectral analysis.

2.5 | Phase and amplitude of the filtered signal

For a more refined, time-resolved analysis of the EGG, the next step is to filter the raw EGG from the selected channel around the participant's peak frequency to better isolate the gastric rhythm. Several types of filters might be considered, bearing in mind that the very low frequency of the EGG imposes additional constraints on filter design and filter stability. We opted for a finite impulse response filter, known to be more stable and less likely to introduce nonlinear phase distortions (Cohen, 2014), and more precisely a third-order frequency sampling designed finite impulse response filter (MATLAB: FIR2), with a bandwidth of ±0.015 Hz around the participant's peak EGG frequency (function “compute_filter_EGG”). For instance, if peak frequency is exactly 0.05 Hz (3 cpm), the filter covers the range between 0.035 and 0.065 Hz (2.1 and 3.9 cpm). If peak frequency is 0.035 Hz (2.1 cpm), close to the lower limit of the normogastric range, the filter range is 0.02–0.05 Hz (1.2–3 cpm) and therefore also includes signal outside the normogastric range. Of note, filtering, especially at low frequencies, is difficult, and the actual filter deviates from the ideal filter, with smoother transitions, extending at higher and lower frequencies, as illustrated in Figure 6a. Filter width is designed to be wide enough to capture physiological fluctuations in the duration of the gastric cycle, but narrow enough to exclude not only respiration, but also the harmonic of the gastric rhythm (Verhagen et al., 1999).

By applying the Hilbert transform to the filtered data, we retrieve the instantaneous phase and amplitude envelope of the gastric rhythm. Figure 5 shows two examples of the filtered signal, and amplitude and phase obtained after applying the Hilbert transform. The distribution of cycle duration is usually Gaussian (Figure 5b), with sometimes outliers (Figure 5d), defined as exceeding mean ± 3 *SD*s. We observed that cycles with abnormally long or short duration also often presented a nonmonotonous phase evolution (inset in Figure 5c).

2.6 | Identification of noisy recordings

We have presented so far good quality recordings. Identifying noisy recordings, or noisy segments of data, is of course

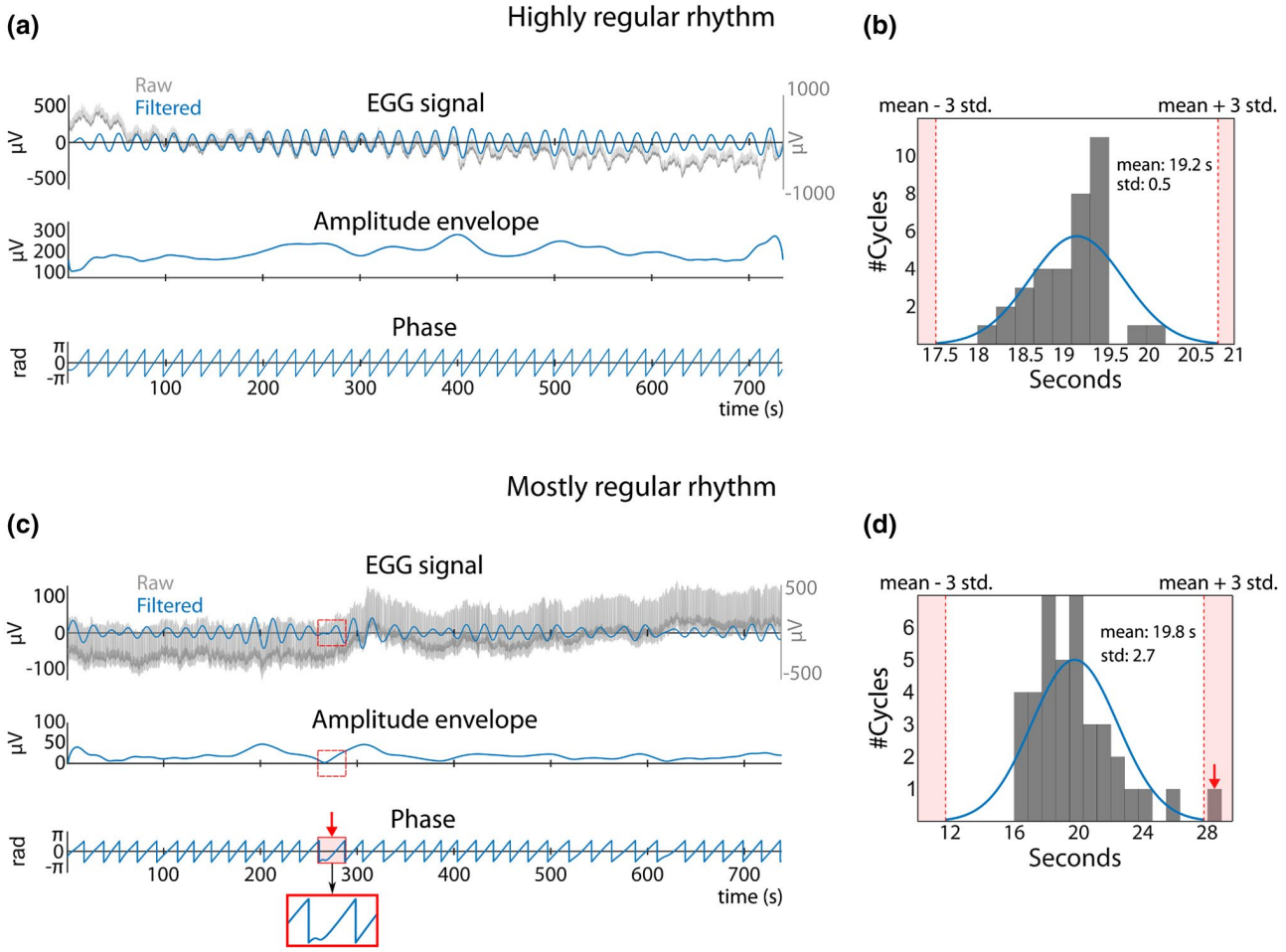

FIGURE 5 Two examples of EGG signal and corresponding amplitude and phase that reveal a highly regular rhythm (top) or a mostly regular rhythm (bottom). (a) Top row: Raw signal (grey) with superimposed filtered EGG (blue), obtained by filtering the raw signal ±0.015 Hz around the peak frequency of the recording. The Hilbert transform generates two time series: the amplitude envelope (middle row) and instantaneous phase of the gastric rhythm in radians (bottom row). (b) Distribution of cycle durations. Red dotted lines indicate mean cycle duration ± three *SD*s. In this example, the distribution of cycle duration is quite narrow, without any outlier. (c) Example of a different recording with mostly regular phase time series. The gastric rhythm is not always visible to the naked eye in the raw signal (top row) and its amplitude is sometimes very low (middle row). A cycle shaded in red and marked by a red arrow shows a nonmonotonous change in phase (bottom row) and concomitant low amplitude. (d) Histogram of cycle duration. The cycle with nonmonotonous change in phase in (c) appears as an outlier (red arrow). The cycle is considered as an artifact (nonmonotonicity and cycle duration) and therefore discarded from further analysis

critical. In the following, we suggest some criteria to guide decisions.

2.6.1 | Power spectra

The power spectrum is a good indicator of data quality. As shown in Figure 6a, a high-quality recording shows a clear spectral peak in normogastric range with a peak frequency that is congruent across several channels. We systematically discarded power spectra with variability in peak frequency between electrodes (Figure 6b-e). We also discarded cases where a clear spectral signature is observed, but at only one location, as in Figure 6f. As detailed in Section 3, the power at peak frequency (between 26 and 8,800 μV^2 in our data) does not appear as a reliable indicator of signal quality.

2.6.2 | Identification of participants with highly variable gastric cycle duration

Once the EGG is filtered at the selected channel around peak frequency, we do a second quality check based on the regularity of the cycle durations. We estimated, in each participant, cycle duration from the phase of the Hilbert transform and computed the *SD* of cycle duration (see function "compute_std_cycle_duration"). The distribution of the *SD* of cycle duration in the 100 participants we recorded is shown

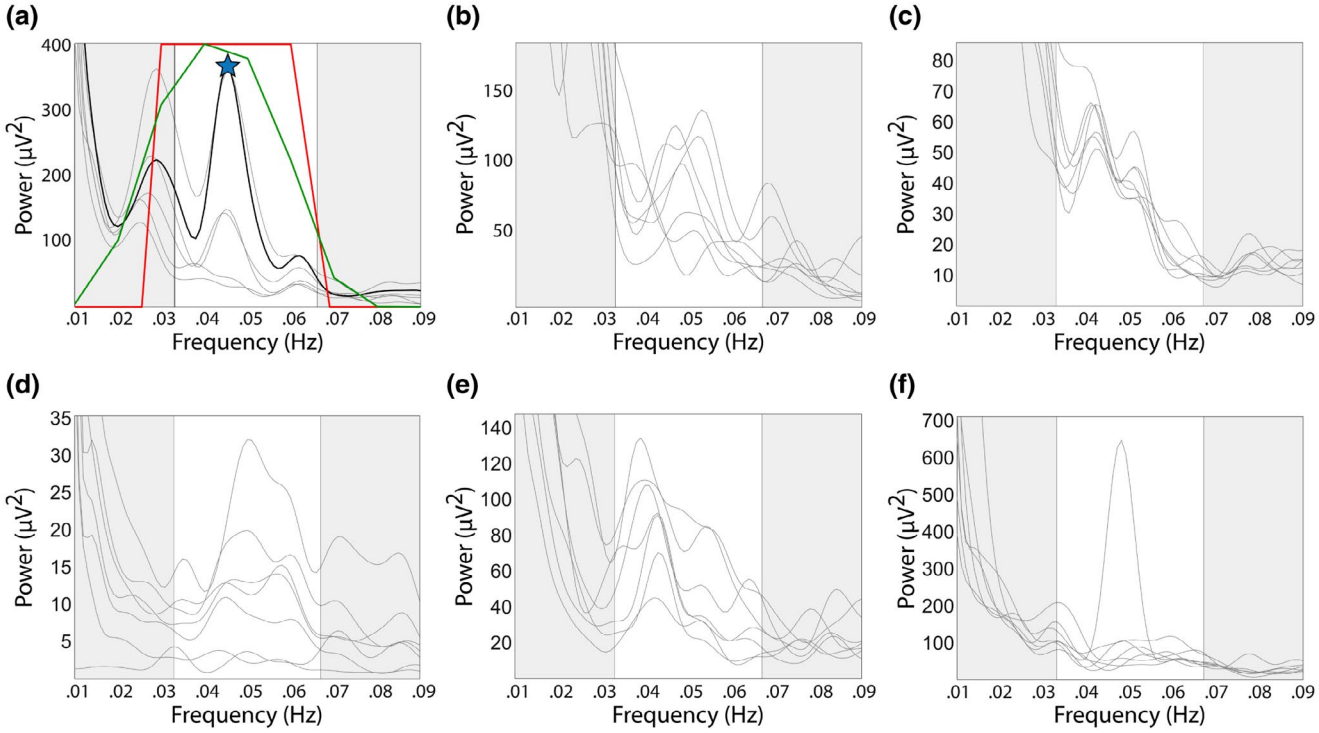

FIGURE 6 Examples of power spectra of data included in further analysis (a) or discarded (b-f). Each line corresponds to a recording channel, and the spectral region highlighted in white corresponds to normogastria. (a) Power spectrum with a well-defined spectral peak in the normogastric range, occurring in several channels at the same frequency. The star indicates peak frequency and the black line corresponds to the channel with the largest power at peak frequency. The red line represents the ideal filter, and the green line the best fit for the ideal filter. (b) Power spectrum with peaks at different frequencies in different channels. (c) Power spectrum with spectral peaks at two different frequencies. (d) Power spectrum with a broad peak, well defined in only one channel. (e) Several channels display a spectral peak but at different frequencies. (f) A well-defined spectral peak is present, but only in one channel

in Figure 7a. Four participants clearly lie outside the distribution and are considered outliers. We retained a criterion of the *SD* of cycle duration smaller than 6 to include participants in further analysis.

We compared this data-driven procedure with a procedure based on the clinical EGG literature (see function "show_prop_normogastria"), where it is held that EGG recordings in a healthy subject should be composed of at least 70% cycles in the normogastric range (2–4 cpm, or cycle duration between 15 and 30 s) (Parkman et al., 2003; Riezzo et al., 2013). *Bradygastria* refers to slow cycles ranging between 30 and 60 s (1–2 cpm) and *tachygastria* to short cycles between 6 and 15 s (4–10 cpm) (Riezzo et al., 2013). We found that those four participants identified as outliers in the distribution of *SD* of cycle duration (Figure 7a) are also outliers in the percentage of cycles in normogastria and exhibit less than 70% cycles in the normogastric range (Figure 7b). The two criteria thus appear equivalent in this data set.

Note that this processing step is dependent on the filter width (ideal and best fit) used. It is not suited for studies attempting to induce shifts in gastric peak frequency, resulting in a larger variability of gastric cycle duration or even in a shift of gastric peak frequency outside the normogastric range, as when eliciting nausea or disgust (Geldof et al., 1989; Harrison et al., 2010; Meissner et al., 2011; Stern et al., 1985).

2.7 | Identification of artifacted data segments

Once recordings of overall good quality have been selected, artifacts transiently affecting the data have to be identified. Any type of artifact which involves a movement of the wires or of the abdominal wall might contaminate the signal. This includes for example movement of the legs, abdomen or torso, touching of the electrodes or wires, talking or coughing. Artifacts perturb the signal not only at the exact time of their occurrence, but spread over time given the very low frequency of the filter used.

The procedure we propose to identify artifacted data segments is based on two criteria: a cycle whose length exceeds the mean ±3 *SD*s of the cycle length distributions (Figure 5b, d), and a cycle that displays a nonmonotonic change in phase (inset in Figure 5c). This procedure is implemented in the function "detect_EGG_artifacts." Any cycle meeting at least one of those criteria is considered as artifacted. Note that whether cycles tagged as artifacted by this procedure represent

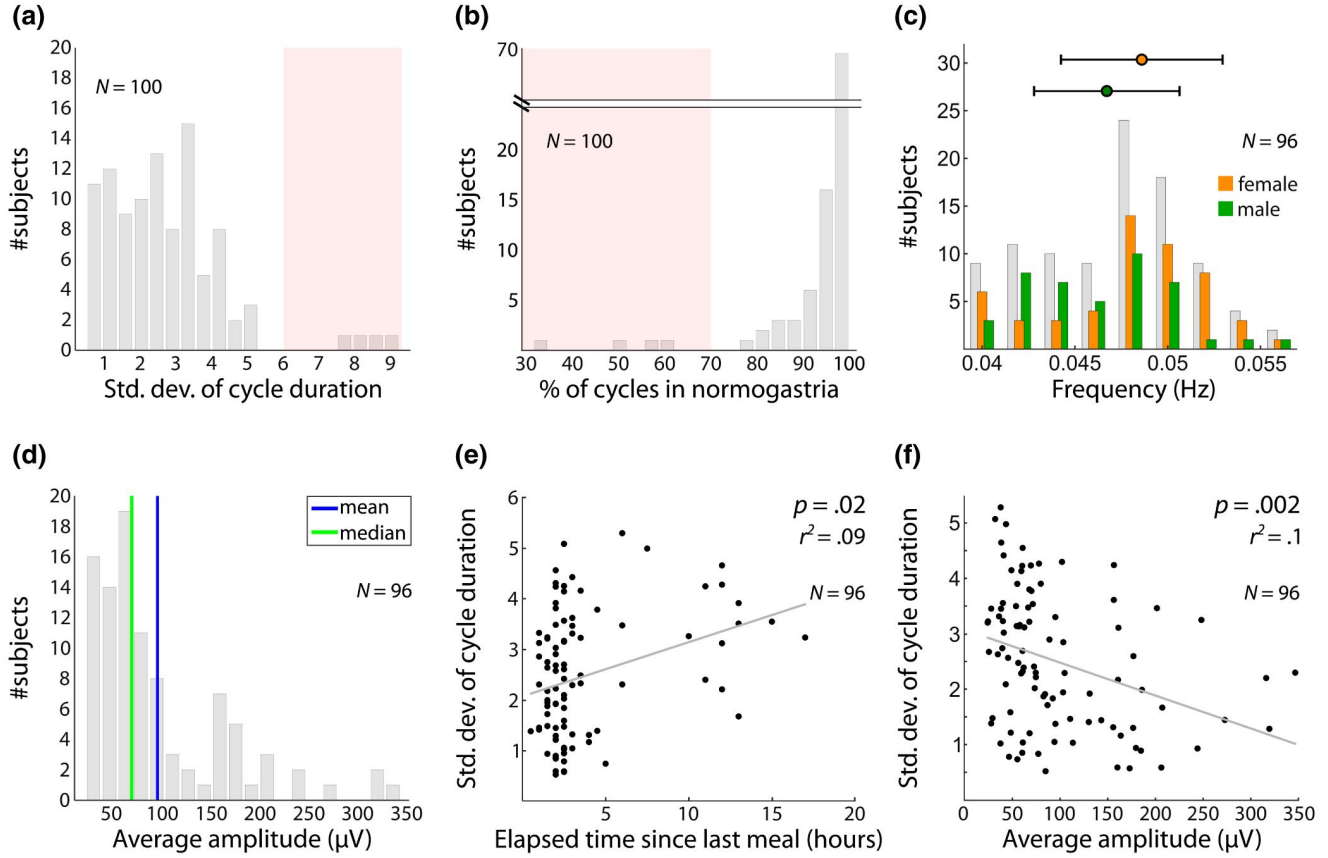

FIGURE 7 Distribution of EGG features across a sample of 100 young healthy participants. (a) Distribution of *SD*s of cycle duration. A cutoff at six *SD*s (red shaded area) isolates four outlier participants with more irregular cycles. (b) Percentage of cycles in normogastria (2–4 cpm). A cut-off at 70% (red shaded area), as proposed by the clinical literature (Riezzo et al., 2013) isolates the same four outlier participants. (c) EGG peak frequency in the 96 remaining participants, with a mean of 0.048 Hz and *SD* of 0.004 Hz. Peak frequency is higher in female ($M = 0.0486$ Hz, $SD = 0.0044$) than male ($M = 0.0467$ Hz, $SD = 0.0039$) participants (rank sum test $z = -2.25$, Bonferroni-corrected $p = .15$). Horizontal bars represent the *SD*. (d) Robust correlation between BMI and average amplitude. BMI shows no significant relationship with mean amplitude (Bonferroni-corrected $p = 1$). (e) Robust correlation between elapsed time since the last meal and variability of cycle duration, expressed in *SD* around the mean for each participant. Longer fasting is associated with higher cycle irregularity (robust regression, Bonferroni-corrected $p = .02$, $r^2 = .09$), an effect mostly driven by prolonged fasting (>10 hr). (f) Robust correlation between average amplitude and *SD* of cycle duration. There is a significant negative relationship, with higher amplitude being associated with lower variability of cycle duration (robust regression, $p = .002$, $r^2 = .10$)

real artifacts or truly irregular gastric activity remains an open question.

It is advisable to complement the semi-automated procedure we propose by a visual inspection to confirm artifact detection (Verhagen et al., 1999), but also to verify that the filtering, which can get unstable at very low frequencies, did not induce signal distortion.

2.8 | Conclusion on preprocessing steps

We propose a preprocessing procedure of the EGG consisting of different steps with associated quality checks. All steps aim at identifying a regular rhythm, with a progression in the refinement of the analysis level. This procedure is summarized in Figure 8: In a first step, we decide whether the peak in the power spectrum is clear enough, with a peak frequency consistent between recording sites, to allow for the selection of a channel and a peak frequency. In a second step, the data are filtered and the phase computed, together with the distribution of cycle length. If at least 70% of the cycles lie in the normogastric range, and/or if the *SD* of cycle length is smaller than 6, the recording is considered to be of sufficient quality, else it is discarded. The last step consists of identifying artifacted data segments, based on cycle duration and phase monotonicity within a cycle.

3 | NORMATIVE DATA AND INTERINDIVIDUAL VARIABILITY IN YOUNG, HEALTHY VOLUNTEERS

Here, we apply the procedures described in Section 2 in a large data set of EGG recordings ($N = 117$) obtained in

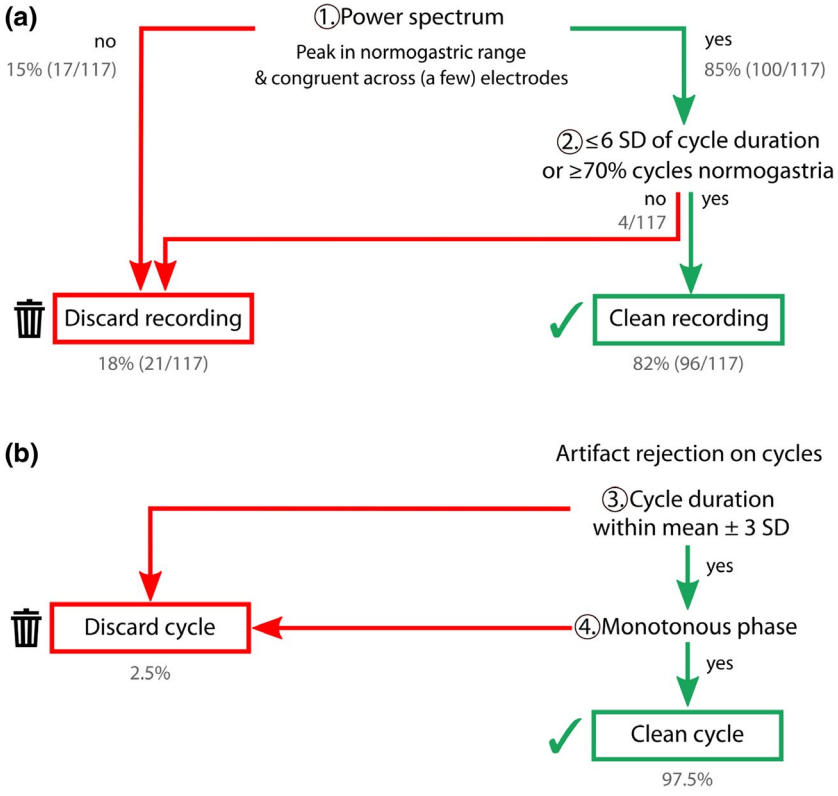

FIGURE 8 Decision tree with processing steps and corresponding criteria for a good quality recording/cycle. Grey numbers document the outcome of this procedure in a data set of 117 participants. (a) Decision tree for whether or not the recording can be retained for further analysis, depending on the presence of the spectral signature of the gastric rhythm and rhythm regularity. (b) Additional decision tree to detect artifacted cycles, based on the cycle duration and monotonicity of phase evolution

our group, from which normative parameters of the gastric rhythm in a healthy, young, and rather lean population can be derived.

3.1 | Material

We used the data from 117 healthy participants (52 male, 65 female) sitting in a reclining chair. Participants were aged between 18 and 30 years (mean: 24, $SD = 3.1$) and had a BMI comprised between 16 and 26 (mean: 21.3, $SD = 2.03$). We aimed at recording participants in a moderate fasting state, where stomach contractions are scarce, and thus asked participants to fast for at least two hours before their appointment. One data set ($N = 17$) corresponds to the re-analysis of published data (Richter et al., 2017), the rest corresponds to various unpublished pilot studies. Most participants ($N = 75$, including the participants from Richter et al., 2017) were recorded for 12–15 min at rest with eyes open using the MEG acquisition system of Elekta Neuromag® with a sampling frequency of 1,000 Hz, DC to 330 Hz. EGG data were also recorded in 25 participants performing an experiment on visual perception at a threshold for 12 min, and 17 subjects viewed a short movie ("Bang! You're Dead" from Alfred Hitchcock, 1961) during 15 min, using a BioSemi acquisition system with a sampling frequency of 2048 Hz, DC to 400 Hz. A subset of 66 participants filled out the Trait Anxiety Inventory (Spielberger, Gorsuch, Lushene, Vagg, & Jacobs, 1983). All participants signed a written informed consent and were paid for participation. The procedures were approved by the Ethics Committee CPP Ile de France III and were in accordance with the Helsinki declaration.

EGG was recorded as described earlier. We used the montage of seven electrodes described above, except in the 17 participants of Richter et al., 2017. Here, we had used a bilateral grid of 19 EGG electrodes (17 active, 1 reference, and 1 ground) placed over four regularly spaced rows, that we subsampled to match the current seven active electrodes schema.

3.2 | Results

3.2.1 | EGG identification in 117 recordings

We applied the procedures described above to the 117 EGG recordings (Figure 8). A well-defined spectral peak within the normogastric range could be observed in 100 participants out of 117 (85%). The BMI of the 100 participants with an identifiable spectral peak ($M = 21.2$, $SD = 2$) was slightly, but significantly, lower than the BMI of the 17 participants where the peak could not be found ($M = 22.3$, $SD = 2$; $t(115) = -1.99$, $p = .049$). We then discarded participants whose gastric rhythm was irregular. Two different criteria could be considered, either a *SD* of gastric cycle duration larger than 6 (Figure 7a), or less than 70% of cycles in normogastria (Parkman et al., 2003; Riezzo et al., 2013). Those two criteria converged on the same four participants. Overall, our procedure was successful at recording and identifying the gastric

rhythm in 82% (96/117) of the participants. Within the 96 remaining participants, 16 come from the study of Richter et al., 2017, and 80 from the new, unpublished data sets. Within the 96 recordings selected, 2.5% of the cycles were identified as artifacted, that is, as having an excessively long or short duration, or as displaying a nonmonotonous change in phase.

3.2.2 | Electrode selection

For each participant, we identified, within the seven electrode grids, the electrode with the strongest peak in the 0.033–0.067 Hz range and selected it for all further analysis. The location of the selected electrode varied on a participant-by-participant basis, with electrode 1 selected in 14% of participants, electrode 2: 4%, electrode 3: 1%, electrode 4: 14%, electrode 5: 15%, electrode 6: 22%, electrode 7: 30%. Figure 4a shows, for each location in the grid, how often it was selected. The electrode showing the highest peak in the normogastric range was in the lower left abdominal region in more than half of the participants (electrodes 6 and 7) but all locations proved useful in at least one participant.

3.2.3 | Analysis of gastric frequency, amplitude and cycle duration variability

We then analyzed several properties of the EGG in the 96 remaining participants. Mean dominant EGG frequency was 0.048 Hz (SD = 0.004) (Figure 7c). Female subjects had a slightly higher mean peak frequency than males, but this difference did not survive correction for multiple comparisons (Figure 7c; M_{female} = 0.0486 Hz, SD = 0.0044; M_{male} = 0.0467 Hz, SD = 0.0039; rank sum test $z = -2.25$, uncorrected $p = .03$; Bonferroni-corrected $p = .15$). As detailed in Table 1, we found no link between EGG peak frequency and age, BMI, anxiety, time of recording (morning versus. afternoon) or elapsed time since the last meal.

The mean average amplitude across participants was 97.3 μV (SD = 70.2) (Figure 7d). None of the demographical variables tested revealed any link with amplitude (Table 1), including BMI.

Last, we estimated fluctuations in EGG frequency by computing the SD of cycle duration. There was a significant positive correlation between longer fasting and higher variation in cycle length (Bonferroni-corrected $p = .02$, $r^2 = 0.09$; Figure 7e), mostly driven by subjects with an elapsed time since last meal larger than 10 hr. Participants with a large EGG amplitude had more regular cycles, as revealed by the negative correlation between amplitude and SD of cycle length ($p = .002$, $r^2 = 0.1$; Figure 7f). None of the other variables measured co-varied with the SD of cycle duration.

TABLE 1 Descriptive statistics for EGG parameters and statistical relationships with sex, age, BMI, anxiety scores, daytime of recording and time from last meal

	Mean	Median	Min	Max	Gender (rank sum test) 43 male, 53 female	Age (robust correlation) $N = 96$	BMI (robust correlation) $N = 96$	Anxiety (robust correlation) $N = 66$	Time of recording (rank sum test morning vs. afternoon) $N = 100$	Elapsed time since last meal (robust corr.) $N = 100$
Peak frequency (Hz)	0.048	0.048	0.04	0.057	$p = .15$	$r = -.06$ $p = 1$	$r = -.04$ $p = 1$	$r = .05$ $p = 1$	$p = 1$	$r = -.07$ $p = 1$
Average amplitude (μV)	97.3	70.7	24	346.6	$p = 1$	$r = .05$ $p = 1$	$r = -.14$ $p = 1$	$r = -.1$ $p = 1$	$p = 1$	$r = -.06$ $p = 1$
%normogastria	96	98	79	100	$p = 1$	$r = .02$ $p = 1$	$r = -.1$ $p = 1$	$r = .05$ $p = 1$	$p = 1$	$r = -.22$ $p = .22$
SD Dev cycle duration	2.5	2.4	0.5	5.2	$p = 1$	$r = -.06$ $p = 1$	$r = .14$ $p = 1$	$r = .11$ $p = 1$	$p = 1$	$r = .3$ $*\mathbf{p = .02}$

Note: p values are Bonferroni-corrected for the six tests performed. Significant results (corrected for multiple comparisons) appear in bold font.
*Indicates Bonferroni-corrected $p < .05$.

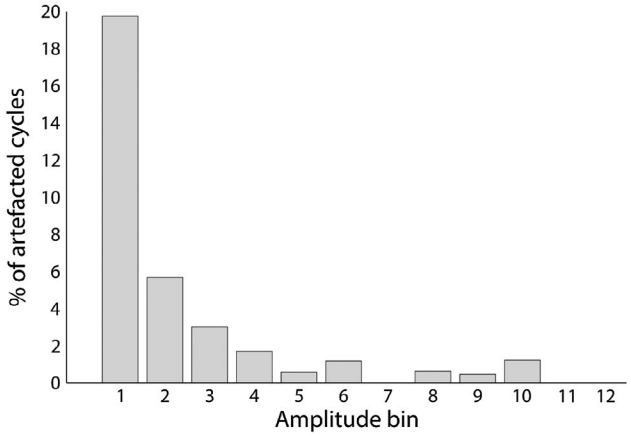

FIGURE 9 Percentage of EGG cycles classified as artifacted because of nonmonotonicity, as a function of EGG amplitude. Only 20% of the nonmonotonous cycles also have a very low amplitude

The data came from different experimental conditions (resting state, acquired with a BioSemi system, and various visual tasks, acquired with a BioMag system). No meaningful differences were found between experiments for any of the EGG parameters tested, apart from a difference in EGG amplitude, which might reflect more a difference in gain calibration between the two recording systems rather than on experimental conditions.

3.2.4 | Amplitude in clean versus artifacted data segments

We finally compared EGG amplitude in "clean" versus artifacted cycles, that is, cycles that were either of extreme duration or nonmonotonous. No significant difference in amplitude was found between clean cycles ($M = 96.6$ μV, $SD = 86.3$) and cycles of extreme duration ($M = 86$ μV, $SD = 51.2$; rank sum test $z = -.4$, $p = .67$). Amplitude in nonmonotonous cycles ($M = 40.3$ μV, $SD = 39$) was significantly lower than in clean cycles ($M = 96.6$ μV, $SD = 86.3$; rank sum test $z = -8.5$, $p < .001$). However, as shown in Figure 9, only a small proportion (20%) of the cycles with very low amplitude were nonmonotonous, and a number of nonmonotonous cycles have a large amplitude.

4 | DISCUSSION

We propose here a procedure for recording and analyzing EGG data, and test this approach in 117 healthy, young, and rather lean male and female participants who had been fasting for at least two hours. The analysis pipeline aims at identifying a regular rhythm that can be safely attributed to the stomach, through multiple steps: by selecting only those participants who have a well-defined spectral signature, with a peak frequency in the normogastric range (2–4 cpm) and regular cycles, and by excluding cycles whose duration exceeds mean ± 3 *SD* or whose phase is irregular.

We could identify the spectral signature of the gastric rhythm in 85% of the participants, most often at lower left abdominal locations. The largest amplitude could often be observed at electrodes located lower than usually recorded in clinical settings (Chen et al., 1999; Riezzo et al., 2013). Peak frequency was centered around 0.05 Hz, consistent with the gastroenterology literature, with a marginal difference in peak frequency between female and male participants. The large majority (96%) of the recordings with a clear spectral signature were also regular, with a *SD* of gastric cycle smaller than 6. The latter criterion proved equivalent to the criterion of 70% of cycles in the normogastric range (2–4 cycles per minute/0.033–0.067 Hz) employed in the clinical EGG literature. The parameter that most influenced the EGG was the time elapsed since last meal, with fasting longer than 10 hr leading to a more irregular rhythm. BMI, anxiety, and age had no noticeable relationship with EGG amplitude, frequency or regularity.

4.1 | Electrode montage

We found that the sharpest spectral signature of the gastric rhythm could most often be found over lower left abdominal regions, that is, locations that are lower than in standard clinical settings (Riezzo et al., 2013; Simonian et al., 2004; Yin & Chen, 2013). This result is in line with recent EGG studies, where electrodes also covered a lower portion of the abdomen, but that were additionally informed, via CT scan analysis, on the precise stomach location and geometry in both patients and healthy controls (Gharibans, Kim, Kunkel, & Coleman, 2017, 2019). Both in the Gharibans et al. studies, and in ours, participants were seated, slightly or half-reclined, thus differing from most clinical studies where a lying position is the norm (e.g., Geldof et al., 1989; Kaneoke et al., 1995; Lin, 1999), potentially leading to a different stomach position. In addition, we used here the reference electrode location commonly advocated in the clinical literature (Chen et al., 1999) over the upper right abdominal location, which might contribute to observing larger EGG amplitudes more often at the lower left location. While distance to reference electrode might contribute to EGG signal amplitude, it is unlikely to be the only determinant, for two reasons. In some participants, the largest EGG amplitude was detected close to the reference (i.e., electrodes 2 and 3). Conversely, the electrode where the largest EGG amplitude is most often detected (#7) is not the electrode the furthest away from the reference electrode. Note that reference-free EGG data can be obtained by a higher density coverage and the surface laplacian transform (Gharibans et al., 2017).

Still, it is important to bear in mind that electrodes at lower locations might be more likely to record not only from the stomach, but also from other organs of the GI tract (Amaris et al., 2002; Erickson et al., 2019). While the rhythmic activity of the small intestine is at higher frequencies, the frequency range of the colon is broader, covering the frequency range between 0.03 and 0.13 Hz (Amaris et al., 2002; Erickson et al., 2019; Homma et al., 1995; Pezzolla et al., 1989; Riezzo et al., 1998), or even up to 0.2 Hz (Taylor et al., 1975). The frequency range of the colon and of the stomach might thus overlap, but the spectral signature of the stomach seems more narrow-band than the spectral signature of the colon. It is thus important to couple the use of the low electrode montage we advocate with strict criteria to identify the spectral signature of the stomach in the recordings.

4.2 | Data set selection based on spectral analysis and percentage in normogastria

The best evidence for gastric activity is a sharp spectral signature with a peak within the normogastric range. We retained two criteria: the sharpness of the spectral peak, and its presence at several recording locations. Applying those criteria in a rather strict manner led to discarding 18% of the participants, which is quite a large proportion, but this conservative approach should guarantee a large contribution of the gastric rhythm to the recorded signal. This first processing step could, and should, be improved in the future by finding a more quantitative approach to characterize the spectral signature.

The absence of the spectral signature of the gastric rhythm in EGG spectra can be attributed to various reasons. The signal might be too small because the stomach is too far away from the selected recorded locations, either because of an unusual stomach position or because abdominal fat increases the distance between stomach and electrode (Chen et al., 1999; Liang & Chen, 1997). Although participants with high BMI (above 26) are more likely to have more abdominal fat and to display a lower EGG amplitude (Riezzo et al., 1991; Simonian et al., 2004; Somarajan et al., 2014), we do not observe a link between EGG amplitude and BMI. However, participants without an EGG spectral peak had a higher BMI than participants with a spectral peak. This might indicate that abdominal fat can decrease the signal-to-noise ratio to the point that the gastric rhythm can no longer be detected. However, if the gastric rhythm can be detected, its amplitude and frequency do not depend on BMI, at least in the restricted BMI range explored in our sample. Signal to noise ratio might also be compromised because of artifacts, in particular, due to movement of the abdominal wall or of wires. Additionally, the gastric rhythm might be disorganized and hence display a blurred spectral signature, even in healthy participants which were screened for gastrointestinal pathologies.

After assessing power spectra, we quantified the regularity of gastric cycles using two independent approaches (*SD* of gastric duration smaller than 6 or 70% of cycles in normogastria), that converged and identified the same four participants with irregular EGG, out of 100. Note that the criteria on spectral signature are somewhat redundant with the criteria on cycle regularity. Indeed, irregular cycles are likely to result in a wide spectral peak, while we selected recordings with a well-defined spectral signature.

4.3 | Data segment selection

To the best of our knowledge, there is currently no standard for artifact rejection in EGG recordings, although some new methods are being developed for ambulatory recordings (Gharibans et al., 2018). Here, we chose to discard gastric cycles, that is, data segments of about 20 s, if the cycle was excessively long or short or if the phase displayed a nonmonotonous evolution within a cycle. Participants with a large EGG amplitude also had more regular cycles. At the single-subject level, nonmonotonous cycles were more numerous when amplitude was low, but could be also observed in data segments with large amplitude. In other words, while there is a link between amplitude and cycle regularity, there is no one-to-one correspondence. It is important to underline that we do not know whether the cycles we discard represent artifacts (motion, electrical noise, …) accompanied with signal loss or a true irregularity of the gastric rhythm. Our procedure aims at extracting a regular rhythm that can be safely assumed to reflect the gastric rhythm. It is obviously unsuitable for clinical studies or cognitive studies in which irregularities of the gastric rhythm are of interest (see, e.g., Harrison et al., 2010).

4.4 | Factors affecting EGG peak frequency, amplitude, and cycle duration variability

We found that women showed on average a slightly higher peaking frequency than men, a difference that was small and not strong enough to survive correction for multiple comparisons. This is in line with two previous studies (Parkman et al., 1996; Tolj, 2007) in comparably large sample sizes ($N = 83$ and $N = 120$). No effect was detected in smaller samples of adults (Pfaffenbach et al., 1995; Simonian et al., 2004) or in children (Riezzo et al., 1998). We did not document the phase of the menstrual cycle, which might impact EGG activity, although different studies yielded contradictory results (Parkman et al., 1996; Pfaffenbach et al., 1995; Tolj, 2007). Age was not related to EGG peak frequency, amplitude or

cycle length variability, in line with previous studies investigating this age range (18–30 years) (Parkman et al., 1996; Pfaffenbach et al., 1995; Riezzo et al., 1991; Shimamoto et al., 2002; Simonian et al., 2004; Tolj, 2007). Note that our data set stems from a quite homogenous population: We did only include participants with a BMI range comprised between 18 and 26 and with an age between 18 and 30 years. EGG parameters are altered for higher values of BMI (Simonian et al., 2004; Tolj, 2007) or age (Parkman et al., 1996; Pfaffenbach et al., 1995; Riezzo et al., 1991; Shimamoto et al., 2002; Simonian et al., 2004; Tolj, 2007).

As time elapsed since the last meal increased, the EGG became more irregular. The correlation was mostly driven by participants having had their last meal more than 10 hr before the recording, that is, participants who had skipped breakfast. This suggests that in order to increase the chance of recording a regular signal, it might be recommended to ask participants to have a meal 2 to 4 hr before the recordings. This finding might potentially be linked to the observation that during very prolonged fasting (typically overnight), the stomach shows transient periods of strong contractions (also called the "phase III of the interdigestive complex"—Koch & Stern, 2004), which could impact the stability of the EGG. Combined with the classical finding that EGG amplitude increases right after a meal, these results emphasize the importance of taking into account the time elapsed since last meal in the experimental design (for instance by counterbalancing the order of presentation of different conditions between participants) and data analysis (for instance by adding time elapsed since last meal as a regressor).

Note that we restricted the analysis to a subset of EGG parameters (peak frequency, amplitude, cycle duration variability, percentage normogastria). Other parameters of interest, not studied here, are related to departure from normogastria (see e.g., Koch & Stern, 2004; Riezzo et al., 2013; Yin & Chen, 2013).

4.5 | Conclusion: strengths and limitations

We propose here a full pipeline to record and analyze the EGG of young, healthy, and rather lean participants in a moderate fasting state, and validate it in a large data set. The pipeline aims at identifying a rhythm with a peak frequency between 0.033 and 0.067 Hz (2–4 cpm), and regular enough over time, so that it can safely be attributed to the stomach. It follows that we do not investigate lower or higher frequencies, for lack of criteria to discriminate signal from noise (Verhagen et al., 1999) and that the procedure we propose is not well suited for psychophysiological studies targeting large changes in gastric rhythm frequency, such as nausea, disgust, and stress. The procedure is also not suitable for investigating the spatial propagation of gastric slow wave along the stomach, and we refer the reader to other approaches (Angeli et al., 2015; Bradshaw et al., 2016; Gharibans et al., 2019; O'Grady et al., 2010, 2012).

The pipeline depends on the definition of the normal range of the gastric rhythm, an issue that is not fully resolved in the clinical literature (Chang, 2005; Parkman et al., 2003). This pipeline allows to estimate the duration of each gastric cycle, thereby providing a finer temporal resolution than approaches based on running spectral analysis (Stern et al., 2007). Gastric cycle duration estimation is dependent on the design and width of the filter used for analysis, which should be wide enough to capture physiological fluctuations of the gastric rhythm but narrow enough to exclude contaminating sources. Finally, the procedure is only semi-automatized. Visual inspection is still required to detect large artifacts before any processing, to select power spectra satisfying all criteria, and to verify the quality of the filtering process.

ACKNOWLEDGMENTS

We thank Margaux Romand-Monnier, Clémence Almeras and Juliette Klamm for help during data acquisition. We also thank Ismael Jose Palacios-García and Janina Hüer for helpful comments on an earlier version of the manuscript.

CONFLICT OF INTEREST

The authors declare that no competing interests exist.

CUSTOM CODE

The custom code used for this article can be accessed online at the following address: https://github.com/niwolpert/EGG_Scripts

ORCID

Nicolai Wolpert https://orcid.org/0000-0003-4381-0970
Ignacio Rebollo https://orcid.org/0000-0002-4119-9955
Catherine Tallon-Baudry https://orcid.org/0000-0001-8480-5831

REFERENCES

Abell, T. L., & Malagelada, J.-R. (1988). Electrogastrography: Current assessment and future perspectives. *Digestive Diseases and Sciences*, *33*(8), 982–992. https://doi.org/10.1007/BF01535995

Agostoni, E., Chinnock, J. E., De Daly, M. B., & Murray, J. G. (1957). Functional and histological studies of the vagus nerve and its branches to the heart, lungs and abdominal viscera in the cat. *The Journal of Physiology*, *135*(1), 182–205. https://doi.org/10.1113/jphysiol.1957.sp005703

Altschuler, S. M., Bao, X. M., Bieger, D., Hopkins, D. A., & Miselis, R. R. (1989). Viscerotopic representation of the upper alimentary tract in the rat : Sensory ganglia and nuclei of the solitary and spinal trigeminal tracts. *The Journal of Comparative Neurology*, *283*(2), 248–268. https://doi.org/10.1002/cne.902830207

Alvarez, W. (1922). The electrogastrogram and what it shows. *JAMA*, *78*, 1116–1118.

Amaris, M. A., Sanmiguel, C. P., Sadowski, D. C., Bowes, K. L., & Mintchev, M. P. (2002). Electrical activity from colon overlaps with normal gastric electrical activity in cutaneous recordings. *Digestive Diseases and Sciences*, *47*(11), 6. https://doi.org/10.1023/a:1020503908304

Amassian, V. E. (1951). Cortical representation of visceral afferents. *Journal of Neurophysiology*, *14*(6), 433–444. https://doi.org/10.1152/jn.1951.14.6.433

Américo, M. F., Miranda, J. R. A., Corá, L. A., & Romeiro, F. G. (2009). Electrical and mechanical effects of hyoscine butylbromide on the human stomach : A non-invasive approach. *Physiological Measurement*, *30*(4), 363–370. https://doi.org/10.1088/0967-3334/30/4/002

Andreis, U., Américo, M. F., Corá, L. A., Oliveira, R. B., Baffa, O., & Miranda, J. R. A. (2008). Gastric motility evaluated by electrogastrography and alternating current biosusceptometry in dogs. *Physiological Measurement*, *29*(9), 1023–1031. https://doi.org/10.1088/0967-3334/29/9/002

Andrews, P. L., & Scratcherd, T. (1980). The gastric motility patterns induced by direct and reflex excitation of the vagus nerves in the anaesthetized ferret. *The Journal of Physiology*, *302*(1), 363–378. https://doi.org/10.1113/jphysiol.1980.sp013248

Angeli, T. R., Cheng, L. K., Du, P., Wang, T.-H., Bernard, C. E., Vannucchi, M.-G., … O'Grady, G. (2015). Loss of Interstitial Cells of Cajal and patterns of gastric dysrhythmia in patients with chronic unexplained nausea and vomiting. *Gastroenterology*, *149*(1), 56–66.e5. https://doi.org/10.1053/j.gastro.2015.04.003

Angeli, T. R., Du, P., Paskaranandavadivel, N., Janssen, P. W. M., Beyder, A., Lentle, R. G., … O'Grady, G. (2013). The bioelectrical basis and validity of gastrointestinal extracellular slow wave recordings : Bioelectrical basis of GI extracellular recordings. *The Journal of Physiology*, *591*(18), 4567–4579. https://doi.org/10.1113/jphysiol.2013.254292

Azpiroz, F., & Malagelada, J.-R. (1990). Perception and reflex relaxation of the stomach in response to gut distention. *Gastroenterology*, *98*(5), 1193–1198. https://doi.org/10.1016/0016-5085(90)90333-V

Azzalini, D., Rebollo, I., & Tallon-Baudry, C. (2019). Visceral signals shape brain dynamics and cognition. *Trends in Cognitive Sciences*, *23*(6), 488–509. https://doi.org/10.1016/j.tics.2019.03.007

Baldaro, B., Battacchi, M. W., Codispoti, M., Tuozzi, G., Trombini, G., Bolzani, R., & Palomba, D. (1996). Modifications of electrogastrographic activity during the viewing of brief film sequences. *Perceptual and Motor Skills*, *82*(3_suppl), 1243–1250. https://doi.org/10.2466/pms.1996.82.3c.1243

Baldaro, B., Battacchi, M. W., Trombini, G., Palomba, D., & Stegagno, L. (1990). Effects of an emotional negative stimulus on the cardiac, electrogastrographic, and respiratory responses. *Perceptual and Motor Skills*, *71*(2), 647–655. https://doi.org/10.2466/pms.1990.71.2.647

Baldaro, B., Mazzetti, M., Codispoti, M., Tuozzi, G., Bolzani, R., & Trombini, G. (2001). Autonomic reactivity during viewing of an unpleasant film. *Perceptual and Motor Skills*, *93*(3), 797–805. https://doi.org/10.2466/pms.2001.93.3.797

Bayguinov, O., Hennig, G. W., & Sanders, K. M. (2011). Movement based artifacts may contaminate extracellular electrical recordings from GI muscles: Movement artifacts in extracellular recording. *Neurogastroenterology & Motility*, *23*(11), 1029–e498. https://doi.org/10.1111/j.1365-2982.2011.01784.x

Berthoud, H. R., Blackshaw, L. A., Brookes, S. J. H., & Grundy, D. (2004). Neuroanatomy of extrinsic afferents supplying the gastrointestinal tract. *Neurogastroenterology and Motility*, *16*(Suppl 1), 28–33. https://doi.org/10.1111/j.1743-3150.2004.00471.x

Bester, H., Besson, J. M., & Bernard, J. F. (1997). Organization of efferent projections from the parabrachial area to the hypothalamus : A Phaseolus vulgaris-leucoagglutinin study in the rat. *The Journal of Comparative Neurology*, *383*(3), 245–281. https://doi.org/10.1002/(SICI)1096-9861(19970707)383:3<245:AID-CNE1>3.0.CO;2-3

Birmingham, A. (1898). The arrangement of the muscular fibres of the stomach. *Transactions of the Royal Academy of Medicine in Ireland*, *16*(1), 432–440. https://doi.org/10.1007/BF03177287

Bishop, V. S., Malliani, A., & Thorén, P. (1983). Handbook of physiology, section 2: The cardiovascular system. In J. T. Shepard (Ed.), *Comprehensive physiology* (pp. 497–555). Baltimore: Waverly Press. https://doi.org/10.1002/cphy.cp020315

Blackshaw, L. A., Brookes, S. J. H., Grundy, D., & Schemann, M. (2007). Sensory transmission in the gastrointestinal tract. *Neurogastroenterology and Motility*, *19*(1 Suppl), 1–19. https://doi.org/10.1111/j.1365-2982.2006.00871.x

Bozler, E. (1945). The action potentials of the stomach. *American Journal of Physiology*, *144*, 693–700. https://doi.org/10.1152/ajplegacy.1945.144.5.693

Bradshaw, L. A., Cheng, L. K., Chung, E., Obioha, C. B., Erickson, J. C., Gorman, B. L., … Richards, W. O. (2016). Diabetic gastroparesis alters the biomagnetic signature of the gastric slow wave. *Neurogastroenterology and Motility*, *28*(6), 837–848. https://doi.org/10.1111/nmo.12780

Brown, B. H., Smallwood, R. H., Duthie, H. L., & Stoddard, C. J. (1975). Intestinal smooth muscle electrical potentials recorded from surface electrodes. *Medical & Biological Engineering*, *13*(1), 97–103. https://doi.org/10.1007/BF02478194

Bruinstroop, E., Cano, G., VanderHorst, V. G. J. M., Cavalcante, J. C., Wirth, J., Sena-Esteves, M., & Saper, C. B. (2012). Spinal projections of the A5, A6 (locus coeruleus), and A7 noradrenergic cell groups in rats. *The Journal of Comparative Neurology*, *520*(9) , 1985–2001. https://doi.org/10.1002/cne.23024

Cannon, W. B. (1927). The James-Lange theory of emotions : A critical examination and an alternative theory. *The American Journal of Psychology*, *39*, 106–124. https://doi.org/10.2307/1415404

Cechetto, D. F., & Saper, C. B. (1987). Evidence for a viscerotopic sensory representation in the cortex and thalamus in the rat. *The Journal of Comparative Neurology*, *262*(1), 27–45. https://doi.org/10.1002/cne.902620104

Chang, F.-Y. (2005). Electrogastrography: Basic knowledge, recording, processing and its clinical applications. *Journal of Gastroenterology and Hepatology*, *20*, 502–516. https://doi.org/10.1111/j.1440-1746.2004.03751.x

Chang, H. Y., Mashimo, H., & Goyal, R. K. (2003). IV. Current concepts of vagal efferent projections to the gut. *American Journal of Physiology-Gastrointestinal and Liver Physiology*, *284*(3), G357–G366. https://doi.org/10.1152/ajpgi.00478.2002

Chen, D. D., Xu, X., Wang, Z., & Chen, J. D. Z. (2005). Alteration of gastric myoelectrical and autonomic activities with audio stimulation in healthy humans. *Scandinavian Journal of Gastroenterology*, *40*, 814–821. https://doi.org/10.1080/00365520510015656

Chen, D. D., Xu, X., Zhao, Q., Yin, J., Sallam, H., & Chen, J. D. (2008). Effects of audio stimulation on gastric myoelectrical activity and sympathovagal balance in healthy adolescents and adults. *Journal*

of Gastroenterology and Hepatology, *23*, 141–149. https://doi.org/10.1111/j.1440-1746.2007.05123.x

Chen, J., & McCallum, R. W. (1992). Gastric slow wave abnormalities in patients with gastroparesis. *American Journal of Gastroenterology*, *87*, 477–482.

Chen, J. D., Schirmer, B. D., & McCallum, R. W. (1994). Serosal and cutaneous recordings of gastric myoelectrical activity in patients with gastroparesis. *American Journal of Physiology-Gastrointestinal and Liver Physiology*, *266*(1), G90–G98. https://doi.org/10.1152/ajpgi.1994.266.1.G90

Chen, J. D. Z., Zou, X., Lin, X., Ouyang, S., & Liang, J. (1999). Detection of gastric slow wave propagation from the cutaneous electrogastrogram. *American Journal of Physiology-Gastrointestinal and Liver Physiology*, *277*(2), G424–G430. https://doi.org/10.1152/ajpgi.1999.277.2.G424

Cheng, L. K., Du, P., & O'Grady, G. (2013). Mapping and modeling gastrointestinal bioelectricity : From Engineering Bench to Bedside. *Physiology*, *28*(5), 310–317. https://doi.org/10.1152/physiol.00022.2013

Chiba, T., Kudara, N., Sato, M., Inomata, M., Orii, S., & Suzuki, K. (2007). Effect of a muscarinic M3 receptor agonist on gastric motility. *Journal of Gastroenterology and Hepatology*, *22*(11), 2039–2041. https://doi.org/10.1111/j.1440-1746.2006.03363.x

Christensen, J., Schedl, H. P., & Clifton, J. A. (1966). The small intestinal basic electrical rhythm (slow wave) frequency gradient in normal men and in patients with a variety of diseases. *Gastroenterology*, *50*(3), 309–315. https://doi.org/10.1016/S0016-5085(66)80069-0

Christensen, J., & Torres, E. I. (1975). Three layers of the opossum stomach : Responses to nerve stimulation. *Gastroenterology*, *69*(3), 641–648. https://doi.org/10.1016/S0016-5085(19)32457-6

Christoff, K., Cosmelli, D., Legrand, D., & Thompson, E. (2011). Specifying the self for cognitive neuroscience. *Trends in Cognitive Sciences*, *15*(3), 104–112. https://doi.org/10.1016/j.tics.2011.01.001

Coen, S. J., Hobson, A. R., & Aziz, Q. (2012). Chapter 23—Processing of gastrointestinal sensory signals in the brain. In L. R. Johnson, F. K. Ghishan, J. D. Kaunitz, J. L. Merchant, H. M. Said, & J. D. Wood (Eds.), *Physiology of the gastrointestinal tract* (5th ed., pp. 689–702). Boston: Academic Press.). https://doi.org/10.1016/B978-0-12-382026-6.00023-3s

Cohen, M. X. (2014). *Analyzing neural time series data: Theory and practice*. Cambridge, MA: The MIT Press.

Coizet, V., Dommett, E. J., Klop, E. M., Redgrave, P., & Overton, P. G. (2010). The parabrachial nucleus is a critical link in the transmission of short latency nociceptive information to midbrain dopaminergic neurons. *Neuroscience*, *168*(1), 263–272. https://doi.org/10.1016/j.neuroscience.2010.03.049

Coleski, R., & Hasler, W. L. (2004). Directed endoscopic mucosal mapping of normal and dysrhythmic gastric slow waves in healthy humans. *Neurogastroenterology and Motility*, *16*(5), 557–565. https://doi.org/10.1111/j.1365-2982.2004.00542.x

Craig, A. D. (2002). How do you feel? Interoception: The sense of the physiological condition of the body. *Nature Reviews Neuroscience*, *3*(8), 655–666. https://doi.org/10.1038/nrn894

Critchley, H. D., & Harrison, N. A. (2013). Visceral influences on brain and behavior. *Neuron*, *77*(4), 624–638. https://doi.org/10.1016/j.neuron.2013.02.008

Cucchiara, S., Salvia, G., Borrelli, O., Ciccimarra, E., Az-Zeqeh, N., Rapagiolo, S., … Riezzo, G. (1997). Gastric electrical dysrhythmias and delayed gastric emptying in gastroesophageal reflux disease. *The American Journal of Gastroenterology*, *92*(7), 1103–1108.

Damasio, A. R. (1996). The somatic marker hypothesis and the possible functions of the prefrontal cortex. *Philosophical Transactions of the Royal Society of London Series B, Biological Sciences*, *351*(1346), 1413–1420. https://doi.org/10.1098/rstb.1996.0125

Davis, R. C., & Berry, F. (1963). Gastrointestinal reactions during a noise avoidance task. *Psychological Reports*, *12*(1), 135–137. https://doi.org/10.2466/pr0.1963.12.1.135

Davis, R. C., Berry, F., & Paden, A. (1969). *The effect of certain tasks and conditions on gastrointestinal activity* (Technical Report). Bloomington, IN: Indiana University.

Davis, R. C., Garafolo, L., & Kveim, K. (1959). Conditions associated with gastrointestinal activity. *Journal of Comparative and Physiological Psychology*, *52*(4), 466–475. https://doi.org/10.1037/h0044130

Deuchars, S. A., & Lall, V. K. (2015). Sympathetic preganglionic neurons: Properties and inputs. *Comprehensive Physiology*, *5*, 829–869.

Downman, C. B. B. (1951). Cerebral destination of splanchnic afferent impulses. *The Journal of Physiology*, *113*(4), 434–441. https://doi.org/10.1113/jphysiol.1951.sp004586

Du, P., O'Grady, G., Cheng, L. K., & Pullan, A. J. (2010). A multiscale model of the electrophysiological basis of the human electrogastrogram. *Biophysical Journal*, *99*(9), 2784–2792. https://doi.org/10.1016/j.bpj.2010.08.067

Dum, R. P., Levinthal, D. J., & Strick, P. L. (2009). The spinothalamic system targets motor and sensory areas in the cerebral cortex of monkeys. *The Journal of Neuroscience*, *29*(45), 14223–14235. https://doi.org/10.1523/JNEUROSCI.3398-09.2009

Ercolani, M., Baldaro, B., Comani, G., De Portu, I., Rossi, N., & Trombini, G. (1982). Evolution de la motilité gastrique, de la fréquence cardiaque et ventilatoire de sujets sains pendant L'exécution d'épreuves de performance. *Aggressologie*, *23*, 263–267.

Ercolani, M., Baldaro, B., & Trombini, G. (1989). Effects of two tasks and two levels of difficulty upon surface electrogastrograms. *Perceptual and Motor Skills*, *69*(1), 99–110. https://doi.org/10.2466/pms.1989.69.1.99

Erickson, J. C., Bruce, L. E., Taylor, A., Richman, J., Higgins, C., Wells, C. I., & O'Grady, G. (2019). Electrocolonography : Non-invasive detection of colonic cyclic motor activity from multielectrode body surface recordings. *IEEE Transactions on Bio-Medical Engineering*, https://doi.org/10.1109/TBME.2019.2941851

Erişir, A., Van Horn, S. C., & Sherman, S. M. (1997). Relative numbers of cortical and brainstem inputs to the lateral geniculate nucleus. *Proceedings of the National Academy of Sciences of the United States of America*, *94*(4), 1517–1520. https://doi.org/10.1073/pnas.94.4.1517

Familoni, B. O., Kingma, Y. J., & Bowes, K. L. (1987). Study of transcutaneous and intraluminal measurement of gastric electrical activity in humans. *Medical & Biological Engineering & Computing*, *25*(4), 397–402. https://doi.org/10.1007/BF02443360

Fedor, J. H., & Russell, R. W. (1965). Gastrointestinal reactions to response-contingent stimulation. *Psychological Reports*, *16*(1), 95–113. https://doi.org/10.2466/pr0.1965.16.1.95

Foley, J. O. (1948). The functional types of nerve fibers and their numbers in the great splanchnic nerve. *The Anatomical Record*, *100*, 766–767.

Fritsch, H., & Kühnel, W. (2008). *Color atlas of human anatomy: Internal organs* (Vol. *2*). Stuttgart, Germany: Georg Thieme Verlag.

Fulwiler, C. E., & Saper, C. B. (1984). Subnuclear organization of the efferent connections of the parabrachial nucleus in the rat. *Brain Research Reviews*, *7*(3), 229–259. https://doi.org/10.1016/0165-0173(84)90012-2

Furness, J. B. (2006). *The enteric nervous system*. Oxford, UK: Blackwell Publishing.

Furness, J. B. (2012). The enteric nervous system and neurogastroenterology. *Nature Reviews Gastroenterology & Hepatology*, *9*(5), 286–294. https://doi.org/10.1038/nrgastro.2012.32

Geldof, H., van der Schee, E. J., Smout, A. J. P. M., van de Merwe, J. P., van Blankenstein, M., & Grashuis, J. L. (1989). Myoelectrical activity of the stomach in gastric ulcer patients: An electrogastrographic study. *Neurogastroenterology & Motility*, *1*(2), 122–130. https://doi.org/10.1111/j.1365-2982.1989.tb00150.x

Gharibans, A. A., Coleman, T. P., Mousa, H., & Kunkel, D. C. (2019). Spatial patterns from high-resolution electrogastrography correlate with severity of symptoms in patients with functional dyspepsia and gastroparesis. *Clinical Gastroenterology and Hepatology*, *17*(13), 2668–2677. https://doi.org/10.1016/j.cgh.2019.04.039

Gharibans, A. A., Kim, S., Kunkel, D. C., & Coleman, T. P. (2017). High-resolution Electrogastrogram: A novel, noninvasive method for determining gastric slow-wave direction and speed. *IEEE Transactions on Biomedical Engineering*, *64*(4), 807–815.https://doi.org/10.1109/TBME.2016.2579310

Gharibans, A. A., Smarr, B. L., Kunkel, D. C., Kriegsfeld, L. J., Mousa, H. M., & Coleman, T. P. (2018). Artifact rejection methodology enables continuous, noninvasive measurement of gastric myoelectric activity in ambulatory subjects. *Scientific Reports*, *8*(1), 1–12. https://doi.org/10.1038/s41598-018-23302-9

Gianaros, P. J., Quigley, K. S., & Mordkoff, J. T. (2001). Gastric myoelectrical and autonomic cardiac reactivity to laboratory stressors. *Psychophysiology*, *38*(4), 540–547.

Gillis, R. A., Quest, J. A., Pagani, F. D., & Norman, W. P. (1989). Control centers in the central nervous system for regulating gastrointestinal motility. In J. D. Wood (Ed.), *Handbook of physiology. The gastrointestinal system. Motility and circulation* (Vol. *1*, pp. 621–683). Bethesda, MD: American Physiological Society. https://doi.org/10.1002/cphy.cp060117

Hall, K. E., el-Sharkawy, T. Y., & Diamant, N. E. (1986). Vagal control of canine postprandial upper gastrointestinal motility. *The American Journal of Physiology*, *250*(4 Pt 1), G501–G510. https://doi.org/10.1152/ajpgi.1986.250.4.G501

Hamilton, J. W., Bellahsene, B. E., Reichelderfer, M., Webster, J. G., & Bass, P. (1986). Human electrogastrograms: Comparison of surface and mucosal recordings. *Digestive Diseases and Sciences*, *31*(1), 33–39. https://doi.org/10.1007/BF01347907

Han, W., Tellez, L. A., Perkins, M. H., Perez, I. O., Qu, T., Ferreira, J., … de Araujo, I. E. (2018). A neural circuit for gut-induced reward. *Cell*, *175*(3), 665–678.e23. https://doi.org/10.1016/j.cell.2018.08.049

Harrison, N. A., Gray, M. A., Gianaros, P. J., & Critchley, H. D. (2010). The embodiment of emotional feelings in the brain. *Journal of Neuroscience*, *30*(38), 12878–12884. https://doi.org/10.1523/JNEUROSCI.1725-10.2010

Hinder, R. A., & Kelly, K. A. (1977). Human gastric pacesetter potential. Site of origin, spread, and response to gastric transection and proximal gastric vagotomy. *The American Journal of Surgery*, *133*, 29–33. https://doi.org/10.1016/0002-9610(77)90187-8

Hirst, G. D. S., & Edwards, F. R. (2006). Electrical events underlying organized myogenic contractions of the guinea pig stomach: Descending propagation of gastric slow waves. *The Journal of Physiology*, *576*, 659–665. https://doi.org/10.1113/jphysiol.2006.116491

Hocke, M., Schöne, U., Richert, H., Görnert, P., Keller, J., Layer, P., & Stallmach, A. (2009). Every slow-wave impulse is associated with motor activity of the human stomach. *American Journal of Physiology-Gastrointestinal and Liver Physiology*, *296*(4), G709–G716. https://doi.org/10.1152/ajpgi.90318.2008

Holzer, P. (2006). Efferent-like roles of afferent neurons in the gut: Blood flow regulation and tissue protection. *Autonomic Neuroscience: Basic & Clinical*, *125*, 70–75. https://doi.org/10.1016/j.autneu.2006.01.004

Holzl, R., Schroder, G., & Kiefer, L. (1979). Indirect gastrointestinal motility measurement for use in experimental psychosomatics: A new method and some data. *Behavior Analysis and Modification*, *3*, 77–97.

Homma, S., Hasegawa, J., Maruta, T., Watanabe, N., Matsuo, H., Tamiya, Y., … Hatakeyama, K. (1999). Isopower maps of the electrogastrogram (EGG) after total gastrectomy or total colectomy. *Neurogastroenterology & Motility*, *11*, 441–448. https://doi.org/10.1046/j.1365-2982.1999.00170.x

Homma, S., Shimakage, N., Yagi, M., Hasegawa, J., Sato, K., Matsuo, H., … Hatakeyama, K. (1995). Electrogastrography prior to and following total gastrectomy, subtotal gastrectomy, and gastric tube formation. *Digestive Diseases and Sciences*, *40*(4), 893–900. https://doi.org/10.1007/BF02064997

Hou, X., Yin, J., Liu, J., Pasricha, P. J., & Chen, J. D. Z. (2005). In vivo gastric and intestinal slow waves in W/W^{v} Mice. *Digestive Diseases and Sciences*, *50*(7), 1335–1341. https://doi.org/10.1007/s10620-005-2783-6

Huizinga, J. D., & Chen, J.-H. (2014). Interstitial Cells of Cajal: Update on basic and clinical science. *Current Gastroenterology Reports*, *16*(1), 363. https://doi.org/10.1007/s11894-013-0363-z

Hylden, J. L., Hayashi, H., Bennett, G. J., & Dubner, R. (1985). Spinal lamina I neurons projecting to the parabrachial area of the cat midbrain. *Brain Research*, *336*(1), 195–198. https://doi.org/10.1016/0006-8993(85)90436-6

Imai, K., & Sakita, M. (2005). Pre- and postoperative electrogastrography in patients with gastric cancer. *Hepato-Gastroenterology*, *52*(62), 639–644.

Indrio, F., Riezzo, G., Raimondi, F., Bisceglia, M., Cavallo, L., & Francavilla, R. (2009). Effects of probiotic and prebiotic on gastrointestinal motility in newborns. *Journal of Physiology and Pharmacology*, *60*(Suppl 6), 27–31.

James, W. (1890). *The Principles of Psychology*. New York: Holt.

Jonderko, K., Kasicka-Jonderko, A., & Blonska-Fajfrowska, B. (2005). Does body posture affect the parameters of a cutaneous electrogastrogram? *Journal of Smooth Muscle Research*, *41*(3), 133–140. https://doi.org/10.1540/jsmr.41.133

Kaiho, T., Shimoyama, I., Nakajima, Y., & Ochiai, T. (2000). Gastric and non-gastric signals in electrogastrography. *Journal of the Autonomic Nervous System*, *79*(1), 60–66. https://doi.org/10.1016/S0165-1838(99)00098-3

Kaneoke, Y., Koike, Y., Sakurai, N., Washimi, Y., Hirayama, M., Hoshiyama, M., & Takahashi, A. (1995). Gastrointestinal dysfunction in Parkinson's disease detected by electrogastroenterography. *Journal of the Autonomic Nervous System*, *50*(3), 275–281. https://doi.org/10.1016/0165-1838(94)00098-5

Kelly, K. A. (1980). Gastric emptying of liquids and solids : Roles of proximal and distal stomach. *American Journal of Physiology-Gastrointestinal and Liver Physiology*, *239*(2), G71–G76. https://doi.org/10.1152/ajpgi.1980.239.2.G71

Kelly, K. A., Code, C. F., & Elveback, L. R. (1969). Patterns of canine gastric electrical activity. *American Journal of Physiology*, *217*, 461–470. https://doi.org/10.1152/ajplegacy.1969.217.2.461

Kern, M., Aertsen, A., Schulze-Bonhage, A., & Ball, T. (2013). Heart cycle-related effects on event-related potentials, spectral power changes, and connectivity patterns in the human ECoG. *NeuroImage*, *81*, 178–190. https://doi.org/10.1016/j.neuroimage.2013.05.042

Khalsa, S. S., Adolphs, R., Cameron, O. G., Critchley, H. D., Davenport, P. W., Feinstein, J. S., … Kupli, R. (2018). Interoception and mental health: A roadmap. *Biological Psychiatry. Cognitive Neuroscience and Neuroimaging*, *3*(6), 501–513. https://doi.org/10.1016/j.bpsc.2017.12.004

Klüppel, M., Huizinga, J. D., Malysz, J., & Bernstein, A. (1998). Developmental origin and kit-dependent development of the Interstitial Cells of Cajal in the mammalian small intestine. *Developmental Dynamics*, *211*(1), 60–71. https://10.1002/(SICI)1097-0177(199801)211:1<60:AID-AJA6>3.0.CO;2-5

Koch, K. L., Bingaman, S., Tan, L., & Stern, R. M. (1998). Visceral perceptions and gastric myoelectrical activity in healthy women and in patients with bulimia nervosa. *Neurogastroenterology & Motility*, *10*, 3–10. https://doi.org/10.1046/j.1365-2982.1998.00080.x

Koch, K. L., Hong, S. P., & Xu, L. (2000). Reproducibility of gastric myoelectrical activity and the water load test in patients with dysmotility-like dyspepsia symptoms and in control subjects. *Journal of Clinical Gastroenterology*, *31*, 125–129. https://doi.org/10.1097/00004836-200009000-00007

Koch, K. L., & Stern, R. M. (2004). *Handbook of electrogastrography*. New York, NY: Oxford University Press.

Květina, J., Varayil, J., Ali, S., Kuneš, M., Bureš, J., Tachecí, I., … Kopáčová, M. (2010). Preclinical electrogastrography in experimental pigs. *Interdisciplinary Toxicology*, *3*(2), 53–58. https://doi.org/10.2478/v10102-010-0011-5

Ladabaum, U., Minoshima, S., Hasler, W. L., Cross, D., Chey, W. D., & Owyang, C. (2001). Gastric distention correlates with activation of multiple cortical and subcortical regions. *Gastroenterology*, *120*(2), 369–376. https://doi.org/10.1053/gast.2001.21201

Lange, C. G. (1885). *The Emotions (William & Wilkins)*. Baltimore, MD: Williams & Wilkins.

Leek, B. F. (1972).Abdominal visceral receptors. In B. Andersson, M. Fillenz, R. F. Hellon, A. Howe, B. F. Leek, E. Neil (Eds.), *Enteroceptors* (pp. 113–160). Berlin, Heidelberg: Springer. https://doi.org/10.1007/978-3-642-65252-3_4

Liang, J., & Chen, J. D. (1997). What can be measured from surface electrogastrography. *Computer Simulationss Digestive Diseases and Sciences*, *42*(7), 1331–1343. https://doi.org/10.1023/a:1018869300296

Lin, H.-H., Chang, W.-K., Chu, H.-C., Huang, T.-Y., Chao, Y.-C., & Hsieh, T.-Y. (2007). Effects of music on gastric myoelectrical activity in healthy humans. *International Journal of Clinical Practice*, *61*(7), 1126–1130. https://doi.org/10.1111/j.1742-1241.2006.01090.x

Lin, Z., Chen, J. D. Z., Schirmer, B. D., & McCallum, R. W. (2000). Postprandial response of gastric slow waves : Correlation of serosal recordings with the electrogastrogram. *Digestive Diseases and Sciences*, *45*(4), 7. https://doi.org/10.1023/a:1005434020310

Lin, Z., Eaker, E. Y., Sarosiek, I., & McCallum, R. W. (1999). Gastric myoelectrical activity and gastric emptying in patients with functional dyspepsia. *American Journal of Gastroenterology*, *94*(9), 2384–2389. https://doi.org/10.1111/j.1572-0241.1999.01362.x

Lindberg, G., Iwarzon, M., & Hammarlund, B. (1996). 24-hour ambulatory electrogastrography in healthy volunteers. *Scandinavian Journal of Gastroenterology*, *31*(7), 658–664. https://doi.org/10.3109/00365529609009146

Linsong, W., Huailin, Z., Xitai, L., Xiaojin, Z., & Pingan, R. (1989). The primary research of electrogastrograms in macaca mulatta of taihang mountains. *Journal of Henan Normal University (Natural Science)*.

Lu, C.-L., Wu, Y.-T., Yeh, T.-C., Chen, L.-F., Chang, F.-Y., Lee, S.-D., … Hsieh, J.-C. (2004). Neuronal correlates of gastric pain induced by fundus distension: A 3T-fMRI study. *Neurogastroenterology and Motility*, *16*(5), 575–587. https://doi.org/10.1111/j.1365-2982.2004.00562.x

Lu, S. M., Guido, W., & Sherman, S. M. (1993). The brain-stem parabrachial region controls mode of response to visual stimulation of neurons in the cat's lateral geniculate nucleus. *Visual Neuroscience*, *10*(4), 631–642. https://doi.org/10.1017/s0952523800005332

Martin, A., Nicolov, N., Ormieres, D., Beloncle, M., & Murat, J. (1982). La motricité gastrique chez 60 sujets normaux sous l'influence d'une tension émotionnelle, premiers résultats. *Aggressologie*, *23*, 269–273.

McCallum, R., Jones, T., Lin, Z., Sarosiek, I., & Moncure, M. (2001). Assessment of gastric emptying and myoelectric activity in the morbidly obese patient. *American Gastroenterological Association*, *120*(5), A290.

Meissner, K., Muth, E. R., & Herbert, B. M. (2011). Bradygastric activity of the stomach predicts disgust sensitivity and perceived disgust intensity. *Biological Psychology*, *86*(1), 9–16. https://doi.org/10.1016/j.biopsycho.2010.09.014

Mintchev, M. P., Kingma, Y. J., & Bowes, K. L. (1993). Accuracy of cutaneous recordings of gastric electrical activity. *Gastroenterology*, *104*(5), 1273–1280. https://doi.org/10.1016/0016-5085(93)90334-9

Mintchev, M., Otto, S., & Bowes, K. (1997). Electrogastrography can recognize gastric electrical uncoupling in dogs. *Gastroenterology*, *112*(6), 2006–2011. https://doi.org/10.1053/gast.1997.v112.pm9178693

Morrison, S. F., Sved, A. F., & Passerin, A. M. (1999). GABA-mediated inhibition of raphe pallidus neurons regulates sympathetic outflow to brown adipose tissue. *American Journal of Physiology-Regulatory, Integrative and Comparative Physiology*, *276*(2), R290–R297.https://doi.org/10.1152/ajpregu.1999.276.2.R290

Munk, M. H., Roelfsema, P. R., König, P., Engel, A. K., & Singer, W. (1996). Role of reticular activation in the modulation of intracortical synchronization. *Science*, *272*, 271–274. https://doi.org/10.1126/science.272.5259.271

Murakami, H., Matsumoto, H., Ueno, D., Kawai, A., Ensako, T., Kaida, Y., … Hirai, T. (2013). Current status of multichannel electrogastrography and examples of its use. *Journal of Smooth Muscle Research*, *49*, 78–88. https://doi.org/10.1540/jsmr.49.78

Muth, E. R., Koch, K. L., Stern, R. M., & Thayer, J. F. (1999). Effect of autonomic nervous system manipulations on gastric myoelectrical activity and emotional responses in healthy human subjects. *Psychosomatic Medicine*, *61*(3), 297–303. https://doi.org/10.1097/00006842-199905000-00008

Norgren, R. (1978). Projections from the nucleus of the solitary tract in the rat. *Neuroscience*, *3*(2), 207–218. https://doi.org/10.1016/0306-4522(78)90102-1

O'Grady, G. (2012). Gastrointestinal extracellular electrical recordings: Fact or artifact? *Neurogastroenterology and Motility*, *24*(1), 1–6. https://doi.org/10.1111/j.1365-2982.2011.01815.x

O'Grady, G., Du, P., Cheng, L. K., Egbuji, J. U., Lammers, W. J. E. P., Windsor, J. A., & Pullan, A. J. (2010). Origin and propagation of human gastric slow-wave activity defined by high-resolution mapping. *American Journal of Physiology-Gastrointestinal and Liver Physiology*, *299*(3), G585–G592. https://doi.org/10.1152/ajpgi.00125.2010

O'Grady, G., Angeli, T. R., Du, P., Lahr, C., Lammers, W. J. E. P., Windsor, J. A., … Cheng, L. K. (2012). Abnormal initiation and conduction of slow-wave activity in gastroparesis, defined by high-resolution electrical mapping. *Gastroenterology*, *143*(3), 589–598.e3. https://doi.org/10.1053/j.gastro.2012.05.036

Obioha, C., Erickson, J., Suseela, S., Hajri, T., Chung, E., … Bradshaw, L. A. (2016). Effect of Body Mass Index on the sensitivity of magnetogastrogram and electrogastrogram. *Journal of Gastroenterology and Hepatology Research*, *2*(4), 513–519.

Oostenveld, R., Fries, P., Maris, E., & Schoffelen, J. (2011). FieldTrip: Open source software for advanced analysis of MEG, EEG, and invasive electrophysiological data. *Computational Intelligence and Neuroscience*, *2011*, 1–9. https://doi.org/10.1155/2011/156869

Pagani, F. D., Norman, W. P., Kasbekar, D. K., & Gillis, R. A. (1985). Localization of sites within dorsal motor nucleus of vagus that affect gastric motility. *The American Journal of Physiology*, *249*(1 Pt 1), G73–G84. https://doi.org/10.1152/ajpgi.1985.249.1.G73

Parkman, H. P., Harris, A. D., Miller, M. A., & Fisher, R. S. (1996). Influence of age, gender, and menstrual cycle on the normal electrogastrogram. *The American Journal of Gastroenterology*, *91*(1), 127–133.

Parkman, H. P., Hasler, W. L., Barnett, J. L., & Eaker, E. Y. (2003). Electrogastrography : A document prepared by the gastric section of the American Motility Society Clinical GI Motility Testing Task Force. *Neurogastroenterology and Motility*, *15*(2), 89–102. https://doi.org/10.1046/j.1365-2982.2003.00396.x

Parkman, H. P., & Orr, W. C. (2007). The gastrointestinal motility laboratory. *Gastroenterology Clinics of North America*, *36*(3), 515–529. https://doi.org/10.1016/j.gtc.2007.07.010

Paton, J. F., & Kasparov, S. (2000). Sensory channel specific modulation in the nucleus of the solitary tract. *Journal of the Autonomic Nervous System*, *80*(3), 117–129. https://doi.org/10.1016/s0165-1838(00)00077-1

Peupelmann, J., Quick, C., Berger, S., Hocke, M., Tancer, M. E., Yeragani, V. K., & Bär, K.-J. (2009). Linear and non-linear measures indicate gastric dysmotility in patients suffering from acute schizophrenia. *Progress in Neuro-Psychopharmacology & Biological Psychiatry*, *33*(7), 1236–1240. https://doi.org/10.1016/j.pnpbp.2009.07.007

Pezzolla, F., Riezzo, G., Maselli, M. A., & Giorgio, I. (1989). Electrical activity recorded from abdominal surface after gastrectomy or colectomy in humans. *Gastroenterology*, *97*(2), 313–320. https://doi.org/10.1016/0016-5085(89)90066-8

Pfaffenbach, B., Adamek, R. J., Kuhn, K., & Wegener, M. (1995). Electrogastrography in healthy subjects: Evaluation of normal values, influence of age and gender. *Digestive Diseases and Sciences*, *40*(7), 1445–1450. https://doi.org/10.1007/BF02285190

Powley, T. L., & Phillips, R. J. (2011). Vagal intramuscular array afferents form complexes with interstitial cells of Cajal in gastrointestinal smooth muscle: Analogues of muscle spindle organs? *Neuroscience*, *186*, 188–200. https://doi.org/10.1016/j.neuroscience.2011.04.036

Powley, T. L., Wang, X.-Y., Fox, E. A., Phillips, R. J., Liu, L. W. C., & Huizinga, J. D. (2008). Ultrastructural evidence for communication between intramuscular vagal mechanoreceptors and interstitial cells of Cajal in the rat fundus. *Neurogastroenterology and Motility*, *20*(1), 69–79. https://doi.org/10.1111/j.1365-2982.2007.00990.x

Pritchard, T. C., Hamilton, R. B., & Norgren, R. (2000). Projections of the parabrachial nucleus in the old world monkey. *Experimental Neurology*, *165*(1), 101–117. https://doi.org/10.1006/exnr.2000.7450

Quadt, L., Critchley, H. D., & Garfinkel, S. N. (2018). The neurobiology of interoception in health and disease. *Annals of the New York Academy of Sciences*, *1428*(1), 112–128. https://doi.org/10.1111/nyas.13915

Rayner, C. K., Hebbard, G. S., & Horowitz, M. (2012). Chapter 35—Physiology of the antral pump and gastric emptying. In L. R. Johnson, F. K. Ghishan, J. D. Kaunitz, J. L. Merchant, H. M. Said, & J. D. Wood (Eds.), *Physiology of the gastrointestinal tract* (5th ed., pp. 959–976). Boston, MA: Academic Press. https://doi.org/10.1016/B978-0-12-382026-6.00035-X

Rebollo, I., Devauchelle, A.-D., Béranger, B., & Tallon-Baudry, C. (2018). Stomach-brain synchrony reveals a novel, delayed-connectivity resting-state network in humans. *Elife*, *7*, e33321. https://doi.org/10.7554/eLife.33321

Richter, C. G., Babo-Rebelo, M., Schwartz, D., & Tallon-Baudry, C. (2017). Phase-amplitude coupling at the organism level: The amplitude of spontaneous alpha rhythm fluctuations varies with the phase of the infra-slow gastric basal rhythm. *NeuroImage*, *146*, 951–958. https://doi.org/10.1016/j.neuroimage.2016.08.043

Riezzo, G., Chiloiro, M., & Guerra, V. (1998). Electrogastrography in healthy children: Evaluation of normal values, influence of age, gender, and obesity. *Digestive Diseases and Sciences*, *43*(8), 1646–1651. https://doi.org/10.1023/a:1018894511181

Riezzo, G., Pezzolla, F., & Giorgio, I. (1991). Effects of age and obesity on fasting gastric electrical activity in man: A cutaneous electrogastrographic study. *Digestion*, *50*, 176–181. https://doi.org/10.1159/000200759

Riezzo, G., Pezzolla, F., Maselli, M. A., & Giorgio, I. (1994). Electrical activity recorded from abdominal surface before and after right hemicolectomy in man. *Digestion*, *55*(3), 185–190. https://doi.org/10.1159/000201146

Riezzo, G., Porcelli, P., Guerra, V., & Giorgio, I. (1996). Effects of different psychophysiological stressors on the cutaneous electrogastrogram in healthy subjects. *Archives of Physiology and Biochemistry*, *104*(3), 282–286. https://doi.org/10.1076/apab.104.3.282.12899

Riezzo, G., Russo, F., & Indrio, F. (2013). Electrogastrography in adults and children: The strength, pitfalls, and clinical significance of the cutaneous recording of the gastric electrical activity. *BioMed Research International*, *2013*, 1–14. https://doi.org/10.1155/2013/282757

Ruhland, C., Koschke, M., Greiner, W., Peupelmann, J., Pietsch, U., Hocke, M., … Bär, K.-J. (2008). Gastric dysmotility in patients with major depression. *Journal of Affective Disorders*, *110*(1–2), 185–190. https://doi.org/10.1016/j.jad.2007.12.236

Sanders, K. M., Koh, S. D., & Ward, S. M. (2006). Interstitial Cells of Cajal as pacemakers in the gastrointestinal tract. *Annual Review of Physiology*, *68*, 307–343. https://doi.org/10.1146/annurev.physiol.68.040504.094718

Sanders, K. M., Ward, S. M., & Koh, S. D. (2014). Interstitial Cells: Regulators of smooth muscle function. *Physiological Reviews*, *94*(3), 859–907. https://doi.org/10.1152/physrev.00037.2013

Saper, C. B. (2002). The central autonomic nervous system: Conscious visceral perception and autonomic pattern generation. *Annual Review of Neuroscience*, *25*(1), 433–469. https://doi.org/10.1146/annurev.neuro.25.032502.111311

Saper, C. B., & Loewy, A. D. (1980). Efferent connections of the parabrachial nucleus in the rat. *Brain Research*, *197*(2), 291–317. https://doi.org/10.1016/0006-8993(80)91117-8

Schemann, M., & Grundy, D. (1992). Electrophysiological identification of vagally innervated enteric neurons in guinea pig stomach. *The American Journal of Physiology*, *263*(5 Pt 1), G709–718. https://doi.org/10.1152/ajpgi.1992.263.5.G709

Shimamoto, C., Hirata, I., Hiraike, Y., Takeuchi, N., Nomura, T., & Katsu, K. (2002). Evaluation of gastric motor activity in the elderly by electrogastrography and the 13C-Acetate Breath Test. *Gerontology*, *48*, 381–386. https://doi.org/10.1159/000065500

Shipley, M. T., & Sanders, M. S. (1982). Special senses are really special: Evidence for a reciprocal, bilateral pathway between insular cortex and nucleus parabrachialis. *Brain Research Bulletin*, *8*(5), 493–501. https://doi.org/10.1016/0361-9230(82)90007-7

Simonian, H. P., Panganamamula, K., Parkman, H. P., Xu, X., Chen, J. Z., Lindberg, G., … Buhl, H. (2004). Multichannel electrogastrography (EGG) in normal subjects: A multicenter study. *Digestive Diseases and Sciences*, *49*(4), 594–601. https://doi.org/10.1023/B:DDAS.0000026304.83214.50

Smirnov, V. M., & Lychkova, A. E. (2003). Mechanism of synergism between sympathetic and parasympathetic autonomic nervous systems in the regulation of motility of the stomach and sphincter of Oddi. *Bulletin of Experimental Biology and Medicine*, *135*(4), 327–329. https://doi.org/10.1023/a:1024692226837

Smout, A. J. P. M., Van Der Schee, E. J., & Grashuis, J. L. (1980). What is measured in electrogastrography? *Digestive Diseases and Sciences*, *25*, 179–187. https://doi.org/10.1007/bf01308136

Somarajan, S., Cassilly, S., Obioha, C., Richards, W. O., & Bradshaw, L. A. (2014). Effects of body mass index on gastric slow wave: A magnetogastrographic study. *Physiological Measurement*, *35*(2), 205–215. https://doi.org/10.1088/0967-3334/35/2/205

Spielberger, C., Gorsuch, R., Lushene, R., Vagg, P., & Jacobs, G. (1983). *Manual for the state-trait anxiety inventory*. Palo Alto, CA: Consulting Psychologists.

Stern, R. M. (1966). A re-examination of the effects of response-contingent aversive tones on gastrointestinal activity. *Psychophysiology*, *2*(3), 217–223. https://doi.org/10.1111/j.1469-8986.1966.tb02645.x

Stern, R. M. (1983). Responsiveness of the stomach to environmental events. *Psychophysiology of the gastrointestinal tract: Experimental and clinical applications* (pp. 181–207). New York, NY: Plenum.

Stern, R. M., Crawford, H. E., Stewart, W. R., Vasey, M. W., & Koch, K. L. (1989). Sham feeding. Cephalic-vagal influences on gastric myoelectric activity. *Digestive Diseases and Sciences*, *34*(4), 521–527. https://doi.org/10.1007/bf01536327

Stern, R. M., Jokerst, M. D., Levine, M. E., & Koch, K. L. (2001). The stomach's response to unappetizing food: cephalic-vagal effects on gastric myoelectric activity. *Neurogastroenterology & Motility*, *13*(2), 151–154. https://doi.org/10.1046/j.1365-2982.2001.00250.x

Stern, R. M., Koch, K. L., Leibowitz, H. W., Lindblad, I. M., Shupert, C. L., & Stewart, W. R. (1985). Tachygastria and motion sickness. *Aviation, Space, and Environmental Medicine*, *56*(11), 1074–1077.

Stern, R. M., Koch, K. L., Levine, M. E., & Muth, E. R. (2007). Gastrointestinal response. In J. T. Cacioppo, L. G. Tassinary, & G. Berntson (Eds.), *Handbook of psychophysiology* (pp. 211–230). Cambridge, UK: Cambridge University Press.

Stern, R. M., Koch, K. L., Stewart, W. R., & Vasey, M. W. (1987). Electrogastrography: Current issues in validation and methodology. *Psychophysiology*, *24*, 55–64. https://doi.org/10.1111/j.1469-8986.1987.tb01862.x

Stern, R. M., Vasey, M. W., Senqi, H., & Koch, K. L. (1991). Effects of cold stress on gastric myoelectric activity. *Neurogastroenterology & Motility*, *3*, 225–228. https://doi.org/10.1111/j.1365-2982.1991.tb00065.x

Suzuki, N., Prosser, C. L., & Dahms, V. (1986). Boundary cells between longitudinal and circular layers: Essential for electrical slow waves in cat intestine. *The American Journal of Physiology*, *250*(3 Pt 1), G287–294. https://doi.org/10.1152/ajpgi.1986.250.3.G287

Sveshnikov, D. S., Smirnov, V. M., Myasnikov, I. L., & Kuchuk, A. V. (2012). Study of the nature of sympathetic trunk nerve fibers enhancing gastric motility. *Bulletin of Experimental Biology and Medicine*, *152*(3), 283–285. https://doi.org/10.1007/s10517-012-1508-z

Tack, J. (2012). Chapter 34—Neurophysiologic mechanisms of gastric reservoir function. In L. R. Johnson, F. K. Ghishan, J. D. Kaunitz, J. L. Merchant, H. M. Said, & J. D. Wood (Eds.), *Physiology of the gastrointestinal tract* (Fifth Edition, pp. 951–957). Boston, MA: Academic Press. https://doi.org/10.1016/B978-0-12-382026-6.00034-8

Taylor, I., Duthie, H. L., Smallwood, R., & Linkens, D. (1975). Large bowel myoelectrical activity in man. *Gut*, *16*(10), 808–814. https://doi.org/10.1136/gut.16.10.808

Thompson, E., & Varela, F. J. (2001). Radical embodiment: Neural dynamics and consciousness. *Trends in Cognitive Sciences*, *5*(10), 418–425. https://doi.org/10.1016/s1364-6613(00)01750-2

Tolj, N. (2007). The impact of age, sex, body mass index and menstrual cycle phase on gastric myoelectrical activity characteristics in a healthy Croatian population. *Collegium Antropologicum*, *31*(4), 955–962.

Tosetti, C., Corinaldesi, R., Stanghellini, V., Pasquali, R., Corbelli, C., Zoccoli, G., … Barbara, L. (1996). Gastric emptying of solids in morbid obesity. *International Journal of Obesity and Related Metabolic Disorders*, *20*, 200–205.

Travagli, R. A., Hermann, G. E., Browning, K. N., & Rogers, R. C. (2006). Brainstem circuits regulating gastric function. *Annual Review of Physiology*, *68*, 279–305. https://doi.org/10.1146/annurev.physiol.68.040504.094635

Tumpeer, I., & Blitsten, P. (1926). Registration of peristalsis by the Einthoven galvanometer. *The American Journal of Diseases of Children*, 454–455.

Uhlrich, D. J., Cucchiaro, J. B., & Sherman, S. M. (1988). The projection of individual axons from the parabrachial region of the brain stem to the dorsal lateral geniculate nucleus in the cat. *The Journal of Neuroscience*, *8*(12), 4565–4575. https://doi.org/10.1523/JNEUROSCI.08-12-04565.1988

Uhlrich, D. J., Tamamaki, N., Murphy, P. C., & Sherman, S. M. (1995). Effects of brain stem parabrachial activation on receptive field properties of cells in the cat's lateral geniculate nucleus. *Journal of Neurophysiology*, *73*(6), 2428–2447. https://doi.org/10.1152/jn.1995.73.6.2428

Umans, B. D., & Liberles, S. D. (2018). Neural sensing of organ volume. *Trends in Neurosciences*, *41*(12), 911–924. https://doi.org/10.1016/j.tins.2018.07.008

van Dyck, Z., Vögele, C., Blechert, J., Lutz, A. P. C., Schulz, A., & Herbert, B. M. (2016). The water load test as a measure of gastric interoception: Development of a two-stage protocol and application to a healthy female population. *PLoS ONE*, *11*(9), e0163574. https://doi.org/10.1371/journal.pone.0163574

van Oudenhove, L., Vandenberghe, J., Dupont, P., Geeraerts, B., Vos, R., Bormans, G., … Tack, J. (2009). Cortical deactivations during gastric fundus distension in health: Visceral pain-specific response or attenuation of «default mode» brain function? A H2 15O-PET study. *Neurogastroenterology and Motility*, *21*(3), 259–271. https://doi.org/10.1111/j.1365-2982.2008.01196.x

Vandenbergh, J., Dupont, P., Fischler, B., Bormans, G., Persoons, P., Janssens, J., & Tack, J. (2005). Regional brain activation during proximal stomach distention in humans: A positron emission tomography study. *Gastroenterology*, *128*(3), 564–573. https://doi.org/10.1053/j.gastro.2004.11.054

Varayil, J. E., Ali, S. M., Tachecí, I., Květina, J., Kopáčová, M., Kuneš, M., … Bureš, J. (2009). Electrogastrography in experimental pigs. *Folia Gastroenterologica Et Hepatologica*, *7*(3–4), 98–104.

Vasavid, P., Chaiwatanarat, T., Pusuwan, P., Sritara, C., Roysri, K., Namwongprom, S., … Gonlachanvit, S. (2014). Normal solid gastric emptying values measured by scintigraphy using asian-style meal: A multicenter study in healthy volunteers. *Journal of Neurogastroenterology and Motility*, *20*(3), 371–378. https://doi.org/10.5056/jnm13114

Verhagen, M. A. M. T., Van Schelven, L. J., Samsom, M., & Smout, A. J. P. M. (1999). Pitfalls in the analysis of electrogastrographic recordings. *Gastroenterology*, *117*(2), 453–460. https://doi.org/10.1053/gast.1999.0029900453

Vianna, E. P. M., Weinstock, J., Elliott, D., Summers, R., & Tranel, D. (2006). Increased feelings with increased body signals. *Social Cognitive and Affective Neuroscience*, *1*(1), 37–48. https://doi.org/10.1093/scan/nsl005

Vogt, B. A., & Derbyshire, S. W. (2009). Visceral circuits and cingulate-mediated autonomic functions. In B. A. Vogt (Ed.), *Cingulate neurobiology and disease* (pp. 219–236). Oxford, UK: Oxford University Press.

Waldhausen, J. H. T., Shaffrey, M. E., Skenderis, B. S., Jones, R. S., & Schirmer, B. D. (1990). Gastrointestinal myoelectric and clinical patterns of recovery after laparotomy. *Annals of Surgery*, *211*(6), 777–785. https://doi.org/10.1097/00000658-199006000-00018

Walker, B. B., & Sandman, C. A. (1977). Physiological response patterns in ulcer patients: Phasic and tonic components of the electrogastrogram. *Psychophysiology*, *14*(4), 393–400. https://doi.org/10.1111/j.1469-8986.1977.tb02971.x

Walldén, J., Lindberg, G., Sandin, M., Thörn, S.-E., & Wattwil, M. (2008). Effects of fentanyl on gastric myoelectrical activity: A possible association with polymorphisms of the mu-opioid receptor gene? *Acta Anaesthesiologica Scandinavica*, *52*(5), 708–715. https://doi.org/10.1111/j.1399-6576.2008.01624.x

Wang, G.-J., Tomasi, D., Backus, W., Wang, R., Telang, F., Geliebter, A., … Volkow, N. D. (2008). Gastric distention activates satiety circuitry in the human brain. *NeuroImage*, *39*(4), 1824–1831. https://doi.org/10.1016/j.neuroimage.2007.11.008

White, E. H. (1964). Additional notes on gastrointestinal activity during avoidance behavior. *Psychological Reports*, *14*(2), 343–347. https://doi.org/10.2466/pr0.1964.14.2.343

Xing, J., Qian, L., & Chen, J. (2006). Experimental gastric dysrhythmias and its correlation with in vivo gastric muscle contractions. *World Journal of Gastroenterology*, *12*(25), 3994–3998. https://doi.org/10.3748/wjg.v12.i25.3994

Yin, J., & Chen, J. D. Z. (2013). Electrogastrography: Methodology, validation and applications. *Journal of Neurogastroenterology and Motility*, *19*(1), 5–17. https://doi.org/10.5056/jnm.2013.19.1.5

How to cite this article: Wolpert N, Rebollo I, Tallon-Baudry C. Electrogastrography for psychophysiological research: Practical considerations, analysis pipeline, and normative data in a large sample. *Psychophysiology*. 2020;00:e13599. https://doi.org/10.1111/psyp.13599

7. Article II: Coupling between the phase of a neural oscillation or bodily rhythm with behavior: evaluation of different statistical procedures

7.1. Introduction

The second methodological challenge for my thesis was to quantify the link between gastric phase and visual perception. Based on the coupling between the gastric rhythm and alpha power (Richter et al., 2017), we hypothesized that hits vs. misses (i.e., seen vs. unseen targets) would cluster at different portions of the gastric phase. While circular tests to assess the statistical relationship between phase and a binary outcome are abundant, only few systematic comparisons exist (van Rullen, 2016; Zoefel et al., 2019), raising the issue of which method is optimal for the question under study.

A specialty of our project was that we wanted to be open to different relationships between phase and behavioral outcome. Most studies, e.g. from the literature on the effect of the phase of a neural oscillation on perception, rely on the assumption that phase-behavior takes a 1:1 relationship, with hits and misses each clustering at one preferred portion of the phase. However, especially for a slow bodily rhythm such as the gastric rhythm, the interaction might be more complex. Behavioral outcome could prefer several phase ranges of the same oscillation, resulting in 2:1 coupling or even higher coupling modes. For example, Richter et al. (2017) found that the modulation of alpha power by gastric phase came in different phase-amplitude profiles. However, it is not clear how different tests perform with regard to those different coupling modes.

Another issue is that tests can be affected by an imbalance in the relative number of observations in the two groups. In near-threshold experiments, which theoretically converge in a 50% hit rate, hits and misses are in principle overall equally probable; however, real experiments typically deviate from this ideal balance. Imbalances in the relative number of observations in turn might reduce the sensitivity of the tests (van Rullen, 2016). While a resampling procedure to recover a potential loss in sensitivity has been proposed (Dugué et al., 2015; Staudigl et al., 2017), it is unclear in how far each of the tests benefits from this procedure. Finally, in addition to the different tests to quantify phase-behavior coupling strength, there are also different options for how to estimate significance on the group level.

We investigated these issues in several simulations, where we imposed statistical relationships between the phases of real data (both the neural alpha rhythm and the gastric rhythm) and artificial binary 'outcomes' (i.e., hits and misses). We first compared the performance of four circular tests (Phase Opposition Sum (POS), Circular Logistic Regression, Watson's test and Modulation Index (MI)) with respect to different coupling modes. For this we generated a time series of 'hits' and 'misses', and systematically increased the strength of phase-outcome coupling. For each strength of phase-outcome coupling, we ran 1,000 virtual experiments with 30 participants. We computed sensitivity as the percentage of experiments correctly detecting an effect and False Positive rate as the percentage of experiments falsely detecting an effect under zero phase-outcome coupling (i.e., when no phase-

outcome effect was injected). As a result, we observed that Circular Logistic regression, POS and Watson's test clearly outperformed MI when the coupling mode was 1:1. The Watson test came with the lowest False Positive rate. In contrast, under higher coupling modes, Circular Logistic Regression and POS showed no sensitivity, with MI and Watson's test being the only sensitive tests. The sensitivity of MI and the Watson test decreased when coupling mode increased, with a sharper decrease for Watson. In other words, MI was the most powerful method for detecting complex phase-outcome relationships.

We also compared different strategies to estimate significance on the group level. First, we tested for significance by directly comparing empirical vs. chance level statistics across participants using a t-test. Second, we used a 'surrogate average' approach which is based on comparing the empirical group-average of phase statistics (e.g. POS values) against a null distribution of surrogate group-averages (Busch et al., 2009). Finally, we included several methods to combine p-values from the subject levels (Edgington, 1972; Fisher, 1938; Stouffer, 1949). We observed that the methods had a similar sensitivity, while the False Positive rate was consistently lower when using the t-test on empirical values vs. chance level.

Next, we investigated how imbalances in the relative number of observations affect the power of the tests. We kept the total number of trials fixed, varied the relative number of hits and misses and performed 1,000 virtual experiments with each ratio in relative number of observations. We computed the phase-outcome test statistics both with and without a resampling procedure which controls for imbalances in number of observations. As a result, we observed that while all tests suffer from a loss in statistical power with larger imbalance in number of observations, POS was the most vulnerable to such imbalances. However, when combining POS with a resampling procedure, POS recovered its sensitivity to the point of becoming the most sensitive method to large imbalances. The other tests did not benefit from the resampling procedure. Thus, POS in combination with resampling is well adapted for situations with large imbalances in the relative number of observations.

In conclusion, our results highlighted the Watson test as a good all-rounder method, with an excellent sensitivity to 1:1 coupling, some sensitivity to higher coupling modes, and good robustness to imbalances in relative number of observations. MI, although least sensitive to 1:1 coupling, was the most sensitive for detecting more complex phase-behavior relationships. These investigations allowed us to optimize our procedure to detect a statistical link between gastric phase and behavioral outcome.

NeuroImage xxx (xxxx) 118050

Contents lists available at ScienceDirect

NeuroImage

journal homepage: www.elsevier.com/locate/ynimg

Coupling between the phase of a neural oscillation or bodily rhythm with behavior: Evaluation of different statistical procedures

Nicolai Wolpert *, Catherine Tallon-Baudry

Laboratoire de Neurosciences Cognitives et Computationnelles, Ecole Normale Supérieure, Inserm u960, PSL University, 24 rue Lhomond, Paris 75005, France

ARTICLE INFO

Keywords:
Oscillations
Rhythms
Behavior
Phase
Simulations
Circular statistics

ABSTRACT

Growing experimental evidence points at relationships between the phase of a cortical or bodily oscillation and behavior, using various circular statistical tests. Here, we systematically compare the performance (sensitivity, False Positive rate) of four circular statistical tests (some commonly used, i.e. Phase Opposition Sum, Circular Logistic Regression, others less common, i.e., Watson test, Modulation Index). We created semi-artificial datasets mimicking real two-alternative forced choice experiments with 30 participants, where we imposed a link between a simulated binary behavioral outcome with the phase of a physiological oscillation. We systematically varied the strength of phase-outcome coupling, the coupling mode (1:1 to 4:1), the overall number of trials and the relative number of trials in the two outcome conditions. We evaluated different strategies to estimate phase-outcome coupling chance level, as well as significance at the individual or group level. The results show that the Watson test, although seldom used in the experimental literature, is an excellent first intention test, with a good sensitivity and low False Positive rate, some sensitivity to 2:1 coupling mode and low computational load. Modulation Index, initially designed for continuous variables but that we find useful to estimate coupling between phase and a binary outcome, should be preferred if coupling mode is higher than 2:1. Phase Opposition Sum, coupled with a resampling procedure, is the only test retaining a good sensitivity in the case of a large unbalance in the number of occurrences of the two behavioral outcomes.

1. Introduction

Oscillations are ubiquitous in the sensory and cognitive brain (Buzsáki et al., 2013). The phase of neural oscillations modulates not only spike rate (Fries et al., 2007) and spike timing (Fiebelkorn and Kastner, 2020) but also behavior. For instance, the phase of infraslow, theta or alpha oscillations at which a near-threshold stimulus is presented correlates with its probability of detection, in the visual (Busch et al., 2009; Dugué et al., 2011; Helfrich et al., 2018; Mathewson et al., 2009), auditory (Ng et al., 2012; Rice and Hagstrom, 1989; Strauß et al., 2015) and somatosensory domain (Ai and Ro, 2013; Baumgarten et al., 2015; Monto et al., 2008). Phase has been also been related to other types of behavior such as reaction time (Callaway and Yeager, 1960; Dustman and Beck, 1965), decision-making (Wyart et al., 2012), visual search performance (Dugué et al., 2015) or auditory discrimination (Kayser et al., 2016; McNair et al., 2019). The timing of eye movements depends on brain alpha phase (Drewes and VanRullen, 2011; Gaarder et al., 1966; Hamm et al., 2012; Staudigl et al., 2017). Finally, the phase of various oscillatory bodily signals, such as the cardiac cycle, the gastric rhythm, or respiration, also influences both neural activity and behavior (for reviews, see Azzalini et al., 2019; Garfinkel and Critchley, 2016; Tort et al., 2018).

Most studies relating the phase of neural or bodily oscillations with behavior aim at establishing a statistical link between phase and a given binary outcome (e.g. “hit” or “miss” in a near-threshold detection experiment). However, just as there is an abundance of paradigms and cognitive variables studied, there is a large variety of statistical methods employed, hindering comparisons between studies. Besides, the reasons why a certain method is favored in a given experimental situation are usually not provided, and only few systematic investigations of the properties of statistical tests relating phase to behavior exist (VanRullen, 2016; Zoefel et al., 2019). Here, we systematically compare the performance of four statistical circular tests (Phase Opposition Sum, Circular Logistic Regression, Watson's test and Modulation Index) to quantify relationships between oscillatory phase and a binary outcome with opposite preferred phases.

* Corresponding author.
E-mail address: nicolaiwolpert@gmail.com (N. Wolpert).

https://doi.org/10.1016/j.neuroimage.2021.118050
Received in revised form 12 February 2021; Accepted 6 April 2021
1053-8119/

We created semi-artificial datasets based on real data acquired from 30 participants at rest, from which we extracted the phase of a neural rhythm (alpha rhythm, 8–12 Hz) and the phase of a bodily rhythm (gastric rhythm, ~0.05 Hz – Wolpert et al., 2020). We simulated a typical two-alternative forced choice experiment, where participants have to choose between two mutually exclusive options at each trial – stimulus seen vs. not in an experiment probing vision at threshold, or dog vs. cat in a categorization experiment with morphed images. Behavior was generated as transient events belonging to two categories ("hits" and "misses") with a flat distribution over time. We then imposed a statistical link between phase and behavior (Fig. 1), with hits more likely (resp. misses less likely) in one phase range, hence creating two behavioral outcomes with opposite preferred phases. The use of a semi-artificial dataset has the advantage of retaining all the complexity of real data, that can be difficult to model, such as the inter- and intra-individual variability in power law exponent (Podvalny et al., 2015; Voytek et al., 2015), individual differences in peak frequencies of oscillations of interest (Haegens et al., 2014), or the cycle duration variability necessary for some statistical procedures (Bahramisharif et al., 2013; Richter et al., 2017). While this approach is ideally suited to derive practical conclusions on the performance of different statistical tests, which is the main aim of this article, it does not allow an in-depth assessment of the effect of data quality and features. We therefore also performed a selected control analysis on synthetic data.

We characterize each of the four tests not only by its sensitivity (the probability of finding an existing phase-outcome effect) but also its False Positive rate (the probability of a significant result despite the absence of a true effect). We systematically varied parameters such as the overall number of observations as well as the relative number of observations in the two outcome conditions. We also varied coupling mode. Indeed, most studies so far relied on the assumption that the phase-behavioral outcome relationship would be a 1:1 coupling with respect to an underlying carrier frequency in an a priori specified frequency band (e.g., 8–12 Hz alpha oscillation or 0.05 Hz gastric rhythm), i.e. with only one phase range associated with a given behavioral outcome. However, phase-behavioral outcome coupling might be more complex, with a given behavioral outcome being more frequent in several phase ranges of the band-specific oscillation, resulting in 2:1 coupling, over even higher coupling modes. Mathematically, a behavioral outcome with 2:1 coupling with an oscillation at frequency f would be equivalent to 1:1 coupling of behavior with an oscillation at frequency f*2. However, data interpretation would be different. Indeed, the brain generates some specific rhythms at a given frequency, like the parieto-occipital rhythm. Bodily rhythms, such as respiration or the gastric rhythm, are defined by their central frequency (respectively ~0.3 Hz and ~0.05 Hz). Thus, from a biological perspective, 2:1 coupling at a (neural or bodily) carrier frequency is not equivalent to 1:1 coupling at twice the carrier frequency. Furthermore, it is possible that there exists inter-subject variability in coupling mode (i.e., with some subjects exhibiting 1:1 coupling, others 2:1 etc.), with regards to the *same* carrier frequency. We thus probed how the four tests compare in relation to such "higher" modes of coupling, and show that Modulation Index (Tort et al., 2010), originally devised for continuous variables, detects the link between (continuous) phase and a binary response variable.

Before presenting the results, we remind the reader of the rationale behind each of the four evaluation methods we test (Fig. 2), which are all *non-parametric* methods. In logistic regression, the phases of the two groups are used as circular predictors in a regression model to predict the outcome (e.g. choice in an auditory discrimination task – Kayser et al., 2016; McNair et al., 2019). Another method that has been proposed is *Phase Opposition Sum* (POS), which measures the extent to which phases of different groups cluster at different portions of a cycle (VanRullen, 2016). It is based on the Inter-Trial phase Coherence (ITC), which quantifies the extent of phase concentration across trials (Lachaux et al., 1999; Tallon-Baudry and Bertrand, 1999). Significance testing is done with non-parametric permutation statistics (VanRullen, 2016). The Watson test is the nonparametric version of the Watson-Williams two-sample test. It computes a test statistic U^2, which is based on the ordering of the phases and computing the cumulative relative frequency distributions. Last, we adapted the *Modulation Index* (MI, Tort et al., 2010), initially proposed to detect phase-amplitude coupling between continuous variables, to coupling between phase and a binary behavioral outcome. Here, MI is computed based on an event *rate* of one of the conditions (e.g., hit rate per phase bin). This method measures the extent to which an empirical distribution (here, hit rate per phase bin) differs from a uniform distribution. Significance is estimated by a surrogate procedure, as for POS.

2. Material and methods

2.1. Experimental data

We used real data to extract physiological phase time series, on which we simulated behavioral output. Data were obtained from 30 healthy participants (16 male, mean age 24, range 19–30) in resting-state with eyes open, 21 corresponding to already analyzed and published data (Richter et al., 2017; Wolpert et al., 2020) and the rest to an unpublished pilot study. All participants signed a written informed consent and were paid for participation. The procedures were approved by the Ethics Committee CPP Île de France III and were in accordance with the Helsinki declaration. Recordings were of 12–15 min length. Brain spontaneous activity was measured with an Elekta Neuromag® TRIUX magnetoencephalography (MEG) system with a sampling frequency of 1000 Hz. Signal Space Separation (tSSS) was performed using MaxFilter (Elekta Neuromag) to remove external noise. Subsequent analysis was conducted on magnetometer signals. The cardiac artifact was corrected using Independent Component Analysis (ICA), as implemented in the FieldTrip toolbox (Oostenveld et al., 2011). Briefly, MEG data were highpass-filtered at 0.5 Hz (zero phase shift 4th order butterworth filter) and epoched from 200 ms before to 200 ms after each R-peak. The number of independent components to be identified was the rank of the time × trial matrix. Continuous magnetometer data were then decomposed according to identified ICA components. The pairwise phase-consistency (PPC, Vinck et al., 2010) was computed between the ICA-decomposed signals and the ECG signal to isolate those components most reflective of ECG activity. Components with PPC values larger than 3 standard deviations than the mean were rejected iteratively from the continuous MEG data from each block until either no component exceeded 3 standard deviations or 3 components were rejected. In practice, this resulted in 3 components being rejected in each subject. Blink artifacts were defined by the EyeLink eyetracker system, padded by ±100 ms. Muscle and movement artifacts were identified automatically based on a z-value threshold on the MEG data filtered into a band of 110–140 Hz and 4–30 Hz respectively.

Concomitant to MEG, electrogastrogram (EGG) data were recorded by means of seven active electrodes placed on the abdominal skin (for details on EGG acquisition and preprocessing see Wolpert et al., 2020). Since we wanted to compare results using phase time series of two oscillations with very different frequencies, we extracted both the phase of MEG alpha oscillations (8–12 Hz) from the magnetometer channel with the largest alpha power, as well as the phase of the gastric slow rhythm (~0.05 Hz) from the abdominal electrode showing the largest EGG signal. To obtain the alpha phase time series, we first applied an 8–12 Hz bandpass 6th order Butterworth zero-phase shift filter using the Fieldtrip toolbox (Oostenveld et al., 2011). The EEG time series were filtered around gastric peak frequency (mean 0.049 ± 0.005 Hz) with a third-order frequency sampling designed finite impulse response filter (MATLAB: FIR2), with a bandwidth of ±0.015 Hz around gastric peak frequency. We then retrieved instantaneous phase applying the Hilbert transform to the filtered data.

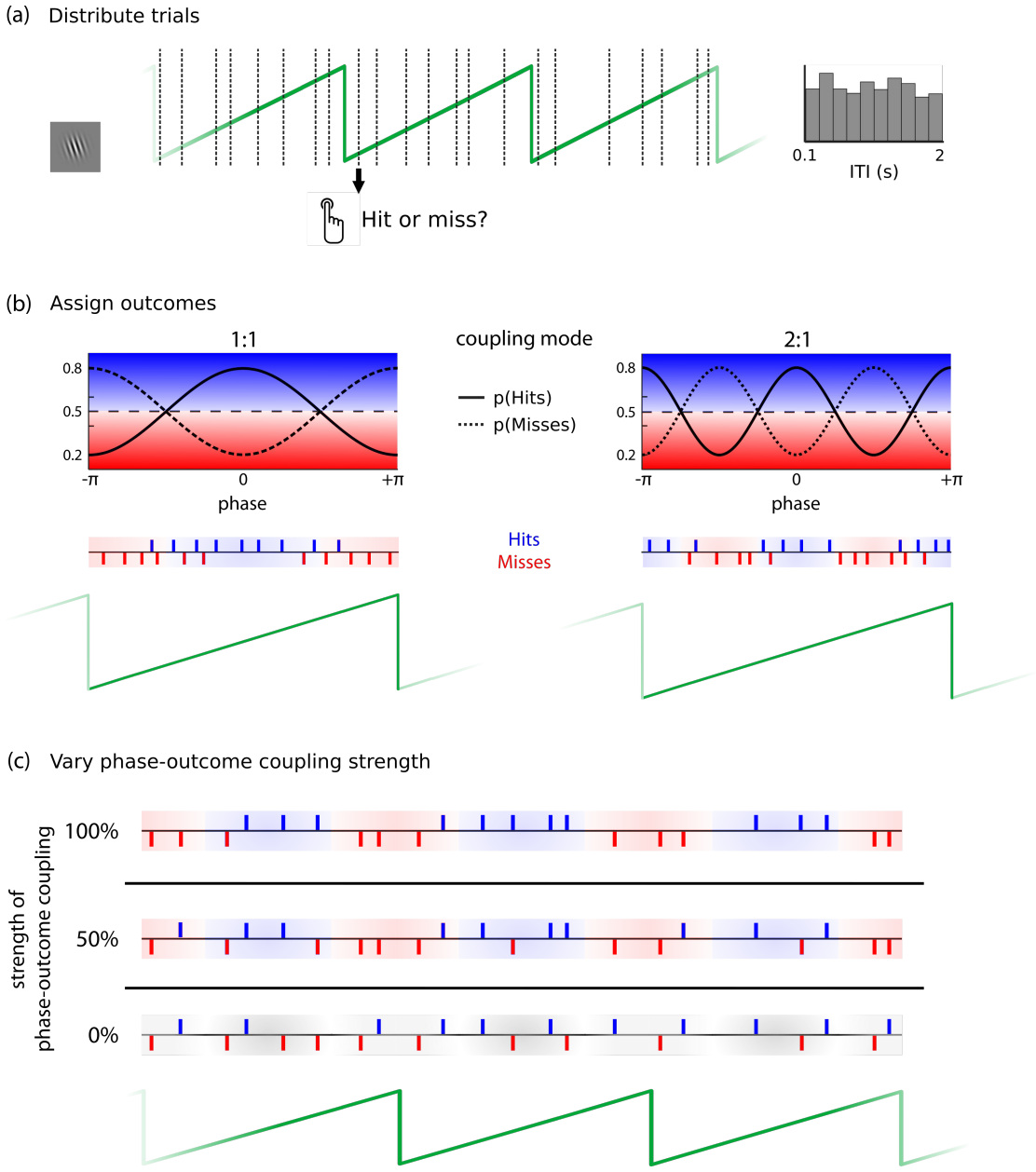

Fig. 1. Procedure for simulating behavior. (a) In a first step, a series of "trials" was distributed with a random Inter-Trial-Interval (ITI) selected from a flat distribution between 100 and 2000 ms, mimicking button presses uniformly distributed over time (b) Next, mutually exclusive behavioral outcomes, as in two-alternative forced choice experiments (hits and misses) were determined for each trial as a function of phase. A hit was assigned with mean probability of 0.5 (dashed lines), which was modulated over a cycle of the carrier frequency by a cosine function, such that hit probability (solid lines) ranged between 0.2 and 0.8. For a 1:1 coupling mode (left), p_{Hit} contained a single peak. For a 2:1 coupling mode (right), the probability function was rescaled to contain two peaks. The probability function for misses (dotted line) was defined as 1-p_{Hit}. By design, hits and misses where therefore distributed to occur at opposite phases. Middle rows show an example of resulting occurrences of hits and misses. Of note, the phase range at which a given outcome was more likely was fixed within a participant, but could vary between participants. (c) Phase-outcome coupling strength was varied by randomly reassigning labels (hits or misses) to a proportion of behavioral outcome. Top row: time series with 100% phase-outcome coupling, no label reassignment. Middle row: time series at 50% phase-outcome coupling strength (random label reassignment in 50% of the trials). Bottom row: time series with 0% phase-outcome coupling (random label reassignment in 100% of trials). Hits and misses are distributed randomly.

2.2. Simulations of phase-behavior relationships

The general rationale for simulations was as follows. We simulated 1000 virtual "experiments" with 30 participants each. For each participant, we created an artificial time series of outcomes, "hits" and "misses" with a two-step procedure. First (Fig. 1a), we created a series of "events" (mimicking "trials" in a perceptual experiment) with a random time interval selected from a flat distribution between 100 and 2000 ms. In this way, trials were distributed uniformly with respect to phase. In a second step (Fig. 1b), the label "hit" or "miss" was assigned to each trial according to a probability function depending on phase. The outcome "hit" was assigned with a mean probability of 0.5, which was modulated as a cosine function of phase defined on $-\pi$ to $+\pi$, rescaled in amplitude to take values between 0.2 and 0.8. The probability function for misses was then defined as $p_{Miss} = 1 - p_{Hit}$. In other words, an event placed at the preferred phase for hits would have an 80% probability of being a hit and 20% probability of being a miss. Note also that because p_{Miss} and p_{Hit} sum up to 1 at each phase, hits and misses have opposite preferred phases. We rotated the probability function to a random degree, such that preferred phases varied across sub-

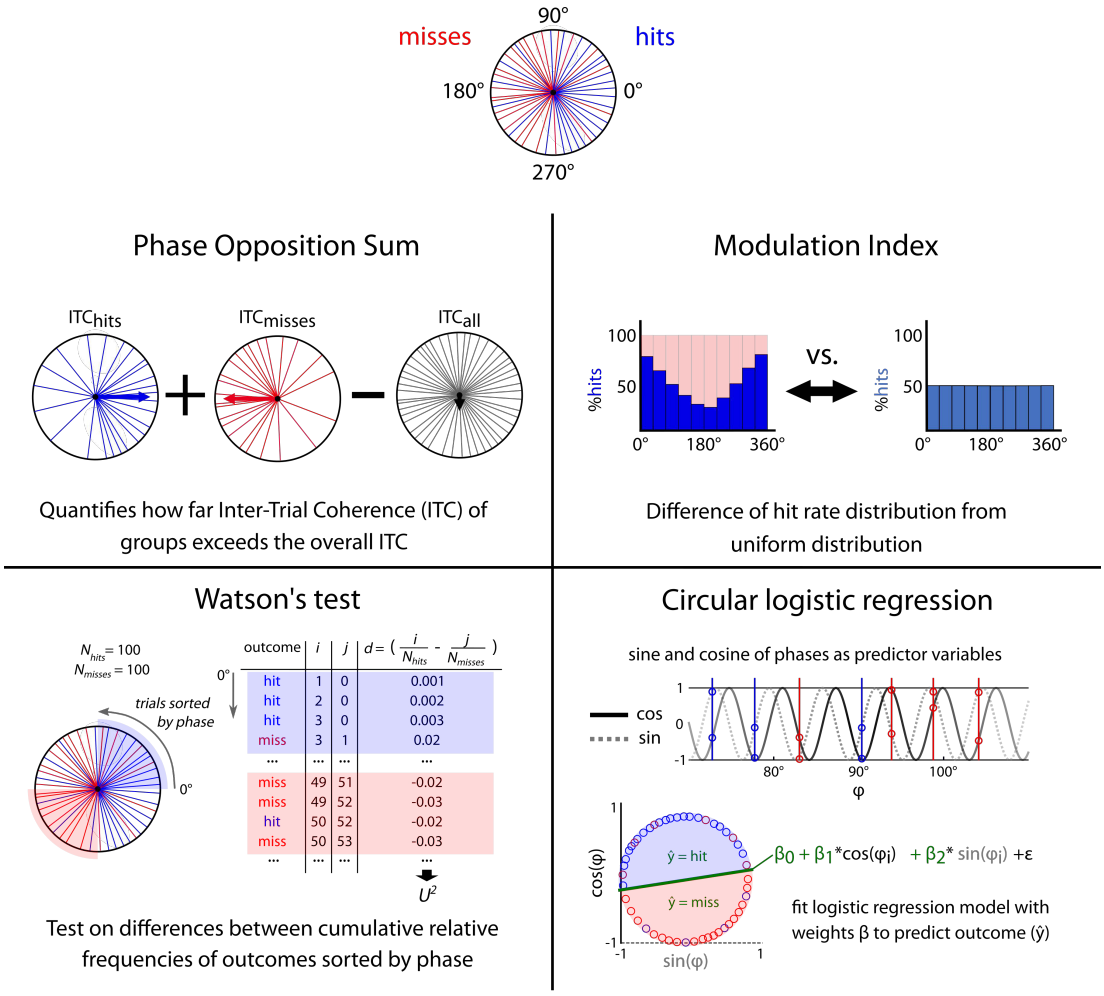

Fig. 2. Illustration of statistical tests compared in this paper. The aim is to assess whether hits (blue) and misses (red) are occurring at different oscillatory phases (polar circle, top). Phase Opposition Sum (VanRullen, 2016): This measure is based on the Inter-Trial Coherence (ITC), which quantifies the extent of phase concentration for a set of trials. Phase Opposition Sum combines the ITCs by subtracting the overall ITC from the separate ITC from each group. It thus becomes positive if the phases separated into hits and misses result in a higher ITC than the overall ITC. Modulation Index (Tort et al., 2010): The phase is binned into *N* phase bins of equal width, and the hit rate per phase bin computed, yielding a hit rate distribution. Note that the hit rate distribution is the mirror image of the miss rate distribution. If hits and misses occur at different portions of the cycle, the distribution will deviate from uniformity. MI measures the extent to which the empirical hit rate distribution deviates from a flat uniform distribution. Watson's test: Phases from hits and misses are sorted in ascending order, and for each trial, index *i* counts the cumulative number of hits and index *j* the cumulative number of misses. At each trial (row), the difference between the respective cumulative relative frequencies (*i*/#hits and *j*/#misses) is then computed. These differences are combined into a test statistic U^2 (for formula see 2.3). Circular logistic regression: The sine and cosine of phases for hits and misses are used as predictors in a circular logistic regression model with coefficients β_1 and β_2 and the intercept term β_0. To quantify the performance of the fit, a root-mean square is then computed using true outcomes and predictor coefficients.)(For interpretation of the references to color in this figure legend, the reader is referred to the web version of this article.)

jects within an experiment, as well as across experiments. To simulate higher coupling modes, probability functions were rescaled to contain two, three or four peaks and troughs per physiological phase cycle, thereby representing different "coupling modes", with either one, two, three or four preferred phases. We refer to these coupling modes as 1:1, 2:1, 3:1 and 4:1.

Finally, we introduced a parameter to vary the strength of the effect, which we call the *strength of phase-outcome coupling* (Fig. 1c). This was done by adding a certain amount of randomness or "noise" to the outcomes of events: A given proportion of trials was selected where a hit or miss was re-assigned with 50:50% chance. For example, with a strength of phase-outcome coupling of 30%, the outcome of trials would depend on phase in 30% of trials, whereas the remaining 70% of trials would be randomly selected, independently of phase. Finally, we randomly subsampled a set of a given size for hits and misses respectively, thereby controlling the number of trials for hits and misses and the relative number of trials in each group.

In sum, our simulations varied the following parameters: 1) *Strength of phase-outcome coupling*, or percentage of trials where outcome depended on phase; 2) *Coupling mode*, or number of peaks of the probability function for outcome by phase, reflecting the number of preferred phase ranges for each behavioral outcome. We refer to these coupling modes as 1:1, 2:1, 3:1 and 4:1, from 1 preferred phase range to 4. 3) Overall *number of trials* in the experiment, and 4) the *relative number of trials* for each behavioral outcome.

2.2.1. Sensitivity-analysis

We aimed to assess which statistical test would be most sensitive to detect phase-behavior relationships under a given coupling mode. For this, we generated a time series of hits and misses, keeping the total number of trials constant at 250 with as many hits as misses, while systematically increasing the strength of phase-outcome coupling. Phase-outcome coupling strength started from 0% (i.e., random behavior, no relationship between behavioral outcome and phase) and was incre-

mented in steps of 5% up to 40% (i.e., behavioral outcome depends on phase in 40% of the trials). We verified that the difference in the number of observations between the two conditions after imposing noise was not more than 10%. For each strength of phase-outcome coupling, we ran 1000 virtual experiments with 30 subjects each. For each virtual experiment, we distributed events in each subject separately, assigned the labels hits and misses to those events according to the probability functions by phase, and computed the phase-outcome statistics for the four different tests (see Section 2.3). We then assessed for each virtual experiment if there was a significant effect at the group-level ($p < \alpha = 0.05$; for how we assess significance at the group level, see Section 2.5). We repeated this procedure for each of the coupling modes investigated from 1:1 to 4:1.

We defined the False Positive rate as the percentage of experiments with 0% strength of phase-outcome coupling, i.e. no effect present, where significant group-level effect was (falsely) detected. Sensitivity (True Positive rate) for phase-outcome coupling strength larger than 0% was computed as the percentage of experiments correctly detecting an injected phase-outcome coupling. This allowed us to compare the performance of different statistical tests as the strength of phase-outcome coupling was gradually increased.

2.2.2. Relative trial number between groups

In a different set of simulations, we addressed how an imbalance in the number of observations for hits and misses would affect the statistical tests. We initially distributed 240 hits and 240 misses, with the strength of phase-outcome coupling fixed at either 15%, to estimate sensitivity, or 0%, to estimate False Positive rate. From this pool of 2×240 events, we subsampled a number of hits and misses, systematically varying the relative proportion in number of observations for hits vs. misses (i.e., 20:80, 30:70, 40:60, 70:30 and 80:20), while keeping the total number of trials constant at 300. To generate the sample with a ratio of 20:80, we subsampled 60 of the initial set of hits and kept all 240 misses. To generate the sample with a ratio of 30:70, we build on the 20:80 sample by adding 30 hits and removing 30 misses, and so on. This was done in 1000 virtual experiments with 30 subjects each.

To assess how a potential loss in sensitivity for an imbalanced number of trials can be recovered, we applied the resampling procedure proposed by (Dugué et al., 2015; Staudigl et al., 2017). This procedure works as follows: For each subject, one resamples (without replacement) as many trials from the group with more trials as there are trials in the smaller group, and recomputes the phase-outcome statistics. This procedure is repeated N times (in our case $N = 100$), resulting in a distribution of N resampled values. The true test statistic is then estimated as the mean of this resample distribution. To quantify the impact of this resampling procedure, we computed for each hit:miss proportion the phase-outcome statistics both with and without resampling. In sum, this yielded 2×2 conditions: Effect present or absent and resampling vs. no resampling.

2.2.3. Amplitude of the underlying oscillation

In an additional analysis, we investigated the impact of the amplitude of the oscillation modulating outcome. For this, we first created a synthetic 10 Hz oscillation as a sinewave of amplitude scaled to [−1;1], with a sampling frequency of 1000 Hz and 15 min duration (Fig. 3). For each of the 30 virtual subjects, hits and misses were assigned based on the synthetic 10 Hz sinewave. We then modulated the amplitude of the 10 Hz oscillation by a scaling factor ranging between 0 and 0.2 before adding it to background noise, generated as pink noise with an amplitude rescaled to [−1, 1]. The resulting combined signal was then filtered around 10 Hz (±1) using a 6th order Butterworth zero-phase shift filter, and the Hilbert transform was applied on the combined signal to extract instantaneous phase. The resulting phase time series thus represented the "empirical" phase time series whose signal-to-noise ratio depended on the amplitude of the true underlying oscillation. Phases for hits and misses were extracted, and the phase-outcome statistics computed for each amplitude. This was repeated in 1000 virtual experiments, to compute sensitivity and False Positive rate.

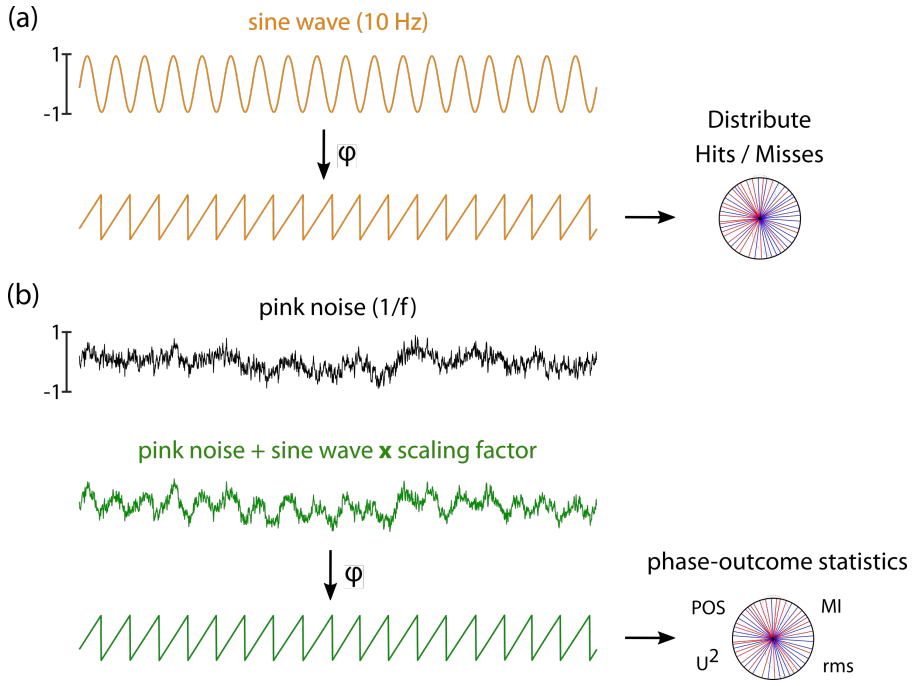

Fig. 3. Simulations on oscillatory amplitude. (a) A pure sine wave at 10 Hz was generated with an amplitude between −1 and 1, and hits and misses were distributed based on its instantaneous phase. (b) Background activity was simulated as pink noise with an amplitude between −1 and 1. The sine wave was multiplied with a scaling factor and added to background activity, and instantaneous phase retrieved. Phases for hits and misses based on the phase time series of this combined signal were then retrieved and the phase-outcome statistics computed for each amplitude.

2.3. Statistical tests

We applied four circular statistical tests commonly used in the field of neuroscience (Fig. 2).

2.3.1. Phase Opposition Sum (POS)

The Phase Opposition Sum (POS) index is a non-parametric method assessing phase differences between conditions (Drewes and VanRullen, 2011; Dugué et al., 2011; VanRullen, 2016). It is based on a comparison of the phase concentration of hits and misses to a phase locking computed over all trials. The extent of phase concentration is quantified using the *Inter-Trial Coherence measure* (ITC – Tallon-Baudry et al., 1996; Lachaux et al., 1999), which is defined as:

$$ITC_{all} = \sum_{i=1}^{N_{all}} \Phi_i / N_{all} \quad (1)$$

$$ITC_{hits} = \sum_{i=1}^{N_{hits}} \Phi_i \ / N_{hits} \quad (2)$$

$$ITC_{misses} = \sum_{i=1}^{N_{misses}} \Phi_i \ / N_{misses} \quad (3)$$

where Φ_i is the phase angle at which the event i occurs, N_{all} the total number of trials, and N_{hits} and N_{misses} are the number of hits and misses. Inter-Trial Coherence quantifies the phase-locking of a circular distribution of phases by taking values between 0 (uniform phase distribution) and 1 (perfect phase-alignment). The *Phase Opposition Sum* (POS) is then defined as:

$$POS = ITC_{hits} + ITC_{misses} - 2ITC_{all} \quad (4)$$

POS is positive when the ITC of each group exceeds the overall ITC. The POS measure is a recent improvement (VanRullen, 2016) of the Phase Bifurcation Index, defined as (ITC_{hits} - ITC_{all}) * (ITC_{misses} - ITC_{all}), which has been the measure of choice for many studies on phase differences (e.g., Busch et al., 2009). Using the additive measure is motivated by the finding that POS is more robust to low trial numbers and differences in relative trial numbers between groups compared to the Phase Bifurcation Index and a number of other measures (Sherman et al., 2016; VanRullen, 2016).

Note that the raw POS value obtained is not yet informative whether significant phase-concentration is present or not. An additional step is required to quantify the deviance from a null distribution estimated by a permutation procedure, as will be detailed in Section 2.4.

2.3.2. Watson's test

The Watson test is the nonparametric version of the Watson-Williams two-sample test, the circular equivalent of a two-sample *t*-test for angular means (Baumgarten et al., 2015; Samaha et al., 2015; VanRullen, 2016), since it does not rely on the assumption that the sampled populations are unimodal. It is computed the following way (Zar, 2010): First, the phases of hits and misses are separately grouped in ascending order. Let N_{hits} and N_{misses} denote the number of samples in each group, and N the total number of samples ($N_{hits} + N_{misses}$). With i as the index of hits and j as index of misses, the cumulative relative frequencies for the observations in the two groups are then computed as i/N_{hits} and j/N_{misses}. Values of d_k (with k running from 1 to N) are defined as the differences between the two cumulative relative frequency distributions ($d_k = i/N_{hits} - j/N_{misses}$). The test statistics, called Watson's U^2, is then computed as:

$$U^2 = \frac{N_{hits} N_{misses}}{N^2} \left[\sum_{k=1}^{N} d_k^2 - \frac{\left(\sum_{k=1}^{N} d_k\right)^2}{N} \right] \quad (5)$$

Significance can be read from significance tables for U^2 (see Zar, 2010). We also estimate significance of U^2 using the same permutation procedure as for POS and MI, described in Section 2.4.

2.3.3. Circular logistic regression

Circular logistic regression is used to test whether phase predicts outcome at the single-trial level. Phases are sine- and cosine transformed and used as circular predictors of the outcome in a regression model (Al-Daffaie and Khan, 2017):

$$\hat{y}_i = \beta_0 + \beta_1 \cos \Phi_i + \beta_2 \sin \Phi_i + \varepsilon \quad (6)$$

where $\hat{y}_i$ is the outcome for trial i, Φ_i is the phase at which the event occurred in trial i and ε the error term. A p-value for each participant can be directly obtained by comparing the full regression model with an intercept-only model using an F-Test, as described in (Zoefel et al., 2019). The root-mean-square of the obtained predictor coefficients $\left(\sqrt{{\beta_1}^2 + {\beta_2}^2}\right)$ is used to quantify how well phase predicts behavioral outcome. As for the other tests, we here computed p-values using a permutation procedure (see Section 2.4) to assess whether the root-mean-square was higher than expected by chance.

2.3.4. Modulation Index (MI)

The Modulation Index (Tort et al., 2010), or MI, measures the extent to which an empirical distribution differs from a uniform distribution with the Kullback-Leibler distance. It was originally applied to detect phase-amplitude coupling (Tort et al., 2008, 2009), i.e. between phase and a *continuous* neural variable. We modified the method to quantify the relationship between phase and a *binary* response variable (hits vs. misses). We transform hits and misses into a hit *rate* per oscillatory phase bin. Phases are sorted into K bins spanning the [-π, π] interval (here: $K = 10$), and the hit rate computed for each bin. MI measures how far the distribution of hit rate deviates from a uniform distribution with respect to phase bins. (Note that MI could also be computed based on miss rate. The two distributions are in fact complementary.) Formally, MI is defined as:

$$MI = \frac{\log(K) + \sum_{j=1}^{K} P(j) * \log P(j)}{\log(K)} \quad (7)$$

Where P(j) is the standardized hit rate in phase bin j:

$$P(j) = \frac{Hit\ rate\varphi(j)}{\sum_{i=1}^{K} Hit\ rate\varphi(i)} \quad (8)$$

And the hit rate per phase bin HR_φ is the number of hits in the phase bin φ divided by the total number of trials in the phase bin:

$$HR_\varphi = \frac{NHits\varphi}{NHits\varphi + NMisses\varphi} \quad (9)$$

Note that MI thus differs from the other tests considered here since it is not directly based on the phases themselves but based on a *proportion* of hits relative to the number of trials in each bin. MI ranges from 0 if there is no phase-modulation of hit rate at all (meaning a perfectly uniform distribution) to 1 if there is perfect coupling (i.e. $P(j) = 1$ for a given bin and 0 for all other bins). With a limited number of trials, it might happen that $P(j)$ is zero, i.e. no hit in that phase bin. The bin can simply be ignored, because adding or removing an event with zero probability does not alter entropy.

2.4. Significance at the single subject level

While Watson's test and circular logistic regression directly return a p-value, POS and MI yield only raw values which do not inform on statistical significance. We use a permutation-based approach to estimate

a distribution of phase statistics under the null-hypothesis of no phase-outcome relationship (Fig. 4a). This step is necessary for POS or MI but can be applied to other phase statistics (Watson's U^2, root mean squares of the logistic regression).

The rationale for this procedure is to abolish the hypothetical effect of phase on behavioral outcome in the original data by randomly reassigning behavioral outcomes in single participants. For each given subject, the event assignment to hit or miss is randomly permuted 100 times, e.g. maintaining the hit/miss proportion and timings but randomizing the link with phase by assigning the hit/miss label randomly. Because we distributed trials uniformly with respect to phase, surrogate phase distributions would also converge to uniformity (with slight departures due to noise – Fig. 4b). Phase statistics are recomputed at each permutation, to generate the distribution of phase statistics under the null hypothesis. Chance level is defined as the mean (or median, but see 3.2) of this null distribution. The comparison of the empirical phase sta-

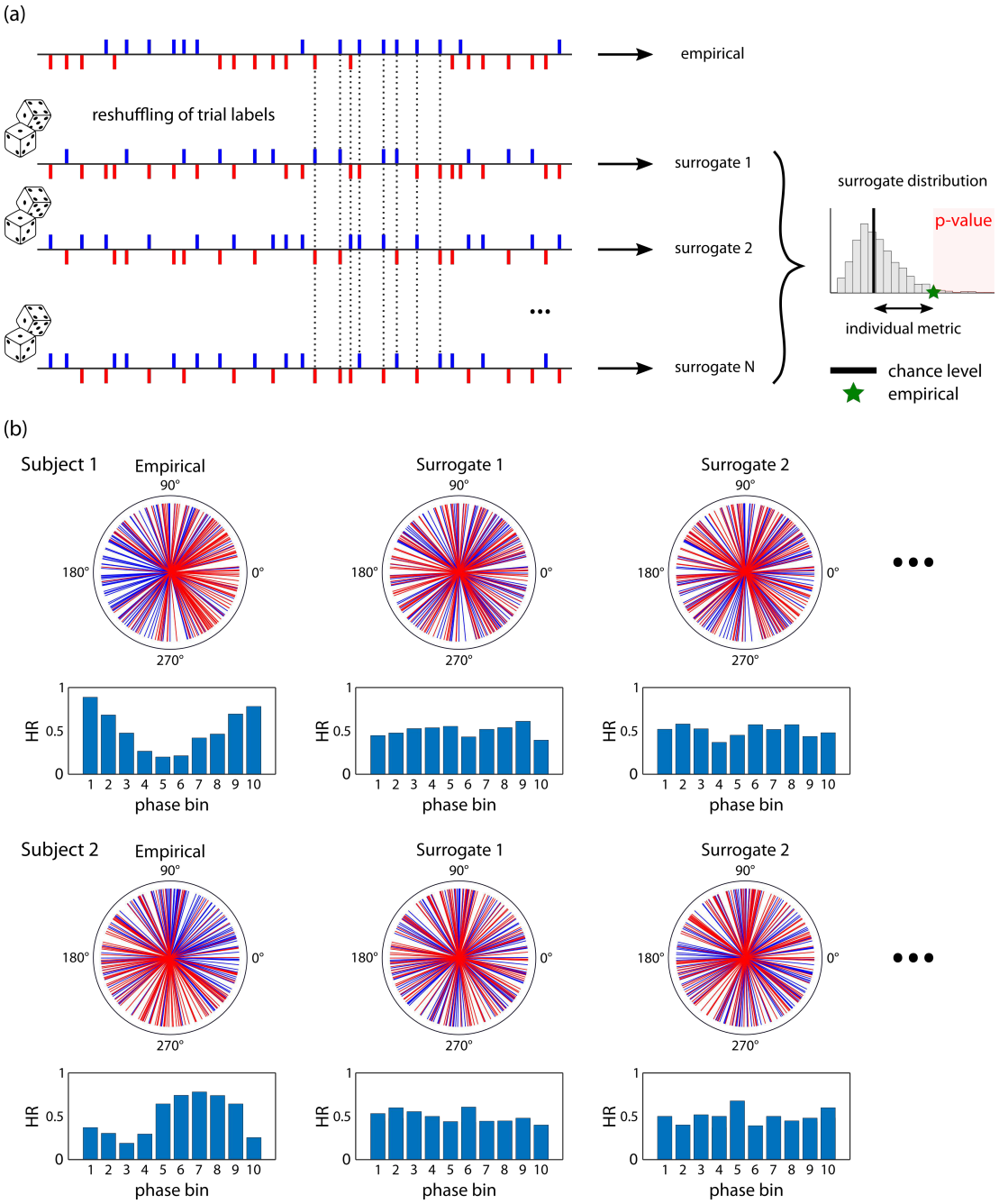

Fig. 4. (a) Permutation approach to estimate null distributions of no phase-outcome relationships. Top row: From the original time series of hits and misses, an empirical phase-outcome statistic is computed. The trial outcomes are then reshuffled (lower rows), with hit and miss labels randomly permuted, resulting in a new time series of hits and misses where the phase-outcome link is abolished while keeping the balance of relative number of observations and inter-stimulus intervals. This is repeated *N* times, and for each reshuffling, the phase-outcome statistic is computed. This results in a surrogate distribution (right). Chance level (black vertical line) is then defined as the mean of this distribution. The difference between the empirical phase-outcome statistic (green star) and chance level provides an individual metric of the strength of the phase-outcome effect. Additionally, an individual *p*-value can be computed as the proportion of surrogate values higher than empirical. (b) Example of empirical (left column) and surrogate (middle and right columns) phase distributions, for a phase-outcome coupling strength of 100% and 250 trials. Upper row: Polar representation, lower row: distributions of hit rate per phase bin.(For interpretation of the references to color in this figure legend, the reader is referred to the web version of this article.)

tistics with the null distribution yields a Monte-Carlo *p*-value at the single subject level (proportion of surrogate values larger than the empirical one). Additionally, the difference between the empirical phase statistics and chance level provides an individual metric of the strength of the phase-outcome coupling.

2.5. Testing for significance at the group level

Significance at the group level can be assessed either by direct comparison between chance level statistics and empirical statistics, by computing surrogate averages, or by combining individual *p*-values.

2.5.1. Empirical vs. chance level

One option consists in comparing the empirical phase statistics to chance level estimates across participants, using a one-tailed paired-sample *t*-test, as in Richter et al., 2017. The test is one-tailed because the hypothesis is that there is more phase coupling than expected by chance.

2.5.2. Surrogate average

An alternative method is based on comparing the empirical group-average of phase statistics (e.g. POS values) against a null distribution of surrogate group-averages (Busch et al., 2009). One value is drawn randomly from the surrogate distribution from each subject, the average across subjects computed, and this is repeated 1000 times. This yields a distribution of 1000 surrogate averages under the null hypothesis. A Monte-Carlo *p*-value is then computed as the proportion of surrogate averages that are larger than the empirical average, and the result is considered as significant if this group-level *p*-value is below the threshold of significance ($p = .05$).

2.5.3. Combining p-values

Another option to calculate group-level significance is to combine the results of the individual subjects (VanRullen, 2016). We used the individual *p*-values corresponding to the proportion of permutations yielding a higher phase-outcome statistic than the empirical value. In case the *p*-value was smaller than $1 / N_{perm}$, we assigned the midpoint between zero and $1 / N_{perm}$, which is $1 / (2 * N_{perm})$. (vanRullen, 2016). To combine *p*-values, a wide range of different methods is available (Alves and Yu, 2014; Heard and Rubin-Delanchy, 2018; Loughin, 2004; Rosenthal, 1978), of which we selected three of the most frequently used.

2.5.3.1. Fisher's method. Fisher's method combines the individual *p*-values from *K* independent tests into the following test statistic (Fisher, 1938):

$$T = -2 * \sum_{i=1}^{K} \ln(p_i) \tag{11}$$

where p_i corresponds to the *p*-value of participant *i*. Under the null hypothesis, *T* follows a chi-square distribution with $2K$ degrees of freedom (Alves and Yu, 2014; Fisher, 1938; Zoefel et al., 2019). From this, a combined *p*-value can be obtained.

Fisher's method has been shown to be asymmetrically sensitive to small compared to large *p*-values (Whitlock, 2005). This might be a drawback depending on the context in which this test is used.

2.5.3.2. Stouffer's method. Stouffer's method (Stouffer, 1949) relies on a transformation of one-tailed *p*-values of *K* independent tests into equivalent *z*-scores, which are combined across observers into one *z*-score, which is finally turned back into a *p*-value:

$$p_{combined} = 1 - F\left(\sum_{i=0}^{K} \mathrm{F}^{-1}(1 - p_i) \;/\; \sqrt{N}\right) \tag{12}$$

Where *F* is the normal cumulative distribution function.

This test does not show any asymmetry with respect to *p*-values as mentioned for the Fisher method. It can be seen as a compromise between methods like Fisher's method with high sensitivity to small *p*-values and other methods with high sensitivity to large *p*-values (Heard and Rubin-Delanchy, 2018).

2.5.3.3. Edgington's method. Edgington proposed to combine *p*-values by a simple sum across *K* observations (Edgington, 1972):

$$S_E = \sum_{i=1}^{K} p_i \tag{13}$$

The combined *p*-value is then obtained from the cumulative distribution function for the resulting sum (Heard and Rubin-Delanchy, 2018; Zaykin et al., 2007).

2.6. Data and code availability statement

The custom code as well as a set of phase time series from real participants for performing the simulations for this article can be accessed online at the following address: https://github.com/niwolpert/Simulations_phase_statistics. Our scripts make use of Matlab's Circular Statistics Toolbox (Berens, 2009, available at: https://fr.mathworks.com/matlabcentral/fileexchange/10676-circular-statistics-toolbox-directional-statistics). In addition, we made use of Rufin van Rullen's code on Phase Opposition (VanRullen, 2016, available at: www.cerco.ups-tlse.fr/~rufin/PhaseOppositionCode/).

3. Results

3.1. Sensitivity of statistical tests across different coupling modes

We investigated the sensitivity of four statistical circular tests (circular logistic regression, Phase Opposition Sum (POS), Watson's test, the Raleigh test and Modulation Index (MI)) to coupling between oscillatory phase and behavioral outcome (i.e., hits vs. misses). We extracted physiological oscillations from real data of 30 participants, and created artificial series of behavioral outcomes where we controlled the statistical relationship between phase and outcome, systematically varying the percentage of events where the outcome probability depended on phase, which we call the phase-outcome coupling strength. We also varied coupling mode from 1:1 to 4:1 (Fig. 1b). For 30 virtual participants, we set the number of trials to 250 and distributed hits and misses with respect to phase, following a given coupling mode and strength of phase-outcome coupling, and applied the four statistical tests. For each subject we estimated a null distribution for the phase-outcome statistics of each test (POS, MI, Watson's U^2, and root-mean-square of circular logistic regression) by a reshuffling procedure (Fig. 4), and defined chance level as the mean of the surrogate distribution. We then tested across subjects if empirical values were significantly higher than chance levels by means of a one-tailed paired samples *t*-test (in the following denoted as the "empirical vs. chance method"). We performed 1000 of such virtual experiments with 30 participants each. Sensitivity was computed as the percentage of experiments detecting a significant effect ($p < .05$). Additionally, we estimated the False Positive rate for each of the tests by computing the number of experiments that yielded a significant difference when outcomes were purely randomly assigned, independently of phase.

We performed these simulations for two types of real oscillations of very different frequencies and origin (alpha 8–12 Hz oscillation measured with MEG and gastric slow wave at ~0.05 Hz, during resting state), to ensure that the results do not depend on the frequency or origin of oscillations. We also ran the same simulations on synthetic data (10 Hz sine wave superimposed on pink noise). As we observed very

similar results for the different types of oscillations, we restrict the presentation of results to the real alpha oscillation.

The results on sensitivity for a 1:1 coupling mode are presented in Fig. 5a,b. We observed that circular logistic regression, POS and the Watson test were similarly sensitive (Fig. 5a), with True Positive rate saturating at 25% phase locking strength. Circular logistic regression was slightly more sensitive than the other two, to the cost of a higher False Positive rate (Fig. 5b). The Watson test appears as a sensitive method with low False Positive rate. The sensitivity of MI was well below these three tests, sensitivity saturating at 35% strength of phase-outcome coupling. The corresponding results for synthetic data are presented in Supplementary Figure 1.

Next, we investigated the influence of coupling mode on sensitivity by varying coupling mode from 1:1 to 4:1. Results are summarized in Fig. 5c. Circular logistic regression and POS do not detect coupling beyond the 1:1 coupling mode. The sensitivity of MI and the Watson test decreases when coupling mode increases, with a sharper decrease for Watson.

We also tested whether sensitivity depended on the overall number of trials for a 1:1 coupling mode by keeping the strength of phase-outcome coupling constant at 20% and gradually increasing the number of trials from 50 to 400 (Fig. 6). Sensitivity increased for all four statistical tests, and circular logistic regression, POS and the Watson test outperformed MI. False Positive Rate did not vary depending on the number of trials for any of the tests and was constantly below 5%.

In summary, we found clear differences in sensitivity between the statistical tests for different modes of coupling between phase and outcome: For 1:1 relationships, circular logistic regression, POS and the Watson test were all similarly sensitive, while MI was substantially less sensitive. In contrast, for higher forms of coupling, circular logistic regression and POS completely failed, with MI and Watson test as only sensitive tests. MI was the most powerful test for higher coupling modes. The Watson test was the only test being sensitive to all types of coupling modes, with a low False Positive rate.

3.2. *Different ways of assessing significance at the group level*

Significance of outcome-phase coupling at the group level can be assessed through various methods. In this section, we compare three different methods: empirical vs. chance (employed in the results described above), surrogate average, and combination of individual *p*-values.

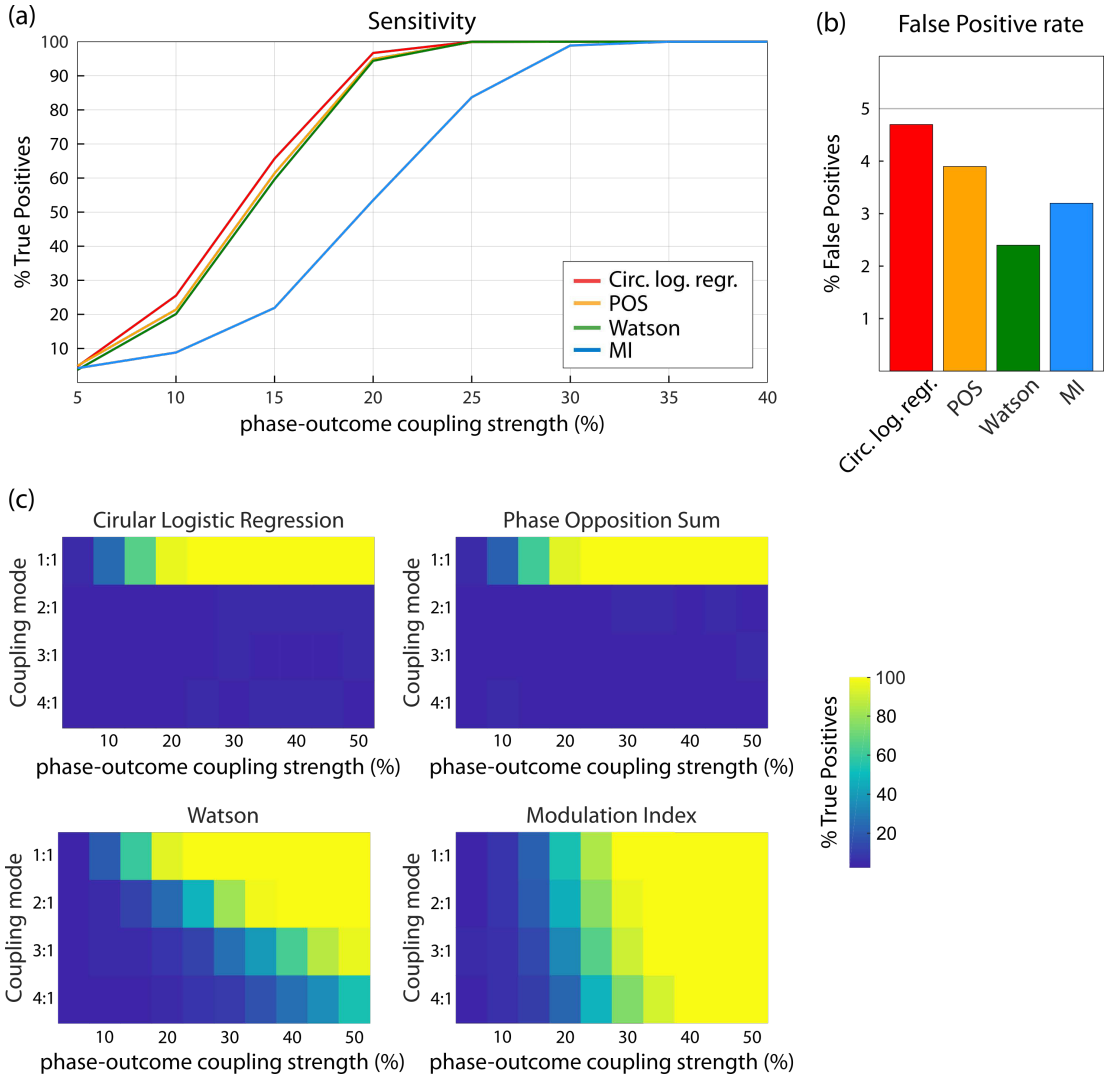

Fig. 5. Sensitivity of different tests to a 1:1 coupling mode (250 trials, 50% hits & misses). (a) Detection rate of True Positives as a function of phase locking strength. Circular logistic regression, POS and Watson's test clearly outperform MI. (b) False Positive rate computed based on outcomes randomly assigned, independently of phase. Red: Circular logistic regression, yellow: POS, green: Watson's test, blue: MI. (c) Sensitivity of the four tests as function of phase-outcome coupling strength and coupling mode. Color codes represent the percentage of True Positives. (For interpretation of the references to color in this figure legend, the reader is referred to the web version of this article.)

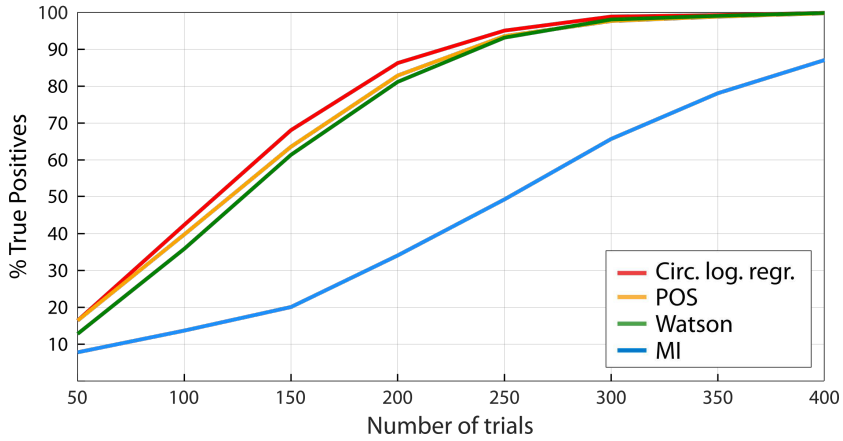

Fig. 6. Sensitivity by number of trials (1:1 coupling mode, 50% hits & misses). Phase-outcome coupling strength is kept constant at 20%, and the number of trials (hits & misses) is gradually increased. Sensitivity increases with number of trials. Circular logistic regression, POS and Watson outperform MI.

In the *T-test empirical* vs. *chance level* approach, chance level is defined in each participant as the mean of the surrogate distribution. One can then test whether empirical values are higher than chance levels across participants with a one-tailed paired *t*-test. An advantage of this approach is that the difference between empirical and chance level coupling is summarized by one value (Richter et al., 2017). In the original proposal by Richter et al., chance level (for a continuous variable) was estimated as the median of the surrogate distribution. With the binary outcomes we test here, we found that using the median of the surrogate distribution inflates False Positive rate (Fig. 7) for all tests, while using the mean of the surrogate distribution produces False Positive rates below 5% for all tests. The reason for this is that our phase distributions resulted in surrogate distributions that were highly right-skewed (Fig. 4a). With right-skewed distributions, the mean is systematically larger than the median, resulting in higher estimate of chance level with the mean and hence a smaller False Positive rate. The skewness of surrogate distributions is thus critical for the resulting False Positive rate and sensitivity. Since skewness depends on data only, it is important to check the resulting False Positive rate and sensitivity for the data at hand to make an informed decision for the definition of chance level. Here, we decided to use the mean of the surrogate distribution as an estimation of chance level.

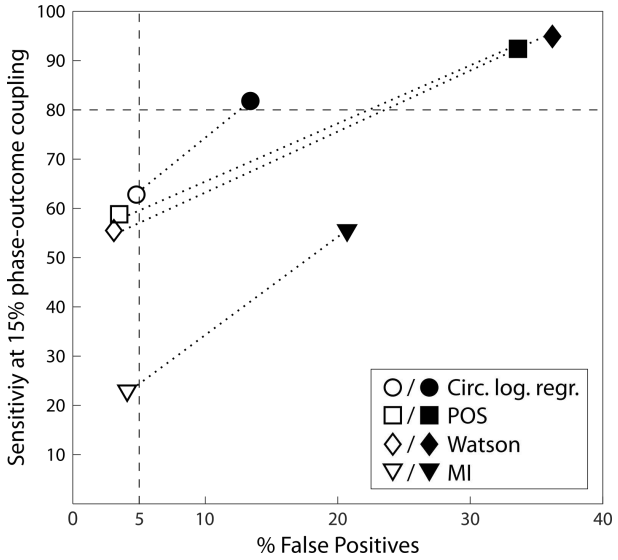

Fig. 7. False Positive rate at 0% phase-outcome coupling strength and sensitivity at 15% phase-outcome coupling strength (1:1 coupling mode, 300 trials, 50% hits & misses), when estimating chance level as the mean (open symbols) vs. the median (filled symbols) of surrogate distributions. Estimating chance level as the median of surrogate distributions increases sensitivity but also False Positive rate for all tests, especially for POS and the Watson test. False Positive rate remains below 5% for all tests when chance level is estimated as the mean of surrogate distributions.

The *surrogate average* procedure directly generates a surrogate value at the group level. Significance is then expressed as the percentage of surrogate averages that are higher than the empirical average across participants. In practice, one first computes the average empirical value of the phase-outcome statistics (e.g. POS) across subjects. Then, a distribution of surrogate group-level averages is computed by randomly drawing one value from the surrogate distribution of each subject, computing the average over these random samples, and repeating this procedure a number of times (Busch et al., 2009). This method is computationally slightly more intensive since it requires an extra-step of surrogate statistics.

Finally, one can combine *p*-values obtained in each participant into a single group-level *p*-value (VanRullen, 2016). Individual *p*-values for each subject correspond to the percentage of surrogate values that are higher than the empirical individual value. Numerous methods exist for combining *p*-values – we here restrain our analyses to the methods of Fisher, Stouffer and Edgington.

For each of the 1000 virtual experiments, we tested for significance at the group level using each of these methods (empirical vs. chance, surrogate averages, and *p*-value combinations: Fisher, Stouffer and Edgington).

Results for a 1:1 coupling mode are presented in Fig. 8 for the Watson test and POS, with circular logistic regression and MI resulting in very similar profiles. All group-level statistics methods had a very similar sensitivity, except for the *p*-value combination using Stouffer's method, which consistently underperformed when strength of phase-outcome coupling was high. However, False Positive rate was consistently lower when using the *t*-test on empirical vs. chance level to assess significance at the group level.

3.3. Relative number of observations

In all previous simulations, the two behavioral outcomes were overall equally probable in each participant. Real experiments typically depart from this ideal balance in numbers of observations between conditions, and differences in the relative number of observations might in turn influence the statistical power of the tests, as already demonstrated for POS (van Rullen, 2016). A “resampling procedure” has been proposed to correct for an imbalance in number of observations (Dugué et al., 2015; Staudigl et al., 2017). In each participant, a random subsample of *N* observations is drawn from the group with more observations, *N* being the number of observations in the condition with fewer obser-

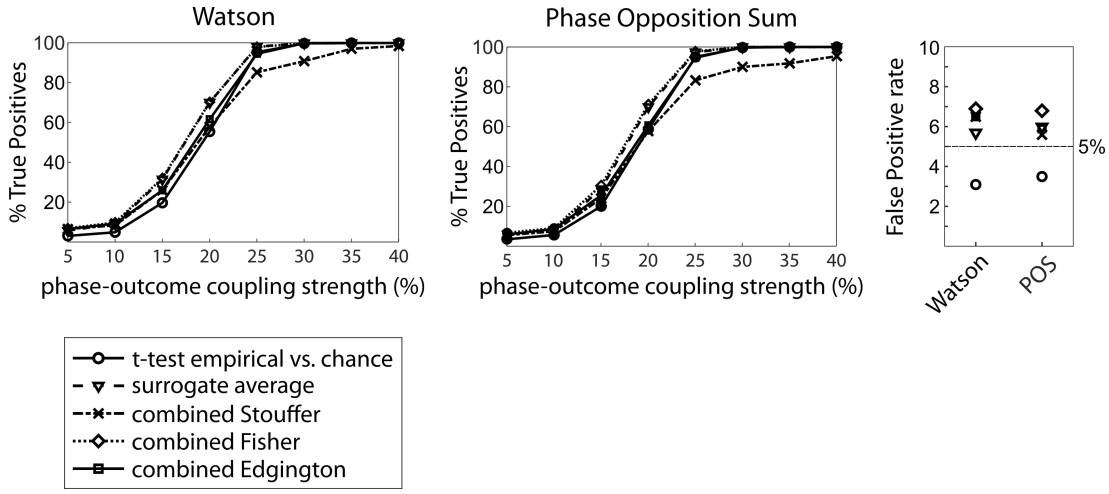

Fig. 8. Comparison of sensitivity and False Positive rate for the four different methods to test for significance at the group-level, with the examples of the Watson test and POS and for a 1:1 coupling mode (250 trials, 50% hits & misses). Circles: *t*-test on empirical vs. chance; triangles: surrogate average; stars: *p*-value combination using the Stouffer method; diamonds: *p*-value combination using the Fisher-method; squares: *p*-value combination using Edgington's method. Left and middle panel: Sensitivity; right panel: False Positive rate. Most methods perform very similarly, although the *p*-value combination using Stouffer's method performs comparably poorly for high strength of phase-outcome coupling, which was consistent across statistical tests. Using the paired *t*-test on empirical vs. chance resulted in the lowest False Positive rate for all the tests.

vations. POS is recomputed, and the process repeated a 100 times, resulting in a distribution of resampled POS values, with the empirical POS being estimated as the mean of this resample distribution.

We assessed to which degree the different statistical tests are impaired by an imbalance in number of observations between conditions and whether statistical power can be recovered using the resampling procedure described above. In the following, we created a time series of hits and misses by setting the total number of trials to 300 and fixing the strength of phase-outcome coupling at 15%. We systematically varied the relative number of observations in each condition from 0.2:0.8 to 0.8:0.2 in steps of 0.1. We computed phase-outcome statistics for each relative number of observations, both with and without a resampling approach, in 1000 virtual experiments with 30 subjects each, with each of the methods for phase-outcome statistics, and estimated group level statistics in each virtual experiment using one sided paired *t*-test between empirical and chance level phase-outcome statistics. True Positive and False Positive rate were computed for each trial balance, with vs. without resampling procedure.

The results are presented in Fig. 9 for a 1:1 coupling mode. For a balanced number of observations (50:50), we replicate the results of Section 3.1 (Fig. 5), with circular logistic regression, POS and the Watson test being the most sensitive tests, and MI performing less well. We observed that all tests suffer from a loss in statistical power with larger imbalance in number of observations between conditions. Loss in power was most pronounced for POS. The resampling procedure (dotted lines) did not change the result for any of the tests except for POS, with a large gain in statistical power at large imbalance. Indeed, although POS performed less well than logistic regression and the Watson test for large imbalance, the use of the resampling procedure increased the statistical power of POS to the point that it performed better than all other methods for large imbalance. Even for an extreme imbalance of 20:80%, the sensitivity was only about 15% lower than for a 50:50% ratio. Note that since resampling removes trials to equalize number of observations, it results in an *overall* lower number of trials, which itself decreases the sensitivity of the test. We observed no systematic change in False Positive rate with relative trial number, which was below 5% for each statistical test and balance in trial number.

With varying ratios in trial numbers, MI showed some asymmetry in the sense that it performed better when the trial imbalance went into the direction of more hits than misses than vice versa. This is because MI is based on *hit* rate (the opposite pattern was observed when computing MI based on miss rate).

To conclude, these results demonstrated that all four statistical tests suffer from an imbalance in number of observations between condi-

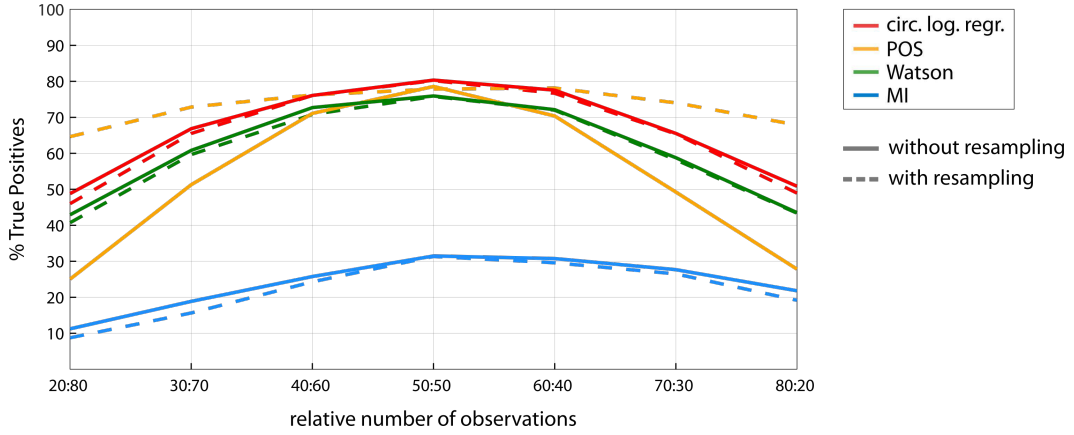

Fig. 9. Sensitivity of the different phase-outcome tests as a function of the relative number of observations for hits vs. misses (1:1 coupling mode, 300 trials, 15% phase-outcome coupling strength). Solid lines: without resampling; dotted lines: with resampling.

tions, with POS being most vulnerable. However, the resampling procedure restores POS sensitivity, which then exceeds the sensitivity of circular logistic regression, Watson and MI.

3.4. Amplitude of the underlying oscillation

In the previous simulations, we presented results using empirical data, and hence could not analyze how the amplitude of the underlying oscillation affects results. To analyze the influence of signal-to-noise ratio, we generated synthetic data. We first generated a synthetic 10 Hz sine wave, representing a "true" underlying oscillation, and assigned behavioral outcomes based on its instantaneous phase. To simulate background neural activity, we generated pink noise time series for 30 virtual subjects, with an amplitude in the range of −1 to 1. We scaled the amplitude of the sinewave by a factor varying between 0 and 0.2 before adding it to pink noise. The resulting signal was filtered around 10 Hz and instantaneous phase computed. We retrieved phases for hits and misses and computed phase-outcome statistics. This procedure was repeated in 1000 virtual experiments, and sensitivity and False Positive rate computed.

The results are presented in Fig. 10 for a 1:1 coupling mode. At zero amplitude (pure pink noise), the sensitivity of all the tests was below 5%, corresponding to their baseline False Positive rate. Sensitivity sharply increased between 0.02 and 0.05 and saturated at an amplitude around 0.15 for all tests. As expected, circular logistic regression, POS and Watson's test showed highest sensitivity while MI performed more poorly.

3.5. Comparing permutation statistics with tabulated statistics

Two tests also directly output a *p*-value: The Watson test yields a U^2-statistic from which a *p*-value can be obtained from significance tables. For circular logistic regression, a *p*-value can be obtained by an *F*-test comparing the full regression model to an intercept-only model. However, in the results presented so far, we combined the Watson test and circular logistic regression with a permutation procedure to estimate a null distribution in each participant for consistency across all methods.

We compared the performance of these two approaches to compute a *p*-value on the individual level. For each of the 1000 virtual experiments, we computed individual *p*-values for each of the 30 virtual subjects using both the permutation *p*-value and the tabular *p*-value. For each strength of phase-outcome coupling, we computed the proportion of subjects with a significant *p*-value, to infer True Positive rate in the case of a strength of phase-outcome coupling above zero and a False Positive rate in the case of zero phase locking strength. Both strategies resulted in roughly equivalent sensitivity and False Positive rate (Fig. 11).

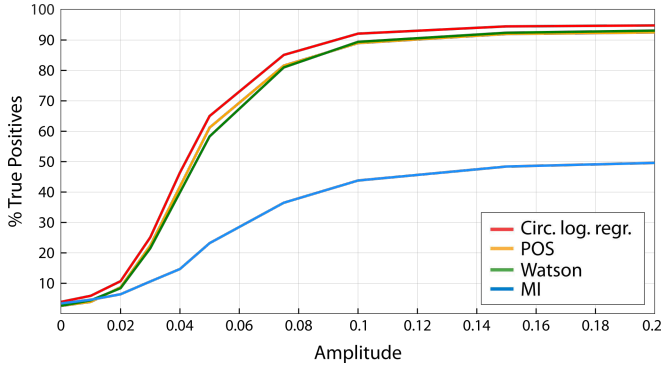

Fig. 10. Sensitivity of the different phase-outcome tests as a function of the amplitude of the 10 Hz oscillation relative to pink noise (1:1 coupling mode, 250 trials, 20% phase-outcome coupling strength).

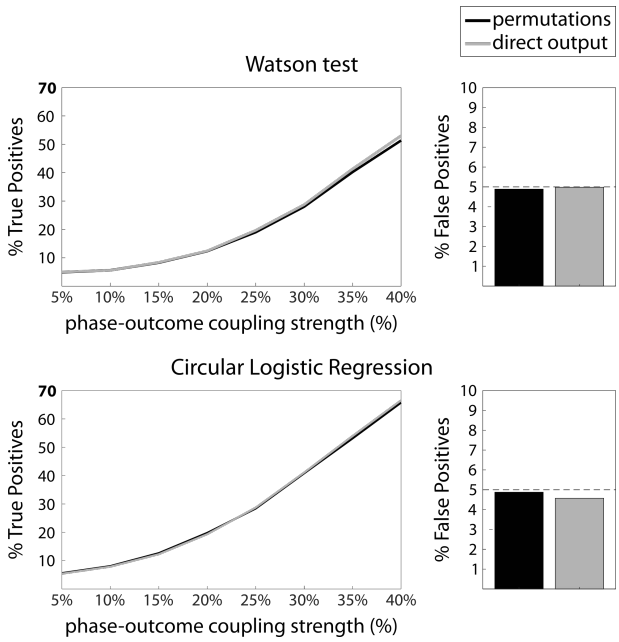

Fig. 11. Computing *p*-value based on permutations or on the direct output of the statistical test, for the Watson test and circular logistic regression, all for a 1:1 coupling mode (250 trials, 50% hits & misses). Left: Sensitivity (%True Positives), right: False Positive rate. Black: Permutation approach; gray: direct output. Both the Watson test and circular logistic regression are equally sensitive with either approach.

4. Discussion

We compared the performance of four statistical circular tests (POS, circular logistic regression, Watson's test and MI) at detecting relationships between phase and behavioral outcome. We created artificial data sets where we injected a statistical link between oscillatory phase and outcome (hit or miss) to compare the tests in terms of sensitivity and False Positive rate. We systematically varied the strength of the phase-outcome coupling and the coupling mode, as well as the total and relative numbers of observations. We observed that circular logistic regression, POS and the Watson test are similarly sensitive to a unimodal coupling mode (one preferred phase for each behavioral outcome). In comparison, MI performed poorly. The Watson test had the lowest False Positive rate, followed by MI, POS and logistic regression. In contrast, when going to higher coupling modes (groups have multiple opposed preferred phases), MI and Watson were the only sensitive tests, while all the other tests completely failed at detecting the effect. For those higher coupling modes, MI showed a higher sensitivity than the Watson test, especially for 3:1 and 4:1 coupling.

4.1. Advantages and limitations of each test for the detection of phase-outcome locking at the participant's level

Phase Opposition Sum has frequently been used to test phase-outcome coupling (e.g., Busch et al., 2009; Drewes and VanRullen, 2011; Dugué et al., 2011; Hamm et al., 2012; McLelland et al., 2016; Ruzzoli et al., 2019; Staudigl et al., 2017). Two methodological studies (VanRullen, 2016; Zoefel et al., 2019) identified POS as a powerful method for detecting (unimodal) coupling. Our findings are in line with these results, but we add to this literature that the sensitivity of POS is on par with the Watson test and circular logistic regression, and that the sensitivity of POS comes at the cost of a higher False Positive rate compared to the Watson test. Moreover, POS is not sensitive to higher coupling modes. POS is based on the Inter-Trial Coherence, which is the norm of the mean vector of all phases of a group of behavioral outcomes. If a behavioral outcome has two (or more) preferred phases, the

resulting mean vector will be small, the two preferred phases tending to cancel each other. Compared to the other tests investigated here, POS is the most vulnerable to an imbalance in relative number of observations. This drop in sensitivity results from two factors: First, an insufficient number of trials in one of the two groups, which equally affects all the methods tested here (Fig. 9b). Second, with high imbalance in relative number of observations, ITC_{all} becomes biased to toward either ITC_{hits} or ITC_{misses} (the one with more observations), which increases ITC_{all} and results in a reduced empirical POS (VanRullen, 2016). The resampling procedure compensates for this second factor, which is specific to POS, and has no effect on the other tests analyzed here. As a drawback, note though that resampling comes at the cost of longer computation time. Permutations can become computationally expensive especially if time-frequency data are analyzed (VanRullen, 2016), which increases exponentially with resampling.

Our results highlight the Watson test as an interesting method with several advantages that has remained underused in the experimental literature. First, the Watson test is among the three most sensitive methods for detecting unimodal coupling, and it also comes with the lowest False Positive rate. Second, it is the only method among the three winning methods for 1:1 coupling mode that was also sensitive to higher coupling modes. It could therefore be described as an "allrounder" method with a good tradeoff between sensitivity and False Positive rate and the potential to detect 2:1 coupling. Finally, the Watson test is computationally cheap: As it yields the same results whether the permutation procedure is used or *p*-values are directly computed, permutations are not strictly necessary for this test. It is also quite robust to moderate imbalances in relative number of observations.

Our findings concerning circular logistic regression as one of the most sensitive methods are in line with the results of Zoefel et al., 2019, who found it to be the best performing method. Still, by distinguishing between sensitivity and False Positive rate, we also observed that it came with the highest False Positive rate among the methods tested here, and it does not detect coupling modes higher than 1:1. The latter is due to the fact that circular logistic regression is fitting weights for an optimal linear separation between groups (Fig. 2), while two distributions clustering at more than one circular portion are not linearly separable.

We observed that among the four methods tested, MI was least sensitive to 1:1 coupling. This observation might be explained by an overestimation of chance level. Indeed, MI measures the departure of a distribution from uniformity (Tort et al., 2010). To determine whether a given MI value could be obtained by chance, we compare empirical MI with chance level MI, where chance level is estimated by reshuffling the behavioral outcomes, while keeping the same timing of behavioral events. Because the number of behavioral outcomes is finite, surrogate hit rate distributions only approximate uniformity, leading to a potential over-estimation of chance level. Additionally, MI values might be biased if behavioral events, irrespective of behavioral outcome, are not distributed evenly across all phase bins. Last, MI does not make any assumption on the *type* of departure from uniformity. What results in the good performance of MI at higher coupling modes comes at a cost at 1:1 coupling mode. In particular, a surrogate phase distribution might by chance display a bimodal distribution, which would be measured as a departure from non-uniformity and lead to an inflated chance level estimation. In contrast to 1:1 coupling, MI was clearly the most sensitive method for detecting higher coupling modes. Note that MI was originally devised for detecting relationships between phase and a continuous variable (e.g., phase-amplitude coupling – Tort et al., 2009). We show here that MI is also valuable to detect coupling between phase and a transient event such as a button press.

4.2. Testing for significance at the group level

We compared five different strategies to estimate significance on the group level: Running a paired *t*-test on empirical vs. chance level, creating a surrogate average distribution, and combining individual *p*-values with Stouffer's, Fisher's and Edgington's method. All methods had very similar sensitivity, except for Stouffer's *p*-value combination, which was substantially less sensitive when the strength of phase-outcome coupling was high. Note that there is an extensive literature investigating the power and properties of the different ways to combine *p*-values (e.g., Heard and Rubin-Delanchy, 2018; Whitlock, 2005). For example, it is considered that Fisher's method is asymmetrically sensitive to small *p*-values, while Stouffer's and Edgington's methods are seen as compromises between higher sensitivity to smaller vs. higher sensitivity to larger *p*-values. We here did not investigate in further detail how these methods compare, but observe that the Stouffer may be not the optimal choice in this context.

Using a *t*-test on empirical vs. chance resulted in a lower False Positive rate than the other four methods. Another advantage of relying on empirical vs. chance level is that one can quantify the strength of coupling on the individual level by computing empirical minus chance. This gives a continuous measure that can be regressed against other parameters of interest (e.g., to identify individual factors like age or daytime of recording that explain interindividual differences in strength of coupling). For those two reasons, the empirical vs. chance test seems a good option. Importantly, we here found that estimating chance level as the mean, rather than the median, of surrogate distributions should be preferred to avoid large False Positive rates. More generally, this result points to the importance of the method retained to estimate chance level when computing statistics on phase. We demonstrate this importance for phase-behavior coupling, but similar issues probably also arise for phase-phase or phase-amplitude coupling.

One important aspect in the design of our simulations is that we randomly vary the preferred phase for hits and misses from one subject to the other. Several previous studies have relied on the assumption that preferred phase would be constant across subjects (e.g., Mathewson et al., 2009; Monto et al., 2008; Rice and Hagstrom, 1989). However, there are different reasons for this to not hold true. For neural data, the measured phase at the scalp level might differ between participants due to factors like conduction relays (VanRullen, 2016). Depending on the context, it might therefore be advisable to focus on relative phase difference instead of absolute measured phase. To circumvent this issue, studies analyzing effects of phase on hit rate (Baumgarten et al., 2015; Zoefel and Heil, 2013) or continuous outcomes like evoked responses (Busch and VanRullen, 2010; Chakravarthi and Vanrullen, 2012; Neuling et al., 2012) have frequently realigned phase bins to the "preferred phase" for each participant (e.g., the phase with highest hit rate), to then run tests (e.g., ANOVA, Rayleigh test, or circular-linear correlation) on the phases pooled across subjects. Here, the tests we are using do not rely on phases being consistent across participants, and therefore do not require this additional realignment step.

Conclusions

In conclusion, we advocate the use of the Watson test, especially if the imbalance between observations in each condition is not larger than 40:60, and one wants to be open to higher coupling modes. POS becomes the measure of choice for 1:1 coupling when there is a large imbalance in the relative number of observations. In case one wants to investigate more complex coupling modes, MI seems as the optimal choice. To estimate significance on the group level, a good strategy is to compare empirical vs. chance levels, which comes with a low False Positive rate and provides an individual metric for the strength of the effect.

Note that we here constrained to the scenario of a binary outcome and did not consider the case of only one condition (e.g., clustering of saccades at a specific portion of the cardiac cycle – Ohl et al., 2016). Among the tests considered here, only MI can be directly used to assess the phase-dependency of events of only one type. MI has the advantage of detecting higher coupling modes, but requires a sufficient number of events to be present in all phase bins, which might not be the case for events whose onset is not in the control of the experimenter. Alternatively, other one-sample tests such as the Rayleigh test can be applied in this scenario (Ai and Ro, 2013; Galvez-Pol et al., 2019; Wyart et al., 2012). In addition, because we modelled a two-alternative forced choice experiment where the two behavioral outcomes are by design of opposite phase, we did not consider other possibilities, such as one outcome clustered at a specific phase, and the other homogenously distributed.

Data and code availability statement

The custom code as well as a set of phase time series from real participants for performing the simulations for this article can be accessed online at the following address: https://github.com/niwolpert/Simulations_phase_statistics. Our scripts make use of Matlab's Circular Statistics Toolbox (Berens, 2009, available at: https://fr.mathworks.com/matlabcentral/fileexchange/10676-circular-statistics-toolbox-directional-statistics). In addition, we made use of Rufin van Rullen's code on Phase Opposition (VanRullen, 2016, available at: www.cerco.ups-tlse.fr/~rufin/PhaseOppositionCode/).

Credit author statement

Catherine Tallon-Baudry: Conceptualization, Funding acquisition, Investigation, Methodology, Project administration, Resources, Supervision, Validation, Writing - review & editing **Nicolai Wolpert**: Conceptualization, Data curation, Formal analysis, Investigation, Methodology, Project administration, Software, Validation, Visualization, Roles/Writing - original draft

, , .

Declaration of Competing Interest

The authors declare that no competing interests exist.

Acknowledgments

This work was supported by funding from the European Research Council (ERC) under the European Union's Horizon 2020 research and innovation program (Grant agreement No. 670325, Advanced grant BRAVIUS) and by a senior fellowship of the Canadian Institute for Advanced Research (CIFAR) program in Brain, Mind and Consciousness to C.T.-B., as well as from ANR-17-EURE-0017. The authors thank Rufin Van Rullen for providing code for Phase Opposition Sum, and Adriano Tort for providing Modulation Index code.

Supplementary materials

Supplementary material associated with this article can be found, in the online version, at doi:10.1016/j.neuroimage.2021.118050.

References

Ai, L., Ro, T., 2013. The phase of prestimulus alpha oscillations affects tactile perception. J. Neurophysiol. 111, 1300–1307. https://doi.org/10.1152/jn.00125.2013.

Al-Daffaie, K., Khan, S., 2017. Logistic regression for circular data. AIP Conf. Proc. 1842, 030022. https://doi.org/10.1063/1.4982860.

Alves, G., Yu, Y.-K., 2014. Accuracy evaluation of the unified P-value from combining correlated P-values. PLoS ONE 9, e91225. https://doi.org/10.1371/journal.pone.0091225.

Azzalini, D., Rebollo, I., Tallon-Baudry, C., 2019. Visceral signals shape brain dynamics and cognition. Trends Cogn. Sci. 23, 488–509. https://doi.org/10.1016/j.tics.2019.03.007.

Bahramisharif, A., Gerven, M.A.J.va., Aarnoutse, E.J., Mercier, M.R., Schwartz, T.H., Foxe, J.J., Ramsey, N.F., Jensen, O., 2013. Propagating neocortical gamma bursts are coordinated by traveling alpha waves. J. Neurosci. 33, 18849–18854. https://doi.org/10.1523/JNEUROSCI.2455-13.2013.

Baumgarten, T.J., Schnitzler, A., Lange, J., 2015. Beta oscillations define discrete perceptual cycles in the somatosensory domain. Proc. Natl. Acad. Sci. USA 112, 12187–12192. https://doi.org/10.1073/pnas.1501438112.

Berens, P., 2009. CircStat: a MATLAB toolbox for circular statistics. J. Stat. Softw. 31, 1–21. https://doi.org/10.18637/jss.v031.i10.

Busch, N.A., VanRullen, R., 2010. Spontaneous EEG oscillations reveal periodic sampling of visual attention. Proc. Natl. Acad. Sci. USA 107, 16048–16053. https://doi.org/10.1073/pnas.1004801107.

Busch, N.A., Dubois, J., VanRullen, R., 2009. The phase of ongoing EEG oscillations predicts visual perception. J. Neurosci. 29, 7869–7876. https://doi.org/10.1523/JNEUROSCI.0113-09.2009.

Buzsáki, G., Logothetis, N., Singer, W., 2013. Scaling brain size, keeping timing: evolutionary preservation of brain rhythms. Neuron 80, 751. https://doi.org/10.1016/j.neuron.2013.10.002.

Callaway, E., Yeager, C.L., 1960. Relationship between reaction time and electroencephalographic alpha phase. Science 132, 1765–1766. https://doi.org/10.1126/science.132.3441.1765.

Chakravarthi, R., VanRullen, R., 2012. Conscious updating is a rhythmic process. Proc. Natl. Acad. Sci. USA 109, 10599–10604. https://doi.org/10.1073/pnas.1121622109.

Drewes, J., VanRullen, R., 2011. This is the rhythm of your eyes: the phase of ongoing electroencephalogram oscillations modulates saccadic reaction time. J. Neurosci. 31, 4698–4708. https://doi.org/10.1523/JNEUROSCI.4795-10.2011.

Dugué, L., Marque, P., VanRullen, R., 2011. The phase of ongoing oscillations mediates the causal relation between brain excitation and visual perception. J. Neurosci. 31, 11889–11893. https://doi.org/10.1523/JNEUROSCI.1161-11.2011.

Dugué, L., Marque, P., VanRullen, R., 2015. Theta oscillations modulate attentional search performance periodically. J. Cogn. Neurosci. 27, 945–958. https://doi.org/10.1162/jocn_a_00755.

Dustman, R.E., Beck, E.C., 1965. Phase of alpha brain waves, reaction time and visually evoked potentials. Electroencephalogr. Clin. Neurophysiol. 18, 433–440. https://doi.org/10.1016/0013-4694(65)90123-9.

Edgington, E.S., 1972. An additive method for combining probability values from independent experiments. J. Psychol. 80, 351–363. https://doi.org/10.1080/00223980.1972.9924813.

Fiebelkorn, I.C., Kastner, S. (2020). Spike timing in the attention network predicts behavioral outcome prior to target selection. BioRxiv 2020.04.03.024109. doi: 10.1016/j.neuron.2020.09.039

Fisher, R.A., 1938. Statistical Methods for Research Workers. Oliver and Boyd, Edinburgh.

Fries, P., Nikolić, D., Singer, W., 2007. The gamma cycle. Trends Neurosci. 30, 309–316. https://doi.org/10.1016/j.tins.2007.05.005.

Gaarder, K.R., Koresko, R.L., Kropfl, W., 1966. The phasic relation of a component of alpha rhythm to fixation saccadic eye movements. Electroencephalogr. Clin. Neurophysiol. 21, 544–551. https://doi.org/10.1016/0013-4694(66)90173-8.

Galvez-Pol, A., McConnell, R., Kilner, J.M., 2019. Active sampling in visual search is coupled to the cardiac cycle. Cognition 196, 104149. https://doi.org/10.1016/j.cognition.2019.104149.

Garfinkel, S.N., Critchley, H.D., 2016. Threat and the body: how the heart supports fear processing. Trends Cogn. Sci. (Regul. Ed.) 20, 34–46. https://doi.org/10.1016/j.tics.2015.10.005.

Haegens, S., Cousijn, H., Wallis, G., Harrison, P.J., Nobre, A.C., 2014. Inter- and intra-individual variability in alpha peak frequency. Neuroimage 92, 46–55. https://doi.org/10.1016/j.neuroimage.2014.01.049.

Hamm, J.P., Dyckman, K.A., McDowell, J.E., Clementz, B.A., 2012. Pre-cue fronto-occipital alpha phase and distributed cortical oscillations predict failures of cognitive control. J. Neurosci. 32, 7034–7041. https://doi.org/10.1523/JNEUROSCI.5198-11.2012.

Heard, N., Rubin-Delanchy, P., 2018. Choosing between methods of combining p-values. Biometrika 105, 239–246. https://doi.org/10.1093/biomet/asx076.

Helfrich, R.F., Fiebelkorn, I.C., Szczepanski, S.M., Lin, J.J., Parvizi, J., Knight, R.T., Kastner, S., 2018. Neural mechanisms of sustained attention are rhythmic. Neuron 99, 854–865 e5 https://doi.org/10.1016/j.neuron.2018.07.032.

Kayser, S.J., McNair, S.W., Kayser, C., 2016. Prestimulus influences on auditory perception from sensory representations and decision processes. Proc. Natl. Acad. Sci. USA 113, 4842–4847. https://doi.org/10.1073/pnas.1524087113.

Lachaux, J.-P., Rodriguez, E., Martinerie, J., Varela, F.J., 1999. Measuring phase synchrony in brain signals. Hum. Brain Mapping 8, 194–208. https://doi.org/10.1002/(SICI)1097-0193(1999)8:4<194::AID-HBM4>3.0.CO;2-C.

Loughin, T.M., 2004. A systematic comparison of methods for combining p-values from independent tests. Comput. Stat. Data Anal. 47, 467–485. https://doi.org/10.1016/j.csda.2003.11.020.

Mathewson, K.E., Gratton, G., Fabiani, M., Beck, D.M., Ro, T., 2009. To see or not to see: prestimulus alpha phase predicts visual awareness. J. Neurosci. 29, 2725–2732. https://doi.org/10.1523/JNEUROSCI.3963-08.2009.

McLelland, D., Lavergne, L., VanRullen, R., 2016. The phase of ongoing EEG oscillations predicts the amplitude of peri-saccadic mislocalization. Sci. Rep. 6, 29335. https://doi.org/10.1038/srep29335.
McNair, S.W., Kayser, S.J., Kayser, C., 2019. Consistent pre-stimulus influences on auditory perception across the lifespan. Neuroimage 186, 22–32 Epub 2018 Nov 2 https://doi.org/10.1016/j.neuroimage.2018.10.085.
Monto, S., Palva, S., Voipio, J., Palva, J.M., 2008. Very slow EEG fluctuations predict the dynamics of stimulus detection and oscillation amplitudes in humans. J. Neurosci. 28, 8268–8272. https://doi.org/10.1523/JNEUROSCI.1910-08.2008.
Neuling, T., Rach, S., Wagner, S., Wolters, C.H., Herrmann, C.S., 2012. Good vibrations: oscillatory phase shapes perception. Neuroimage 63, 771–778. https://doi.org/10.1016/j.neuroimage.2012.07.024.
Ng, B.S.W., Schroeder, T., Kayser, C., 2012. A precluding but not ensuring role of entrained low-frequency oscillations for auditory perception. J. Neurosci. 32, 12268–12276. https://doi.org/10.1523/JNEUROSCI.1877-12.2012.
Ohl, S., Wohltat, C., Kliegl, R., Pollatos, O., Engbert, R., 2016. Microsaccades are coupled to heartbeat. J. Neurosci. 36, 1237–1241. https://doi.org/10.1523/JNEUROSCI.2211-15.2016.
Oostenveld, R., Fries, P., Maris, E., Schoffelen, J., 2011. FieldTrip: open source software for advanced analysis of MEG, EEG, and invasive electrophysiological data. Comput. Intell. Neurosci.. https://doi.org/10.1155/2011/156869.
Podvalny, E., Noy, N., Harel, M., Bickel, S., Chechik, G., Schroeder, C.E., Mehta, A.D., Tsodyks, M., Malach, R., 2015. A unifying principle underlying the extracellular field potential spectral responses in the human cortex. J Neurophysiol 114, 505–519. https://doi.org/10.1152/jn.00943.2014.
Rice, D.M., Hagstrom, E.C., 1989. Some evidence in support of a relationship between human auditory signal-detection performance and the phase of the alpha cycle. Percept. Mot. Skills 69, 451–457. https://doi.org/10.2466/pms.1989.69.2.451.
Richter, C.G., Babo-Rebelo, M., Schwartz, D., Tallon-Baudry, C., 2017. Phase-amplitude coupling at the organism level: the amplitude of spontaneous alpha rhythm fluctuations varies with the phase of the infra-slow gastric basal rhythm. Neuroimage 146, 951–958. https://doi.org/10.1016/j.neuroimage.2016.08.043.
Rosenthal, R., 1978. Combining results of independent studies. Psychol. Bull. 85, 185–193. https://doi.org/10.1037/0033-2909.85.1.185.
Ruzzoli, M., Torralba, M., Morís Fernández, L., Soto-Faraco, S., 2019. The relevance of alpha phase in human perception. Cortex 120, 249–268. https://doi.org/10.1016/j.cortex.2019.05.012.
Samaha, J., Bauer, P., Cimaroli, S., Postle, B.R., 2015. Top-down control of the phase of alpha-band oscillations as a mechanism for temporal prediction. Proc. Natl. Acad. Sci. USA 112, 8439–8444. https://doi.org/10.1073/pnas.1503686112.
Sherman, M.T., Kanai, R., Seth, A.K., VanRullen, R., 2016. Rhythmic influence of top-down perceptual priors in the phase of prestimulus occipital alpha oscillations. J. Cogn. Neurosci. 28, 1318–1330. https://doi.org/10.1162/jocn_a_00973.
Staudigl, T., Hartl, E., Noachtar, S., Doeller, C.F., Jensen, O., 2017. Saccades are phase-locked to alpha oscillations in the occipital and medial temporal lobe during successful memory encoding. PLoS Biol. 15, e2003404. https://doi.org/10.1371/journal.pbio.2003404.
Stouffer, S.A., 1949. The American Soldier, Vol.1: Adjustment during Army Life. Princeton University Press, Princeton.
Strauß, A., Henry, M.J., Scharinger, M., Obleser, J., 2015. Alpha phase determines successful lexical decision in noise. J. Neurosci. 35, 3256–3262. https://doi.org/10.1523/JNEUROSCI.3357-14.2015.
Tallon-Baudry, C., Bertrand, O., 1999. Oscillatory gamma activity in humans and its role in object representation. Trends Cogn. Sci. 3, 151–162. https://doi.org/10.1016/S1364-6613(99)01299-1.
Tallon-Baudry, C., Bertrand, O., Delpuech, C., Pernier, J., 1996. Stimulus specificity of phase-locked and non-phase-locked 40Hz visual responses in human. J. Neurosci. 16 (13), 4240–4249. https://doi.org/10.1523/JNEUROSCI.16-13-04240.1996.
Tort, A.B.L., Kramer, M.A., Thorn, C., Gibson, D.J., Kubota, Y., Graybiel, A.M., Kopell, N.., 2008. Dynamic cross-frequency couplings of local field potential oscillations in rat striatum and hippocampus during performance of a T-maze task. Proc. Natl. Acad. Sci. USA 105, 20517–20522. https://doi.org/10.1073/pnas.0810524105.
Tort, A.B.L., Komorowski, R.W., Manns, J.R., Kopell, N.J., Eichenbaum, H., 2009. Theta-gamma coupling increases during the learning of item-context associations. PNAS 106, 20942–20947. https://doi.org/10.1073/pnas.0911331106.
Tort, A.B.L., Komorowski, R., Eichenbaum, H., Kopell, N., 2010. Measuring phase-amplitude coupling between neuronal oscillations of different frequencies. J. Neurophysiol. 104, 1195–1210. https://doi.org/10.1152/jn.00106.2010.
Tort, A.B.L., Brankačk, J., Draguhn, A., 2018. Respiration-entrained brain rhythms are global but often overlooked. Trends Neurosci. 41, 186–197. https://doi.org/10.1016/j.tins.2018.01.007.
VanRullen, R., 2016. How to evaluate phase differences between trial groups in ongoing electrophysiological signals. Front. Neurosci. 10, 426. https://doi.org/10.3389/fnins.2016.00426.
Vinck, M., van Wingerden, M., Womelsdorf, T., Fries, P., Pennartz, C.M.., 2010. The pairwise phase consistency: a bias-free measure of rhythmic neuronal synchronization. Neuroimage 51, 112–122. https://doi.org/10.1016/j.neuroimage.2010.01.073.
Voytek, B., Kramer, M.A., Case, J., Lepage, K.Q., Tempesta, Z.R., Knight, R.T., Gazzaley, A., 2015. Age-related changes in 1/f neural electrophysiological noise. J Neurosci 35, 13257–13265. https://doi.org/10.1523/JNEUROSCI.2332-14.2015.
Whitlock, M.C., 2005. Combining probability from independent tests: the weighted Z-method is superior to Fisher's approach. J. Evol. Biol. 18, 1368–1373. https://doi.org/10.1111/j.1420-9101.2005.00917.x.
Wolpert, N., Rebollo, I., Tallon-Baudry, C., 2020. Electrogastrography for psychophysical research: practical considerations, analysis pipeline, and normative data in a large sample. Psychophysiology 57, e13599. https://doi.org/10.1111/psyp.13599.
Wyart, V., de Gardelle, V., Scholl, J., Summerfield, C., 2012. Rhythmic fluctuations in evidence accumulation during decision making in the human brain. Neuron 76, 847–858. https://doi.org/10.1016/j.neuron.2012.09.015.
Zar, J.H., 2010. Biostatistical Analysis. (Prentice Hall).
Zaykin, D.V., Zhivotovsky, L.A., Czika, W., Shao, S., Wolfinger, R.D., 2007. Combining p-values in large scale genomics experiments. Pharm. Stat. 6, 217–226. https://doi.org/10.1002/pst.304.
Zoefel, B., Heil, P., 2013. Detection of near-threshold sounds is independent of EEG phase in common frequency bands. Front. Psychol. 4. https://doi.org/10.3389/fpsyg.2013.00262.
Zoefel, B., Davis, M.H., Valente, G., Riecke, L., 2019. How to test for phasic modulation of neural and behavioral responses. Neuroimage 202, 116175. https://doi.org/10.1016/j.neuroimage.2019.116175.

8. Probing the link between near-threshold target perception and the gastric rhythm

8.1. Introduction

In the following, I am going to present the experimental project of my PhD, in which we addressed the question whether the slow rhythm of the stomach has a link with visual perception at threshold. Several lines of evidence speak to a **potential link between the gastric rhythm and visual perception**. First, anatomy suggest that visual occipital regions might receive input from the stomach. For example, the lateral geniculate nucleus, the thalamic relay station in the visual pathway, receives massive input from the parabrachial nucleus (Erişir et al., 1997a, 1997b; Uhlrich et al., 1988), and stimulation of the parabrachial nucleus affects visual responses in cats (Lu et al., 1993). Moreover, occipital regions are activated in response to gastric distension in humans (Ladabaum et al., 2001; Lu et al., 2004b; van Oudenhove et al., 2009) and electrical stimulation in rats (Cao et al., 2019). Richter et al., 2017 also showed that spontaneous fluctuations in occipital alpha power are modulated by the phase of the gastric rhythm. Spontaneous fluctuations in electrophysiological signals have been related to variability in perception, with ongoing alpha power predicting the perception of visual near-threshold stimuli (Busch et al., 2009; Dijk et al., 2008; Ergenoglu et al., 2004; Hanslmayr et al., 2007; Mathewson et al., 2009). Furthermore, it has been found that neural responses to cardiac inputs affect visual detection (Park et al., 2014), suggesting that visceral input interacts with behaviorally relevant ongoing cortical activity. Finally, anatomy suggests that gastric input might be projected to neuromodulatory centers that regulate arousal, vigilance and sustained attention (Elam et al., 1986; Saito et al., 2002), processes that should influence perceptual performance in a prolonged visual task.

Based on these arguments, we formulated the hypothesis that the gastric rhythm drives a slow fluctuation in cortical excitability that modulates alpha power. Gastric phase would thus influence visual perception. **We predicted that the probability to perceive a near-threshold visual stimulus would show a link with the phase of the gastric rhythm, with seen and unseen targets (hits vs. misses) clustering at different portions of the gastric phase.**

To test the idea that gastric phase modulates the probability for a visual target to be perceived, we developed an **experimental protocol** (Figure 25) to target fluctuations in perceptual performance. Standard paradigms of near-threshold perception experiments, where participants are warned at the beginning of a trial, are not well suited for our purposes, for different reasons. First, we aimed to obtain slow fluctuations in arousal, which we hypothesized to be linked with the gastric rhythm. We reasoned that these slow fluctuations would best be obtained with long uninterrupted recordings. Moreover, in 'standard' paradigms relying on a classical 'trial' structure, the potential occurrence of a target is very predictable. Problematically, it is known that when the brain can detect a rhythm in a task, the amplitude of slow neural oscillations can be entrained to the predictable stimulus stream via top-down attentional mechanisms (Lakatos et al., 2008). It is also known that the sudden onset of stimuli in the visual or other modalities can 'reset' cortical oscillations, including alpha (Lakatos et al., 2009; Mercier et al., 2013;

Romei et al., 2012). It was thus crucial to design a paradigm with unpredictable stimulus occurrences and avoid any events that could interfere with fluctuations in arousal, slow spontaneous oscillations in the gastric slow wave or coupled fast brain oscillations. Lastly, we chose to present targets with long inter-stimulus intervals (3.5-10 seconds) to minimally interrupt fluctuations in vigilance. This together with the slow frequency of the gastric slow wave required long uninterrupted recordings, in order to sample enough data from all portions of the gastric cycle.

The task consisted in the detection of randomly oriented Gabor patches which appeared at random uncued moments, superimposed on a near-foveal annulus consisting of flickering noise of grey shaded pixels (Figure 25). Subjects fixated a central bull's eye and responded by pressing a button whenever they perceived a Gabor. The visibility of the targets was controlled so that subjects would perceive it around 50% of the time. The details of the stimuli, experimental protocol and participants included are specified in the following.

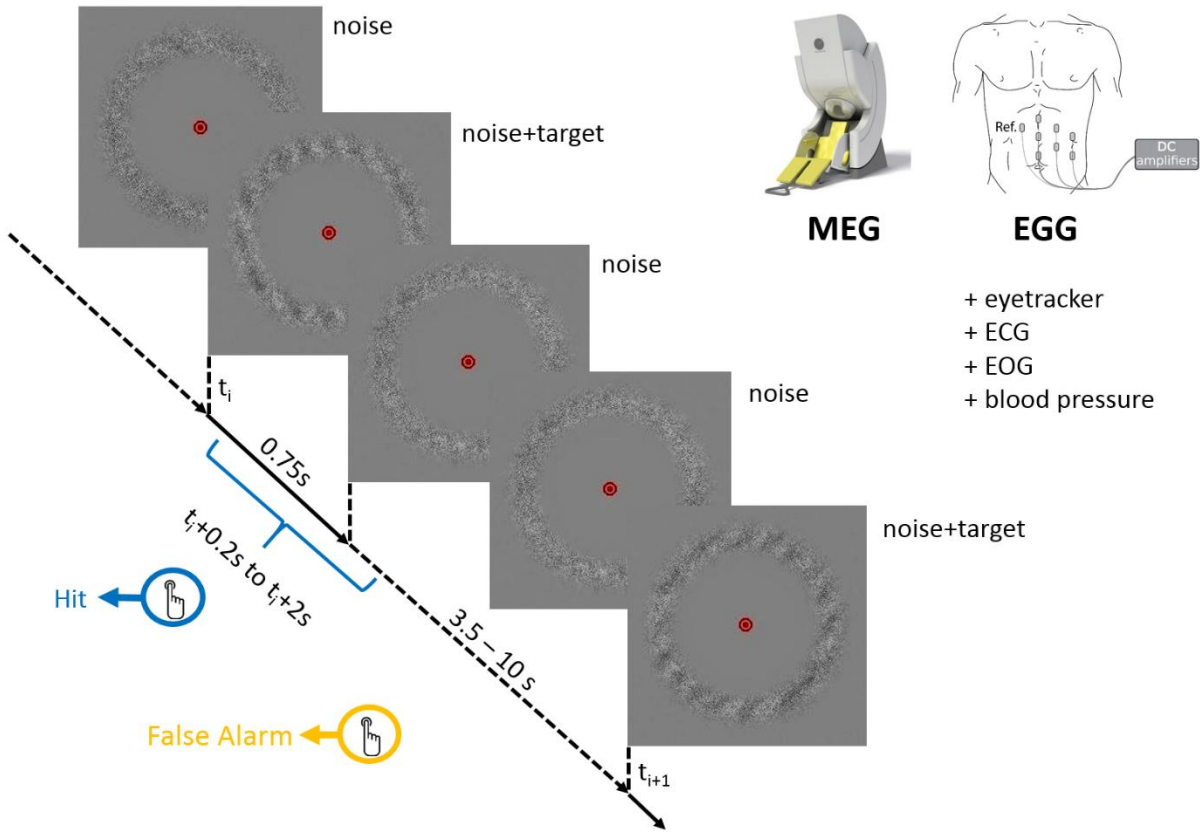

***Figure 25**: Experimental paradigm. Subjects fixated a central red bull's eye. A near foveal annulus (inner diameter 2°, outer diameter 4°) filled with grey shaded pixels was displayed. At random uncued moments, with an inter-stimulus-interval of 3.5-10 seconds (flat hazard rate), a target (t_i) consisting in a randomly oriented Gabor was superimposed on the noise for 0.75 seconds. Responses in a window of 0.2s to 2 seconds relative to target onset were considered as hits, responses outside these windows as*

False Alarms. Simultaneously, magnetencephalography (MEG) and electrogastrogram (EGG) signals were collected. Additionally, eye position, the electrocardiam (ECG), electrooculogram (EOG) and momentaneous blood pressure were recorded.

8.2. Material and methods

8.2.1. Participants

Thirty-two participants with normal vision and no reported psychological, neurological, cardiac or digestive/gastric problems participated in the experiment. All participants provided informed written consent and were paid for their participation. Subjects were required not to eat or drink anything the two hours preceding the testing. All procedures were approved by the local ethics committee, and participants were informed that they could stop the experiment at any time.

We excluded one participant where not enough data could be acquired due to time constraints (3 experimental blocks, while the other participants performed 4 to 5 blocks). We excluded one participant with an exceptionally elevated blink rate, with more than 30% of samples contaminated by blinks. This left thirty subjects (seventeen female; thirteen male; 19-30 years; mean age: 24±2.7; mean body mass index: 20.2±1.3) for analysis.

The participants included had their last meal between one and seventeen hours (mean: four hours) preceding the appointment (i.e, between two and eighteen hours before the beginning of the first experimental block).

8.2.2. Stimuli

Subjects were seated in a dimmed room and required to fixate a central red "bull's eye" (diameter: 0.2° of visual angle) on a gray background, at a viewing distance of 80 cm. The "target absent" stimuli corresponded to a near-foveal annulus (2-4° radius) composed of weak grey-shaded pixels of a pink noise pattern (frequency spectrum of $1/f$), spatially smoothed towards the borders by a Gaussian distribution. 'Target present' stimuli consisted of Gabor patches (2.5 cycles per degree) superimposed on the noise background, with Gaussian smoothing towards the edges of the annulus. Gabors were superimposed by a modulation of the noise values by adding the Gabor profile with positive and negative values. Target visibility was controlled by a 'mask' consisting of zeros and ones. The mask controlled for each pixel of the Gabor whether it was added onto the noise background (=1) or ignored (=0). Gabor visibility was controlled by the percentage of pixels of the Gabor that were added/subtracted to the noise vs. masked out. We call this factor 'transparency level'. Noise and noise + Gabor had the same mean luminance, equal to the background luminance, and the same luminance variance. On each trial, the orientation of the grating was randomly chosen, excluding ± 20° around the cardinal orientations.

8.2.3. Experimental protocol

The protocol consisted of different steps which are schematized in Figure 26 and which will be detailed here.

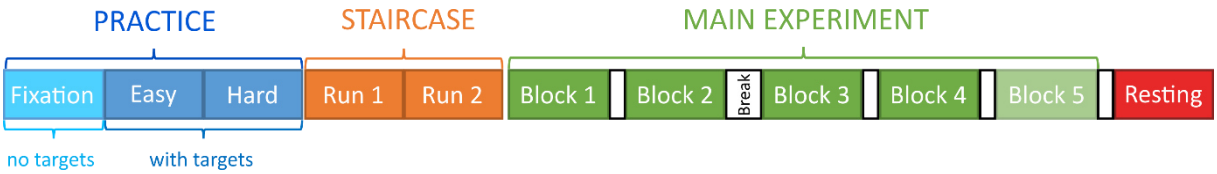

***Figure 26**: Protocol of the experiment. See text for details.*

The **main experiment** consisted of four to five blocks of approximately 12 minutes each, with 90 presentations of the near-threshold Gabor in each block. The stimuli occurred at random moments and lasted 750 ms. Inter-stimulus-intervals were randomly drawn from a triangular distribution, taking into account the hazard rate (min: 3.5 s, max: 10 s). Subjects were instructed to maintain fixation at all times and press a button as soon as they had the impression of seeing a Gabor in the noise. Some additional data (at least 40 seconds) where acquired before the start and the end of the experiment of each block, which were later discarded to avoid edge effects due to the very slow frequency of the gastric rhythm. Between blocks, subjects could take small breaks, with an optional longer break outside the scanner after the second block.

The experiment was preceded by a practice and a staircase session. The **practice session** consisted of two parts: The first part served to train subjects to keep fixation at the center by giving them online-feedback on the accuracy of their fixation, with white coloring of the fixation bull's eye when fixation was inaccurate. Only noise backgrounds without any targets were presented. In the second part of the practice, subjects were familiarized with the target stimuli. Gabors were made clearly visible by using a higher contrast, in order to ensure that subjects got a clear idea of the appearance of the targets. Subsequently, Gabors were made more difficult to see, with a low luminance contrast as in the final experiment and a transparency level of 100%. During these exercises, inter-stimulus intervals were the same as for the main experiment, but at a given inter-stimulus interval, the probability of a grating being presented was only 50%, mimicking the temporal expectation a participant with a 50% hit rate would have. Each target-present practice contained 8 trials, so subjects perceived 2 times 4 gratings on average.

During the **staircase session**, subjects performed the same task as during the main experiment, except that the transparency level changed from trial to trial depending on the response of the previous trial, according to a one-up one-down staircase procedure, which theoretically converges to a 50% detection rate. The transparency level started at 90% and the initial step-size was 25%, then 17% (two-third of the initial step-size) and finally 8% (one third of the initial step-size). The staircase procedure was terminated after a total of 14 reversals. The procedure was applied twice to ensure a proper estimation of perception threshold. Trials without accurate fixation target presence were repeated. The average of the two resulting staircases was then used for the actual experiment. If the two staircases were not clearly converging, the staircase procedure was repeated.

If at the chosen transparency level, subjects had too low (<30%) or too high (>70%) hit rate in the first minutes of the first block, the block was interrupted, a new staircase started to determine transparency threshold, and the block restarted with the adjusted transparency level (the true reason for interrupting the block was hidden to the subject).

After the end of the experiments, we also acquired a block of 12 minutes **resting state**. Participants fixated the central red "bull's eye" on a gray background and were instructed to stay still.

Before the experiment, subjects filled out the French versions of two questionnaires. The Daydreaming Frequency Scale (Giambra, 1993) contains 12 questions about the extent of daydreaming and mindwandering during daily life, with a five-point Likert-scale to answer. The Sate-Trait Anxiety Inventory (STAI, Spielberger et al., 1983) is a commonly used measure of trait and state anxiety. We used the part assessing trait anxiety, containing 20 questions about how subjects generally feel (e.g. "I am a content; I am a steady person", "I worry too much over something that really doesn't matter"), which are rated on a 4-point scale reaching from 'Almost Never' to 'Almost Always'.

8.2.4.Data acquisition

Continuous MEG signals were collected using a whole-head MEG system with 102 magnetometers and 204 planar gradiometers (Elekta Neuromag TRIUX MEG system) at a sampling rate of 1000 Hz and online low-pass filtered at 330 Hz. The electrogastrogram (EGG) was recorded with via nine disposable electrodes (seven active, one reference and one ground) placed on the abdomen and acquired simultaneously with MEG data, using the protocol detailed in Wolpert, Rebollo & Tallon-Baudry, 2020. The only difference was that the ground electrode was placed over the right shoulder. An electrocardiogram (ECG) with one electrode on the left clavicle and one electrode on the right lower abdominal location, as well as a vertical electrooculogram (EOG) were simultaneously recorded. The impedance of the electrodes was monitored for consistency between channels and to not exceed 10kΩ. In addition, peripheral blood pressure was measured on the left arm using Caretaker® software. Because of a number of technical problems, good-quality peripheral blood pressure data could be acquired in 15 subjects only. Horizontal/vertical eye position and pupil diameter were monitored using an EyeLink 1000 system (SR Research©) recorded together with MEG, ECG and EOG data.

8.2.5.Preprocessing

The EGG was preprocessed following exactly the procedure described in Wolpert, Rebollo & Tallon-Baudry, 2020: In a first step, for each block spectral power was computed at each electrode via a Fast Fourier Transform (FFT) with a Hanning taper, as implemented in the fieldtrip toolbox (Oostenveld et al., 2011). The electrode with the largest peak in the normogastric range of 0.033-0.067 Hz (2-4 cycles per minute) was then selected. The raw EGG from the selected channel in the given block was then then filtered using a frequency sampling designed finite impulse response filter (Matlab: *FIR2*), with a bandwidth of ± 0.015 Hz of the EGG peak frequency. The instantaneous phase and amplitude

envelope of the gastric rhythm was then retrieved by applying the Hilbert transform to filtered data. We discarded recordings based on the quality of the EGG, as described in the paper (Wolpert, Rebollo & Tallon-Baudry, 2020). First, we kept only blocks where the power spectrum exhibits a clear peak in normogastric range at a congruent frequency across several channels. Second, for those blocks with a clean power spectrum, we did a second quality check based on the regularity of cycle durations, discarding recordings with a standard deviation of cycle duration higher than 6 (a threshold defined based on empirical distributions as described in the paper). In practice, only one resting state block had to be discarded, due to a high standard deviation of cycle duration. Within blocks, we removed cycles whose length exceeds the mean ± 3 standard deviations of the given block, as well as cycles with nonmonotonous change in phase.

For MEG data, Signal Space Separation (tSSS) was performed using MaxFilter (Elekta Neuromag) to remove external noise. Subsequent analysis was conducted on magnetometer signals. The cardac artifact was corrected using Independent Component Analysis (ICA), as implemented in the FieldTrip toolbox (Oostenveld et al., 2011). The MEG data were highpass-filtered at 0.5 Hz and epoched to R-peaks from 200 ms before to 200 ms after each R-peak. The number of independent components to be identified was the rank of the time × trial matrix. The continuous magnetometer data were then decomposed according to identified ICA components. The pairwise phase-consistency (PPC, Vinck et al., 2010) was computed between the ICA-decomposed signals and the ECG signal to isolate those components most reflective of ECG activity. Components with PPC values larger than 3 standard deviations than the mean were rejected iteratively from the continuous MEG data from each block until either no component exceeded 3 standard deviations or 3 components were rejected (in practice, this always resulted in 3 components being rejected). Blink artifacts were detected automatically by the EyeLink eyetracker system, and padded by ±100 ms. Muscle artifacts were identified based on a z-value threshold of 20 on the MEG data filtered into a band of 110-140 Hz. Movement artifacts were identified based on a z-value threshold of 40 on the MEG data filtered into a band of 4-30 Hz.

We extracted MEG power in the 10-11 Hz band in which MEG power has been found to be coupled to the gastric rhythm. For this we applied a 10-11 Hz bandpass 6^{th} order Butterworth zero-phase shift filter on the ICA-corrected magnetometer data, using the Fieldtrip toolbox (Oostenveld et al., 2011). The instantaneous amplitude envelope of the filtered MEG data was then retrieved by applying the Hilbert transform, and downsampled to 20 Hz.

We preprocessed pupil diameter in resting state blocks by removing blinks and saccades larger than 1.5 degrees, with 100 ms padding. Artifact periods were linearly interpolated if the duration of the artifact was not longer than 1.5 seconds. Artifacted windows separated by less than 200 ms were combined and treated as a single artifact. Pupil diameter was transformed to be in the positive range by

subtracting the minimum value of pupil diameter and dividing by the difference between maximum and minimum value ($pupil = (pupil - minVal) / (maxVal - minVal)$).

Behavioral responses between 200 ms and 2 seconds after target onset were defined as hits, while responses 2.5 seconds after target onset were considered as False Alarms. (These time windows were defined based on pilot data not shown here and will be validated in the results section.) Responses in the remaining time windows (i.e., between 0 and 200 ms after target onset, and between 2 and 2.5 seconds after target onset) were considered as "uncategorized" due to their ambiguity with regard to their classification as "Hit" vs. "False Alarm", and not further considered. Note that we here could not compute a sensitivity index and decision criterion in the framework of signal-detection theory, since these rely on a false alarm rate. In turn, a false alarm rate could not be computed due to the absence of a classical trial structure with "target absent" and "target present trials".

We discarded trials in which participants made a blink during presentation of the target Gabor. We also discarded trials with saccades larger than 1.5° during target presentation. On average, 24.6% of trials contained blinks, 11.1% contained saccades larger than 1.5° of visual angle, and on average 7.3% of trials had to be rejected due to EGG artifacts. This resulted in 56% of clean trials on average, with 135 to 356 trials per subject (mean: 256) entered into the analysis.

8.2.6. Statistical analysis

8.2.6.1. Gastric phase & behavior

We aimed at determining the relationship between gastric phase and perceptual outcome, hypothesizing that hits vs. misses would cluster at different phases of the gastric cycle. As shown in Wolpert & Tallon-Baudry, 2021, the Watson test is a good allrounder method with high sensitivity to unimodal coupling modes and some sensitivity to higher coupling modes. Modulation Index is less sensitive to 1:1 coupling but highly sensitive to more complex coupling modes. We therefore included both tests into our analysis.

Watson test

The Watson test is the nonparametric version of the Watson-Williams two-sample test, since it does not rely on the assumption that the sampled populations are unimodal. It is computed the following way (Zar, 2010): First, the phases of hits and misses are separately grouped in ascending order. Let N_{hits} and N_{misses} denote the number of samples in each group, and N the total number of samples ($N_{hits}+N_{misses}$). With i as the index of hits and j as index of misses, the cumulative relative frequencies for the observations in the two groups are then computed as i/N_{hits} and j/N_{misses}. Values of d_k (with k running from 1 to N) are defined as the differences between the two cumulative relative frequency distributions ($d_k = i/N_{hits} - j/N_{misses}$). The test statistics, called the Watson U^2, is then computed as:

$$U^2 = \frac{N_{hits}N_{misses}}{N^2}\left[\sum_{k=1}^{N} d_k^2 - \frac{(\sum_{k=1}^{N} d_k)^2}{N}\right]$$

Significance can be read from significance tables for U^2 (see Zar, 2010). Here, we estimate significance of the U^2 using a permutation procedure (as for Modulation Index), which will be detailed later.

Modulation Index (MI)

The Modulation Index (MI) of Tort et al., 2010 is an adaption of the Kullback-Leibler distance, a measure used to quantify the amount of difference between two distributions. It measures the extent to which an empirical distribution differs from a uniform distribution. It was originally applied for detecting coupling between the phase of a slower oscillation and the amplitude of a faster oscillation (Tort et al. 2008, 2009), i.e. between phase and a *continuous* response variable. Here, we applied the method to quantify the relationship between phase and a *dichotomous* response variable (hits and misses) (Wolpert & Tallon-Baudry, 2021). For this we transform hits and misses into a hit *rate* per oscillatory phase bin: The phases are sorted into *K* bins spanning the [-pi, pi] interval (here: $K = 10$), and the hit rate computed for each bin (i.e. number of hits divided by total number of events in that bin). The MI measures how far the distribution of hit rate deviates from a flat/uniform distribution with respect to phase bins. (Note that MI could also be computed based on miss rate. The two distributions are in fact complementary.) Formally, it is defined as:

$$\mathrm{MI} = \frac{\log(K) + \sum_{j=1}^{K} P(j) * \log P(j)}{\log(K)}$$

Where P(*j*) is the standardized hit rate in phase bin *j*:

$$\mathrm{P}(j) = \frac{Hit\ rate\varphi(\mathrm{j})}{\sum_{i=1}^{K} Hit\ rate\varphi(\mathrm{i})}$$

And the hit rate per phase bin HR_φ is the number of hits in the phase bin φ divided by the total number of trials in the phase bin:

$$\mathrm{HR}_\varphi = \frac{NHits\varphi}{NHits\varphi + NMisses\varphi}$$

MI is 0 if there is no phase-modulation of hit rate at all (meaning a perfectly uniform distribution) and 1 if there is perfect coupling (i.e. P(*j*)=1 for a given bin and 0 for all other bins).

Estimation of chance level and coupling strength

For each subject, we estimated chance level of no phase-behavior relationship. For this, we used a "permutation-based" approach to estimate a surrogate distribution of U^2 or MI values with no phase-outcome relationship. The rationale for this procedure is to abolish the hypothetical effect in the original data by randomly reassigning trial outcomes in single participants. For each given subject, the trial

assignment to hit or miss was randomly permuted 1000 times, and the phase statistics recomputed at each permutation, which yields a distribution of surrogate U^2 or MI values. We defined chance level for each participant as the mean of the respective surrogate distribution. The difference of the empirical value from chance level then gives a measure of the strength of the phase-behavior relationship in the individual subject. We refer to this difference as "coupling strength".

Estimation of significance at the group level

To assess significant coupling on the group level, we then ran a one-tailed t-test on empirical values vs. chance levels, testing if empirical values are higher than chance level.

8.2.6.2. Computing gastric-brain coupling

We investigated coupling between gastric phase and brain alpha oscillations in the task blocks, in the 10-11 Hz range where significant coupling was found during rest in Richter et al., 2017. We then assessed whether the strength of this coupling between individuals shows a link with individual performance in the experiment of vision at threshold. In the following, the procedure to assess gastric-alpha coupling will be detailed.

Phase-amplitude coupling (PAC)

As a result of the preprocessing steps, we obtained the amplitude envelope of the 10-11 Hz MEG signal at each sensor, as well as the phase of the gastric rhythm, in each of the 4 to 5 task blocks. We targeted moments without artifacts and where participants were not exposed to target stimuli nor preparing or executing a motor response. All samples coinciding with a blink, muscle, movement or EGG artifact were rejected. We also discarded all samples within response windows (i.e., 0.2-2 seconds relative to target onset) as well as button presses (Hits and False Alarms) ± 1 second. EGG phase and MEG alpha power were each concatenated across blocks. The EGG phase was partitioned into 18 bins spanning the [-pi pi] interval, and corresponding MEG power was averaged for each phase bin, yielding a phase-amplitude profile. We then computed the Modulation Index (MI) (Tort et al., 2010) to quantify the deviation of this profile from a uniform distribution.

Statistical determination of significant clusters of PAC

We identified significant clusters of phase-amplitude coupling using a two-step process, as in Richter et al., 2017. In a first step, we estimated in each participant and sensor the chance level MI. Next, we assessed on the group level which sensors show a significant difference between the empirical MI and chance level. The steps are detailed in the following.

We estimated chance level MI for each participant and sensor by creating null distributions of surrogate MI values. The EGG phase was shifted relative to the MEG signals for each block in random time intervals between at least 60 seconds and at maximum the duration of the respective block minus 60 seconds. Data at the end of the recording were wrapped to the beginning. In this way, the original

relationship between EGG and MEG signals was disrupted while best preserving the characteristics of the phase time series. Because the filtered EGG signal and MEG power envelope are not pure sine waves, but physiological signals with spontaneous variations in frequency, any link between gastric phase and brain alpha oscillations is disrupted in the surrogate data. We recomputed MI across blocks based on the rotated EGG phase time series, and repeated this procedure 1,000 times, yielding a distribution of surrogate Mis expected under the null hypothesis. We defined chance level as the median of the respective surrogate distribution for each participant and sensor.

To test whether the empirical MI significantly differed from chance level MI at the group level, we used a cluster-based permutation procedure (Maris and Oostenveld, 2007) as implemented in Fieldtrip (Oostenveld et al., 2011). In this procedure, empirical MIs are compared with the corresponding chance level MIs across participants using a one-tailed t-test at each sensor. Candidate clusters are defined in space as sensors exceeding the first level *t*-threshold ($p < 0.05$) and that are connected to at least 2 neighboring sensors also exceeding this threshold. Each candidate cluster then is characterized by a summary statistic corresponding to the sum of the *t*-values across the sensors defining the cluster. To determine whether the candidate cluster with its given sum of *t*-values can be obtained by chance, the distribution of cluster statistics under the null hypothesis is computed. This is done by randomly shuffling the labels "empirical" and "chance" 10,000 times, applying the clustering procedure, and retaining the largest positive and negative clusters from each permutation. The 10,000 permutations then yield a distribution of cluster t-sum statistics under the null hypothesis, which is then used to assess the empirical cluster for significance. Because the largest positive and negative clusters are retained at each permutation, this method intrinsically controls for multiple comparisons over sensors (Maris and Oostenveld, 2007). The resulting clusters are then described by their summary statistics, i.e. the sum of *t*-values, and their Monte Carlo *p*-value indicating significance at the cluster level corrected for multiple comparisons across sensors and frequencies. Finally, we estimated the False Positive rate of this statistical approach, i.e. how likely it is that the observed cluster statistics could be obtained by chance. For this we picked (without replacement) surrogate MIs from the chance distributions for each participant and sensor, labeled them as "empirical" and repeated the cluster based permutation test with each surrogate value as "empirical MI", to count the number of iterations yielding a higher sum(*t*) than the empirical data.

8.2.6.3. Correlations and Bayes Factor

We were interested in the link between individual mean EGG-alpha coupling strength in the identified cluster and performance, as well as with a number of control parameters. To be less sensitive to the presence of outliers, correlations were performed using robust regression (Matlab's *robustfit*) with iteratively reweighted least squares using the bisquare weighting function.

Bayesian statistics on correlation coefficients were computed and interpreted according to the method of (Wetzels and Wagenmakers, 2012), which is based on the correlation coefficient and the number of observations. Bayesian statistics on two sample (unpaired) t-tests where computed according to (Rouder and Morey, 2011). A Bayes Factor greater than 1 indicates evidence for the presence of a correlation, and a Bayes factor smaller than 1 indicates evidence for the absence of a correlation, i.e. the null hypothesis H_0 (1-3: Anectodal evidence for H_1; 1/3 - 1: Anecdotal evidence for H_0; 1/10-1/3: Substantial evidence for H_0, <1/10: Strong evidence for H_0).

8.2.6.4. Prestimulus alpha power and behavior

We also analyzed whether prestimulus power in the 8-12 Hz band differed for hits vs. misses. For this we selected the 15 sensors showing highest power in the second preceding target onset. For each hit and miss, mean alpha power over the channels was computed in the second preceding target onset. For each subject, alpha power was then averaged across epochs and time points for hits and misses. We tested whether mean prestimulus alpha power differed for hits vs. misses across subjects by a two-sample t-test.

8.2.6.5. Computing gastric-pupil coupling

We also computed coupling between pupil diameter and EGG phase in the resting state. The statistical analysis was the same as for computing coupling between EGG phase and alpha power. I.e., the preprocessed pupil time series was partitioned into 18 bins, pupil diameter averaged for each phase bin, and MI computed to quantify the deviation of this profile from a uniform distribution. Chance level MI was estimated for each participant by shifting EGG phase relative to the pupil time course. We then tested across participants if empirical MI was larger than chance level by a one-tailed t-test.

8.3. Results

8.3.1. Behavior

An inspection of the latencies of all button presses with respect to the last preceding target onset (**Figure 27**) confirmed that the distribution of button presses was mostly confined to a window of 0.2 to 2 seconds, validating the window chosen to define hits. Mean reaction time in hits was 0.957±0.21 seconds.

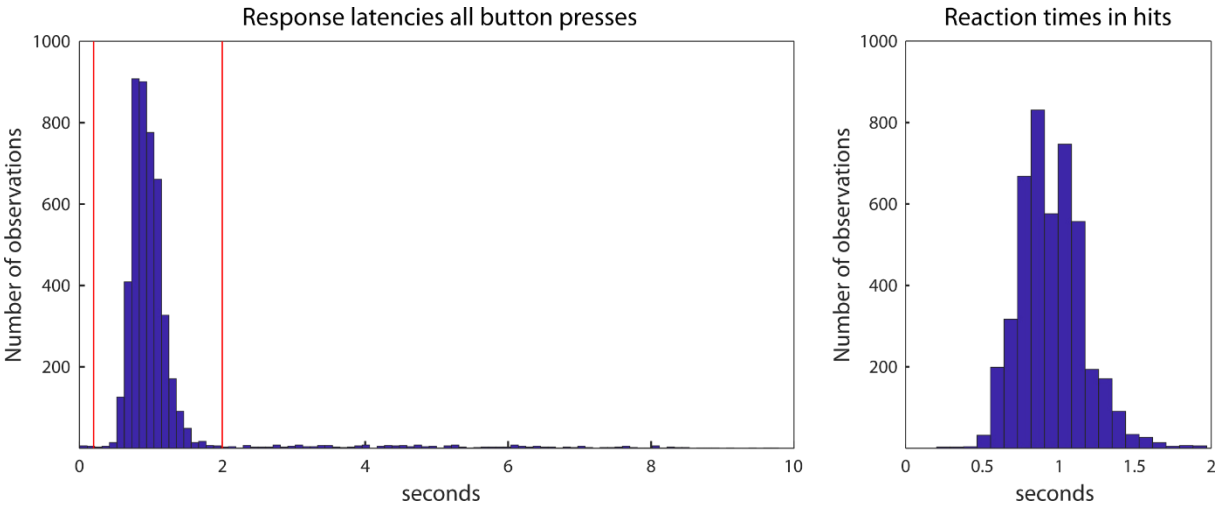

Figure 27*: Left: Distribution of latencies of button presses with respect to the last preceding target onset (time point 0), across all trials and subjects. A clear peak is visible that is completely contained in the response window of 0.2-2 s (red lines) relative to target onset, with a flat distribution outside this window. Right: Zoom on the distribution of reaction time in hits.*

After rejecting artifacted trials, the mean hit rate across participants was 0.436±0.076 (range: 0.324-0.612). The mean number of false alarms was 4.75±5.98 (range: 0-23). Participants therefore made overall few false alarms.

8.3.2. Gastric phase & behavior

We first tested whether hits were more likely at specific points of the gastric cycle. We computed Watson's U^2 and MI on hits vs. misses and gastric phase, and estimated chance level by a permutation procedure for each participant. We then compared empirical values and chance levels at the group level. Empirical values were not higher than chance level for Watson's test (empirical $\mu = 0.071 \pm 0.035$, chance level $\mu = 0.084 \pm 0.002$; one-tailed t-test $t(29)=-1.96$, $p=0.97$) nor MI (empirical $\mu = 0.007 \pm 0.004$, chance level $\mu = 0.008 \pm 0.003$; $t(29)=-1.88$, $p=0.96$) (Figure 28). There was therefore no evidence for a link between gastric phase and hits vs. misses.

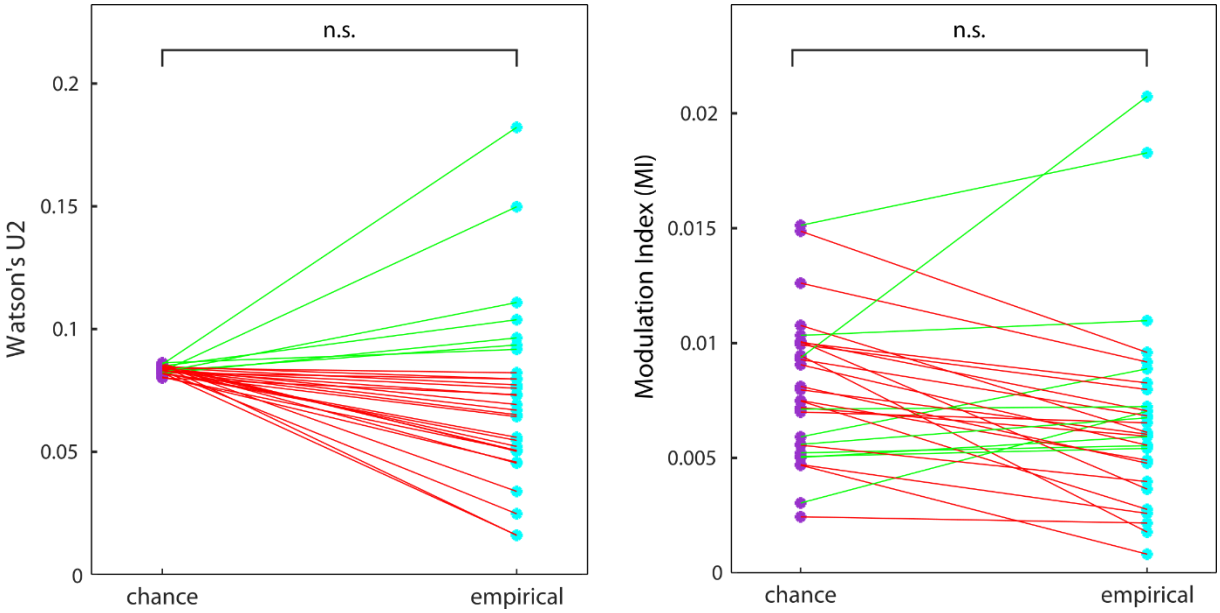

***Figure 28**: Empirical vs. chance level coupling between gastric phase and behavior, assessed by Watson (left) and MI (right). Each pair of dots corresponds to one participant. Green dot-connecting lines indicate positive coupling strength (empirical > chance), red lines negative coupling. Empirical values were not significantly higher than chance level for either of the tests.*

Correlation with questionnaires

We also assessed whether coupling between gastric phase and behavior was linked to scores in two questionnaires participants filled out after the experiment. First, we used the Daydreaming Frequency Scale, to test whether there was a link with the propensity of participants to follow off-task thoughts (N = 29, range = 14 – 43, mean = 29 ± 7.1). Second, we measured trait anxiety due to the common association of stomach sensations with emotions, although we did not have any more specific hypothesis on this aspect (N = 30, range = 6 – 35, mean = 19 ± 7.3).

There was no correlation between daydreaming frequency and gastric-behavior coupling strength for neither Watson's test (robust correlation, t(27) = 0.26, p = 0.8, r^2 = 0) nor MI (t(27) = -1.49, p = 0.15, r^2 = 0.08). There was also no correlation between STAI scores and gastric-behavior coupling strength neither for Watson's test (t(28) = 0.3, p = 0.77, r^2 = 0) nor MI (t(28) = -0.51, p = 0.62, r^2 = 0.01).

8.3.3. Gastric phase and alpha power during the task

Richter et al. observed coupling between gastric phase and alpha power in the 10-11 Hz band. We thus tested whether we could find coupling in this frequency band, during moments where participants were watching the screen but were not exposed to the target stimulus nor responding. We quantified the coupling between gastric phase and amplitude of the alpha rhythm using Modulation

Index (MI) (Tort et al., 2010). We compared empirical MI values with chance level estimated using a cluster-based procedure (Maris and Oostenveld, 2007) intrinsically correcting for multiple comparisons at the group level across sensors. Significant gastric-brain coupling occurred in a large cluster spanning parieto-occipital as well as central to frontal regions (Figure 29A) (sum(t) = 96.81, MonteCarlo p < 0.001). We also estimated the False Positive rate of our statistical procedure, testing whether any of the 1000 surrogate data sets created to estimate chance level could yield cluster statistics as large as those produced by the original data. We observed that only 1% of surrogate data sets resulted in a cluster statistic as large as the real data set, thereby showing that the Monte-Carlo probability of obtaining the empirical cluster by chance was 0.01. The cluster overlapped, but only partially, with the channels showing strongest alpha power across samples and participants (Figure 29B). Although MI is in principle independent from power (Tort et al., 2010), we controlled whether EGG-alpha coupling was driven by alpha power. However, there was no significant correlation across participants between MI coupling strength and mean alpha power averaged across the channels in the cluster (robust correlation, t(28) = 0.56, p = 0.58, r^2 = 0.01, Bayes factor = 0.15, substantial evidence for the null hypothesis). Coupling strength was also not related to the power (t(28) = 0.83, p = 0.42, r^2 = 0.03, Bayes factor = 0.2, substantial evidence for the null) or regularity of the EGG signal as quantified by the standard deviation of cycle duration (t(28) = 0.2, p = 0.84, r^2 = 0, Bayes factor =0.14, substantial evidence for the null).

By visual inspection, we observed that gastric-alpha coupling involved 1:1 but also higher coupling modes. Examples phase-amplitude profiles from the subject with highest, intermediary and lowest coupling are plotted in Figure 29C.

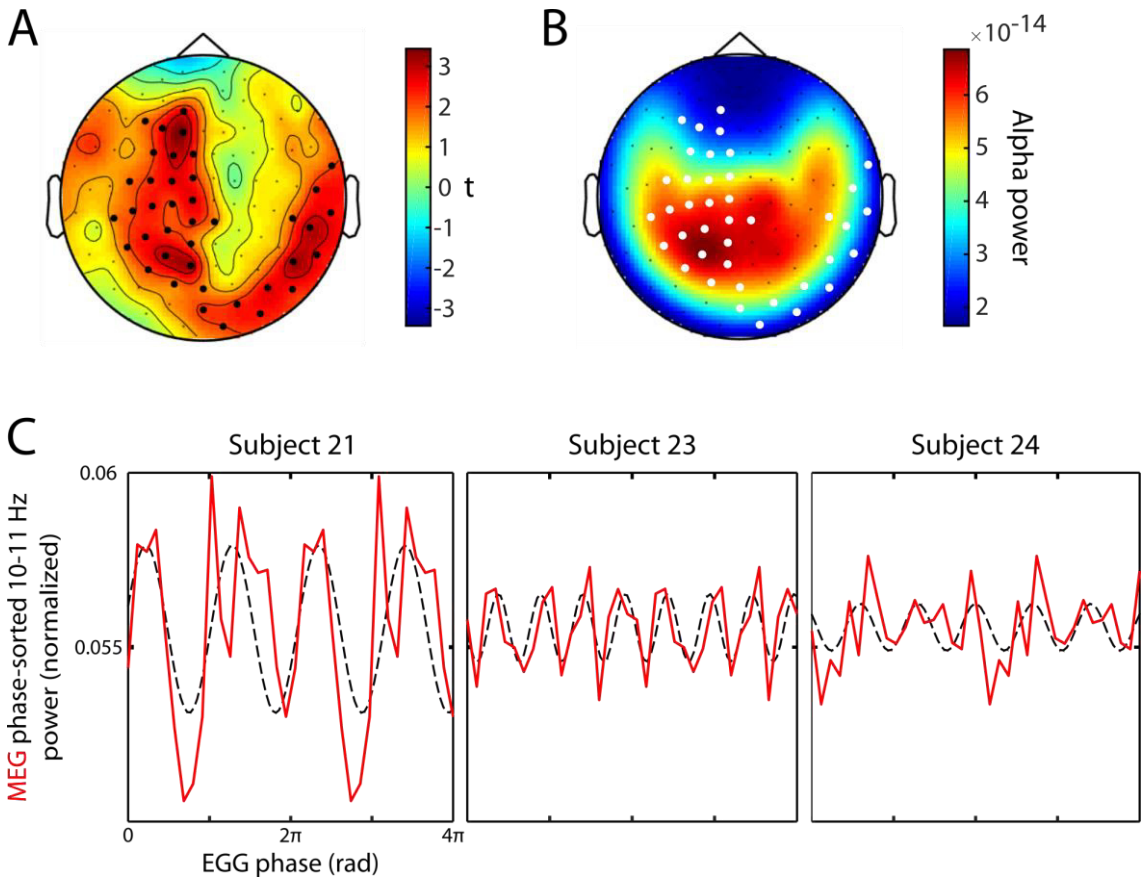

***Figure 29**: Gastric-alpha coupling. **A**: Statistical map of t-values on empirical vs. chance level MI quantifying coupling between gastric phase and MEG power at 10-11 Hz during task blocks. Channels in the cluster are indicated by larger block dots. **B**: Topographical map of 10-11 Hz power during the task, grand average across participants and samples analyzed, with channels in the EGG-alpha cluster for the task blocks marked by larger white dots. **C**: Three examples of phase-amplitude profiles for the participant with highest (left), intermediate (middle) and lowest coupling strength (right). Profiles are presented over two gastric cycles (4π) for visualization. MEG power in each bin was normalized by the sum of the average power across bins. Dashed black lines represent cosine fits.*

8.3.4.Inter-subject variability in gastric-alpha coupling during task

We correlated coupling strength in the significant cluster in the task blocks (Figure 29A) with scores in the questionnaires and several demographical and experimental variables. Results are reported in Table 1. None of the variables tested revealed any link with EGG-alpha coupling strength, apart from a weak trend for a higher coupling strength in female than male participants (two-sample t-test, t(28) = -2.03, $p = 0.052$ not corrected for multiple comparisons). For all other variables, Bayes statistics indicate substantial evidence for H_0. This replicates Rebollo et al., 2018, who found no link between gastric-BOLD coupling strength with STAI scores, gender or BMI. Note though that BMI and age was more restricted in our sample than in the general population.

STAI	Daydreaming	Gender	BMI	Age	Time of recording (morning vs. afternoon)	Time elapsed since last meal (hours)
Range : 6 - 35 Mean: 19.3	Range : 14 - 43 Mean : 29.2	13 male, 17 female	Range : 18.2 - 22.9 Mean : 20.2	Range : 19 - 30 Mean : 23.8	18 morning, 12 afternoon	Range : 1 - 17 Mean : 4.2
Robust corr. $r^2 = 0$ $p = 0.92$ BF = 0.14	Robust corr. $r^2 = 0.02$ $p = 0.52$ BF = 0.18	T-test $t = -2.03$ $p = 0.05$ BF = 1.55	Robust corr. $r^2 = 0.01$ $p = 0.62$ BF = 0.16	Robust corr. $r^2 = 0.05$ $p = 0.24$ BF = 0.29	T-test $t = 1.14$ $p = 0.27$ BF = 0.57	Robust corr. $r^2 = 0.03$ $p = 0.39$ BF = 0.21

***Table 1**: Effects of STAI/daydreaming scores and demographical variables on mean coupling strength in the cluster. P-values not corrected for multiple comparisons. BF: Bayes Factor. Interpretations of Bayes Factors are as follows: 1-3: Anecdotal evidence for H_1; 0.33 - 1: Anecdotal evidence for H_0; 0.1-0.33: Substantial evidence for H_0, <0.1: Strong evidence for H_0.*

8.3.5. Gastric-alpha coupling & performance during the task

We next tested whether the individual strength of EGG-alpha coupling during the task showed any relationship with behavioral performance in the experiment of vision at threshold. However, individual EGG-alpha coupling strength did not show a significant link with hit rate (robust correlation, t(28) = 0, $p = 1$, $r^2 = 0$) or mean reaction time (t(28) = 0.-1.14, $p = 0.26$, $r^2 = 0.05$) (Figure 30).

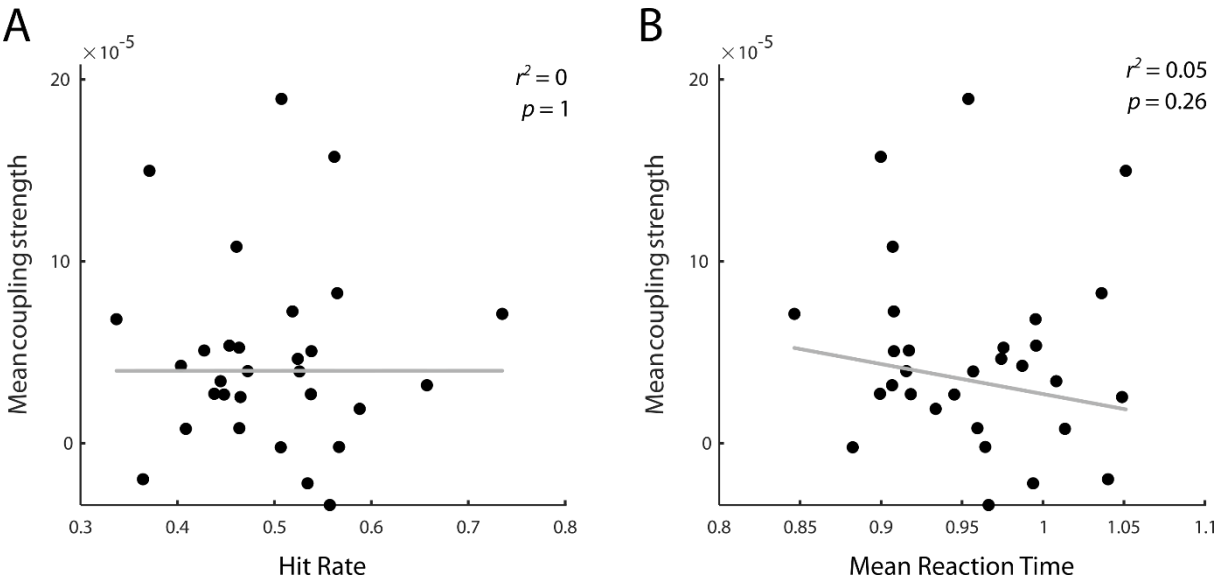

***Figure 30**: **A**: Correlation between individual hit rate and mean gastric-alpha coupling strength in the significant task-cluster. **B**: Correlation between individual mean reaction time and mean gastric-alpha coupling strength.*

We also assessed whether the individual degree of gastric-alpha coupling in task blocks was linked to the coupling strength between gastric phase and hits vs. misses. There was a trend for gastric-alpha coupling strength to be associated with stronger EGG-behavior coupling strength which did not reach significance (robust correlation, t(28) = 1.75, p = 0.09, r^2 = 0.1) (Figure 31). In other words, participants in which alpha power was strongly modulated by gastric phase also tended to show a higher modulation of hit rate by gastric phase.

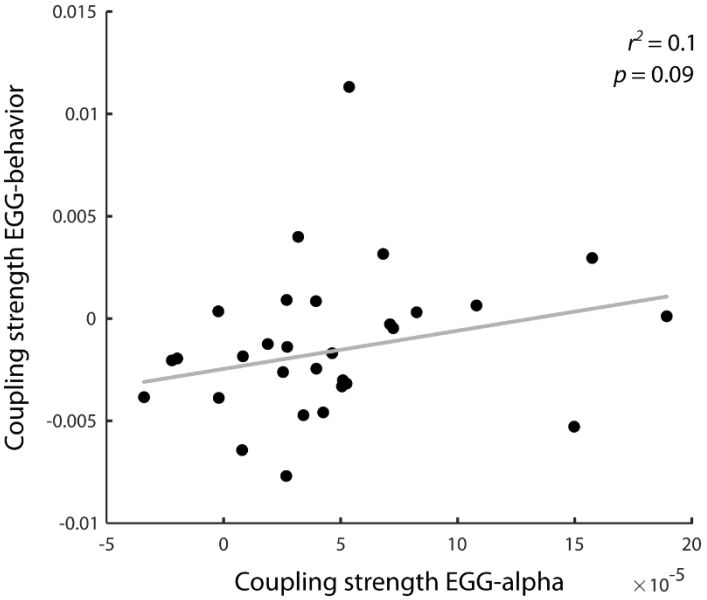

***Figure 31**: Correlation between gastric-alpha coupling in the cluster (x-axis) and gastric-behavior coupling (y-axis). There was a trend for a positive link between gastric-alpha coupling strength and coupling between gastric phase and behavior.*

8.3.6.Alpha power & performance during the task

We tested whether prestimulus alpha power differed between hits and misses. For this we computed the mean power in the 8-12 Hz band across the 15 channels with strongest alpha power in the second preceding target onsets (Figure 32A). Across participants, mean prestimulus alpha power for hits vs. misses did not differ significantly (unpaired t-test, t(58) = -0.06, p = 0.95, Bayes Factor = 0.26, substantial evidence for the null – Figure 32B). Next, we tested whether individual mean alpha power in the 8-12 Hz band across the 15 channels with strongest alpha power correlated with hit rate *between* subjects. However, there was no significant correlation (robust regression, t(28) = 0.17, p = 0.86, r^2 = 0, Bayes Factor = 0.14, substantial evidence for the null – Figure 32C). We did the same analysis with a narrower frequency band of 10-11 Hz, which still yielded no significant link between prestimulus alpha power and perceptual outcome.

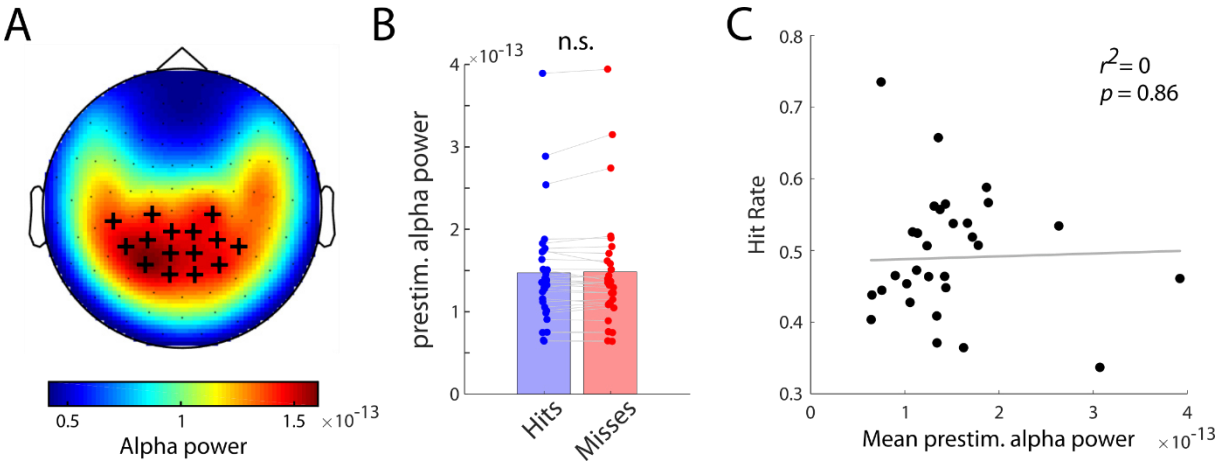

***Figure 32**: **A**: Topographical map of the mean 8-12 Hz power in the second preceding target onsets. Sensors marked by crosses were used for the comparison between hits and misses. **B**: Bar graph of the mean prestimulus alpha power at the sensors indicated in the map and in the second preceding target onsets, in hits (blue) and misses (red). **C**: Correlation between individual mean prestimulus alpha power and hit rate across participants.*

8.3.7. Gastric phase and alpha power during rest

We also analyzed EGG-alpha coupling during the resting state. Two candidate clusters were obtained that did not reach significance, one right lateralized parietal-temporal that was marginally significant (sum(t) = 18.4, MonteCarlo p = 0.098) and one smaller frontal cluster (sum(t) = 5.38, MonteCarlo p = 0.354) (Figure 33).

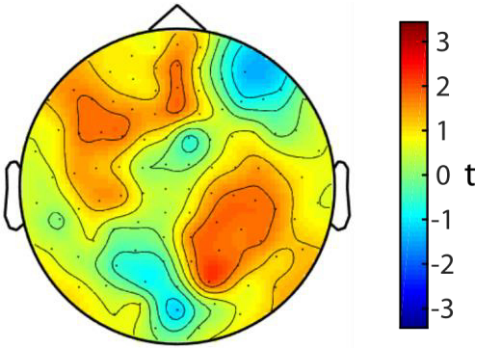

***Figure 33**: T-value map for gastric-MEG coupling during the resting state. The right occipito-temporal cluster was only marginally significant (p = 0.098).*

8.3.8. Gastric phase and pupil diameter during rest

We also analyzed whether EGG phase modulated pupil diameter, an index of arousal. Since the pupil diameter in task blocks represents a mixture between tonic pupil fluctuations and evoked responses to the visual targets or motor responses, we analyzed this coupling in the resting state blocks. Empirical

MI was not higher than chance (one-tailed t-test t(28) = -0.93, p = 0.82), indicating no significant coupling of pupil diameter to gastric phase.

8.4. Discussion

8.4.1. Summary experimental results

We experimentally tested the hypothesis that the gastric rhythm has an influence on perceptual performance by modulating brain alpha oscillations. We developed a continuous task with visual targets at threshold, to reveal slow fluctuations in the probability of target detection. We acquired MEG data and recorded the gastric rhythm using the Electrogastrogram while participants performed this task. Perceptual outcome was not modulated by gastric phase more than expected by chance, and we thus could not confirm our initial hypothesis. Next, in a more exploratory analysis, we first assessed whether we could find coupling between the gastric rhythm and brain alpha power during the task as previously observed at rest (Richter et al., 2017). We indeed observed significant phase-amplitude coupling between gastric phase and alpha power in task blocks, during moments where participants were watching the screen but were not exposed to the target stimulus nor responding. Coupling was localized in an extended cluster spanning posterior to central sensors. Only marginally significant coupling was found in the resting state. We then asked if the individual strength of gastric-alpha coupling in the task blocks had functional correlates with performance, by correlating individual EGG-alpha coupling strengths with individual hit rates and mean reaction times. However, no significant link was observed. There was a marginal trend for coupling between gastric phase and alpha power to be associated with higher coupling between gastric phase and hit rate. Finally, we did not replicate the often reported effect of prestimulus alpha power on hits vs. misses (Busch et al., 2009; Dijk et al., 2008; Ergenoglu et al., 2004; Mathewson et al., 2009). Mean alpha power also did not predict hit rate between participants. In conclusion, while for the first time describing coupling between the gastric rhythm and cortical alpha power while participants are engaged in a task, this study could not provide evidence for a behavioral correlate of this coupling.

In the following, I will discuss the different findings in relation to the ideas proposed in the introduction. Specifically, I will consider several factors that might account for the absence of a link of gastric phase with performance, and discuss possible interpretations regarding the observed coupling between gastric phase and alpha power.

8.4.2. Experimental aspects

First of all, it is important to consider the special nature of our experimental paradigm. We used a **continuous experiment** in which participants were seeing an uninterrupted stream of flickering noise during an extended period, with targets superimposed at random uncued moments, and without any stimulus that marked the start or end of a trial. We chose this design for several reasons. One of our central hypotheses was that vigilance or arousal might share a link with the gastric rhythm. Gastric phase might exert a rhythmic modulation of arousal through its projections to neuromodulatory systems, with arousal thus varying within the gastric cycle. Alternatively, it might be that the gastric rhythm influences arousal over longer time periods, e.g. by the degree of coupling to the brain alpha rhythm over a given

period. With both possible cases in mind, we aimed to minimize interruptions with these ongoing fluctuations in arousal or vigilance, which would have hindered the detection of a link with gastric phase. Next, at the cortical level, it is known that the sudden onset of stimuli in the visual or other modalities can 'reset' cortical oscillations (Lakatos et al., 2009; Mercier et al., 2015; Romei et al., 2012), which would have disrupted their spontaneous fluctuations. Moreover, the brain is good at detecting rhythms, and it has been shown that the amplitude of slow neural oscillations can be entrained to the predictable stimulus stream via top-down attentional mechanisms (Lakatos et al., 2008), and that expectations of stimulus presentation modulate alpha power specifically (Praamstra et al., 2006; van Diepen et al., 2015). More speculatively, it might be that sudden events also interact with the spontaneous gastric slow wave. In sum, this design might make our task more "natural", as in the real world we are also continuously receiving a chain of visual input not as well defined as experimental trials (Huk et al., 2018). Although this can be considered as a strength and interesting aspect, it also makes the experiment less controlled.

One consequence of the experiment being less controlled is that introduces **many determinants of perception**. For example, it might be that a stimulus is missed due to low sensitivity, fatigue, a drop in arousal or vigilance, or task-unrelated thoughts. However, we do not know in how far each of these processes is linked to the gastric rhythm. These different concepts, despite subtle differences in their definitions, are hard to disentangle operationally. Indeed, changes in vigilance, sustained attention, off-task focus and fatigue of all been operationalized very similarly, namely by decreases in performance (Esterman et al., 2013, 2014; Hinds et al., 2013; Langner et al., 2010, 2012; Rosenberg et al., 2015).

Finally, our experiment is faced with the common problem of a **limited sample size** and statistical power. We here could include 30 participants, with around 250 artifact-free trials that could be obtained for each, which might be too low or at the lower limit to detect a potentially small effect of gastric phase on behavioral outcome. More trials could have been obtained by reducing the durations of inter-stimulus intervals. However, this might have prevented the development of slow fluctuations in vigilance which we targeted here.

8.4.3. Only marginally significant coupling in the resting state

A finding that deserves attention is that while we did find significant coupling in the task blocks, we observed only marginally significant coupling in the resting state, i.e., we do not readily replicate Richter et al., 2017.

We obtained a right parieto-occipital cluster which overlaps with the parieto-occipital cluster found by Richter et al. However, we also obtained a mid/left frontal candidate cluster not overlapping with clusters by Richter et al. Interestingly, this could suggest that the **type of occupation of the participants before** affects coupling during the resting state. In Richter et al., the resting state was acquired after an interrupted-thought paradigm (Babo-Rebelo et al., 2016b), which is close to

spontaneous mind-wandering. Here, the resting state was acquired after a visual task of an extended duration. In the literature on resting state networks, it has been extensively reported that the performance of a task (such as a learning task or memory load) affects brain dynamics during subsequent resting state (e.g., Gordon et al., 2012; Lewis et al., 2009; Pyka et al., 2009; Tambini et al., 2010; Wang et al., 2012). For example, prolonged exposure to visual stimuli affects functional connectivity of visual regions in subsequent resting state (Stevens et al., 2010). Here, one might thus speculate that the previous task of near-threshold target perception has affected dynamics during resting state. Perhaps, the visual nature of the task could have driven participants' attention more towards the visual modality in the subsequent resting block, and made them engage less into processes decoupled from the environment. Also, with the long duration of the experimental procedure that precedes the resting state (practices+staircases+4-5 task blocks), it is likely that participants were in a fatigued state, or at least more so than in the study by Richter et al, where participants reported more boredom than visual fatigue. It would be an interesting option to analyze the influence of task on resting state gastric-alpha coupling.

Finally, one could also consider the possibility that gastric-alpha coupling in the task blocks was not specific to the fact that participants were performing the task. It might be that the monotonous and unchallenging task, with long intervals up to 10 seconds between the targets, was still functionally close to a resting state, e.g. with participants still engaged in task-unrelated thoughts. Gastric-alpha coupling might have also been detected in the resting state if more data would have been available. While the task included four to five blocks of 12 minutes each, we acquired only one block of resting state of 12 minutes. Moreover, one participant less was available for the resting state due to a poor quality of the EGG. Finally, we here restricted to the 10-11 Hz band in which gastric-alpha coupling was previously reported (Richter et al., 2017), and did not analyze the frequency specificity in task vs. rest.

8.4.4.Significant gastric-alpha coupling in the task

We here observed for the first time that brain alpha power was coupled to the gastric phase during the performance of a task. We obtained one large cluster that seemed to be composed of two parts; one that extended mostly over midline channels and one right-lateralized from outer temporal to occipital channels. The cluster partially overlapped with the channels showing strongest alpha power.

This **topography** of the cluster differs from the topography of significant gastric-alpha coupling previously reported during resting state (Richter et al., 2017). In the study of Richter et al., coupling occurred in two bilateral parieto-occipital clusters with an extension over right fronto-temporal sensors. The cluster here observed in the task overlaps with the parieto-occipital cluster of Richter et al., which was source localized to the parieto-occipital sulcus. Given this and also the fact that our cluster overlapped with the channels showing strongest alpha power, one can assume that the coupling observed here in the task is at least partly driven by occipito-parietal regions. However, we also find coupling in

more frontal channels not reported in Richter et al. This might suggest that gastric phase is coupled to alpha power in additional regions than during resting state.

The exciting finding of gastric-alpha coupling during the task makes the question for the **functional consequences** of this coupling even more relevant. Here, we could not find evidence for our initial hypothesis that gastric phase would modulate the probability of perceiving the targets. Gastric phase did also not modulate pupil diameter during the resting state. This might suggest that our hypothesis of a fluctuation in arousal along the gastric cycle might not be appropriate. We next wondered if the strength of gastric-alpha coupling might be linked to *interindividual* differences in arousal state. This could be reflected in measures of performance such as hit rate and reaction time. However, we observed that coupling strength in the cluster did not correlate with hit rate or reaction time. This analysis is so far explorative and has several limitations. First, it does not take into account that the topography of gastric-alpha coupling might vary within participants. Next, it might be that correlating performance with overall coupling strength in the cluster obtained in the scalp level mixes the contributions of functionally heterogeneous regions, and that there is a behavioral correlate for gastric-alpha coupling in specific (e.g. occipital or frontal) regions. Determining the cortical sources of gastric-alpha coupling would thus be an important next step.

One possibility is that gastric-alpha coupling over longer periods within participants is related to hit rate. This could be tested by comparing coupling strength in windows of low vs. high hit rate. The difficulty with testing this hypothesis is that it is not clear over which time windows gastric-alpha coupling predicts behavior. Indeed, when we explored this idea, we found that results are unstable and highly depend on parameters such as the duration or percentage overlap of windows within which coupling and hit rate is computed.

Interestingly, we observed a trend for coupling strength between gastric phase and perceptual outcome to be positively correlated with coupling strength between gastric phase and alpha power. In other words, participants where alpha was more strongly modulated by gastric phase, perceptual outcome tended to depend more on gastric phase. This could suggest that the link between gastric phase and behavior holds mostly or only for individuals with high gastric-alpha coupling. This hypothesis could be tested with a larger sample size of participants. Also, even within participants, gastric phase might not *continuously* modulate arousal and performance, but only during certain moments or in given individual states. Future works are needed to investigate what could characterize those states, or in other words, explain what drives the variability in the strength of gastric-alpha coupling. This question is one of the important issues that need to be addressed to identify the functional significance of stomach-brain coupling.

8.4.5.Reconsidering the link between alpha power and perception

Our hypothesis of a potential link between the gastric rhythm and performance was based on the finding that the gastric rhythm modulates ongoing alpha power, because alpha power has frequently been reported to modulate visual perception at threshold. However, in the present experiment, alpha power did not modulate perceptual outcome.

In fact, our experiment is not the first with an absent link between prestimulus alpha power and visual perception at threshold. For example, Hanslmayr et al., 2007; Harris et al., 2018; Park et al., 2014; Wyart and Tallon-Baudry, 2008 reported that trial-to-trial prestimulus alpha power did not predict hits vs. misses. Babiloni et al., 2006 even found a link going into the opposite direction, with stronger prestimulus alpha predicting hits. The proportion of studies finding no link with alpha might also be underestimated because of a bias to not report missing effects. Generally, the reasons for the conflicting results are not understood. Here, the special design of our experiment is one possible factor that would potentially explain a missing influence of alpha power. Indeed, a question that has received more attention in recent years is how findings obtained in well controlled experiments using simplistic stimuli and paradigms translate to more ecologically valid settings (Leopold and Park, 2020). For example, it might be that the effect of prestimulus alpha is less pronounced with more smooth transitions from noise to target periods and a continuous setting with no clear trial structure.

In the recent years, the excitability/inhibition hypothesis has been somewhat revised. Indeed, several studies show that alpha decreases response criterion (i.e., resulting in a higher propensity to report 'seen') rather than improving detection sensitivity itself (Benwell et al., 2017, 2021; Iemi et al., 2017; Limbach and Corballis, 2016; Samaha et al., 2017b, 2020). The precise nature of the link between prestimulus alpha power and perception is thus still an ongoing investigation. Here, it is open whether in our experiment participants missed targets due to a lower sensitivity vs. response criterion. Our training procedure attempted to stabilize criterion. A further improvement of the experiment would have been to introduce additional 'catch' trials with no target, at moments where targets would normally have been presented. This would have allowed to compute a false alarm rate and hence estimate sensitivity and criterion.

8.4.6.Conclusion

In sum, with the current study, we could not find evidence for a link between the gastric rhythm and the probability to detect a visual stimulus at threshold. However, we do find for the first time that the gastric rhythm modulates brain alpha oscillations during performance of a task, likely in occipital regions. The functional role of this coupling remains to be characterized.

9. General discussion

9.1. Summary main results

In my PhD, I studied the coupling between the phase of the gastric rhythm and the power of alpha oscillations and its functional consequences for visual perception. Our hypothesis was that the gastric rhythm drives slow fluctuations in arousal and cortical excitability that have an impact on fluctuations in visual perception.

A first step to test this hypothesis was to obtain good quality EGG recordings and develop an analysis pipeline to extract the gastric phase in healthy human participants. Building on the nascent expertise in the group, I refined recording procedures and developed a semi-automated analysis pipeline to identify a regular gastric rhythm. We applied these recording and analysis procedures in a large sample of participants. This, together with EGG recordings from other projects in the group, resulted in more than a hundred EGG recordings. From on these recordings, we derived normative distributions of EGG parameters. We found that 85% of recordings showed a clear spectral peak in the normogastric range (0.033-0.067 Hz). We then analyzed properties of the EGG in the recordings with clean power spectra. We found that women showed a higher peak frequency than men, replicating two previous studies with comparably large sample sizes (Parkman et al., 1996; Tolj, 2007). Age and BMI were not related to any EGG parameter. Next, we found that most recordings showed a standard deviation of cycle duration lower than 6, with recordings above this threshold clearly representing outliers. This threshold converged with the criterion from the clinical literation of at least 70% of cycles being in the normogastric range (i.e., 10-30 seconds) (Parkman et al., 2003; Riezzo et al., 2013). We thus consider this threshold useful as an inclusion criterion for EGG recordings. We also observed that prolonged fasting resulted in a more irregular distribution of cycle duration.

Once we established how to extract a regular gastric phase, the next step was to evaluate how to detect a statistical relationship between gastric phase and a binary behavioral outcome (i.e., hits vs. misses). We addressed this question in a set of simulations, where we mimicked relationships between the phase of real data and an artificial outcome. We varied the strength of the injected phase-outcome effect, coupling mode, and the relative number of observations in the two groups. We compared the performance of four circular tests (Phase Opposition Sum (POS), circular logistic regression, the Watson test, and Modulation Index (MI)), and evaluated different methods to assess significance on the group level (comparing empirical vs. chance values, creating surrogate average distributions, and three ways of combining individual p-values). As a result, we observed that POS, circular logistic regression and the Watson test were most sensitive to 1:1 relationships between gastric phase and outcome, while MI, and to some lesser extent the Watson test, where the only sensitive methods to detect more complex modes of coupling. The Watson test also came with the lowest False Positive rate. Additionally, the Watson test was also robust to moderate imbalances in the relative number of trials between groups. In sum, our results highlighted the Watson test as a good allrounder method for detecting phase-behavior

relationships, while the advantage of MI is its high sensitivity to more complex coupling modes. All the considered methods for evaluating significance at the group level showed a similar sensitivity, but comparing empirical vs. chance level came with the lowest False Positive rate. This approach was thus retained for estimating for significance at the group level.

Finally, we experimentally addressed the question whether the gastric rhythm has an influence on the probability to detect a near-threshold visual target. We designed a task targeting fluctuations in visual perception and recorded the MEG and EGG in 30 participants while performing the task. Gastric phase showed no link with the probability of targets to be perceived. However, we found that alpha power (10-11 Hz) was significantly modulated by gastric phase during the task, with marginally significant coupling in the resting state. The individual strength of gastric-alpha coupling was not related to individual hit rate or reaction time. There was a marginal trend that participants with higher modulation of alpha power also showed a higher modulation of hit rate by gastric phase. Prestimulus alpha power did not differ for hits vs. misses, and there was no correlation between individual mean prestimulus alpha power and hit rate. Finally, we tested if pupil in the resting block was related to gastric phase, but found no significant coupling between pupil diameter and gastric phase.

In the following, I will discuss these results from a broader perspective. I will first discuss some aspects related to the results of both the methodological and experimental projects. I will then present two hypotheses on the potential function of stomach-brain coupling, and conclude with further outstanding questions and future perspectives.

9.2. How do EGG parameters relate to gastric-alpha coupling?

Frequency

We made several interesting observations that were linked to EGG frequency. As a reminder, although the gastric rhythm is mostly driven by the ICCs intrinsic pacemaker activity, there is evidence that it can also be modulated by vagal/parasympathetic and spinal/sympathetic descending projections (Andrews and Scratcherd, 1980; Pagani et al., 1985; Smirnov and Lychkova, 2003; Teckentrup et al., 2020; Tsuchiya et al., 1974). The orchestration and relative contributions of vagal and spinal projections on gastric frequency are still unknown. Gastric frequency is thus an interesting parameter that deserves further consideration. In the following, I will discuss several of the findings from the thesis and argue that gastric frequency might be of relevance for stomach-brain coupling.

To start with, we found in our EGG data set (Wolpert et al., 2020) that female participants had a slightly but consistently faster gastric rhythm than male participants. How does this finding relate to the EGG literature? Unfortunately there are only few studies on differences in EGG parameters in healthy participants. While Pfaffenbach et al., 1995 and Simonian et al., 2004 found no effect of gender

on dominant frequency, two studies with larger sample size comparable to ours (Parkman et al., 1996; Tolj, 2007) equally found female participants to have a faster gastric rhythm. No functional interpretation has been offered to explain those gender-differences in peak frequency. Women were also found to show fewer bradygastria (i.e., cycle of longer duration than the normal range) and more tachygastria (i.e., cycle of shorter duration than the normal range) compared to men (Tolj, 2007). It might thus be that the effect is more subtle than a difference in peak frequency, being potentially driven by occurrences of EGG cycles of faster or slower duration. Alternatively, the occurrence of more cycles in tachygastria might also be trivially explained by a shift in the *overall* distribution of cycle durations toward the normogastric limits, which would then naturally result in a proportion of cycles in normogastria.

Several studies have been interested in gastric frequency changes in stress (Gianaros et al., 2001), nausea (Hu et al., 1991; Stern et al., 1985) and disgust (Harrison et al., 2010). Increased amounts of periods with tachygastria have also been found in patients with schizophrenia (Peupelmann et al., 2009) and depression (Ruhland et al., 2008). While the literature is rather mute on interpretations of differences in overall peak frequency, studies reporting periods with faster rhythms proposed that these are caused by an increased sympathetic and decreased parasympathetic activation. In support of this, periods of tachygastric are accompanied by an increased skin-conductance and decreased differences in heart rate (Hu et al., 1991). In clinical patients, tachygastria would reflect a disturbance in the balance of autonomic branches, with an increased sympathetic relative to parasympathetic activation (Peupelmann et al., 2009; Ruhland et al., 2008).

Changes in gastric frequency could therefore be a physiological marker of the vagal/parasympathetic vs. spinal/sympathetic output. Another such marker is heart rate variability (HRV). Low frequencies (0.04-0.15 Hz) in HRV (LF-HRV) are assumed to reflect parasympathetic outputs, while high frequencies (0.15-0.4 Hz, HF-HRV) additionally reflect sympathetic outputs. Harrison et al., 2010 found that the magnitude of experienced disgust was predicted both by tachygastria and HF-HRV, suggesting that HRV and gastric frequency might be linked and both can be used to assess changes in sympathetic activation.

Some findings tentatively make a **link between these physiological changes and cortical coupling to gastric signals**. For example, Harrison et al., 2010 went on to show that some cortical regions, including the bilateral mid-anterior insula, co-varied with changes in gastric frequency. Moreover, Rebollo et al., 2018, found that regions of the gastric BOLD network fluctuated either with LF-HRV or HF-HRV. For example, dorsal occipital regions were more related to high frequency HRV, suggesting that they might be more related to parasympathetic output. Faster EGG rhythms could thus provide a measure that isolates sympathetic output (even though the 1:1 mapping between tachygastria and sympathetic activation might be an oversimplification). Potentially, studying changes or differences

in EGG frequency might thus be an interesting measure to disentangle the contribution of vagal vs. spinal projections to gastric-alpha coupling.

While we did not investigate tachygastria or bradygastria, we found no correlation between gastric-alpha coupling strength and EGG peak frequency. The only finding that indirectly linked between frequency and coupling strength was that female participants showed marginally higher coupling strength than male participants. Given the small sample size (17 female, 13 male), this finding has of course to be taken with caution. Rebollo et al., 2018, found no link between gender and gastric-BOLD coupling strength in any of the nodes of the gastric network. However, it might be that the effect is more specific to MEG alpha oscillations, or more related transient changes in gastric frequency and not overall peak frequency.

In conclusion, the foregoing considerations emphasize that our EGG preprocessing and analysis pipeline to extract gastric phase needs further developments. It is currently designed to extract a gastric rhythm with stable and regular frequency. We here discarded recordings with no peak within the normogastric range (in the EGG data set analyzed (Wolpert et al., 2020), this happened in 18% of all cases), and also excluded cycles with an excessively long or short duration. It might be that these recordings or portions are functionally interesting. However, the important challenge is to develop criteria to determine if these signals represent noise (electronical, movements, …) or true irregularities in the gastric rhythm. Indeed, not all cutaneously recorded irregularities frequency can be attributed to true irregularities in gastric frequency (Mintchev and Bowes, 1997). In future, these limitations could be also be overcome by measuring gastric activity invasively, for example by using endoscopy (Coleski and Hasler, 2004), serosal surface electrodes in patients undergoing surgery (Lin et al., 2000), or new measurement technology such as pills that can be swallowed and thus enter the stomach in a minimally invasive way (Monti et al., 2021).

EGG amplitude, stomach distension and fed vs. fasted state

EGG amplitude is another parameter of importance and might equally share a link with gastric-alpha coupling.

The amplitude of the gastric signal in cutaneous recordings depends to a large extent on the fed vs. fasted state of the participant. In the fasted state, when the stomach is empty, only few contractions occur and the EGG reflects mostly intrinsic activity of ICC pacemaker potentials. As an exception, very prolonged fasting (typically overnight) can lead to periods of transient strong contractions, called the "phase III of the interdigestive complex" (Koch and Stern, 2004). We here found that prolonged fasting (>10 hours) leads to a more irregular gastric rhythm (Wolpert et al., 2020), which might be explained by the irregular contractions of the phase III that could distort the measured rhythm. During digestion, when the stomach is full, smooth muscle contractions are triggered with additional input from enteric

motor neurons (Sanders et al., 2014), and the EGG now becomes more driven by the contractile activity. This results in a stronger EGG amplitude in healthy participants (Riezzo et al., 2013).

In our experiment of vision at threshold, we targeted a moderately fasted state by asking participants to fast for the 2 hours preceding the appointment. In practice, participants seem to have mostly followed this request, with reported time elapsed since their last meal ranging from two to seventeen hours. Since only about 10% of a solid meal remains in the stomach 2 to 3 hours after meal ingestion (Vasavid et al., 2014), participants thus were indeed in a fasted state. Irregular contractions driven by prolonged fasting and feelings of hunger might have occurred; however, we found no correlation between time elapsed since last meal and gastric-alpha coupling. **Overall, this suggests that the gastric-alpha coupling we found probably represents cortical coupling to the intrinsic pacemaker activity of the stomach rather than smooth muscle contractions.**

Even though we studied coupling during a fasted state, there are several reasons why the fed state might affect coupling and could therefore be interesting to study. First, studies applying an artificial distension of the stomach (Ladabaum et al., 2001; Lu et al., 2004) showed that distensions of increasing intensity resulted in similar topographies but increasing strength of BOLD activations. Even though these studies are possibly confounded with pain, it might be that also a naturally increasing gastric distension (i.e., by ingestion of food) results in stronger gastric input to cortical structures. It has also been shown in rats that gastric distension by infusion of a saline solution (which might represent a more natural condition) increases vagal activations (Schwartz et al., 1991, 1993).

Another argument that **stomach fullness in humans might modulate gastric ascending signals** can also been made from the study of Schulz et al., 2017. The authors proposed a new methodology to study visceral afferent processing, which is based on the electromyographic eye blink responses to acoustic startle stimuli (short the 'startle reflex'). Previous studies from the group had shown that the startle reflex is modulated by cardiac (Schulz et al., 2009a, 2009b) and respiratory phase (Schulz et al., 2016), with a diminished cardiac modulation in patients with degeneration of autonomous afferents (Schulz et al., 2009b). This suggests that the modulation of startle reflex indirectly reflects visceral afferents. Here, they applied this method to signals from the stomach. Startle stimuli were applied in healthy participants at baseline as well as 0, 7 and 14 minutes after the ingestion of a standardized amount of water (0, 300 or 600 ml). The authors found that startle reflexes were decreased by water ingestion, with the magnitude depending on the time elapsed since ingestion and the amount of water (Figure 34). This suggests that natural stomach distension interacts with brainstem loops mediating the startle reflex. Ingestions of water also led to a decrease in heart rate and an increase in heart rate variability, which was interpreted as an increase in parasympathetic activation. The study therefore suggests that gastric distension induces an increase in parasympathetic signal transmissions to subcortical regions, and that the modulation of the startle reflex provides a measure of this 'visceral-

afferent neural traffic'. Potentially, the amount of stomach fullness could also affect the projections of gastric input to higher cortical structures. Of note, the effects occurred quite early after ingestion and were quite transient. However, while liquids are emptied from the stomach within minutes (Hausken et al., 1998), more long-lasting effects could be expected with solid food.

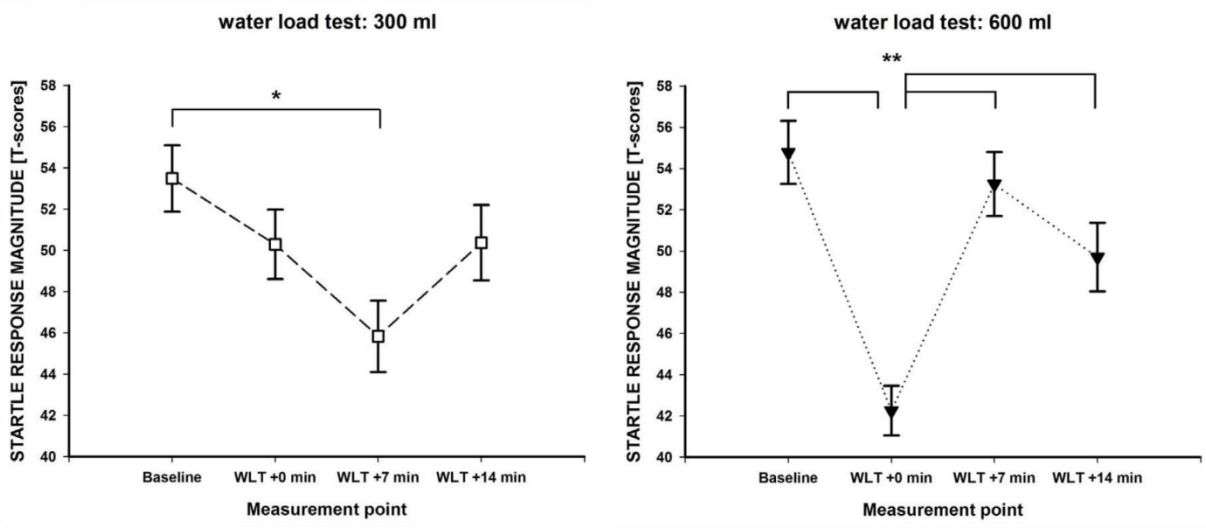

***Figure 34**: Startle response magnitudes (measured by the electromyogram), at baseline and at three measurement points after the ingestion of 300 (left) and 600 (right) ml of water. Startle responses were decreased 7 minutes after ingestion of 300 ml of water, and directly after ingestion of 600 ml. Schulz et al., 2017*

In conclusion, several lines of evidence suggest that the fed vs. fasted state of participants, as (partially) reflected in EGG amplitude, could influence cortical projections of visceral afferents and thus affect gastric-alpha coupling. In the narrow range investigated here, we found no link between time elapsed since last meal or EGG amplitude and gastric-alpha coupling strength. However, future experiments could assess the impact of those parameters on stomach-brain coupling more systematically, and investigate coupling after the administration of standardized amounts of meals.

9.3. Coupling modes

The results of our statistical simulations demonstrate that it is important to consider the expected form of coupling when testing for links between the phase of an oscillation and a behavioral outcome. Among the different circular tests compared, some were more sensitive to 1:1 relationships between phase and outcome, while others were more sensitive to higher coupling modes, with hits and misses each clustering at more than one preferred phase. Such higher forms of coupling between the phase of an oscillation and outcome have so far rarely been considered. For example, studies on the link between

alpha phase and perception have implicitly assumed a 1:1 coupling. In the case of alpha oscillations, this relationship is likely the most plausible since phase is thought to reflect rhythmic changes in the level of depolarization of a group of neurons, reflecting alternating periods of excitability vs. inhibition (Klimesch et al., 2007). However, in the case of a (slower) bodily oscillation, the relationship between phase and the behaviorally relevant brain rhythm, and thus also behavioral outcome, might be more complex. For example, Kluger et al., 2021 found that the respiratory rhythm modulated perceptual sensitivity in a form that was best approximated by a sinusoid fid at 1.55x the respiration frequency. Moreover, we here observed that gastric-alpha coupling showed complex profiles that varied between participants (Figure 16D). In this case, it is therefore important to be sensitive to different forms of coupling.

An unresolved question with regard to coupling modes is what is their **underlying mechanism**. At first glance, a 1:1 relationship between gastric phase and alpha power would perhaps be the most intuitive relationship. For example, the rhythmically occurring ICC pacemaker potentials could be sensed by vagal afferent neurons and relayed to the brain in a phasic way, resulting in a 1:1 modulation with a given delay. However, there are arguments that the picture is not that simple. While it has long been assumed that only one slow wave is propagating over the stomach at a time, more recent studies found that two, three or more wavefronts propagate along the stomach simultaneously (O'Grady et al., 2010; Schulze, 2006). Adding to the complexity, the frequency and amplitude of gastric waves depends on the location of the stomach (O'Grady et al., 2010), such that pacesetter potentials at different sites are likely not combined in a linear way. In general, how sources are combined to give rise to the signal on the cutaneous level is still under investigation (Cheng et al., 2013; Du et al., 2010). It is thus difficult to know how the pacemaker potentials simultaneously present at different sites of the stomach are transmitted to the brain. Potentially, the superposition of multiple pacemaker potentials being transduced from different anatomical locations with different delays could give rise to more complex relationships between cutaneous EGG phase and coupled brain rhythms, thus explaining the higher coupling modes.

A related question is why coupling modes **varies between participants**. Although the mechanistic part of this question is hard to answer at the current state, different coupling profiles might arise due to factors such as interindividual differences in individual gastric frequency, subject-differences in slow wave propagation profiles (O'Grady et al., 2010), and the fed vs. fasted state of the stomach. It would be interesting to investigate whether coupling modes are stable or vary in the same participants across repeated or extended recordings. Another aspect of the question is the *functional* significance of different modes of coupling. The functional consequences of particular modes of coupling could be explored in follow-up studies. E.g., one could test whether a 2:1 modulation of alpha power by gastric phase is associated with a 2:1 relationship between hit rate and gastric phase.

Finally, we so far relied on a visual inspection of coupling modes. A possible extension would be to develop a procedures for *explicitly* testing for different modes of coupling, for example by sinusoidal fits as in Kluger et al., 2021.

9.4. Hypotheses on functions of stomach-brain coupling

While the results of this thesis do not provide a conclusive answer to the functional role of gastric-alpha coupling, several possibilities can be considered. In the following, I will present two not mutually exclusive hypotheses, which, though speculative at this point, may point to fruitful future investigations.

9.4.1.Arousal hypothesis

A first hypothesis is that gastric coupling of alpha oscillations represents a mechanism for the regulation of arousal. Such a role could be suspected based on the notion that occipital alpha power indexes neural excitability, and due to the potential access of gastric signals to neuromodulatory systems. In the following, I will consider two possible relationships between the gastric rhythm and arousal: A modulation of arousal by the gastric cycle and a modulation reflected in the strength of gastric-alpha coupling over given periods.

A modulation of arousal within the gastric cycle?

Concerning the first possibility, it might be that gastric phase exerts a rhythmic influence, with arousal varying within the gastric cycle. For example, the ICC pacemaker potentials (and possibly contractions) could be sensed by vagal afferent neurons and relayed to the parabrachial nucleus, effecting rhythmic modulations of norepinephrine levels by the projections to the locus coeruleus. Interestingly, the idea that visceral signals might influence autonomic arousal is not new, but has already been formulated for cardiac signals (Critchley and Garfinkel, 2015). The beat-to-beat operations of the heart are important to prepare for fight or flight and the processing of threat, and therefore important to be represented in the brain. This state of **cardiovascular arousal** is transmitted to the brain in a phasic manner. The cardiac cycle undergoes phases of atrial and ventricular filling and discharge of blood from the heart. With each heartbeat, blood is ejected from the ventricle and activates stretch receptors, so-called baroreceptors in the aortic arch and carotid sinuses, which induce the baroreflex controlling blood pressure by a slowing or acceleration of the heart. These phasic bursts from arterial baroreceptors might thus underpin representations of cardiovascular arousal signaled to the brain and integrated with the processing of stimuli (Garfinkel and Critchley, 2016).

The idea of a cyclic modulation of arousal by cardiac phase has received widespread empirical support. Numerous studies showed that incoming stimuli are differentially processed at systole (the period of ventricular contractions), compared to diastole (the period in which heart chambers relax and fill with blood). For example, perception of emotional stimuli is enhanced at systole compared to

diastole (Garfinkel et al., 2014). Painful stimuli at systole lead to enhanced amygdala activation (Gray et al., 2009) and higher unpleasantness ratings (Martins et al., 2009). Systole not only facilitates the processing of emotional or threatening stimuli, but also the detection of somatosensory stimuli (Edwards et al., 2009), masked visual stimuli (Pramme et al., 2014) and visual search (Pramme et al., 2016). Self-initiated actions (Kunzendorf et al., 2019) and eye movements in visual search (Galvez-Pol et al., 2019) have also been found to be locked to the systolic portion of cardiac phase.

The **functional advantage** for this phasic modulation of arousal by the cardiac cycle is still an open question. In the case of emotional stimuli, it might be that it is a mechanism that helps the brain in prioritizing threatening stimuli in states of high bodily arousal (Azzalini et al., 2019; Garfinkel and Critchley, 2016). However, the reason why non-emotional stimuli are differently processed by cardiac phase is even more elusive. In the same way, it is speculative what would be the benefit of (additional) arousal fluctuations at a slower time scale of the gastric rhythm. It could be that gastric phase prevents arousal from undergoing too extreme fluctuations and helps it to stay in a restricted range, which would be more optimal to sustain attention and performance over a prolonged period of time.

So far, evidence for a relationship between arousal and gastric phase is missing. This theory would predict that hit rate varies by the gastric cycle, which we did not find here. We also did not find pupil diameter, an index of arousal, to be modulated by gastric phase.

Arousal reflected in gastric-brain coupling?

A second possible way in which gastric coupling could modulate arousal is that instead of gastric phase, it is the *degree* of gastric-alpha coupling over several cycles and longer periods that reflects different states of arousal. In other words, it might be that how much the amplitude of alpha oscillations is modulated by gastric phase indexes different arousal states. The directionality could be either way, with higher gastric coupling indexing lower or higher arousal. On the one hand, it could be that when cortical rhythms are susceptible to being modulated by bodily rhythms, the brain is in a mode where it is more decoupled from the external environment and becomes more a listener of bodily information, being less vigilant towards incoming information from the external senses. On the other hand, the gastric rhythm could have a role in maintaining alertness to information from the external world. This could work in a similar way as speculated above, i.e. by 'pacing' fluctuations in arousal and thus keeping them in a manageable range.

With regards to empirical evidence, it is not clear whether stomach-brain coupling should be expected to **increase or decrease arousal**. Several studies link arousal with organ distension. While distension of the stomach, colon, rectum or bladder stimulates locus coeruleus and increases arousal (Elam et al., 1986; Saito et al., 2002), distension of the small intestine induces sleep (Kukorelli and Juhász, 1977). It might be that these discrepancies are explained by organ differences or the experimental manipulation. For example, Elam et al., 1986 found that the stomach stimulated locus

coeruleus only with abrubt, sudden distension. As discussed in Rebollo et al., 2021, it might thus be that sudden stomach distension increases arousal due to a link with pain, while more progressive distension signals satiation and induces sleep. Schulz et al., 2017 found that natural distension of the stomach in humans (by water ingestion) decreased the eyeblink reflex to startle stimuli and was accompanied by a decrease in heart rate. Speculatively, this would speak to the idea that arousal decreases with ecological distension and stronger afferent visceral signals.

The notion that gastric-brain coupling is stronger during lower periods of arousal would be consistent with studies by the group of Pigarev et al., who suggest that the brain and especially the visual cortex are tuned to gastrointestinal stimulation motility patterns during **sleep and drowsiness**. In monkeys, electrical stimulation of the peritoneum (the membrane lining the abdominal cavity and covering the abdominal organs) evoked responses in primary visual cortex during slow wave sleep, but this effect disappeared during wakefulness (Pigarev et al., 2006). Magnetic pulses to the stomach in monkeys induced evoked responses over occipital portions of the skull during sleep (Pigarev et al., 2008). During sleep, neurons in visual cortices in cats also changed their firing rate dependent on the phase of the duodenal cycle (Pigarev et al., 2013). The authors propose that cortical neurons processing exteroceptive information of different modalities during wakefulness switch to the processing of visceral signals when transitioning into sleep (Pigarev and Pigareva, 2012). Thus, a speculative idea is that when becoming drowsy, gastrointestinal information is gated to the sensory thalamus and cortical regions that during wakefulness are processing information from the external senses, e.g. visual regions.

Either way, if stomach-brain coupling is linked to arousal, it would predict a relationship between coupling and indices of behavioral performance such as hit rate or reaction time. Here, we found no correlation between gastric-alpha coupling and performance across subjects. It might be that there is a link *within* subjects, with periods of low vs. high hit rate or reaction time being linked with lower or higher gastric-alpha coupling. Such a link would be methodologically more difficult to address, since it is unclear over which time windows gastric-alpha coupling could be expected to share a link with performance.

9.4.2.The role of visceral monitoring for an egocentric reference frame

A recently proposed theory (Azzalini et al., 2019; Park and Tallon-Baudry, 2014) suggests that neural monitoring of visceral input plays a role in the generation of a self-centered frame of reference or 'neural subjective frame', that underlies the first-person perspective.

In the brain, information is encoded in sensory and cognitive maps each of which has its own egocentric reference frame or coordinate system (e.g. head-, limb- or gaze-centered, retinotopic, …). Other brain regions are using allocentric (world-centered), or more abstract coordinates (Figure 35). Nevertheless, conscious experience is unified, meaning that we don't perceive the world with its sensory features in a fragmented way, but as a unitary construct in which the different modalities are seamlessly

bound into each other, and experienced from a single point of view. The theory suggests that the mechanism underlying this integration could be a common input that aligns and coordinates these different frames of reference by providing a common point of reference. Visceral signals could provide such an input, as they are constantly present and reach a wide array of cortical and subcortical areas. Moreover, they are coming from the center of our body, and are independent from bodily orientation and from external sensory information. **The brain's monitoring of visceral information could thus provide the 'glue' that coregisters sensory and more abstract information into an egocentric reference frame that would play a role in any conscious experience.**

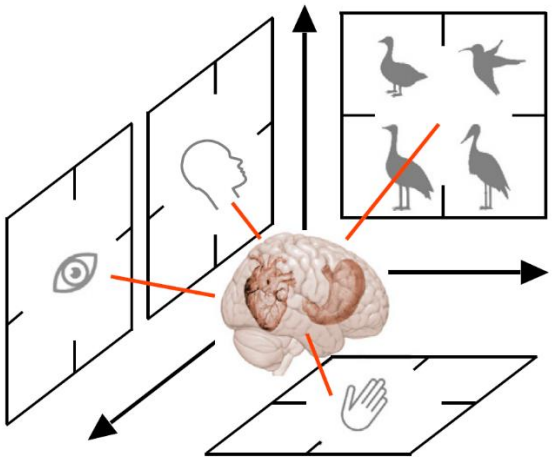

***Figure 35**: Visceral input forms an egocentric reference frame. Visual, proprioceptive, motor and more abstract representations each possess their own coordinate system. The brain's monitoring of visceral input of organs such as the stomach or the heart aligns these different systems into a unified self-centered reference frame. From Azzalini et al., 2019.*

The theory thus predicts that the brain's monitoring of visceral signals interacts with sensory or cognitive processes. Indeed, evidence for this has been found for cardiac signals. In regions overlapping with the default mode network, neural responses to heartbeats using MEG signals predict visual detection (Park et al., 2014) and encode the self-relevance of spontaneous thoughts (Babo-Rebelo et al., 2016a, 2016b). These heart-evoked responses could thus index an enhanced binding of sensory information into a neural subjective frame that produces the subjective experience.

The gastric rhythm might be another visceral input underlying the neural subjective frame. In contrast to heartbeats, we here find gastric-alpha coupling most likely in occipito-parietal regions. Gastric-alpha coupling at resting state reported in Richter et al., 2017 was source-localized not in default mode regions but more occipito-parietal regions and in the right anterior insula. It could be that there is an organ-specific dissociation, with cardiac signals targeting more default-mode regions and gastric signals targeting sensory-motor regions. Congruent with this notion, the occipital alpha rhythm is thought to underlie rhythmic sampling of visual information (VanRullen, 2016). It might be that the coupling of alpha oscillations to the gastric rhythm helps to integrate the visual modality into a common reference frame, bound together with information from the other modalities or abstract mental representations.

Again, we here could not yet provide evidence for the gastric rhythm to interact with sensory processing. As discussed above, it might be that we did not yet target the right type of stomach-brain interaction. I.e., it could be that the integration of sensory information into the neural subjective frame by gastric signals depends on the strength of gastric-alpha coupling over given time windows.

9.5. Outstanding questions and future directions

The electrical activity of the stomach and its coupling with cortical rhythms is still understudied, leaving open many questions about its functional significance for brain and behavior. In the following I will discuss some possible future directions for studying stomach-brain coupling, some of which have been presented in the article of Rebollo et al., 2021 in which I collaborated.

One of the central questions raised by the finding that gastric phase modulates cortical alpha power is on which **anatomical substrates** this coupling is based. For example, in how far is the coupling driven by the vagal vs. spinal pathway, and how is the input from the two systems combined? Moreover, it would be interesting to know whether and how input from the stomach converges with input from other viscera, such as the heart.

Several aspects revolve around the question of how gastric coupling of cortical alpha oscillations relates to **individual state and arousal**. Our study provided first evidence that coupling is present during task performance. However, whether this generalizes to different tasks settings that are more engaging (e.g., difficult or stress inducing), and that could translate into more arousing tasks, is open. Future studies could try to link stomach-brain coupling with different indices of arousal such as pupil diameter, blink rate (Chang et al., 2016; Wang et al., 2016), or the ratio of power in different frequency bands (Chang et al., 2016; Horovitz et al., 2008; Olbrich et al., 2009; Strijkstra et al., 2003). Alternatively, one could systematically compare coupling in different settings inducing different levels of arousal. Moreover, it would be highly interesting to investigate if gastric-alpha coupling is present not only during wakefulness but during sleep. This could build a link to the studies that found visual areas to process gastrointestinal information during sleep (Pigarev and Pigareva, 2012).

Furthermore, even though the gastric rhythm itself is not accessible to conscious awareness, it would be interesting to know if the unconscious coupling investigated is modulated by **conscious gastric interoception**. For example, both the conscious and unconscious processing of cardiac signals has been presumed to converge in similar cortical structures (Berntson and Khalsa, 2021; Garfinkel et al., 2014), and interoceptive attention to the heart modulates cortical responses to heartbeats (Petzschner et al., 2019). While interoception has so far been measured by awareness of cardiac signals (Critchley et al., 2004), a novel method to measure gastric interoception has recently been proposed (van Dyck et al., 2016).

More insight into the mechanisms and functions of stomach-brain coupling could be gained by **causal manipulations** of stomach activity. For example, in humans, noninvasive vagus nerve stimulation leads to changes in gastric frequency (Teckentrup et al., 2020) and amplitude (Hong et al., 2019), as well as functional connectivity in the brain (Bartolomei et al., 2016). It could thus be used in future studies to assess the vagal contributions to stomach-brain coupling. Next, newly developed devices could help to stimulate the stomach in healthy participants, without relying on gastric distension with balloon inflation, a procedure that might result in confounds with pain and stress. For example, a vibrating capsule that can easily be swallowed has recently been developed to stimulate the stomach, and which can be combined with EGG and EEG to study cortical responses to gastric stimulation (Mayeli et al., 2021).

Another avenue for future research is to study more in detail the different **characteristics of stomach activity** and how they relate to coupling with cortical fluctuations and behavior. One example are the spontaneous changes in gastric frequency over time (Koch and Stern, 2004). Another property of stomach activity that has so far not been considered on the brain imaging side is that the gastric rhythm is not spatially fixed, but propagates across the stomach (Angeli et al., 2015; Bradshaw et al., 2016; Gharibans et al., 2019; O'Grady et al., 2010). Moreover, other parameters of gastric activity such as temperature, pressure and pH-level will be easier to measure in the future (Monti et al., 2021), and it will be interesting to see how they relate to the electrical activity of the stomach and cortical coupling. Furthermore, novel ambulatory recordings for the EGG (Gharibans et al., 2018), in combination with EEG, might in future allow for prolonged acquisition of the gastric rhythm, and enable to study the evolution of stomach-brain communication over much longer periods.

Finally, though this thesis focused on the rhythm of the stomach, cortical activity might be modulated by **multiple bodily rhythms** at different time scales. For example, respiration (~0.3 Hz) has been found to entrain brain rhythms (Herrero et al., 2018; Kluger and Gross, 2020; Tort et al., 2018), with behavioral consequences (Kluger et al., 2021; Zelano et al., 2016). Further, a network of brain regions is correlated with fluctuations in heart rate (Rebollo et al., 2018). Spontaneous brain activity might also be shaped by the rhythms of other gastrointestinal organs such as the intestine (Hashimoto et al., 2015) or duodenum (Pigarev et al., 2013). Eventually, what is needed is a unifying account that encompasses all those different bodily rhythms, and explains how they shape spontaneous brain activity and cognition.

10. Appendix

10.1. Article: Brain-stomach coupling: Anatomy, functions and future avenues of research

Available online at www.sciencedirect.com

ScienceDirect

Current Opinion in Biomedical Engineering

Brain–stomach coupling: Anatomy, functions, and future avenues of research

Ignacio Rebollo[1], Nicolai Wolpert[2] and Catherine Tallon-Baudry[2]

Abstract

We have recently discovered the existence in humans of a cortical network synchronized to the gastric rhythm, a constantly generated 0.05 Hz oscillation that paces the contractions of the stomach necessary for digestion. We present here those recent results, and discuss them in the light of known ascending and descending pathways putatively connecting brain and stomach. We discuss possible functional roles of gastric–brain coupling in homeostasis, arousal, and brain function, and review possible causal manipulations of gastric afferents that could be used to test hypotheses about gastric–brain functions beyond rest as well as current methodological limitations.

Addresses

[1] German Institute of Human Nutrition Potsdam-Rehbrücke, Arthur-Scheunert-Allee 114-116, 14558, Nuthetal, Germany

[2] Laboratoire de Neurosciences Cognitives et Computationnelles, Ecole Normale Supérieure, Inserm U960, PSL University, Paris, France

Corresponding author: Rebollo, Ignacio (ignarebo@gmail.com)

Current Opinion in Biomedical Engineering 2021, **18**:100270

This review comes from a themed issue on **Neural Engineering: Brain-computer interface and functional brain imaging**

Edited by **Bin He** and **Zhongming Liu**

Received 20 November 2020, revised 12 January 2021, accepted 20 January 2021

Available online xxx

https://doi.org/10.1016/j.cobme.2021.100270

Keywords

Resting-state networks, Gastric, Gut, Electrogastrogram.

The gastric network

Signals from the inside of the body are constantly being relayed to different levels of the central nervous system, which can in turn adjust bodily function to meet actual or expected changes in the internal and external environment [1,2]. Signals from within the body, whether consciously perceived or not, can modulate perception, cognition, and emotion [3]. Here, we focus on the stomach, and review how the continuous stream of ascending gastric signals that reaches the brain, as well as descending autonomic control, contribute to the rich repertoire of intrinsic brain dynamics.

The stomach can be considered as an electrical pacemaker because it creates its own slow rhythm with a frequency around 0.05 Hz (i.e., 1 cycle every 20 s). The muscular layers of the stomach wall contain a specialized type of cell, the interstitial cells of Cajal (ICCs), which intrinsically generate and propagate slow pacemaker currents through the ICC network and coupled smooth muscles, making synapse-like connections with afferent fibers of vagal sensory neurons with cell bodies located in the nodose ganglion (Figure 1a). During digestion, these currents set the pace for gastric contractions, but pacemaker activity is present at all times, even outside digestion. Although contraction frequency is under the control of ICCs, contraction amplitude is under tight control of the central nervous system. The gastric rhythm can be measured noninvasively using the electrogastrogram [4,5], that is, with cutaneous electrodes placed on the abdomen (Figure 1b). We have recently proposed [5] a procedure for recording and analyzing EGG data to identify regular gastric rhythms in healthy participants and applied this approach to recordings in 117 healthy young participants to derive normative distributions of EGG parameters. We observed that while prolonged fasting leads to a more irregular rhythm, neither body mass index and age nor, more unexpectedly, trait anxiety has substantial relationships with EGG amplitude, frequency, or regularity.

Given the rhythmic properties of the stomach and the possibility that the gastric rhythm is detected by sensory neurons and relayed up to the neocortex, we hypothesized that it could interact with spontaneous brain activity, even in the absence of conscious perception of gastric activity. We tested whether the gastric rhythm interacts with the resting-state networks (RSNs) described using functional magnetic resonance imaging (fMRI), composed of brain regions with correlated activity and complementary functions [6]. To test this hypothesis, we recorded fMRI and EGG in healthy human participants at rest, and discovered a widespread network of cortical regions synchronized with the phase of the gastric rhythm [7]. The gastric network stands in contrast to classical RSNs in two ways. First, it does not overlap with one RSN, but encompasses portions of different classical RSNs including visual, somatosensory, and motor modalities (Figure 1c). Second, the different regions of the gastric network are connected between them and to the stomach with specific, nonzero time delays, as opposed to a classical RSN which is

Figure 1

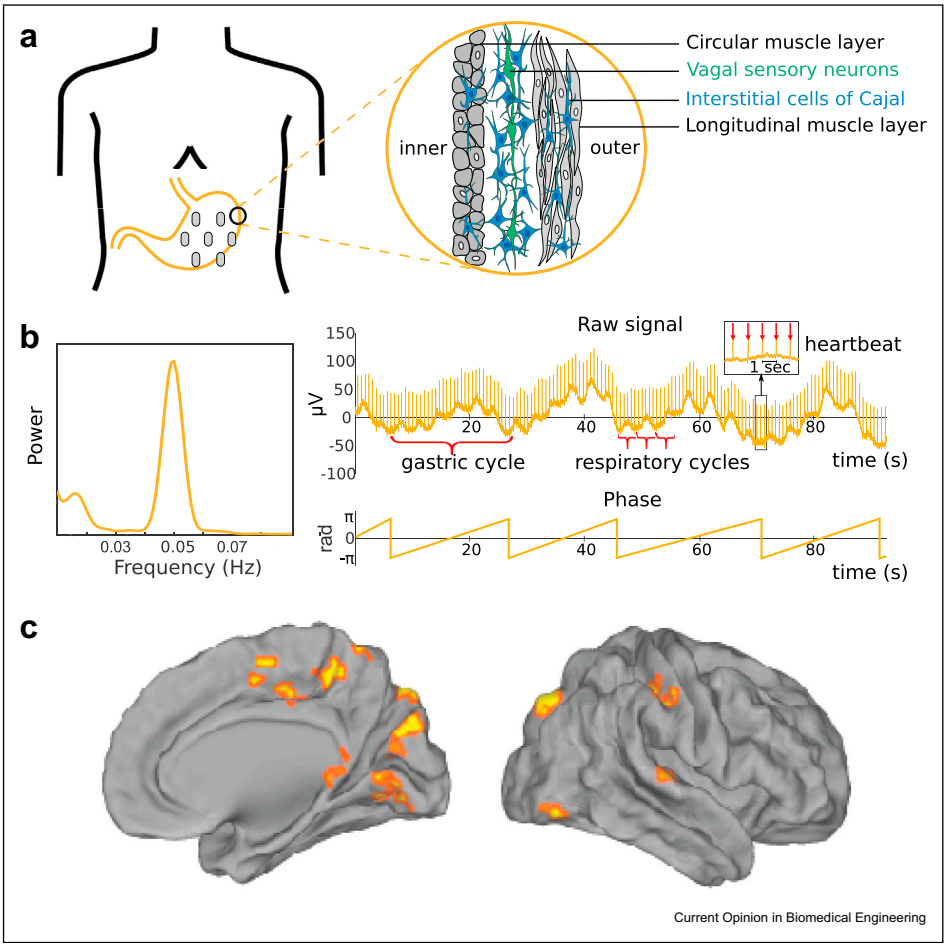

The electrogastrogram and the gastric network. **(a)-** The electrogastrogram (EGG) is recorded with cutaneous electrodes placed on the abdomen. The pacemaker cells generating the gastric rhythm, known as the interstitial cells of Cajal (ICCs, blue), are located between the circular and longitudinal muscle layers of the stomach wall. Pacemaker currents are passed through the ICC network and passively conducted into coupled muscle cells. ICCs also make synapse-like contact with afferent fibers of vagal sensory neurons (green) that can detect mechanical changes in smooth muscles. **(b)-** Left: The power spectrum from an EGG electrode typically shows a sharp peak around 0.05 Hz. Right, upper panel: Example of a raw signal from an EGG electrode. The gastric rhythm is visible as cycles of ~20 s length. Respiratory cycles are much faster (typically 3–5 s length), while heartbeats appear as transients every ~0.8 s (inset). Lower panel: Instantaneous phase of the gastric rhythm. **(c)-** Coupling between gastric phase and fMRI BOLD fluctuations reveals the gastric network. Figure redrawn from Refs. [5,7].

characterized by zero-delay connectivity. The method used to identify the gastric network (phase locking value [8]) does not allow distinguishing between ascending vs. descending regions. However, three arguments indicate a strong contribution of ascending gastric-to-brain neural transmission. First, the gastric rhythm is generated in the stomach even when is decoupled from brain [9]. Second, using magnetoencephalography and time-series causality analysis, we found that the phase of the gastric rhythm modulates the amplitude of the occipital alpha rhythm, the most salient brain rhythm in humans during quiet wakefulness [10]. Finally, the electrical stimulation of the rat stomach elicits BOLD and neural responses in the rat brain in a network showing many similarities to the human gastric network, despite known anatomical differences between the two [11–13].

The gastric network appears quite widespread in the brain, encompassing regions that are usually considered to be part of distinct functional ensembles. In the next section, we show how current knowledge on anatomical pathways might account for the spread of the gastric network.

Anatomical connections between the brain and stomach

How information from the external senses reaches the brain is relatively well understood, even if it is still an active area of research [14]. Much less is known about visceral pathways, which seem to have two outstanding characteristics. First, vision, audition, and touch all have a single specialized thalamic relay nucleus and a primary cortical sensory region. We argue that for visceral signals this view might not hold. Signals from the viscera have multiple entry points (Figure 2a) and target numerous cortical areas, notably through thalamic relays (Figure 2b). Second, visceral organs have also privileged access to the different neuromodulatory systems (Figure 2c) as well as to major behavioral and autonomic effectors, providing a continuous stream of interoceptive information that could modulate behavior and cognition [15]. We examine these two points in more detail below.

Gastric innervation reaches the brain via two pathways: vagal and spinal (Figure 2a). Vagal neurons project to the nucleus of the solitary tract (NST), the first relay and integration center of visceral signals, and then to the parabrachial nuclei (PBN), which integrate vagal and spinal information. Spinal neurons relay information to the parabrachial as well as directly to the thalamus and cortex via the spinothalamic pathway. In turn, the parabrachial nuclei relay gastric input to multiple subcortical and neuromodulatory structures, including major behavioral, autonomic, and endocrine effectors [15], such as the periaqueductal gray, the bed nuclei of the stria terminalis, the central nucleus of the amygdala, and several hypothalamic nuclei, as well as the cerebellum, striatum, and thalamus. The mapping of gastric and visceral signals at the level of the thalamus is unclear at best. Although there are direct projections from the PBN to frontal and insular cortices in rodents, in primates, PBN projections reach the cortex exclusively through the thalamus [12]. Moreover, there are reports of parabrachial–thalamic projections to unimodal and polymodal thalamic nuclei, including somatosensory [16], interoceptive [17], and visual [18] thalamic relays, but whether these projections originate from the visceral or gustatory portions of the PBN is unknown. In addition, there are direct spinothalamic projections to somatosensory thalamus [19]. Properly establishing the thalamic targets of visceral signals is thus an important unanswered research question.

Regarding the cortex, we still do not know with certainty which regions receive gastric input. Evidence from electrophysiological, neuroimaging, and anatomical tracing in other visceral organs suggest that visceral signals reach a large set of cortical regions, including primary and secondary somatosensory cortices, cingulate motor regions, primary visual cortex, insula, hippocampus, and ventromedial prefrontal cortex [17,19–23]. Viral tracers are ideal tools to tackle this question, as the

Figure 2

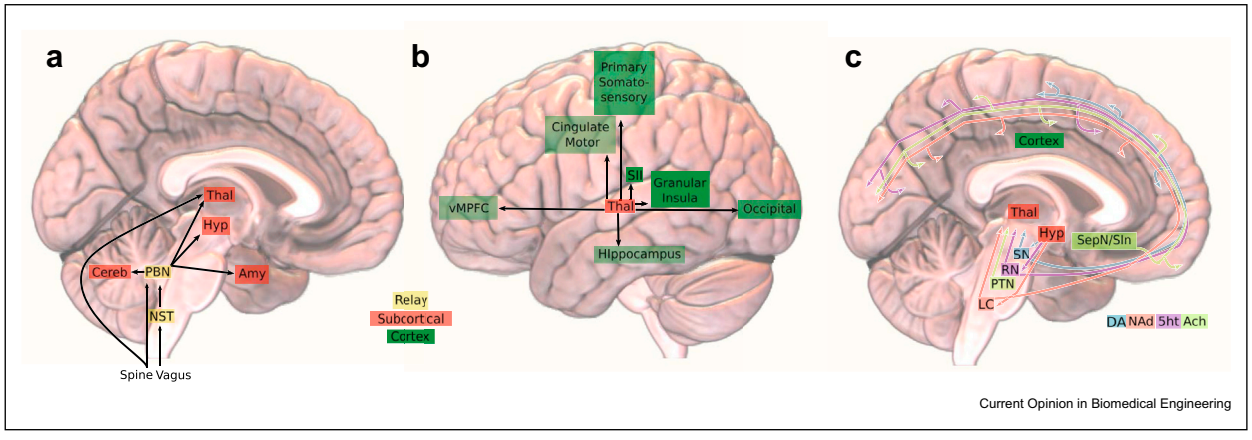

Anatomy of ascending stomach projections suggests multiple mechanisms via which gastric signals could influence brain activity. **(a)-** Overview of entry points of gastric signals in the brain through the vagus nerve and spinal cord. The vagus projects to the nucleus of the solitary tract (NST), and together with the spinal cord projects to the parabrachial nuclei (PBN). In turn, the PBN provide most inputs to other subcortical structures. In addition, the spine projects directly to the thalamus via the spinothalamic tract. **(b)-** Potential cortical targets of gastric signals, based on functional studies in humans using gastric distention [20], tracing studies of the stomach and other visceral organs in rodents and monkeys [14,18,22] and electrophysiological studies in several species [19]. Regions located on the medial wall appear in a lighter shade of green. **(c)-** Parabrachial input to neuromodulatory structures could be an additional source for gastric input modulating cortical activity. Gastric afferents reach all major neuromodulatory systems (dopaminergic, noradrenergic, histaminic, cholinergic, and glutamatergic). These neuromodulatory systems receive additional inputs from the orexinergic lateral hypothalamic nuclei, that also receive gastric input and have widespread projections to the rest of the brain. Redrawn based on previous studies [14,23]. **Abbreviations:** 5 ht, serotoninergic; Amy, amygdala; AP, area postrema; Cereb, cerebellum; DA, dopaminergic; Glu, glutamatergic; Hyp, hypothalamus; LC, locus ceruleus; Nad, noradrenergic; PAG, periaqueductal gray; PTN, pontine tegmental nuclei; SII, secondary somatosensory cortex; SepN, septal nucleus; SIn, substantia innominata; SN, substantia nigra; Thal, thalamus; vMPFC, ventromedial prefrontal cortex.

virus can travel anterogradely through several synapses. The examination of postmortem slices obtained after increasingly long survival times reveals the location of infected neurons through increasingly long pathways. Viral tracing revealed projections from the stomach to the agranular insula and perirhinal cortex [15], with longer survival times needed to detect infections in other cortical regions. Using fMRI, we have found many of the expected targets of visceral inputs, including somatosensory, cingulate motor, and visual cortex [7], indicating that whole-brain functional imaging is a useful methodology for mapping brain–gut interactions, complementing the intrinsic limitations of anatomical tracing.

A further difference between exteroceptive and visceral signals is that visceral signals seem to have privileged access to neuromodulatory structures (Figure 2c), even in the absence of conscious visceral sensations. Indeed, gastric–parabrachial inputs reach most neuromodulatory systems, as well as the orexinergic lateral hypothalamic [14], which also regulates neuromodulatory activity [15]. Thus, by its anatomical connection to neuromodulatory structures, the stomach has the potential to regulate cortical tone, attention, arousal, learning, and reward, and more generally, the integration and segregation of sensory information in the thalamus and cortex [24]. Although this interesting possibility is supported by the existence of anatomical connections, functional studies are needed to verify whether the stomach modulates neural activity in parabrachial and neuromodulatory structures. A recent study has provided conclusive evidence for a link between gastric signals and dopamine-induced reinforced behavior [25] in mice. Further anatomo-functional tracing from body to the brain in rodents is needed, as well as studies using high-field mapping in humans, to verify functional links with other neurotransmitter systems.

Descending projections from brain to stomach are also beginning to be better understood. A recent study has provided a comprehensive mapping of cortical and subcortical efferents in the rat [26], and by either cutting the vagus or leaving it intact, has allowed to distinguish between spinal and vagal cortical regions. The sympathetic/spinal system, allegedly involved in the 'fight or flight' response, arises mainly in the trunk representation of the primary motor cortex, and to a lesser extent, in primary somatosensory and secondary motor cortices. Vagal cortical neurons, allegedly involved in 'rest and digest' functions, are located mostly in anterior insula and to a lesser degree in the medial prefrontal cortex, and in the central nucleus of the amygdala. While in humans it is not easy to disentangle ascending and descending regions, it is likely that the resting-state gastric network reflects both ascending and descending influences.

Functions of the gastric network

What are the functions of the gastric network? Given that the function of the stomach is to store and process food, a link with feeding is expected. Interestingly, a recent study has found links between brain activity in the gastric network and weight loss [27]. Across 90 individuals undergoing a weight reduction lifestyle intervention, brain activity at 0.05 Hz predicted prospective weight loss, with subjects displaying reduced weight loss displaying more power at 0.05 Hz in the gastric network we identified [7]. Although this study did not measure gastric activity directly, it provides important clues linking homeostatic regulation of energy balance and brain activity in the gastric network.

Gastric inputs also appear tightly related to arousal and sleep. Increases in locus coeruleus activity, associated with increased arousal, follow abrupt changes in stomach activity in anesthetized rats [28], while progressive distension of the small intestine induces sleep in cats [29]. This pattern of results might indicate that gradual changes in the small intestine signal satiation and a decrease in arousal, but sudden, potentially painful increases gastric distention leads to sudden increases in arousal. Beyond arousal fluctuations, several reports have linked gastrointestinal activity to specific sleep stages [30,31]. This goes in line with a recent report of an increase in fMRI activity at 0.05 Hz during light sleep [32], suggesting the possibility that activity at gastric frequency during sleep might be important for energy homeostasis and the restorative functions of sleep.

Some of the brain regions where gastric–brain coupling was observed both with fMRI and MEG in humans are quite puzzling: why would the occipital cortex, devoted to vision, be part of the gastric network? Of note, these are not isolated results, because in humans, the visual cortex deactivates when the stomach is artificially distended [21], and in cats, neurons in visual cortices tightly follow the myoelectrical activity of the small intestine during non-REM sleep [31]. Several interpretations can be considered. First, the occipital cortex might be actively engaged in homeostatic functions, a hypothesis that would be supported by the direct connections between the (visceral or gustatory) parabrachial nuclei to the visual thalamic relay [18]. Second, activity in the occipital cortex might be gated by gastric inputs through neuromodulation, reflecting an overall modulation effect related to arousal. This second hypothesis would fit well with the fact that the amplitude of the alpha rhythm, a brain rhythm associated with relaxed states of wakefulness, is partially determined by the phase of the gastric rhythm [10]. Alternatively, changes due to neuromodulation could be related to a more specific process regulating the integration of interoceptive and exteroceptive signals, as well as the allocation of mental resources to the monitoring of the

body versus the external environment. Finally, it has been proposed that a distributed representation of visceral inputs across numerous brain regions could be used as a kind of "topological glue", that is a common reference point facilitating the alignment of the different coordinate systems in which information is encoded in different brain areas [3]. This fits well with the observation that the gastric network contains regions displaying topographical maps active when seeing, touching, or moving the body, as well as regions involved in transforming between egocentric and allocentric reference frame. Alternatively, gastric-brain coupling could be related to bodily self-consciousness, which has been shown to be modulated by temporal contingencies between interoceptive and exteroceptive signals [33].

Thus, gastric–brain coupling might be related to energy homeostasis and vigilance, with an intriguing role for visual cortices that suggests the possibility that the rhythm of the stomach could influence perception and cognition. Given the anatomical pathways connecting the stomach to the amygdala and to neuromodulatory structures, the stomach could also have an influence on conditioned behavior and affective state, but this hypothesis requires further evidence.

Causal manipulations of gastric activity

Causal manipulations of gastric activity in humans and animals could shed light on the mechanisms and functions of brain–stomach synchrony. Feeding is an ecological manipulation of gastric state that could potentially be used to compare brain–stomach synchrony in fasted versus fed states. Transcutaneous vagal stimulation or noninvasive stimulation of the vagus nerve is also an interesting lead as it has recently been shown to reduce gastric frequency [34] and increase its amplitude [35], but its effect on gastric–brain coupling is unknown. More invasive manipulations such as mechanical distention of the stomach with inflatable balloons have long been used in combination with functional neuroimaging to map gastric afferents in humans [21], but the stress and discomfort associated with the procedure might bias results. Another causal manipulation of the stomach is the application of magnetic pulses to the abdominal wall, which has been performed in macaques [36] to reveal cortical evoked responses to abdominal stimulations that vary in magnitude in the different stages of the sleep–wake cycle. While such a technique could in theory be applied in humans, twitches in abdominal muscles are to be expected—and might well have occurred in monkeys—which hinders the interpretability of the results.

The most drastic intervention is gastrectomy, a procedure to treat obesity or gastric cancer. Depending on the type of gastrectomy, either a portion, or extremely rarely the totality, of the stomach is removed or bypassed. The integrity of stomach–brain pathways, and remaining pacemaker properties, vary depending on the type of surgery. After sleeve gastrectomy, a procedure which reduces the stomach content to approximately 15% of its original size, patients with obesity [37] display widespread changes in gray matter, notably in occipital, insular, somatosensory, fusiform, amygdala, and hippocampal regions. Because these changes are significantly associated with postoperative weight loss, they reflect a mixture of recovery from obesity and reduced gastric input to the brain. Not that while there have been reports of functional connectivity changes after gastrectomy in obese patients [38], notably in default network regions, these results might be artifactual, as gastrectomy-induced changes in BMI are associated with changes in head movement, a major confound in functional connectivity analysis [39]. Thus, while gastrectomy could provide important insights on gastric–brain coupling, results must be interpreted carefully, and plasticity, metabolic, and artifactual changes need to be considered.

More subtle manipulations of gastric afferents are currently being developed in animal models. The method developed by Cao et al or electrically stimulating the external wall of the stomach is a great example. If combined with the severing of the vagus nerve branch innervating the stomach, this model could be used to determine the influence of vagal and spinal pathways in gastric–brain coupling. This method builds on gastric electrical stimulation (GES), an invasive therapeutic strategy for the treatment of refractory gastroparesis, that is, difficulties in gastric emptying. By electrically stimulating the stomach surface with surgically implanted electrodes, this treatments aims to reduce vomiting and nausea symptoms. The effects of GES on human brain activity has been assessed in a single study, which revealed increases in metabolic activity in thalamic and caudate nuclei after chronic GES therapy using positron emission tomography [40]. GES has also been used concomitantly with fMRI, revealing evoked responses in occipital cortices and brainstem regions in dogs [41], and the modulation of neural activity in the nucleus of the solitary tract in rats [42]. GES thus appears at an interesting manipulation for probing gastric–brain coupling in animal models as well as humans.

Back to the gut

In this article, we have mostly focused on the brain and reduced the stomach to a simple current generator. However, the stomach is a more complex organ. The gastric rhythm consists of propagating waves that travel through the stomach [43], a property that has not yet been considered on the brain imaging side. In addition, important biological information could be obtained by

measuring other gastric parameters beyond electrical activity, such as the pH of the stomach, or the regulation of gastric distention, contractions and size by the autonomic and central nervous system. Similarly, the influence of other gut organs such as the large and small intestine on intrinsic brain activity have remained largely unexplored (but see Ref. [44]). Finally, there would be great potential for ambulatory EGG recordings, a method which is still technically challenging but currently in development [45]. Potentially in conjunction with ambulatory EEG, this would allow for prolonged monitoring of gastric activity during daily activity and sleep, and open up exciting opportunities for research with clinical applications. Thus, studying brain–stomach synchrony has opened a wide avenue of research with translational potential that calls for further development of biomedical methods.

Funding

This work was supported by the European Research Council (ERC) under the European Union's Horizon 2020 research and innovation program (grant agreement No 670325, Advanced grant BRAVIUS) and by a senior fellowship of the Canadian Institute For Advance Research (CIFAR) program in Brain, Mind and Consciousness to C.T.-B., as well as by Agence Nationale de la Recherche (ANR-17-EURE-0017). IR was supported by a grant from DIM Cerveau et Pensée and Fondation Bettencourt-Schueller.

Declaration of competing interest

The authors declare that they have no known competing financial interests or personal relationships that could have appeared to influence the work reported in this paper.

References

1. Craig AD: **How do you feel? Interoception: the sense of the physiological condition of the body**. *Nat Rev Neurosci* 2002, **3**: 655–666.

2. Saper CB: **The central autonomic nervous system: conscious visceral perception and autonomic pattern generation**. *Annu Rev Neurosci* 2002, **25**:433–469.

3. Azzalini D, Rebollo I, Tallon-Baudry C: **Visceral signals shape brain dynamics and cognition**. *Trends Cogn Sci (Regul Ed)* 2019. https://doi.org/10.1016/j.tics.2019.03.007.

4. Koch KL, Stern Robert M: *Handbook of electrogastrography*. Oxford University Press; 2004.

5. Wolpert N, Rebollo I, Tallon-Baudry C: **Electrogastrography for psychophysiological research: practical considerations, analysis pipeline, and normative data in a large sample**. *Psychophysiology* 2020, e13599.
Methological recommendations for the recording of Electrogastrogram in humans and normative values in healthy participants

6. Yeo BTT, *et al.*: **The organization of the human cerebral cortex estimated by intrinsic functional connectivity**. *J Neurophysiol* 2011, **106**:1125–1165.

7. Rebollo I, Devauchelle A-D, Béranger B, Tallon-Baudry C: **Stomach-brain synchrony reveals a novel, delayed-connectivity resting-state network in humans**. *eLife Sci* 2018, **7**, e33321.
First report of gastric network in humans using resting-state fMRI and electrogastrogram

8. Lachaux J-P, Rodriguez E, Martinerie J, Varela FJ: **others, Measuring phase synchrony in brain signals**. *Hum Brain Mapp* 1999, **8**:194–208.

9. Suzuki N, Prosser CL, Dahms V: **Boundary cells between longitudinal and circular layers: essential for electrical slow waves in cat intestine**. *Am J Physiol Gastrointest Liver Physiol* 1986, **250**:G287–G294.

10. Richter CG, Babo-Rebelo M, Schwartz D, Tallon-Baudry C: **Phase-amplitude coupling at the organism level: the amplitude of spontaneous alpha rhythm fluctuations varies with the phase of the infra-slow gastric basal rhythm**. *Neuroimage* 2017, **146**:951–958.
First report that the phase of the gastric rhythm constrains the amplitude of ongoing brain oscillations

11. Cao J, *et al.*: **Gastric stimulation drives fast BOLD responses of neural origin**. *Neuroimage* 2019, **197**:200–211.
Causal model of the gastric network using fMRI and electrical stimulation of the stomach in rats

12. Pritchard TC, Hamilton RB, Norgren R: **Projections of the parabrachial nucleus in the old world monkey**. *Exp Neurol* 2000, **165**:101–117.

13. Amiez C, Petrides M: **Neuroimaging evidence of the anatomo-functional organization of the human cingulate motor areas**. *Cerebr Cortex* 2014, **24**:563–578.

14. Zhang G-W, *et al.*: **A non-canonical reticular-limbic central auditory pathway via medial septum contributes to fear conditioning**. *Neuron* 2018, **97**. 406-417.e4.

15. Rinaman L, Schwartz G: **Anterograde transneuronal viral tracing of central viscerosensory pathways in rats**. *J Neurosci* 2004, **24**:2782–2786.
A detailed anatomical tracing study of subcortical targets of gastric inputs in rats

16. Coen SJ, Hobson AR, Aziz Q. In *"Chapter 23 - processing of gastrointestinal sensory signals in the brain" in Physiology of the gastrointestinal tract*. Edited by Johnson LR, *et al.*, 5th ed., Academic Press; 2012:689–702.

17. Cechetto DF, Saper CB: **Evidence for a viscerotopic sensory representation in the cortex and thalamus in the rat**. *J Comp Neurol* 1987, **262**:27–45.

18. Erişir A, Van Horn SC, Sherman SM: **Relative numbers of cortical and brainstem inputs to the lateral geniculate nucleus**. *Proc Natl Acad Sci USA* 1997, **94**:1517–1520.

19. Dum RP, Levinthal DJ, Strick PL: **The spinothalamic system targets motor and sensory areas in the cerebral cortex of monkeys**. *J Neurosci* 2009, **29**:14223–14235.

20. Amassian VE: **Cortical representation of visceral afferents**. *J Neurophysiol* 1951, **14**:433–444.

21. Van Oudenhove I, *et al.*: **Cortical deactivations during gastric fundus distension in health: visceral pain-specific response or attenuation of 'default mode' brain function? A $H_2{}^{15}O$-PET study**. *Neuro Gastroenterol Motil* 2009, **21**: 259–271.

22. Castle M, Comoli E, Loewy A: **Autonomic brainstem nuclei are linked to the hippocampus**. *Neuroscience* 2005, **134**: 657–669.

23. Vogt BA, Derbyshire SW: **Visceral circuits and cingulate-mediated autonomic functions**. *Cingulate Neurobiol Dis* 2009: 219–236.

24. Shine JM: **Neuromodulatory influences on integration and segregation in the brain**. *Trends Cognit Sci* 2019. https://doi.org/10.1016/j.tics.2019.04.002 (June 2, 2019).

25. Han W, *et al.*: **A neural circuit for gut-induced reward**. *Cell* 2018, **175**. 665-678.e23.
An elegant study combining tracing and optogenetics demonstrating the link between gut sensory neurons and reward in mice

26. Levinthal DJ, Strick PL: **Multiple areas of the cerebral cortex influence the stomach**. *Proc Natl Acad Sci USA* 2020, **117**: 13078–13083.
First anatomical tracing study revealing the brain regions controlling the stomach in rodents

27. Levakov G, *et al.*: **Neural correlates of future weight loss reveal a possible role for brain-gastric interactions**. *Neuroimage* 2020, **224**:117403.
This fMRI study in humans suggests that weigh loss induces changes in the gastric network

28. Elam M, Thorén P, Svensson TH: **Locus coeruleus neurons and sympathetic nerves: activation by visceral afferents**. *Brain Res* 1986, **375**:117–125.

29. Kukorelli T, Juhász G: **Sleep induced by intestinal stimulation in cats**. *Physiol Behav* 1977, **19**:355–358.

30. Pigarev IN: **Neurons of visual cortex respond to visceral stimulation during slow wave sleep**. *Neuroscience* 1994, **62**: 1237–1243.

31. Pigarev IN, Bagaev VA, Levichkina EV, Fedorov GO, Busigina II: **Cortical visual areas process intestinal information during slow-wave sleep**. *Neuro Gastroenterol Motil* 2013, **25**. 268–275, e169.

32. Song C, Boly M, Tagliazucchi E, Laufs H, Tononi G: **BOLD signatures of sleep**. *bioRxiv* 2019:531186.

33. Park H-D, Blanke O: **Coupling inner and outer body for self-consciousness**. *Trends Cognit Sci* 2019, **23**:377–388.

34. Teckentrup V, *et al.*: **Non-invasive stimulation of vagal afferents reduces gastric frequency**. *Brain Stimul* 2020, **13**: 470–473.

35. Hong G-S, *et al.*: **Effect of transcutaneous vagus nerve stimulation on muscle activity in the gastrointestinal tract (transVaGa): a prospective clinical trial**. *Int J Colorectal Dis* 2019, **34**:417–422.

36. Pigarev I, *et al.*: **Visceral signals reach visual cortex during slow wave sleep: study in monkeys**. *Acta Neurobiol Exp* 2006, **66**:69–73.

37. Michaud A, *et al.*: **Neuroanatomical changes in white and grey matter after sleeve gastrectomy**. *Neuroimage* 2020, **213**: 116696.

38. Li G, *et al.*: **Bariatric surgery in obese patients reduced resting connectivity of brain regions involved with self-referential processing**. *Hum Brain Mapp* 2018, **39**:4755–4765.

39. Beyer F, *et al.*: **Weight loss reduces head motion: revisiting a major confound in neuroimaging**. *Hum Brain Mapp* 2020, **41**: 2490–2494.

40. Mccallum RW, *et al.*: **Mechanisms of symptomatic improvement after gastric electrical stimulation in gastroparetic patients**. *Neuro Gastroenterol Motil* 2010, **22**. 161-e51.

41. Yu X, *et al.*: **Antiemesis effect and brain fMRI response of gastric electrical stimulation with different parameters in dogs**. *Neuro Gastroenterol Motil* 2014, **26**:1049–1056.

42. Qin C, Sun Y, Chen JDZ, Foreman RD: **Gastric electrical stimulation modulates neuronal activity in nucleus tractus solitarii in rats**. *Auton Neurosci* 2005, **119**:1–8.

43. Allegra AB, Gharibans AA, Schamberg GE, Kunkel DC, Coleman TP: **Bayesian inverse methods for spatiotemporal characterization of gastric electrical activity from cutaneous multi-electrode recordings**. *PloS One* 2019, **14**, e0220315.

44. Hashimoto T, *et al.*: **Neural correlates of electrointestinography: insular activity modulated by signals recorded from the abdominal surface**. *Neuroscience* 2015, **289**:1–8.

45. Gharibans AA, *et al.*: **Artifact rejection methodology enables continuous, noninvasive measurement of gastric myoelectric activity in ambulatory subjects**. *Sci Rep* 2018, **8**:5019.

11. References

Addis, D.R., Wong, A.T., and Schacter, D.L. (2007). Remembering the past and imagining the future: common and distinct neural substrates during event construction and elaboration. *Neuropsychologia* 45, 1363–1377.

Agostoni, E., Chinnock, J.E., De Daly, M.B., and Murray, J.G. (1957). Functional and histological studies of the vagus nerve and its branches to the heart, lungs and abdominal viscera in the cat. *J. Physiol*. (Lond.) 135, 182–205.

Ai, L., and Ro, T. (2013). The phase of prestimulus alpha oscillations affects tactile perception. *J. Neurophysiol.* 111, 1300–1307.

Alamia, A., VanRullen, R., Pasqualotto, E., Mouraux, A., and Zenon, A. (2019). Pupil-Linked Arousal Responds to Unconscious Surprisal. *J. Neurosci.* 39, 5369–5376.

Alcaro, A., Huber, R., and Panksepp, J. (2007). Behavioral Functions of the Mesolimbic Dopaminergic System: an Affective Neuroethological Perspective. *Brain Res Rev* 56, 283–321.

Altschuler, S.M., Bao, X.M., Bieger, D., Hopkins, D.A., and Miselis, R.R. (1989). Viscerotopic representation of the upper alimentary tract in the rat: sensory ganglia and nuclei of the solitary and spinal trigeminal tracts. *J. Comp. Neurol.* 283, 248–268.

Alvarez, W.C. (1922). Action currents in stomach and intestine. *American Journal of Physiology-Legacy Content* 58, 476–493.

Amassian, V.E. (1951). Cortical representation of visceral afferents. *J. Neurophysiol.* 14, 433–444.

Amiez, C., and Petrides, M. (2014). Neuroimaging evidence of the anatomo-functional organization of the human cingulate motor areas. *Cereb. Cortex* 24, 563–578.

Anderson, J.S., Lampl, I., Gillespie, D.C., and Ferster, D. (2000). The contribution of noise to contrast invariance of orientation tuning in cat visual cortex. *Science* 290, 1968–1972.

Andrews, P.L., and Scratcherd, T. (1980). The gastric motility patterns induced by direct and reflex excitation of the vagus nerves in the anaesthetized ferret. *J. Physiol.* 302, 363–378.

Andrews, P.L., Grundy, D., and Scratcherd, T. (1980). Reflex excitation of antral motility induced by gastric distension in the ferret. *J. Physiol.* 298, 79–84.

Angeli, T.R., Cheng, L.K., Du, P., Wang, T.H.-H., Bernard, C.E., Vannucchi, M.-G., Faussone-Pellegrini, M.S., Lahr, C., Vather, R., Windsor, J.A., et al. (2015). Loss of Interstitial Cells of Cajal and Patterns of Gastric Dysrhythmia in Patients With Chronic Unexplained Nausea and Vomiting. *Gastroenterology* 149, 56-66.e5.

Apkarian, A.V. (2007). Thalamus, Visceral Representation. In R.F. Schmidt, and W.D. Willis (Ed.) *Encyclopedia of Pain* (pp. 2457–2460). Berlin, Heidelberg: Springer.

Arieli, A., Sterkin, A., Grinvald, A., and Aertsen, A. (1996). Dynamics of Ongoing Activity: Explanation of the Large Variability in Evoked Cortical Responses. *Science* 273, 1868–1871.

Aston-Jones, G., and Cohen, J.D. (2005). An integrative theory of locus coeruleus-norepinephrine function: adaptive gain and optimal performance. *Annu Rev Neurosci* 28, 403–450.

Azzalini, D., Rebollo, I., and Tallon-Baudry, C. (2019). Visceral Signals Shape Brain Dynamics and Cognition. *Trends in Cognitive Sciences* 23, 488–509.

Azzalini, D., Buot, A., Palminteri, S., and Tallon-Baudry, C. (2020). Responses to heartbeats in ventromedial prefrontal cortex contribute to subjective preference-based decisions. *BioRxiv* 776047.

Babiloni, C., Vecchio, F., Bultrini, A., Luca Romani, G., and Rossini, P.M. (2006). Pre- and poststimulus alpha rhythms are related to conscious visual perception: a high-resolution EEG study. *Cereb Cortex* 16, 1690–1700.

Babo-Rebelo, M., Wolpert, N., Adam, C., Hasboun, D., and Tallon-Baudry, C. (2016a). Is the cardiac monitoring function related to the self in both the default network and right anterior insula? *Philos Trans R Soc Lond B Biol Sci* 371.

Babo-Rebelo, M., Richter, C.G., and Tallon-Baudry, C. (2016b). Neural Responses to Heartbeats in the Default Network Encode the Self in Spontaneous Thoughts. *J Neurosci* 36, 7829–7840.

Baldaro, B., Battacchi, M.W., Trombini, G., Palomba, D., and Stegagno, L. (1990). Effects of an emotional negative stimulus on the cardiac, electrogastrographic, and respiratory responses. *Percept Mot Skills* 71, 647–655.

Baldaro, B., Battacchi, M.W., Codispoti, M., Tuozzi, G., Trombini, G., Bolzani, R., and Palomba, D. (1996). Modifications of Electrogastrographic Activity during the Viewing of Brief Film Sequences. *Percept Mot Skills* 82, 1243–1250.

Baldaro, B., Mazzetti, M., Codispoti, M., Tuozzi, G., Bolzani, R., and Trombini, G. (2001). Autonomic reactivity during viewing of an unpleasant film. *Percept Mot Skills* 93, 797–805.

Barbas, H., Saha, S., Rempel-Clower, N., and Ghashghaei, T. (2003). Serial pathways from primate prefrontal cortex to autonomic areas may influence emotional expression. *BMC Neurosci* 4, 25.

Bartley, S.H., and Bishop, Geo.H. (1932). The cortical response to stimulation of the optic nerve in the rabbit. *American Journal of Physiology-Legacy Content* 103, 159–172.

Bartolomei, F., Bonini, F., Vidal, E., Trébuchon, A., Lagarde, S., Lambert, I., McGonigal, A., Scavarda, D., Carron, R., and Benar, C.G. (2016). How does vagal nerve stimulation (VNS) change EEG brain functional connectivity? *Epilepsy Research* 126, 141–146.

Bates, J.F., and Goldman-Rakic, P.S. (1993). Prefrontal connections of medial motor areas in the rhesus monkey. *J Comp Neurol* 336, 211–228.

Bayliss, W.M., and Starling, E.H. (1899). The movements and innervation of the small intestine. *J Physiol* 24, 99–143.

Beckmann, C.F., DeLuca, M., Devlin, J.T., and Smith, S.M. (2005). Investigations into resting-state connectivity using independent component analysis. *Philos. Trans. R. Soc. Lond., B, Biol. Sci.* 360, 1001–1013.

Bentley, P., Vuilleumier, P., Thiel, C.M., Driver, J., and Dolan, R.J. (2003). Cholinergic enhancement modulates neural correlates of selective attention and emotional processing. *Neuroimage* 20, 58–70.

Benwell, C.S.Y., Tagliabue, C.F., Veniero, D., Cecere, R., Savazzi, S., and Thut, G. (2017). Prestimulus EEG Power Predicts Conscious Awareness But Not Objective Visual Performance. *ENeuro* 4.

Benwell, C.S.Y., Coldea, A., Harvey, M., and Thut, G. (2021). Low pre-stimulus EEG alpha power amplifies visual awareness but not visual sensitivity. *Eur. J. Neurosci.* 00, 1-16.

Berger, H. (1929). Über das Elektrenkephalogramm des Menschen. *Archiv f. Psychiatrie* 87, 527–570.

Berkes, P., Orbán, G., Lengyel, M., and Fiser, J. (2011). Spontaneous Cortical Activity Reveals Hallmarks of an Optimal Internal Model of the Environment. *Science* 331, 83–87.

Berntson, G.G., and Khalsa, S.S. (2021). Neural Circuits of Interoception. Trends Neurosci. 44, 17–28.

Berntson, G.G., Sarter, M., and Cacioppo, J.T. (2003). Ascending visceral regulation of cortical affective information processing. *Eur. J. Neurosci.* 18, 2103–2109.

Berridge, C.W. (2008). Noradrenergic Modulation of Arousal. *Brain Res Rev* 58, 1–17.

Berridge, K.C., and Kringelbach, M.L. (2015). Pleasure systems in the brain. *Neuron* 86, 646–664.

Berthoud, H.-R. (1996). Morphological analysis of vagal input to gastrin releasing peptide and vasoactive intestinal peptide containing neurons in the rat glandular stomach. *Journal of Comparative Neurology* 370, 61–70.

Berthoud, H.R., and Neuhuber, W.L. (2000). Functional and chemical anatomy of the afferent vagal system. *Auton Neurosci* 85, 1–17.

Berthoud, H.R., Carlson, N.R., and Powley, T.L. (1991). Topography of efferent vagal innervation of the rat gastrointestinal tract. *Am J Physiol* 260, R200-207.

Birmingham, A. (1898). The arrangement of the muscular fibres of the stomach. *Trans RAM Ireland* 16, 432.

Bishop, Geo.H. (1932). Cyclic changes in excitability of the optic pathway of the rabbit. *American Journal of Physiology-Legacy Content* 103, 213–224.

Bissonette, G.B., and Roesch, M.R. (2016). Development and function of the midbrain dopamine system: what we know and what we need to. *Genes Brain Behav* 15, 62–73.

Biswal, B., Yetkin, F.Z., Haughton, V.M., and Hyde, J.S. (1995). Functional connectivity in the motor cortex of resting human brain using echo-planar mri. Magnetic Resonance in Medicine 34, 537–541.

Blessing, W.W., Jaeger, C.B., Ruggiero, D.A., and Reis, D.J. (1982). Hypothalamic projections of medullary catecholamine neurons in the rabbit: a combined catecholamine fluorescence and HRP transport study. *Brain Res Bull* 9, 279–286.

Blevins, J.E., and Baskin, D.G. (2010). Hypothalamic-Brainstem Circuits Controlling Eating. *Forum Nutr* 63, 133–140.

Bonvallet, M., Dell, P., and Hiebel, G. (1954). Sympathetic tonus and cortical electrical activity. *Electroencephalogr Clin Neurophysiol* 6, 119–144.

Bozler, E. (1945). The action potentials of the stomach. *Am. J. Physiol.* 693–700.

Bradley, M.M., Miccoli, L., Escrig, M.A., and Lang, P.J. (2008). The pupil as a measure of emotional arousal and autonomic activation. *Psychophysiology* 45, 602–607.

Bradshaw, L.A., Cheng, L.K., Chung, E., Obioha, C.B., Erickson, J.C., Gorman, B.L., Somarajan, S., and Richards, W.O. (2016). Diabetic gastroparesis alters the biomagnetic signature of the gastric slow wave. *Neurogastroenterol. Motil.* 28, 837–848.

Brehmer, A., Rupprecht, H., and Neuhuber, W. (2010). Two submucosal nerve plexus in human intestines. *Histochem Cell Biol* 133, 149–161.

Breton-Provencher, V., and Sur, M. (2019). Active control of arousal by a locus coeruleus GABAergic circuit. *Nat Neurosci* 22, 218–228.

Brookes, S.J.H., Spencer, N.J., Costa, M., and Zagorodnyuk, V.P. (2013). Extrinsic primary afferent signalling in the gut. *Nature Reviews Gastroenterology & Hepatology* 10, 286–296.

Brown, B.H., Smallwood, R.H., Duthie, H.L., and Stoddard, C.J. (1975). Intestinal smooth muscle electrical potentials recorded from surface electrodes. *Medical & Biological Engineering* 13, 97–103.

Busch, N.A., and Herrmann, C.S. (2003). Object-load and feature-load modulate EEG in a short-term memory task. *Neuroreport* 14, 1721–1724.

Busch, N.A., Dubois, J., and VanRullen, R. (2009). The phase of ongoing EEG oscillations predicts visual perception. *J. Neurosci.* 29, 7869–7876.

Buzsáki, G. (2006). Rhythms of the brain. New York, NY, US: Oxford University Press.

Buzsáki, G., and Draguhn, A. (2004). Neuronal oscillations in cortical networks. *Science* 304, 1926–1929.

Cannon, W.B. (1898). Movements of the Stomach, Studied by Means of the Röntgen Rays. *Journal of the Boston Society of Medical Sciences* 2, 59.

Cannon, W.B. (1930). The autonomic nervous system. *The Lancet* 215, 1109–1115.

Cao, J., Lu, K.-H., Oleson, S.T., Phillips, R.J., Jaffey, D., Hendren, C.L., Powley, T.L., and Liu, Z. (2019). Gastric stimulation drives fast BOLD responses of neural origin. *NeuroImage* 197, 200–211.

Carlini, V.P., Varas, M.M., Cragnolini, A.B., Schiöth, H.B., Scimonelli, T.N., and de Barioglio, S.R. (2004). Differential role of the hippocampus, amygdala, and dorsal raphe nucleus in regulating feeding, memory, and anxiety-like behavioral responses to ghrelin. *Biochemical and Biophysical Research Communications* 313, 635–641.

Carter, M.E., Yizhar, O., Chikahisa, S., Nguyen, H., Adamantidis, A., Nishino, S., Deisseroth, K., and de Lecea, L. (2010). Tuning arousal with optogenetic modulation of locus coeruleus neurons. *Nat Neurosci* 13, 1526–1533.

Castle, M., Comoli, E., and Loewy, A.D. (2005). Autonomic brainstem nuclei are linked to the hippocampus. *Neuroscience* 134, 657–669.

Cechetto, D.F., and Saper, C.B. (1987). Evidence for a viscerotopic sensory representation in the cortex and thalamus in the rat. *J. Comp. Neurol.* 262, 27–45.

Chang, F.-Y. (2005). Electrogastrography: Basic knowledge, recording, processing and its clinical applications. *Journal of Gastroenterology and Hepatology* 20, 502–516.

Chang, C., Leopold, D.A., Schölvinck, M.L., Mandelkow, H., Picchioni, D., Liu, X., Ye, F.Q., Turchi, J.N., and Duyn, J.H. (2016). Tracking brain arousal fluctuations with fMRI. *Proc Natl Acad Sci USA* 113, 4518–4523.

Chang, H.Y., Mashimo, H., and Goyal, R.K. (2003). IV. Current concepts of vagal efferent projections to the gut. *American Journal of Physiology-Gastrointestinal and Liver Physiology* 284, G357–G366.

Chang, L.J., Yarkoni, T., Khaw, M.W., and Sanfey, A.G. (2013). Decoding the role of the insula in human cognition: functional parcellation and large-scale reverse inference. *Cereb Cortex* 23, 739–749.

Chaumon, M., and Busch, N.A. (2014). Prestimulus neural oscillations inhibit visual perception via modulation of response gain. *J Cogn Neurosci* 26, 2514–2529.

Chen, J.D., Schirmer, B.D., and McCallum, R.W. (1994). Serosal and cutaneous recordings of gastric myoelectrical activity in patients with gastroparesis. *American Journal of Physiology-Gastrointestinal and Liver Physiology* 266, G90–G98.

Cheng, L.K., Du, P., and O'Grady, G. (2013). Mapping and Modeling Gastrointestinal Bioelectricity: From Engineering Bench to Bedside. *Physiology* 28, 310–317.

Choe, A.S., Tang, B., Smith, K.R., Honari, H., Lindquist, M.A., Caffo, B.S., and Pekar, J.J. (2021). Phase-locking of resting-state brain networks with the gastric basal electrical rhythm. *PLoS One* 16, e0244756.

Christensen, J., and Torres, E.I. (1975). Three Layers of the Opossum Stomach: Responses to Nerve Stimulation. *Gastroenterology* 69, 641–648.

Christoff, K., Gordon, A.M., Smallwood, J., Smith, R., and Schooler, J.W. (2009). Experience sampling during fMRI reveals default network and executive system contributions to mind wandering. *PNAS* 106, 8719–8724.

Christoff, K., Cosmelli, D., Legrand, D., and Thompson, E. (2011). Specifying the self for cognitive neuroscience. *Trends Cogn. Sci. (Regul. Ed.)* 15, 104–112.

Coen, S.J., Hobson, A.R., and Aziz, Q. (2012). Chapter 23 - Processing of Gastrointestinal Sensory Signals in the Brain. In L. R. Johnson, F. K. Ghishan, J. D. Kaunitz, J. L. Merchant, H. M. Said, & J. D. Wood (Ed.): *Physiology of the Gastrointestinal Tract* (Fifth Edition, pp. 689–702). Academic Press.

Coizet, V., Dommett, E.J., Klop, E.M., Redgrave, P., and Overton, P.G. (2010). The parabrachial nucleus is a critical link in the transmission of short latency nociceptive information to midbrain dopaminergic neurons. *Neuroscience* 168, 263–272.

Coleski, R., and Hasler, W.L. (2004). Directed endoscopic mucosal mapping of normal and dysrhythmic gastric slow waves in healthy humans. *Neurogastroenterol. Motil.* 16, 557–565.

Cools, R. (2019). Chemistry of the Adaptive Mind: Lessons from Dopamine. *Neuron* 104, 113–131.

Cooper, N.R., Croft, R.J., Dominey, S.J.J., Burgess, A.P., and Gruzelier, J.H. (2003). Paradox lost? Exploring the role of alpha oscillations during externally vs. internally directed attention and the implications for idling and inhibition hypotheses. *Int J Psychophysiol* 47, 65–74.

Cordes, D., Haughton, V.M., Arfanakis, K., Wendt, G.J., Turski, P.A., Moritz, C.H., Quigley, M.A., and Meyerand, M.E. (2000). Mapping functionally related regions of brain with functional connectivity MR imaging. *AJNR Am J Neuroradiol* 21, 1636–1644.

Coste, C.P., and Kleinschmidt, A. (2016). Cingulo-opercular network activity maintains alertness. *NeuroImage* 128, 264–272.

Craig, A.D. (2002). How do you feel? Interoception: the sense of the physiological condition of the body. *Nat. Rev. Neurosci.* 3, 655–666.

Craig, A.D., Bushnell, M.C., Zhang, E.T., and Blomqvist, A. (1994). A thalamic nucleus specific for pain and temperature sensation. *Nature* 372, 770–773.

Critchley, H.D., and Garfinkel, S.N. (2015). Interactions between visceral afferent signaling and stimulus processing. *Front Neurosci* 9.

Critchley, H.D., and Harrison, N.A. (2013). Visceral influences on brain and behavior. *Neuron* 77, 624–638.

Critchley, H.D., Wiens, S., Rotshtein, P., Öhman, A., and Dolan, R.J. (2004). Neural systems supporting interoceptive awareness. *Nat Neurosci* 7, 189–195.

Cul, A.D., Baillet, S., and Dehaene, S. (2007). Brain Dynamics Underlying the Nonlinear Threshold for Access to Consciousness. *PLOS Biology* 5, e260.

Davies, D., and Parasuraman, R. (1982). The psychology of vigilance. London: Academic Press.

Davis, R.C., Berry, F., and Paden, A. (1969). The effect of certain tasks and conditions on gastrointestinal activity. Indiana Univer. at Bloomington.

Deco, G., Hagmann, P., Hudetz, A.G., and Tononi, G. (2014). Modeling resting-state functional networks when the cortex falls asleep: local and global changes. *Cereb Cortex* 24, 3180–3194.

Deen, B., Pitskel, N.B., and Pelphrey, K.A. (2011). Three systems of insular functional connectivity identified with cluster analysis. *Cereb Cortex* 21, 1498–1506.

Dehaene, S. (1993). Temporal Oscillations in Human Perception. *Psychological Science* 4, 264–270.

Dijk, H. van, Schoffelen, J.-M., Oostenveld, R., and Jensen, O. (2008). Prestimulus Oscillatory Activity in the Alpha Band Predicts Visual Discrimination Ability. *J. Neurosci.* 28, 1816–1823.

Dosenbach, N.U.F., Visscher, K.M., Palmer, E.D., Miezin, F.M., Wenger, K.K., Kang, H.C., Burgund, E.D., Grimes, A.L., Schlaggar, B.L., and Petersen, S.E. (2006). A core system for the implementation of task sets. *Neuron* 50, 799–812.

Dosenbach, N.U.F., Fair, D.A., Miezin, F.M., Cohen, A.L., Wenger, K.K., Dosenbach, R.A.T., Fox, M.D., Snyder, A.Z., Vincent, J.L., Raichle, M.E., et al. (2007). Distinct brain networks for adaptive and stable task control in humans. *PNAS* 104, 11073–11078.

Downman, C.B.B. (1951). Cerebral destination of splanchnic afferent impulses. *J. Physiol.* (Lond.) 113, 434–441.

Du, P., O'Grady, G., Cheng, L.K., and Pullan, A.J. (2010). A Multiscale Model of the Electrophysiological Basis of the Human Electrogastrogram. *Biophysical Journal* 99, 2784–2792.

Dugué, L., Marque, P., and VanRullen, R. (2011). The phase of ongoing oscillations mediates the causal relation between brain excitation and visual perception. *J. Neurosci.* 31, 11889–11893.

Dum, R.P., and Strick, P.L. (1991). The origin of corticospinal projections from the premotor areas in the frontal lobe. *J. Neurosci.* 11, 667–689.

Dum, R.P., Levinthal, D.J., and Strick, P.L. (2009). The spinothalamic system targets motor and sensory areas in the cerebral cortex of monkeys. *J. Neurosci.* 29, 14223–14235.

Dum, R.P., Levinthal, D.J., and Strick, P.L. (2016). Motor, cognitive, and affective areas of the cerebral cortex influence the adrenal medulla. *Proc Natl Acad Sci U S A* 113, 9922–9927.

van Dyck, Z., Vögele, C., Blechert, J., Lutz, A.P.C., Schulz, A., and Herbert, B.M. (2016). The Water Load Test As a Measure of Gastric Interoception: Development of a Two-Stage Protocol and Application to a Healthy Female Population. *PLOS ONE* 11, e0163574.

Eason, R.G., Harter, M.R., and White, C.T. (1969). Effects of attention and arousal on visually evoked cortical potentials and reaction time in man. *Physiology & Behavior* 4, 283–289.

Edgington, E.S. (1972). An additive method for combining probability values from independent experiments. *The Journal of Psychology: Interdisciplinary and Applied* 80, 351–363.

Edwards, L., Ring, C., McIntyre, D., Winer, J.B., and Martin, U. (2009). Sensory detection thresholds are modulated across the cardiac cycle: Evidence that cutaneous sensibility is greatest for systolic stimulation. *Psychophysiology* 46, 252–256.

Einhäuser, W., Stout, J., Koch, C., and Carter, O. (2008). Pupil dilation reflects perceptual selection and predicts subsequent stability in perceptual rivalry. *Proc Natl Acad Sci U S A* 105, 1704–1709.

Elam, M., Thorén, P., and Svensson, T.H. (1986). Locus coeruleus neurons and sympathetic nerves: Activation by visceral afferents. *Brain Research* 375, 117–125.

Ercolani, M., Baldaro, B., Comani, G., De Portu, I., Rossi, N., and Trombini, G. (1982). Evolution de la motiliti gastrique, de la frequence cardiaque et ventilatoire de sujets sains pendant I'execution d'epreuves de performance. *Aggressologie* 23, 263–267.

Ercolani, M., Baldaro, B., and Trombini, G. (1989). Effects of Two Tasks and Two Levels of Difficulty upon Surface Electrogastrograms. *Percept Mot Skills* 69, 99-110.

Ergenoglu, T., Demiralp, T., Bayraktaroglu, Z., Ergen, M., Beydagi, H., and Uresin, Y. (2004). Alpha rhythm of the EEG modulates visual detection performance in humans. *Brain Res Cogn Brain Res* 20, 376–383.

Erişir, A., Van Horn, S.C., Bickford, M.E., and Sherman, S.M. (1997a). Immunocytochemistry and distribution of parabrachial terminals in the lateral geniculate nucleus of the cat: a comparison with corticogeniculate terminals. *J Comp Neurol* 377, 535–549.

Erişir, A., Van Horn, S.C., and Sherman, S.M. (1997b). Relative numbers of cortical and brainstem inputs to the lateral geniculate nucleus. *Proc. Natl. Acad. Sci. U.S.A.* 94, 1517–1520.

Esterman, M., Noonan, S.K., Rosenberg, M., and Degutis, J. (2013). In the zone or zoning out? Tracking behavioral and neural fluctuations during sustained attention. *Cereb. Cortex* 23, 2712–2723.

Esterman, M., Rosenberg, M.D., and Noonan, S.K. (2014). Intrinsic Fluctuations in Sustained Attention and Distractor Processing. *J Neurosci* 34, 1724–1730.

Evrard, H.C. (2018). Von Economo and fork neurons in the monkey insula, implications for evolution of cognition. *Current Opinion in Behavioral Sciences* 21, 182–190.

Evrard, H.C. (2019). The Organization of the Primate Insular Cortex. *Front Neuroanat* 13.

Fahrenfort, J.J., Scholte, H.S., and Lamme, V. a. F. (2007). Masking disrupts reentrant processing in human visual cortex. *J Cogn Neurosci* 19, 1488–1497.

Familoni, B.O., Kingma, Y.J., and Bowes, K.L. (1987). Study of transcutaneous and intraluminal measurement of gastric electrical activity in humans. *Medical & Biological Engineering & Computing* 25, 397–402.

Fisher, R.A. (1938). Statistical methods for research workers. Edinburgh: Oliver and Boyd.

Fogel, R., Zhang, X., and Renehan, W.E. (1996). Relationships between the morphology and function of gastric and intestinal distention-sensitive neurons in the dorsal motor nucleus of the vagus. *J Comp Neuro*l 364, 78–91.

Foley, J.O. (1948). The functional types of nerve fibers and their numbers in the great splanchnic nerve. *The Anatomical Record*, 100, 766–767.

Forsythe, P., Bienenstock, J., and Kunze, W.A. (2014). Vagal pathways for microbiome-brain-gut axis communication. *Adv Exp Med Biol* 817, 115–133.

Fortenbaugh, F.C., Rothlein, D., McGlinchey, R., DeGutis, J., and Esterman, M. (2018). Tracking behavioral and neural fluctuations during sustained attention: A robust replication and extension. *Neuroimage* 171, 148–164.

Fossati, P., Hevenor, S.J., Graham, S.J., Grady, C., Keightley, M.L., Craik, F., and Mayberg, H. (2003). In Search of the Emotional Self: An fMRI Study Using Positive and Negative Emotional Words. *AJP* 160, 1938–1945.

Fox, M.D., and Raichle, M.E. (2007). Spontaneous fluctuations in brain activity observed with functional magnetic resonance imaging. *Nat. Rev. Neurosci.* 8, 700–711.

Fox, M.D., Snyder, A.Z., Vincent, J.L., Corbetta, M., Essen, D.C.V., and Raichle, M.E. (2005). The human brain is intrinsically organized into dynamic, anticorrelated functional networks. *PNAS* 102, 9673–9678.

Fox, M.D., Corbetta, M., Snyder, A.Z., Vincent, J.L., and Raichle, M.E. (2006). Spontaneous neuronal activity distinguishes human dorsal and ventral attention systems. *PNAS* 103, 10046–10051.

Fries, P. (2015). Rhythms For Cognition: Communication Through Coherence. *Neuron* 88, 220–235.

Fritsch, H., and Kühnel, W. (2008). Color Atlas of Human Anatomy: Internal organs. Volume 2 (Thieme).

Fuchs, S.A., Edinger, H.M., and Siegel, A. (1985). The role of the anterior hypothalamus in affective defense behavior elicited from the ventromedial hypothalamus of the cat. *Brain Res* 330, 93–107.

Fuller, P.M., Sherman, D., Pedersen, N.P., Saper, C.B., and Lu, J. (2011). Reassessment of the structural basis of the ascending arousal system. *J Comp Neurol* 519, 933–956.

Furness, J.B. (2006). The enteric nervous system. Oxfort, UK: Blackwell Publishing.

Furness, J.B. (2012). The enteric nervous system and neurogastroenterology. *Nat Rev Gastroenterol Hepatol* 9, 286–294.

Furness, J.B., Rivera, L.R., Cho, H.-J., Bravo, D.M., and Callaghan, B. (2013). The gut as a sensory organ. *Nat Rev Gastroenterol Hepatol* 10, 729–740.

Furness, J.B., Callaghan, B.P., Rivera, L.R., and Cho, H.-J. (2014). The enteric nervous system and gastrointestinal innervation: integrated local and central control. *Adv Exp Med Biol* 817, 39–71.

Galvez-Pol, A., McConnell, R., and Kilner, J.M. (2019). Active sampling in visual search is coupled to the cardiac cycle. *Cognition* 196, 104149.

Garfinkel, S.N., and Critchley, H.D. (2016). Threat and the Body: How the Heart Supports Fear Processing. *Trends Cogn. Sci. (Regul. Ed.)* 20, 34–46.

Garfinkel, S.N., Minati, L., Gray, M.A., Seth, A.K., Dolan, R.J., and Critchley, H.D. (2014). Fear from the heart: sensitivity to fear stimuli depends on individual heartbeats. *J. Neurosci.* 34, 6573–6582.

de Gee, J.W., Colizoli, O., Kloosterman, N.A., Knapen, T., Nieuwenhuis, S., and Donner, T.H. (2017). Dynamic modulation of decision biases by brainstem arousal systems. *ELife* 6, e23232.

Geeraerts, B., Oudenhove, L.V., Dupont, P., Vanderghinste, D., Bormans, G., Laere, K.V., and Tack, J. (2011). Different regional brain activity during physiological gastric distension compared to balloon distension: a H215O-PET study. *Neurogastroenterology & Motility* 23, 533-e203.

Geldof, H., Schee, E.J. van der, Smout, A.J.P.M., Merwe, J.P. van de, Blankenstein, M. van, and Grashuis, J.L. (1989). Myoelectrical Activity of the Stomach in Gastric Ulcer Patients: An Electrogastrographic Study. *Neurogastroenterology & Motility* 1, 122–130.

Gershon, M.D. (2010). Developmental determinants of the independence and complexity of the enteric nervous system. *Trends Neurosci* 33, 446–456.

Gharibans, A.A., Smarr, B.L., Kunkel, D.C., Kriegsfeld, L.J., Mousa, H.M., and Coleman, T.P. (2018). Artifact Rejection Methodology Enables Continuous, Noninvasive Measurement of Gastric Myoelectric Activity in Ambulatory Subjects. *Sci Rep* 8, 1–12.

Gharibans, A.A., Coleman, T.P., Mousa, H., and Kunkel, D.C. (2019). Spatial Patterns From High-Resolution Electrogastrography Correlate With Severity of Symptoms in Patients With Functional Dyspepsia and Gastroparesis. *Clin. Gastroenterol. Hepatol* 17, 2668-2677.

Giambra LM (1993) The influence of aging on spontaneous shifts of attention from external stimuli to the contents of consciousness. *Exp Gerontol* 28:485– 492.

Gianaros, P.J., Quigley, K.S., and Mordkoff, J.T. (2001). Gastric myoelectrical and autonomic cardiac reactivity to laboratory stressors. *Psychophysiology* 38, 540-547.

Gilden, D.L. (2001). Cognitive emissions of 1/f noise. *Psychol Rev* 108, 33–56.

Gilden, D.L., and Wilson, S.G. (1995a). On the nature of streaks in signal detection. *Cognitive Psychology* 28, 17–64.

Gilden, D.L., and Wilson, S.G. (1995b). Streaks in skilled performance. *Psychon Bull Rev* 2, 260–265.

Gilden, D.L., Thornton, T., and Mallon, M.W. (1995). 1/f noise in human cognition. *Science* 267, 1837–1839.

Gillis, R.A., Quest, J.A., Pagani, F.D., and Norman, W.P. (2011). Control centers in the central nervous system for regulating gastrointestinal motility. In J. D. Wood (Ed.): *Handbook of physiology. The gastrointestinal system. Motility and circulation.* (Vol. 1, pp. 621-683). Bethesda, MD: Americal Physiological Society.

Glasser, M.F., Coalson, T.S., Robinson, E.C., Hacker, C.D., Harwell, J., Yacoub, E., Ugurbil, K., Andersson, J., Beckmann, C.F., Jenkinson, M., et al. (2016). A multi-modal parcellation of human cerebral cortex. Nature 536, 171–178.

Goldman, R.I., Stern, J.M., Engel, J., and Cohen, M.S. (2002). Simultaneous EEG and fMRI of the alpha rhythm. *Neuroreport* 13, 2487–2492.

Gonzalez Andino, S.L., Michel, C.M., Thut, G., Landis, T., and Grave de Peralta, R. (2005). Prediction of response speed by anticipatory high-frequency (gamma band) oscillations in the human brain. *Hum Brain Mapp* 24, 50–58.

Gordon, E.M., Breeden, A.L., Bean, S.E., and Vaidya, C.J. (2012). Working memory-related changes in functional connectivity persist beyond task disengagement. *Hum Brain Mapp* 35, 1004–1017.

Gray, M.A., Rylander, K., Harrison, N.A., Wallin, B.G., and Critchley, H.D. (2009). Following One's Heart: Cardiac Rhythms Gate Central Initiation of Sympathetic Reflexes. *J. Neurosci.* 29, 1817–1825.

Greicius, M.D., Krasnow, B., Reiss, A.L., and Menon, V. (2003). Functional connectivity in the resting brain: a network analysis of the default mode hypothesis. *Proc. Natl. Acad. Sci. U.S.A.* 100, 253–258.

Grundy, D. (2002). Neuroanatomy of visceral nociception: vagal and splanchnic afferent. *Gut* 51, i2–i5.

Guillery, R.W., and Sherman, S.M. (2002). Thalamic relay functions and their role in corticocortical communication: generalizations from the visual system. *Neuron* 33, 163–175.

Haegens, S., Nácher, V., Luna, R., Romo, R., and Jensen, O. (2011). α-Oscillations in the monkey sensorimotor network influence discrimination performance by rhythmical inhibition of neuronal spiking. *Proc. Natl. Acad. Sci. U.S.A.* 108, 19377–19382.

Hahn, B., Ross, T.J., and Stein, E.A. (2007). Cingulate activation increases dynamically with response speed under stimulus unpredictability. *Cereb Cortex* 17, 1664–1671.

Hamaguchi, T., Kano, M., Rikimaru, H., Kanazawa, M., Itoh, M., Yanai, K., and Fukudo, S. (2004). Brain activity during distention of the descending colon in humans. *Neurogastroenterol Motil* 16, 299–309.

Hamilton, J.W., Bellahsene, B.E., Reichelderfer, M., Webster, J.G., and Bass, P. (1986). Human electrogastrograms: Comparison of surface and mucosal recordings. *Digestive Diseases and Sciences* 31, 33–39.

Han, W., Tellez, L.A., Perkins, M.H., Perez, I.O., Qu, T., Ferreira, J., Ferreira, T.L., Quinn, D., Liu, Z.-W., Gao, X.-B., et al. (2018). A Neural Circuit for Gut-Induced Reward. *Cell* 175, 665-678.e23.

Hanslmayr, S., Klimesch, W., Sauseng, P., Gruber, W., Doppelmayr, M., Freunberger, R., and Pecherstorfer, T. (2005). Visual discrimination performance is related to decreased alpha amplitude but increased phase locking. *Neurosci. Lett.* 375, 64–68.

Hanslmayr, S., Aslan, A., Staudigl, T., Klimesch, W., Herrmann, C.S., and Bäuml, K.-H. (2007). Prestimulus oscillations predict visual perception performance between and within subjects. Neuroimage 37, 1465–1473.

Hanslmayr, S., Gross, J., Klimesch, W., and Shapiro, K.L. (2011). The role of alpha oscillations in temporal attention. *Brain Research Reviews* 67, 331–343.

Hardaway, J.A., Halladay, L.R., Mazzone, C.M., Pati, D., Bloodgood, D.W., Kim, M., Jensen, J., DiBerto, J.F., Boyt, K.M., Shiddapur, A., et al. (2019). Central Amygdala Prepronociceptin-Expressing Neurons Mediate Palatable Food Consumption and Reward. *Neuron* 102, 1037-1052.e7.

Harris, A.M., Dux, P.E., and Mattingley, J.B. (2018). Detecting Unattended Stimuli Depends on the Phase of Prestimulus Neural Oscillations. *J Neurosci* 38, 3092–3101.

Harrison, N.A., Gray, M.A., Gianaros, P.J., and Critchley, H.D. (2010). The Embodiment of Emotional Feelings in the Brain. *J Neurosci* 30, 12878–12884.

Hashimoto, T., Kitajo, K., Kajihara, T., Ueno, K., Suzuki, C., Asamizuya, T., and Iriki, A. (2015). Neural correlates of electrointestinography: insular activity modulated by signals recorded from the abdominal surface. *Neuroscience* 289, 1–8.

Hausken, T., Gilja, O.H., Odegaard, S., and Berstad, A. (1998). Flow across the human pylorus soon after ingestion of food, studied with duplex sonography. Effect of glyceryl trinitrate. *Scand J Gastroenterol* 33, 484–490.

Herrero, J.L., Khuvis, S., Yeagle, E., Cerf, M., and Mehta, A.D. (2018). Breathing above the brain stem: volitional control and attentional modulation in humans. *J. Neurophysiol.* 119, 145–159.

Hervé-Minvielle, A., and Sara, S.J. (1995). Rapid habituation of auditory responses of locus coeruleus cells in anaesthetized and awake rats. *Neuroreport* 6, 1363–1368.

Hesselmann, G., Kell, C.A., and Kleinschmidt, A. (2008a). Ongoing Activity Fluctuations in hMT+ Bias the Perception of Coherent Visual Motion. *J. Neurosci.* 28, 14481–14485.

Hesselmann, G., Kell, C.A., Eger, E., and Kleinschmidt, A. (2008b). Spontaneous local variations in ongoing neural activity bias perceptual decisions. *Proc. Natl. Acad. Sci. U.S.A.* 105, 10984–10989.

Hinder, R.A., and Kelly, K.A. (1977). Human gastric pacesetter potential. Site of origin, spread, and response to gastric transection and proximal gastric vagotomy. *Am. J. Surg.* 133, 29–33.

Hinds, O., Thompson, T.W., Ghosh, S., Yoo, J.J., Whitfield-Gabrieli, S., Triantafyllou, C., and Gabrieli, J.D.E. (2013). Roles of default-mode network and supplementary motor area in human vigilance performance: evidence from real-time fMRI. *J Neurophysiol* 109, 1250–1258.

Hirst, G.D.S., and Edwards, F.R. (2006). Electrical events underlying organized myogenic contractions of the guinea pig stomach: Descending propagation of gastric slow waves. *The Journal of Physiology* 576, 659–665.

Holcman, D., and Tsodyks, M. (2006). The Emergence of Up and Down States in Cortical Networks. *PLOS Computational Biology* 2, e23.

Holst, M.C., Kelly, J.B., and Powley, T.L. (1997). Vagal preganglionic projections to the enteric nervous system characterized with Phaseolus vulgaris-leucoagglutinin. *J Comp Neurol* 381, 81–100.

Holzer, P. (2006). Efferent-like roles of afferent neurons in the gut: blood flow regulation and tissue protection. *Auton Neurosci* 125, 70–75.

Holzl, R., Schroder, G., and Kiefer, L. (1979). Indirect gastrointestinal motihty measurement for use in experimental psychosomatics: a new method and some data. *Behavior Analysis and Modification* 3, 77–97.

Hong, G.-S., Pintea, B., Lingohr, P., Coch, C., Randau, T., Schaefer, N., Wehner, S., Kalff, J.C., and Pantelis, D. (2019). Effect of transcutaneous vagus nerve stimulation on muscle activity in the gastrointestinal tract (transVaGa): a prospective clinical trial. *Int J Colorectal Dis* 34, 417–422.

Hornby, P.J., and Wade, P.R. (2011). Central Control of Gastrointestinal Function. Oxford University Press.

Hornung, J.-P. (2003). The human raphe nuclei and the serotonergic system. *J Chem Neuroanat* 26, 331–343.

Horovitz, S.G., Fukunaga, M., de Zwart, J.A., van Gelderen, P., Fulton, S.C., Balkin, T.J., and Duyn, J.H. (2008). Low frequency BOLD fluctuations during resting wakefulness and light sleep: a simultaneous EEG-fMRI study. *Hum Brain Mapp* 29, 671–682.

Hu, S., Grant, W.F., Stern, R.M., and Koch, K.L. (1991). Motion sickness severity and physiological correlates during repeated exposures to a rotating optokinetic drum. *Aviat Space Environ Med* 62, 308–314.

Huk, A., Bonnen, K., and He, B.J. (2018). Beyond Trial-Based Paradigms: Continuous Behavior, Ongoing Neural Activity, and Natural Stimuli. *J Neurosci* 38, 7551–7558.

Hutchins, K.D., Martino, A.M., and Strick, P.L. (1988). Corticospinal projections from the medial wall of the hemisphere. *Experimental Brain Research* 71, 667–672.

Iemi, L., and Busch, N.A. (2018). Moment-to-Moment Fluctuations in Neuronal Excitability Bias Subjective Perception Rather than Strategic Decision-Making. *ENeuro* 5.

Iemi, L., Chaumon, M., Crouzet, S.M., and Busch, N.A. (2017). Spontaneous Neural Oscillations Bias Perception by Modulating Baseline Excitability. *J Neurosci* 37, 807–819.

Ito, S.-I. (2002). Visceral region in the rat primary somatosensory cortex identified by vagal evoked potential. *J. Comp. Neurol*. 444, 10–24.

Ito, S.-I., and Craig, A.D. (Bud) (2003). Vagal Input to Lateral Area 3a in Cat Cortex. *Journal of Neurophysiology* 90, 143–154.

Jensen, O., and Mazaheri, A. (2010). Shaping Functional Architecture by Oscillatory Alpha Activity: Gating by Inhibition. *Front Hum Neurosci* 4, 186.

Jensen, O., Gelfand, J., Kounios, J., and Lisman, J.E. (2002). Oscillations in the alpha band (9-12 Hz) increase with memory load during retention in a short-term memory task. *Cerebral Cortex* 12, 877–882.

Johnson, J.S., Hamidi, M., and Postle, B.R. (2010). Using EEG to explore how rTMS produces its effects on behavior. *Brain Topogr* 22, 281–293.

Jones, B.E. (2020). Arousal and sleep circuits. *Neuropsychopharmacology* 45, 6–20.

Ju, G., Liu, S., and Tao, J. (1986). Projections from the hypothalamus and its adjacent areas to the posterior pituitary in the rat. *Neuroscience* 19, 803–828.

Juhász, G., and Kukorelli, T. (1973). EEG-synchronizing effect of small intestinal and splanchnic nerve stimulation. *Acta physiol hung* 340–341.

Kaiser, M., Senkowski, D., Busch, N.A., Balz, J., and Keil, J. (2019). Single trial prestimulus oscillations predict perception of the sound-induced flash illusion. *Scientific Reports* 9, 5983.

Kanoski, S.E., and Grill, H.J. (2017). Hippocampus contributions to food intake control: mnemonic, neuroanatomical, and endocrine mechanisms. *Biol Psychiatry* 81, 748–756.

Kello, C.T., Brown, G.D.A., Ferrer-I-Cancho, R., Holden, J.G., Linkenkaer-Hansen, K., Rhodes, T., and Van Orden, G.C. (2010). Scaling laws in cognitive sciences. *Trends Cogn. Sci. (Regul. Ed.)* 14, 223–232.

Kelly, K.A. (1980). Gastric emptying of liquids and solids: roles of proximal and distal stomach. *Am J Physiol* 239, G71-76.

Kelly, K.A., Code, C.F., and Elveback, L.R. (1969). Patterns of canine gastric electrical activity. *American Journal of Physiology-Legacy Content* 239, G71-G76.

Kelly, S.P., Gomez-Ramirez, M., and Foxe, J.J. (2009). The strength of anticipatory spatial biasing predicts target discrimination at attended locations: a high-density EEG study. *Eur. J. Neurosci.* 30, 2224–2234.

Kenet, T., Bibitchkov, D., Tsodyks, M., Grinvald, A., and Arieli, A. (2003). Spontaneously emerging cortical representations of visual attributes. *Nature* 425, 954–956.

Kern, M., Aertsen, A., Schulze-Bonhage, A., and Ball, T. (2013). Heart cycle-related effects on event-related potentials, spectral power changes, and connectivity patterns in the human ECoG. *Neuroimage* 81, 178–190.

Klimesch, W., Sauseng, P., and Hanslmayr, S. (2007). EEG alpha oscillations: the inhibition-timing hypothesis. *Brain Res Rev* 53, 63–88.

Kloosterman, N.A., Meindertsma, T., van Loon, A.M., Lamme, V.A.F., Bonneh, Y.S., and Donner, T.H. (2015). Pupil size tracks perceptual content and surprise. *Eur J Neurosci* 41, 1068–1078.

Kluger, D.S., and Gross, J. (2020). Respiration modulates oscillatory neural network activity at rest. *BioRxiv* 2020.04.23.057216.

Kluger, D.S., Balestrieri, E., Busch, N.A., and Gross, J. (2021). Respiration aligns perception with neural excitability. *BioRxiv* 2021.03.25.436938.

Klüppel, M., Huizinga, J.D., Malysz, J., and Bernstein, A. (1998). Developmental origin and kit-dependent development of the interstitial cells of cajal in the mammalian small intestine. *Developmental Dynamics* 211, 60–71.

Koch, Eb. (1932). Die Irradiation der Pressoreceptorischen Kreislaufreflexe. *Klin Wochenschr* 11, 225–227.

Koch, K.L., and Stern, R.M. (2004). Handbook of Electrogastrography. New York, NY: Oxford University Press.

Konishi, M., Brown, K., Battaglini, L., and Smallwood, J. (2017). When attention wanders: Pupillometric signatures of fluctuations in external attention. *Cognition* 168, 16–26.

van der Kooy, D., Koda, L.Y., McGinty, J.F., Gerfen, C.R., and Bloom, F.E. (1984). The organization of projections from the cortex, amygdala, and hypothalamus to the nucleus of the solitary tract in rat. *J Comp Neurol* 224, 1–24.

Koyama, M.S., Kelly, C., Shehzad, Z., Penesetti, D., Castellanos, F.X., and Milham, M.P. (2010). Reading networks at rest. *Cereb Cortex* 20, 2549–2559.

Kressel, M., Berthoud, H.R., and Neuhuber, W.L. (1994). Vagal innervation of the rat pylorus: an anterograde tracing study using carbocyanine dyes and laser scanning confocal microscopy. *Cell Tissue Res* 275, 109–123.

Kucyi, A., Hove, M.J., Esterman, M., Hutchison, R.M., and Valera, E.M. (2017). Dynamic Brain Network Correlates of Spontaneous Fluctuations in Attention. *Cereb. Cortex* 27, 1831–1840.

Kukorelli, T., and Juhász, G. (1976). Electroencephalographic synchronization induced by stimulation of small intestine and splanchnic nerve in cats. *Electroencephalogr Clin Neurophysiol* 41, 491–500.

Kukorelli, T., and Juhász, G. (1977). Sleep induced by intestinal stimulation in cats. *Physiol*. *Behav*. 19, 355–358.

Kunzendorf, S., Klotzsche, F., Akbal, M., Villringer, A., Ohl, S., and Gaebler, M. (2019). Active information sampling varies across the cardiac cycle. *Psychophysiology* 56, e13322.

Ladabaum, U., Minoshima, S., Hasler, W.L., Cross, D., Chey, W.D., and Owyang, C. (2001). Gastric distention correlates with activation of multiple cortical and subcortical regions. *Gastroenterology* 120, 369–376.

Ladabaum, U., Roberts, T.P., and McGonigle, D.J. (2007). Gastric fundic distension activates fronto-limbic structures but not primary somatosensory cortex: a functional magnetic resonance imaging study. *Neuroimage* 34, 724–732.

Lakatos, P., Karmos, G., Mehta, A.D., Ulbert, I., and Schroeder, C.E. (2008). Entrainment of neuronal oscillations as a mechanism of attentional selection. *Science* 320, 110–113.

Lakatos, P., O'Connell, M.N., Barczak, A., Mills, A., Javitt, D.C., and Schroeder, C.E. (2009). The leading sense: supramodal control of neurophysiological context by attention. *Neuron* 64, 419–430.

Laming, D.R.J. (1968). Information theory of choice-reaction times. Oxford, England: Academic Press.

Lange, J., Halacz, J., van Dijk, H., Kahlbrock, N., and Schnitzler, A. (2012). Fluctuations of prestimulus oscillatory power predict subjective perception of tactile simultaneity. *Cereb Cortex* 22, 2564–2574.

Lange, J., Oostenveld, R., and Fries, P. (2013). Reduced occipital alpha power indexes enhanced excitability rather than improved visual perception. *J*. *Neurosci*. 33, 3212–3220.

Lange, J., Keil, J., Schnitzler, A., van Dijk, H., and Weisz, N. (2014). The role of alpha oscillations for illusory perception. *Behav*. *Brain Res*. 271, 294–301.

Langner, R., Steinborn, M.B., Chatterjee, A., Sturm, W., and Willmes, K. (2010). Mental fatigue and temporal preparation in simple reaction-time performance. *Acta* Psychol *(Amst)* 133, 64–72.

Langner, R., Kellermann, T., Eickhoff, S.B., Boers, F., Chatterjee, A., Willmes, K., and Sturm, W. (2012). Staying responsive to the world: modality-specific and -nonspecific contributions to speeded auditory, tactile, and visual stimulus detection. *Hum Brain Mapp* 33, 398–418.

Larsen, R.S., and Waters, J. (2018). Neuromodulatory Correlates of Pupil Dilation. *Front. Neural Circuits* 12, 21.

Laufs, H., Krakow, K., Sterzer, P., Eger, E., Beyerle, A., Salek-Haddadi, A., and Kleinschmidt, A. (2003a). Electroencephalographic signatures of attentional and cognitive default modes in spontaneous brain activity fluctuations at rest. P*roc. Natl. Acad. Sci. U.S.A.* 100, 11053–11058.

Laufs, H., Kleinschmidt, A., Beyerle, A., Eger, E., Salek-Haddadi, A., Preibisch, C., and Krakow, K. (2003b). EEG-correlated fMRI of human alpha activity. *NeuroImage* 19, 1463–1476.

Laufs, H., Holt, J.L., Elfont, R., Krams, M., Paul, J.S., Krakow, K., and Kleinschmidt, A. (2006). Where the BOLD signal goes when alpha EEG leaves. *NeuroImage* 31, 1408–1418.

Leek, B. F. (1972).Abdominal visceral receptors. In B. Andersson, M. Fillenz, R. F. Hellon, A. Howe, B. F. Leek, E. Neil (Eds.), *Enteroceptors* (pp. 113–160). Berlin, Heidelberg: Springer.

Leopold, D.A., and Park, S.H. (2020). Studying the visual brain in its natural rhythm. *NeuroImage* 216, 116790.

Leopold, D.A., Murayama, Y., and Logothetis, N.K. (2003). Very slow activity fluctuations in monkey visual cortex: implications for functional brain imaging. *Cereb. Cortex* 13, 422–433.

Levinthal, D.J., and Strick, P.L. (2012). The motor cortex communicates with the kidney. *J. Neurosci.* 32, 6726–6731.

Levinthal, D.J., and Strick, P.L. (2020). Multiple areas of the cerebral cortex influence the stomach. *PNAS* 117, 13078–13083.

Lewis, C.M., Baldassarre, A., Committeri, G., Romani, G.L., and Corbetta, M. (2009). Learning sculpts the spontaneous activity of the resting human brain. *PNAS* 106, 17558–17563.

Limbach, K., and Corballis, P.M. (2016). Prestimulus alpha power influences response criterion in a detection task. *Psychophysiology* 53, 1154–1164.

Lin, H.-H., Chang, W.-K., Chu, H.-C., Huang, T.-Y., Chao, Y.-C., and Hsieh, T.-Y. (2007). Effects of music on gastric myoelectrical activity in healthy humans. *Int. J. Clin. Pract.* 61, 1126–1130.

Lin, Z., Chen, J.D.Z., Schirmer, B.D., and McCallum, R.W. (2000). Postprandial Response of Gastric Slow Waves: Correlation of Serosal Recordings with the Electrogastrogram. *Digestive Diseases and Sciences* 45, 7.

Linkenkaer-Hansen, K., Nikouline, V.V., Palva, J.M., and Ilmoniemi, R.J. (2001). Long-range temporal correlations and scaling behavior in human brain oscillations. *J. Neurosci.* 21, 1370–1377.

Linkenkaer-Hansen, K., Nikulin, V.V., Palva, S., Ilmoniemi, R.J., and Palva, J.M. (2004). Prestimulus oscillations enhance psychophysical performance in humans. *J. Neurosci.* 24, 10186–10190.

Lopes da Silva, F. (1991). Neural mechanisms underlying brain waves: from neural membranes to networks. *Electroencephalography and Clinical Neurophysiology* 79, 81–93.

Lu, C.-L., Wu, Y.-T., Yeh, T.-C., Chen, L.-F., Chang, F.-Y., Lee, S.-D., Ho, L.-T., and Hsieh, J.-C. (2004). Neuronal correlates of gastric pain induced by fundus distension: a 3T-fMRI study. *Neurogastroenterol. Motil.* 16, 575–587.

Lu, S.M., Guido, W., and Sherman, S.M. (1993). The brain-stem parabrachial region controls mode of response to visual stimulation of neurons in the cat's lateral geniculate nucleus. *Vis. Neurosci.* 10, 631–642.

Luft, C.D.B., and Bhattacharya, J. (2015). Aroused with heart: Modulation of heartbeat evoked potential by arousal induction and its oscillatory correlates. *Scientific Reports* 5, 15717.

Makeig, S., and Inlow, M. (1993). Lapse in alertness: coherence of fluctuations in performance and EEG spectrum. *Electroencephalography and Clinical Neurophysiology* 86, 23–35.

Maris, E., and Oostenveld, R. (2007). Nonparametric statistical testing of EEG- and MEG-data. *J Neurosci Methods* 164, 177–190.

Martins, A.Q., Ring, C., McIntyre, D., Edwards, L., and Martin, U. (2009). Effects of unpredictable stimulation on pain and nociception across the cardiac cycle. *Pain* 147, 84–90.

Mathewson, K.E., Gratton, G., Fabiani, M., Beck, D.M., and Ro, T. (2009). To see or not to see: prestimulus alpha phase predicts visual awareness. *J. Neurosci.* 29, 2725–2732.

Mathewson, K.E., Lleras, A., Beck, D.M., Fabiani, M., Ro, T., and Gratton, G. (2011). Pulsed Out of Awareness: EEG Alpha Oscillations Represent a Pulsed-Inhibition of Ongoing Cortical Processing. *Front Psychol* 2, 99.

Mayeli, A., Zoubi, O.A., White, E.J., Chappelle, S., Kuplicki, R., Smith, R., Feinstein, J.S., Bodurka, J., Paulus, M.P., and Khalsa, S.S. (2021). Neural indicators of human gut feelings. *BioRxiv* 2021.02.11.430867.

Mayer, E.A., Aziz, Q., Coen, S., Kern, M., Labus, J.S., Lane, R., Kuo, B., Naliboff, B., and Tracey, I. (2009). Brain imaging approaches to the study of functional GI disorders: A Rome Working Team Report. *Neurogastroenterology & Motility* 21, 579–596.

Mazaheri, A., van Schouwenburg, M.R., Dimitrijevic, A., Denys, D., Cools, R., and Jensen, O. (2014). Region-specific modulations in oscillatory alpha activity serve to facilitate processing in the visual and auditory modalities. *NeuroImage* 87, 356–362.

McDougall, S.J., Guo, H., and Andresen, M.C. (2017). Dedicated C-fibre viscerosensory pathways to central nucleus of the amygdala. *J Physiol* 595, 901–917.

McGuire, P.K., Paulesu, E., Frackowiak, R.S., and Frith, C.D. (1996). Brain activity during stimulus independent thought. *Neuroreport* 7, 2095–2099.

Menon, V., and Uddin, L.Q. (2010). Saliency, switching, attention and control: a network model of insula function. *Brain Struct Funct* 214, 655–667.

Mercier, M.R., Molholm, S., Fiebelkorn, I.C., Butler, J.S., Schwartz, T.H., and Foxe, J.J. (2015). Neuro-Oscillatory Phase Alignment Drives Speeded Multisensory Response Times: An Electro-Corticographic Investigation. *J Neurosci* 35, 8546–8557.

Mintchev, M.P., and Bowes, K.L. (1997). Do increased electrogastrographic frequencies always correspond to internal tachygastria? *Ann Biomed Eng* 25, 1052–1058.

Mintchev, M.P., Kingma, Y.J., and Bowes, K.L. (1993). Accuracy of cutaneous recordings of gastric electrical activity. *Gastroenterology* 104, 1273–1280.

Miranda, M.I., Ferreira, G., Ramirez-Lugo, L., and Bermudez-Rattoni, F. (2002). Glutamatergic activity in the amygdala signals visceral input during taste memory formation. Proc Natl Acad Sci *U S A* 99, 11417–11422.

Monti, J.M. (2010). The role of dorsal raphe nucleus serotonergic and non-serotonergic neurons, and of their receptors, in regulating waking and rapid eye movement (REM) sleep. *Sleep Medicine Reviews* 14, 319–327.

Monti, J.M. (2011). Serotonin control of sleep-wake behavior. *Sleep Medicine Reviews* 15, 269–281.

Monti, A., Porciello, G., Panasiti, M.S., and Aglioti, S.M. (2021). Gut markers of bodily self-consciousness. *BioRxiv* 2021.03.05.434072.

Monto, S., Palva, S., Voipio, J., and Palva, J.M. (2008). Very slow EEG fluctuations predict the dynamics of stimulus detection and oscillation amplitudes in humans. *J. Neurosci.* 28, 8268–8272.

Moosmann, M., Ritter, P., Krastel, I., Brink, A., Thees, S., Blankenburg, F., Taskin, B., Obrig, H., and Villringer, A. (2003). Correlates of alpha rhythm in functional magnetic resonance imaging and near infrared spectroscopy. *NeuroImage* 20, 145–158.

Morecraft, R.J., and Van Hoesen, G.W. (1992). Cingulate input to the primary and supplementary motor cortices in the rhesus monkey: evidence for somatotopy in areas 24c and 23c. *J Comp Neurol* 322, 471–489.

Neuhuber, W.L., Kressel, M., Stark, A., and Berthoud, H.R. (1998). Vagal efferent and afferent innervation of the rat esophagus as demonstrated by anterograde DiI and DiA tracing: focus on myenteric ganglia. *J Auton Nerv Syst* 70, 92–102.

Noda, H., and Adey, W.R. (1970). Firing variability in cat association cortex during sleep and wakefulness. *Brain Res.* 18, 513–526.

Nomi, J.S., Schettini, E., Broce, I., Dick, A.S., and Uddin, L.Q. (2018). Structural Connections of Functionally Defined Human Insular Subdivisions. *Cereb Cortex* 28, 3445–3456.

O'Callaghan, C., Walpola, I.C., and Shine, J.M. (2021). Neuromodulation of the mind-wandering brain state: the interaction between neuromodulatory tone, sharp wave-ripples and spontaneous thought. *Philos Trans R Soc Lond B Biol Sci* 376, 20190699.

O'Grady, G., Du, P., Cheng, L.K., Egbuji, J.U., Lammers, W.J.E.P., Windsor, J.A., and Pullan, A.J. (2010). Origin and propagation of human gastric slow-wave activity defined by high-resolution mapping. *American Journal of Physiology-Gastrointestinal and Liver Physiology* 299, G585–G592.

Oken, B.S., Salinsky, M.C., and Elsas, S.M. (2006). Vigilance, alertness, or sustained attention: physiological basis and measurement. *Clin Neurophysiol* 117, 1885–1901.

Okumura, T., and Namiki, M. (1990). Vagal motor neurons innervating the stomach are site-specifically organized in the dorsal motor nucleus of the vagus nerve in rats. *Journal of the Autonomic Nervous System* 29, 157–162.

Olbrich, S., Mulert, C., Karch, S., Trenner, M., Leicht, G., Pogarell, O., and Hegerl, U. (2009). EEG-vigilance and BOLD effect during simultaneous EEG/fMRI measurement. *NeuroImage* 45, 319–332.

Olivier, B. (2015). Serotonin: a never-ending story. *Eur J Pharmacol* 753, 2–18.

Ongür, D., An, X., and Price, J.L. (1998). Prefrontal cortical projections to the hypothalamus in macaque monkeys. *J Comp Neurol* 401, 480–505.

Oostenveld, R., Fries, P., Maris, E., and Schoffelen, J. (2011). FieldTrip: Open Source Software for Advanced Analysis of MEG, EEG, and Invasive Electrophysiological Data. *Computational Intelligence and Neuroscience* 2011, 1–9.

van Oudenhove, L., Vandenberghe, J., Dupont, P., Geeraerts, B., Vos, R., Bormans, G., van Laere, K., Fischler, B., Demyttenaere, K., Janssens, J., et al. (2009). Cortical deactivations during gastric fundus distension in health: visceral pain-specific response or attenuation of "default mode" brain function? A H2 15O-PET study. *Neurogastroenterol. Motil.* 21, 259–271.

Pagani, F.D., Norman, W.P., Kasbekar, D.K., and Gillis, R.A. (1985). Localization of sites within dorsal motor nucleus of vagus that affect gastric motility. *Am. J. Physiol.* 249, G73-84.

Palmiter, R.D. (2018). The Parabrachial Nucleus: CGRP Neurons Function as a General Alarm. *Trends in Neurosciences* 41, 280–293.

Palva, J.M., and Palva, S. (2012). Infra-slow fluctuations in electrophysiological recordings, blood-oxygenation-level-dependent signals, and psychophysical time series. *NeuroImage* 62, 2201–2211.

Palva, S., and Palva, J.M. (2007). New vistas for alpha-frequency band oscillations. *Trends Neurosci.* 30, 150–158.

Palva, J.M., Palva, S., and Kaila, K. (2005). Phase Synchrony among Neuronal Oscillations in the Human Cortex. *J. Neurosci.* 25, 3962–3972.

Parasuraman, R., Warm, J.S., and See, J.E. (1998). Brain systems of vigilance. In: R. Parasuman (Ed.) *The Attentive Brain* (pp. 221–256). Cambridge, MA, US: The MIT Press.

Park, H.-D., and Tallon-Baudry, C. (2014). The neural subjective frame: from bodily signals to perceptual consciousness. *Philos. Trans. R. Soc. Lond., B, Biol. Sci.* 369, 20130208.

Park, H.-D., Correia, S., Ducorps, A., and Tallon-Baudry, C. (2014). Spontaneous fluctuations in neural responses to heartbeats predict visual detection. *Nat Neurosci* 17, 612–618.

Parkman, H.P., Harris, A.D., Miller, M.A., and Fisher, R.S. (1996). Influence of age, gender, and menstrual cycle on the normal electrogastrogram. *Am. J. Gastroenterol.* 91, 127–133.

Parkman, H.P., Hasler, W.L., Barnett, J.L., and Eaker, E.Y. (2003). Electrogastrography: a document prepared by the gastric section of the American Motility Society Clinical GI Motility Testing Task Force. *Neurogastroenterology and Motility* 15, 89–102.

Paulus, M.P., and Frank, L.R. (2003). Ventromedial prefrontal cortex activation is critical for preference judgments. *NeuroReport* 14, 1311–1315.

Peelle, J.E., and Davis, M.H. (2012). Neural Oscillations Carry Speech Rhythm through to Comprehension. *Front. Psychol.* 3.

Penfield, W., and Boldrey, E. (1937). Somatic motor and sensory representation in the cerebral cortex of man as studied by electrical stimulation. *Brain: A Journal of Neurology* 60, 389–443.

Penfield, W., and Faulk, M.E., JR. (1955). The insula: Further observation on its function. *Brain* 78, 445–470.

Persson, B., and Svensson, T.H. (1981). Control of behaviour and brain noradrenaline neurons by peripheral blood volume receptors. *J. Neural Transmission* 52, 73–82.

Petzschner, F.H., Weber, L.A., Wellstein, K.V., Paolini, G., Do, C.T., and Stephan, K.E. (2019). Focus of attention modulates the heartbeat evoked potential. *NeuroImage* 186, 595–606.

Peupelmann, J., Quick, C., Berger, S., Hocke, M., Tancer, M.E., Yeragani, V.K., and Bär, K.-J. (2009). Linear and non-linear measures indicate gastric dysmotility in patients suffering from acute schizophrenia. *Prog. Neuropsychopharmacol. Biol. Psychiatry* 33, 1236–1240.

Pfaffenbach, B., Adamek, R.J., Kuhn, K., and Wegener, M. (1995). Electrogastrography in healthy subjects: Evaluation of normal values, influence of age and gender. *Digestive Diseases and Sciences* 40, 1445–1450.

Pfurtscheller, G. (1976). Ultra-slow changes in the rhythmic activity within the alpha band and their probable origin. *Pflügers Archiv European Journal of Physiology* 367, 55–66.

Pfurtscheller, G., Stancák, A., and Neuper, C. (1996). Post-movement beta synchronization. A correlate of an idling motor area? E*lectroencephalography and Clinical Neurophysiology* 98, 281–293.

Pigarev, I.N., and Pigareva, M.L. (2012). Sleep and the Control of Visceral Functions. *Neurosci Behav Physi* 42, 948–956.

Pigarev, I., Almirall, H., Pigareva, M.L., Bautista, V., Sánchez-Bahillo, A., Barcia, C., and Herrero, M.T. (2006). Visceral signals reach visual cortex during slow wave sleep: study in monkeys. *Acta Neurobiol Exp (Wars)* 66, 69–73.

Pigarev, I., Almirall, H., and Pigareva, M. (2008). Cortical evoked responses to magnetic stimulation of macaque's abdominal wall in sleep-wake cycle. *Acta Neurobiol Exp (Wars)* 68, 91–96.

Pigarev, I.N., Bagaev, V.A., Levichkina, E.V., Fedorov, G.O., and Busigina, I.I. (2013). Cortical visual areas process intestinal information during slow-wave sleep. *Neurogastroenterol Motil* 25, 268–275, e169.

Pollatos, O., Gramann, K., and Schandry, R. (2007). Neural systems connecting interoceptive awareness and feelings. *Human Brain Mapping* 28, 9–18.

Portas, C.M., Bjorvatn, B., and Ursin, R. (2000). Serotonin and the sleep/wake cycle: special emphasis on microdialysis studies. *Prog Neurobiol* 60, 13–35.

Powley, T.L. (2013). Chapter 34 - Central Control of Autonomic Functions: Organization of the Autonomic Nervous System. In: L.R. Squire, D. Berg, F.E. Bloom, S. du Lac, A. Ghosh, and N.C. Spitzer (Ed.). *Fundamental Neuroscience* (Fourth Edition, pp. 729–747). San Diego: Academic Press.

Powley, T.L., and Phillips, R.J. (2011). Vagal intramuscular array afferents form complexes with interstitial cells of Cajal in gastrointestinal smooth muscle: analogues of muscle spindle organs? *Neuroscience* 186, 188–200.

Powley, T.L., Wang, X.-Y., Fox, E.A., Phillips, R.J., Liu, L.W.C., and Huizinga, J.D. (2008). Ultrastructural evidence for communication between intramuscular vagal mechanoreceptors and interstitial cells of Cajal in the rat fundus. *Neurogastroenterol. Motil.* 20, 69–79.

Powley, T.L., Hudson, C.N., McAdams, J.L., Baronowsky, E.A., and Phillips, R.J. (2016). Vagal Intramuscular Arrays: The Specialized Mechanoreceptor Arbors That Innervate the Smooth Muscle Layers of the Stomach Examined in the Rat. *J Comp Neurol* 524, 713–737.

Praamstra, P., Kourtis, D., Kwok, H.F., Oostenveld, R. (2006). Neurophysiology of implicit timing in serial choice reaction-time performance. *J. Neurosci.* 26, 5448-55.

Pramme, L., Larra, M.F., Schächinger, H., and Frings, C. (2014). Cardiac cycle time effects on mask inhibition. *Biological Psychology* 100, 115–121.

Pramme, L., Larra, M.F., Schächinger, H., and Frings, C. (2016). Cardiac cycle time effects on selection efficiency in vision. *Psychophysiology* 53, 1702–1711.

Price, J.L. (1999). Prefrontal cortical networks related to visceral function and mood. *Ann N Y Acad Sci* 877, 383–396.

Pritchard, T.C., Hamilton, R.B., and Norgren, R. (2000). Projections of the Parabrachial Nucleus in the Old World Monkey. *Experimental Neurology* 165, 101–117.

Pyka, M., Beckmann, C.F., Schöning, S., Hauke, S., Heider, D., Kugel, H., Arolt, V., and Konrad, C. (2009). Impact of working memory load on FMRI resting state pattern in subsequent resting phases. *PLoS One* 4, e7198.

Qin, P., and Northoff, G. (2011). How is our self related to midline regions and the default-mode network? *NeuroImage* 57, 1221–1233.

Qiu, M.H., Chen, M.C., Fuller, P.M., and Lu, J. (2016). Stimulation of the Pontine Parabrachial Nucleus Promotes Wakefulness via Extra-thalamic Forebrain Circuit Nodes. *Curr Biol* 26, 2301–2312.

Racké, K., Reimann, A., Schwörer, H., and Kilbinger, H. (1996). Regulation of 5-HT release from enterochromaffin cells. Beha*v. Brain Res.* 73, 83–87.

Raichle, M.E. (2009). A Paradigm Shift in Functional Brain Imaging. *J. Neurosci.* 29, 12729–12734.

Raichle, M.E., MacLeod, A.M., Snyder, A.Z., and Powers, W.J. (2001). Inaugural article: a default mode of brain function. *Proc. Natl. Acad. Sci. USA* 676–682.

Rao, M., and Gershon, M.D. (2016). The bowel and beyond: the enteric nervous system in neurological disorders. *Nat Rev Gastroenterol Hepatol* 13, 517–528.

Ray, W.J., and Cole, H.W. (1985). EEG alpha activity reflects attentional demands, and beta activity reflects emotional and cognitive processes. *Science* 228, 750–752.

Rayner, C., Hebbard, G., and Horowitz, M. (2012). Physiology of the Antral Pump and Gastric Emptying. In L. R. Johnson, F. K. Ghishan, J. D. Kaunitz, J. L. Merchant, H. M. Said, & J. D. Wood (Ed.): *Physiology of the Gastrointestinal Tract* (Fifth Edition, pp. 959–976). Academic Press.

Rebollo, I., Devauchelle, A.-D., Béranger, B., and Tallon-Baudry, C. (2018). Stomach-brain synchrony reveals a novel, delayed-connectivity resting-state network in humans. *Elife* 7:e33321.

Rebollo, I., Wolpert, N., and Tallon-Baudry, C. (2021). Brain–stomach coupling: Anatomy, functions, and future avenues of research. *Current Opinion in Biomedical Engineering* 18, 100270.

Reimer, J., McGinley, M.J., Liu, Y., Rodenkirch, C., Wang, Q., McCormick, D.A., and Tolias, A.S. (2016). Pupil fluctuations track rapid changes in adrenergic and cholinergic activity in cortex. *Nat Commun* 7, 13289.

Ren, K., and Dubner, R. (2008). 5.49 - Descending Control Mechanisms. In: R.H. Masland, T.D. Albright, T.D. Albright, R.H. Masland, P. Dallos, D. Oertel, S. Firestein, G.K. Beauchamp, M. Catherine Bushnell, A.I. Basbaum, et al. (Ed.). *The Senses: A Comprehensive Reference* (pp. 723–762). New York: Academic Press.

Ress, D., Backus, B.T., and Heeger, D.J. (2000). Activity in primary visual cortex predicts performance in a visual detection task. *Nat Neurosci* 3, 940–945.

Rhee, P.-L., Lee, J.Y., Son, H.J., Kim, J.J., Rhee, J.C., Kim, S., Koh, S.D., Hwang, S.J., Sanders, K.M., and Ward, S.M. (2011). Analysis of pacemaker activity in the human stomach: Pacemaker activity in the human stomach. *The Journal of Physiology* 589, 6105–6118.

Richter, C.G., Babo-Rebelo, M., Schwartz, D., and Tallon-Baudry, C. (2017). Phase-amplitude coupling at the organism level: The amplitude of spontaneous alpha rhythm fluctuations varies with the phase of the infra-slow gastric basal rhythm. *NeuroImage* 146, 951–958.

Riezzo, G., Porcelli, P., Guerra, V., and Giorgio, I. (1996). Effects of different psychophysiological stressors on the cutaneous electrogastrogram in healthy subjects. *Arch. Physiol. Biochem.* 104, 282–286.

Riezzo, G., Russo, F., and Indrio, F. (2013). Electrogastrography in Adults and Children: The Strength, Pitfalls, and Clinical Significance of the Cutaneous Recording of the Gastric Electrical Activity. *BioMed Research International* 2013, 1–14.

Rihs, T.A., Michel, C.M., and Thut, G. (2007). Mechanisms of selective inhibition in visual spatial attention are indexed by alpha-band EEG synchronization. *Eur. J. Neurosci*. 25, 603–610.

Rodenkirch, C., Liu, Y., Schriver, B.J., and Wang, Q. (2019). Locus coeruleus activation enhances thalamic feature selectivity via norepinephrine regulation of intrathalamic circuit dynamics. *Nat Neurosci* 22, 120–133.

Rogers, R.C., Kita, H., Butcher, L.L., and Novin, D. (1980). Afferent projections to the dorsal motor nucleus of the vagus. *Brain Res Bull* 5, 365–373.

Romei, V., Brodbeck, V., Michel, C., Amedi, A., Pascual-Leone, A., and Thut, G. (2008). Spontaneous fluctuations in posterior alpha-band EEG activity reflect variability in excitability of human visual areas. *Cereb. Cortex* 18, 2010–2018.

Romei, V., Gross, J., and Thut, G. (2010). On the role of prestimulus alpha rhythms over occipito-parietal areas in visual input regulation: correlation or causation? *J. Neurosci.* 30, 8692–8697.

Romei, V., Gross, J., and Thut, G. (2012). Sounds Reset Rhythms of Visual Cortex and Corresponding Human Visual Perception. *Curr Biol* 22, 807–813.

Rosenberg, M.D., Finn, E.S., Constable, R.T., and Chun, M.M. (2015). Predicting moment-to-moment attentional state. *NeuroImage* 114, 249–256.

Rouder, J.N., and Morey, R.D. (2011). A Bayes factor meta-analysis of Bem's ESP claim. *Psychon Bull Rev* 18, 682–689.

Ruhland, C., Koschke, M., Greiner, W., Peupelmann, J., Pietsch, U., Hocke, M., Yeragani, V.K., and Bär, K.-J. (2008). Gastric dysmotility in patients with major depression. *J Affect Disord* 110, 185–190.

Sadaghiani, S., and D'Esposito, M. (2015). Functional Characterization of the Cingulo-Opercular Network in the Maintenance of Tonic Alertness. *Cereb Cortex* 25, 2763–2773.

Sadaghiani, S., and Kleinschmidt, A. (2013). Functional interactions between intrinsic brain activity and behavior. *NeuroImage* 80, 379–386.

Sadaghiani, S., Hesselmann, G., and Kleinschmidt, A. (2009). Distributed and Antagonistic Contributions of Ongoing Activity Fluctuations to Auditory Stimulus Detection. *J. Neurosci.* 29, 13410–13417.

Sadaghiani, S., Hesselmann, G., Friston, K.J., and Kleinschmidt, A. (2010). The relation of ongoing brain activity, evoked neural responses, and cognition. *Front Syst Neurosci* 4, 20.

Saito, K., Kanazawa, M., and Fukudo, S. (2002). Colorectal distention induces hippocampal noradrenaline release in rats: an in vivo microdialysis study. *Brain Res*. 947, 146–149.

Sakaguchi, T., and Ohtake, M. (1985). Inhibition of gastric motility induced by activation of the hypothalamic paraventricular nucleus. *Brain Res*. 335, 365–367.

Salmelin, R., and Hari, R. (1994). Characterization of spontaneous MEG rhythms in healthy adults. *Electroencephalogr Clin Neurophysiol* 91, 237–248.

Samaha, J., Gosseries, O., and Postle, B.R. (2017a). Distinct Oscillatory Frequencies Underlie Excitability of Human Occipital and Parietal Cortex. *J. Neurosci.* 37, 2824–2833.

Samaha, J., Iemi, L., and Postle, B.R. (2017b). Prestimulus alpha-band power biases visual discrimination confidence, but not accuracy. *Consciousness and Cognition* 54, 47–55.

Samaha, J., Iemi, L., Haegens, S., and Busch, N.A. (2020). Spontaneous Brain Oscillations and Perceptual Decision-Making. *Trends in Cognitive Sciences* 24, 639–653.

Samuels, E.R., and Szabadi, E. (2008). Functional neuroanatomy of the noradrenergic locus coeruleus: its roles in the regulation of arousal and autonomic function part I: principles of functional organisation. *Curr Neuropharmacol* 6, 235–253.

Sanders, K.M. (2019). Spontaneous Electrical Activity and Rhythmicity in Gastrointestinal Smooth Muscles. In: H. Hashitani, and R.J. Lang (Ed.). *Smooth Muscle Spontaneous Activity: Physiological and Pathological Modulation* (pp. 3–46). Singapore: Springer.

Sanders, K.M., Koh, S.D., and Ward, S.M. (2006). Interstitial cells of cajal as pacemakers in the gastrointestinal tract. *Annu. Rev. Physiol.* 68, 307–343.

Sanders, K.M., Ward, S.M., and Koh, S.D. (2014). Interstitial Cells: Regulators of Smooth Muscle Function. *Physiological Reviews* 94, 859–907.

Sanmiguel, C.P., Mintchev, M.P., and Bowes, K.L. (1998). Electrogastrography: A Noninvasive Technique to Evaluate Gastric Electrical Activity. *Canadian Journal of Gastroenterology* 12, 423–430.

Saper, C.B. (2002). The Central Autonomic Nervous System: Conscious Visceral Perception and Autonomic Pattern Generation. *Annu. Rev. Neurosci.* 25, 433–469.

Saper, C.B., and Loewy, A.D. (1980). Efferent connections of the parabrachial nucleus in the rat. *Brain Res.* 197, 291–317.

Saper, C.B., Scammell, T.E., and Lu, J. (2005). Hypothalamic regulation of sleep and circadian rhythms. *Nature* 437, 1257–1263.

Sapir, A., d'Avossa, G., McAvoy, M., Shulman, G.L., and Corbetta, M. (2005). Brain signals for spatial attention predict performance in a motion discrimination task. *PNAS* 102, 17810–17815.

Sara, S.J. (2009). The locus coeruleus and noradrenergic modulation of cognition. *Nature Reviews Neuroscience* 10, 211–223.

Sarter, M., Givens, B., and Bruno, J.P. (2001). The cognitive neuroscience of sustained attention: where top-down meets bottom-up. *Brain Res Brain Res Rev* 35, 146–160.

Sauseng, P., Klimesch, W., Gerloff, C., and Hummel, F.C. (2009). Spontaneous locally restricted EEG alpha activity determines cortical excitability in the motor cortex. *Neuropsychologia* 47, 284–288.

Saxe, R., and Kanwisher, N. (2003). People thinking about thinking people. The role of the temporo-parietal junction in "theory of mind." *NeuroImage* 19, 1835–1842.

Schack, B., and Klimesch, W. (2002). Frequency characteristics of evoked and oscillatory electroencephalic activity in a human memory scanning task. *Neurosci. Lett.* 331, 107–110.

Schemann, M., and Grundy, D. (1992). Electrophysiological identification of vagally innervated enteric neurons in guinea pig stomach. *Am. J. Physiol.* 263, G709-718.

Schoffelen, J.-M., Oostenveld, R., and Fries, P. (2005). Neuronal coherence as a mechanism of effective corticospinal interaction. *Science* 308, 111–113.

Schölvinck, M.L., Friston, K.J., and Rees, G. (2012). The influence of spontaneous activity on stimulus processing in primary visual cortex. *NeuroImage* 59, 2700–2708.

Schooler, J.W., Smallwood, J., Christoff, K., Handy, T.C., Reichle, E.D., and Sayette, M.A. (2011). Meta-awareness, perceptual decoupling and the wandering mind. *Trends Cogn Sci* 15, 319–326.

Schulz, A., Reichert, C.F., Richter, S., Lass-Hennemann, J., Blumenthal, T.D., and Schächinger, H. (2009a). Cardiac modulation of startle: effects on eye blink and higher cognitive processing. *Brain Cogn* 71, 265–271.

Schulz, A., Lass-Hennemann, J., Nees, F., Blumenthal, T.D., Berger, W., and Schachinger, H. (2009b). Cardiac modulation of startle eye blink. *Psychophysiology* 46, 234–240.

Schulz, A., Schilling, T.M., Vögele, C., Larra, M.F., and Schächinger, H. (2016). Respiratory modulation of startle eye blink: a new approach to assess afferent signals from the respiratory system. *Philos Trans R Soc Lond B Biol Sci* 371.

Schulz, A., van Dyck, Z., Lutz, A.P.C., Rost, S., and Vögele, C. (2017). Gastric modulation of startle eye blink. *Biological Psychology* 127, 25–33.

Schulze, K. (2006). Imaging and modelling of digestion in the stomach and the duodenum. *Neurogastroenterol Motil* 18, 172–183.

Schwartz, G.J., McHugh, P.R., and Moran, T.H. (1991). Integration of vagal afferent responses to gastric loads and cholecystokinin in rats. *American Journal of Physiology - Regulatory Integrative and Comparative Physiology* 261, R64–R69.

Schwartz, G.J., McHugh, P.R., and Moran, T.H. (1993). Gastric loads and cholecystokinin synergistically stimulate rat gastric vagal afferents. American Journal of Physiology - Regulatory Integrative and Comparative Physiology 265, R872–R876.

Seashore, C., and Kent, G. (1905). Periodicity And Progressive Change In Continuous Mental Work. *Psychological Monographs: General and Applied* 6, 47–101.

Semba, T., and Mizonishi, T. (1978). Atropine-resistant excitation of motility of the dog stomach and colon induced by stimulation of the extrinsic nerves and their centers. *Jpn J Physiol* 28, 239–248.

Sergent, C., Baillet, S., and Dehaene, S. (2005). Timing of the brain events underlying access to consciousness during the attentional blink. *Nat Neurosci* 8, 1391–1400.

Shahrestani, J., and M Das, J. (2020). Neuroanatomy, Auerbach Plexus. Treasure Island (FL): StatPearls Publishing.

Shipley, M.T., and Sanders, M.S. (1982). Special senses are really special: Evidence for a reciprocal, bilateral pathway between insular cortex and nucleus parabrachialis. *Brain Research Bulletin* 8, 493–501.

Shulman, G.L., Fiez, J.A., Corbetta, M., Buckner, R.L., Miezin, F.M., Raichle, M.E., and Petersen, S.E. (1997). Common Blood Flow Changes across Visual Tasks: II. Decreases in Cerebral Cortex. *J Cogn Neurosci* 9, 648–663.

Simonian, H.P., Panganamamula, K., Parkman, H.P., Xu, X., Chen, J.Z., Lindberg, G., Xu, H., Shao, C., Ke, M.-Y., Lykke, M., et al. (2004). Multichannel Electrogastrography (EGG) in Normal Subjects: A Multicenter Study. *Digestive Diseases and Sciences* 49, 594–601.

Sinz, R., and Stebel, J. (1970). On central nervous minute-periodicity and its coordination. *Act Nerv Super (Praha)* 12, 146–147.

Smallwood, J., and Andrews-Hanna, J. (2013). Not all minds that wander are lost: the importance of a balanced perspective on the mind-wandering state. *Front Psychol* 4.

Smirnov, V.M., and Lychkova, A.E. (2003). Mechanism of synergism between sympathetic and parasympathetic autonomic nervous systems in the regulation of motility of the stomach and sphincter of Oddi. *Bull. Exp. Biol. Med.* 135, 327–329.

Softky, W.R., and Koch, C. (1993). The highly irregular firing of cortical cells is inconsistent with temporal integration of random EPSPs. *J. Neurosci.* 13, 334–350.

Song, K., Meng, M., Chen, L., Zhou, K., and Luo, H. (2014). Behavioral Oscillations in Attention: Rhythmic α Pulses Mediated through θ Band. *J. Neurosci.* 34, 4837–4844.

Spielberger, C.D. (1983). Manual for the State-Trait Inventory STAI (Form Y). Palo Alto, CA: Mind Garden.

Stern, R.M., Koch, K.L., Leibowitz, H.W., Lindblad, I.M., Shupert, C.L., and Stewart, W.R. (1985). Tachygastria and motion sickness. *Aviat Space Environ Med* 56, 1074–1077.

Stevens, W.D., Buckner, R.L., and Schacter, D.L. (2010). Correlated low-frequency BOLD fluctuations in the resting human brain are modulated by recent experience in category-preferential visual regions. *Cereb Cortex* 20, 1997–2006.

Stouffer, S.A. (1949). The American Soldier, Vol.1: Adjustment during Army Life. Princeton: Princeton University Press.

Strigo, I.A., and Craig, A.D. (Bud) (2016). Interoception, homeostatic emotions and sympathovagal balance. *Philosophical Transactions of the Royal Society B: Biological Sciences* 371, 20160010.

Strijkstra, A.M., Beersma, D.G.M., Drayer, B., Halbesma, N., and Daan, S. (2003). Subjective sleepiness correlates negatively with global alpha (8-12 Hz) and positively with central frontal theta (4-8 Hz) frequencies in the human resting awake electroencephalogram. *Neurosci Lett* 340, 17–20.

Suarez, A.N., Hsu, T.M., Liu, C.M., Noble, E.E., Cortella, A.M., Nakamoto, E.M., Hahn, J.D., de Lartigue, G., and Kanoski, S.E. (2018). Gut vagal sensory signaling regulates hippocampus function through multi-order pathways. *Nat Commun* 9, 2181.

Suzuki, N., Prosser, C.L., and Dahms, V. (1986). Boundary cells between longitudinal and circular layers: essential for electrical slow waves in cat intestine. *Am. J. Physiol.* 250, G287-294.

Sveshnikov, D.S., Smirnov, V.M., Myasnikov, I.L., and Kuchuk, A.V. (2012). Study of the nature of sympathetic trunk nerve fibers enhancing gastric motility. *Bull. Exp. Biol. Med.* 152, 283–285.

Tagliazucchi, E., and Laufs, H. (2014). Decoding wakefulness levels from typical fMRI resting-state data reveals reliable drifts between wakefulness and sleep. *Neuron* 82, 695–708.

Tallon-Baudry, C., and Bertrand, O. (1999). Oscillatory gamma activity in humans and its role in object representation. *Trends Cogn. Sci. (Regul. Ed.)* 3, 151–162.

Tambini, A., Ketz, N., and Davachi, L. (2010). Enhanced brain correlations during rest are related to memory for recent experiences. *Neuron* 65, 280–290.

Teckentrup, V., Neubert, S., Santiago, J.C.P., Hallschmid, M., Walter, M., and Kroemer, N.B. (2020). Non-invasive stimulation of vagal afferents reduces gastric frequency. *Brain Stimulation* 13, 470–473.

Thut, G., and Miniussi, C. (2009). New insights into rhythmic brain activity from TMS-EEG studies. *Trends Cogn. Sci. (Regul. Ed.)* 13, 182–189.

Thut, G., Nietzel, A., Brandt, S.A., and Pascual-Leone, A. (2006). Alpha-band electroencephalographic activity over occipital cortex indexes visuospatial attention bias and predicts visual target detection. *J. Neurosci.* 26, 9494–9502.

Tiihonen, J., Kajola, M., and Hari, R. (1989). Magnetic mu rhythm in man. *Neuroscience* 32, 793–800.

Tolj, N. (2007). The Impact of Age, Sex, Body Mass Index and Menstrual Cycle Phase on Gastric Myoelectrical Activity Characteristics in a Healthy Croatian Population. *Coll. Antropol.* 8.

Tort, A.B.L., Kramer, M.A., Thorn, C., Gibson, D.J., Kubota, Y., Graybiel, A.M., and Kopell, N.J. (2008). Dynamic cross-frequency couplings of local field potential oscillations in rat striatum and hippocampus during performance of a T-maze task. *Proc. Natl. Acad. Sci. U. S. A.* 105, 20517–20522.

Tort, A.B.L., Komorowski, R.W., Manns, J.R., Kopell, N.J., and Eichenbaum, H. (2009). Theta-gamma coupling increases during the learning of item-context associations. *Proc. Natl. Acad. Sci.* 106, 20942-20947.

Tort, A.B.L., Komorowski, R., Eichenbaum, H., and Kopell, N. (2010). Measuring phase-amplitude coupling between neuronal oscillations of different frequencies. *J. Neurophysiol.* 104, 1195–1210.

Tort, A.B.L., Brankačk, J., and Draguhn, A. (2018). Respiration-Entrained Brain Rhythms Are Global but Often Overlooked. *Trends Neurosci.* 41, 186–197.

Travagli, R.A., Hermann, G.E., Browning, K.N., and Rogers, R.C. (2006). Brainstem circuits regulating gastric function. *Annu. Rev. Physiol.* 68, 279–305.

Tsuchiya, K., Kozawa, E., Iriki, M., and Manchanda, S.K. (1974). Changes of gastrointestinal motility evoked by spinal cord cooling and heating. *Pflugers Arch.* 351, 275–286.

Tumpeer, I., and Blitsten, P. (1926). Registration of peristalsis by the Einthoven galvanometer. *Am J Dis Child* 454–455.

Uhlrich, D.J., Cucchiaro, J.B., and Sherman, S.M. (1988). The projection of individual axons from the parabrachial region of the brain stem to the dorsal lateral geniculate nucleus in the cat. *J. Neurosci.* 8, 4565–4575.

van Diepen, R.M., Cohen, M.X., Denys, D., and Mazaheri, A. (2015). Attention and temporal expectations modulate power, not phase, of ongoing alpha oscillations. *J. Cogn. Neurosci.* 27, 1573–1586.

Van Diepen, R.M., Foxe, J.J., and Mazaheri, A. (2019). The functional role of alpha-band activity in attentional processing: the current zeitgeist and future outlook. *Curr Opin Psychol* 29, 229–238.

Van Orden, G.C., Holden, J.G., and Turvey, M.T. (2003). Self-organization of cognitive performance. *J Exp Psychol Gen* 132, 331–350.

Van Oudenhove, L., Dupont, P., Vandenberghe, J., Geeraerts, B., van Laere, K., Bormans, G., Demyttenaere, K., and Tack, J. (2008). The role of somatosensory cortical regions in the processing of painful gastric fundic distension: an update of brain imaging findings. *Neurogastroenterol Motil* 20, 479–487.

VanRullen, R. (2016). Perceptual Cycles. *Trends Cogn. Sci. (Regul. Ed.)* 20, 723–735.

Varela, F., Lachaux, J.-P., Rodriguez, E., and Martinerie, J. (2001). The brainweb: Phase synchronization and large-scale integration. *Nature Reviews Neuroscience* 2, 229–239.

Vasavid, P., Chaiwatanarat, T., Pusuwan, P., Sritara, C., Roysri, K., Namwongprom, S., Kuanrakcharoen, P., Premprabha, T., Chunlertrith, K., Thongsawat, S., et al. (2014). Normal Solid Gastric Emptying Values Measured by Scintigraphy Using Asian-style Meal:A Multicenter Study in Healthy Volunteers. *J Neurogastroenterol Motil* 20, 371–378.

Verhagen, M.A.M.T., Van Schelven, L.J., Samsom, M., and Smout, A.J.P.M. (1999). Pitfalls in the analysis of electrogastrographic recordings. *Gastroenterology* 117, 453–460.

Verplanck, W.S., Collier, G.H., and Cotton, J.W. (1952). Nonindependence of successive responses in measurements of the visual threshold. *Journal of Experimental Psychology* 44, 273–282.

Vianna, E.P.M., Weinstock, J., Elliott, D., Summers, R., and Tranel, D. (2006). Increased feelings with increased body signals. *Social Cognitive and Affective Neuroscience* 1, 37–48.

Vinck, M., Batista-Brito, R., Knoblich, U., and Cardin, J.A. (2015). Arousal and locomotion make distinct contributions to cortical activity patterns and visual encoding. *Neuron* 86, 740–754.

Vogt, B.A., and Derbyshire, S.W. (2009). Visceral circuits and cingulate-mediated autonomic functions. In Vogt, B.A. (ed.). *Cingulate Neurobiology and disease* (pp. 220-235). Oxford, UK: Oxford University Press.

Wagenmakers, E.-J., Farrell, S., and Ratcliff, R. (2004). Estimation and interpretation of 1/fα noise in human cognition. *Psychonomic Bulletin & Review* 11, 579–615.

Walker, B.B., and Sandman, C.A. (1977). Physiological response patterns in ulcer patients: Phasic and tonic components of the electrogastrogram. *Psychophysiology* 14, 393–400.

Wang, F.B., and Powley, T.L. (2000). Topographic inventories of vagal afferents in gastrointestinal muscle. *Journal of Comparative Neurology* 421, 302–324.

Wang, C., Ong, J.L., Patanaik, A., Zhou, J., and Chee, M.W.L. (2016). Spontaneous eyelid closures link vigilance fluctuation with fMRI dynamic connectivity states. *PNAS* 113, 9653–9658.

Wang, E., Du Sert, N., and Rudd, J. (2012). Effects of nicotine on gastric myoelectrical activity in ICR mice. *Molecular Neurodegeneration* 7, S13.

Wang, G.-J., Tomasi, D., Backus, W., Wang, R., Telang, F., Geliebter, A., Korner, J., Bauman, A., Fowler, J.S., Thanos, P.K., et al. (2008). Gastric distention activates satiety circuitry in the human brain. *NeuroImage* 39, 1824–1831.

Ward, L.M. (2003). Synchronous neural oscillations and cognitive processes. *Trends in Cognitive Sciences* 7, 553–559.

Weiss, B., Coleman, P.D., and Green, R.F. (1955). A stochastic model for time-ordered dependencies in continuous scale repetitive judgments. *Journal of Experimental Psychology* 50, 237–244.

Wertheimer, M. (1953). An investigation of the "randomness" of threshold measurements. *Journal of Experimental Psychology* 45, 294–303.

Wetzels, R., and Wagenmakers, E.-J. (2012). A default Bayesian hypothesis test for correlations and partial correlations. *Psychon Bull Rev* 19, 1057–1064.

Wohlschläger, A.M., Glim, S., Shao, J., Draheim, J., Köhler, L., Lourenço, S., Riedl, V., and Sorg, C. (2016). Ongoing Slow Fluctuations in V1 Impact on Visual Perception. *Front Hum Neurosci* 10.

Wolpert, N., Rebollo, I., and Tallon-Baudry, C. (2020). Electrogastrography for psychophysiological research: Practical considerations, analysis pipeline, and normative data in a large sample. *Psychophysiology* 57, e13599.

Wolpert, N., and Tallon-Baudry, C. (2021). Coupling between the phase of a neural oscillation or bodily rhythm with behavior: evaluation of different statistical procedures. *NeuroImage* 118050.

Womelsdorf, T., Fries, P., Mitra, P.P., and Desimone, R. (2006). Gamma-band synchronization in visual cortex predicts speed of change detection. *Nature* 439, 733–736.

Worden, M.S., Foxe, J.J., Wang, N., and Simpson, G.V. (2000). Anticipatory biasing of visuospatial attention indexed by retinotopically specific alpha-band electroencephalography increases over occipital cortex. *J. Neurosci.* 20, RC63.

Wyart, V., and Tallon-Baudry, C. (2008). Neural Dissociation between Visual Awareness and Spatial Attention. *J. Neurosci.* 28, 2667–2679.

Wyart, V., and Tallon-Baudry, C. (2009). How Ongoing Fluctuations in Human Visual Cortex Predict Perceptual Awareness: Baseline Shift versus Decision Bias. *J Neurosci* 29, 8715–8725.

Yamamoto, T., Shimura, T., Sako, N., Yasoshima, Y., and Sakai, N. (1994). Neural substrates for conditioned taste aversion in the rat. *Behavioural Brain Research* 65, 123–137.

Yang, M., Li, Z.-S., Xu, X.-R., Fang, D.-C., Zou, D.-W., Xu, G.-M., Sun, Z.-X., and Tu, Z.-X. (2006). Characterization of cortical potentials evoked by oesophageal balloon distention and acid perfusion in patients with functional heartburn. *Neurogastroenterol Motil* 18, 292–299.

Yeo, T.B.T., Krienen, F.M., Sepulcre, J., Sabuncu, M.R., Lashkari, D., Hollinshead, M., Roffman, J.L., Smoller, J.W., Zöllei, L., Polimeni, J.R., et al. (2011). The organization of the human cerebral cortex estimated by intrinsic functional connectivity. *J Neurophysiol* 106, 1125–1165.

Yin, J., and Chen, J.D.Z. (2013). Electrogastrography: Methodology, Validation and Applications. *Journal of Neurogastroenterology and Motility* 19, 5–17.

Zar, J.H. (2010). Biostatistical Analysis. Prentice-Hall/Pearson.

Zelano, C., Jiang, H., Zhou, G., Arora, N., Schuele, S., Rosenow, J., and Gottfried, J.A. (2016). Nasal Respiration Entrains Human Limbic Oscillations and Modulates Cognitive Function. *J. Neurosci.* 36, 12448–12467.

Zhang, Y., and Ding, M. (2010). Detection of a weak somatosensory stimulus: role of the prestimulus mu rhythm and its top-down modulation. *J Cogn Neurosci* 22, 307–322.

Zheng, H., and Berthoud, H.R. (2000). Functional vagal input to gastric myenteric plexus as assessed by vagal stimulation-induced Fos expression. *Am. J. Physiol. Gastrointest. Liver Physiol.* 279, G73-81.

Zhigalov, A., and Jensen, O. (2020). Alpha oscillations do not implement gain control in early visual cortex but rather gating in parieto-occipital regions. *Human Brain Mapping* 41, 5176-5186.

Zoefel, B., Davis, M.H., Valente, G., and Riecke, L. (2019). How to test for phasic modulation of neural and behavioural responses. *NeuroImage* 202, 116175.

RÉSUMÉ

L'activité spontanée du cerveau joue un rôle important pour la perception et la cognition. En particulier, les oscillations alpha indexent l'excitabilité corticale et ont été liées aux fluctuations de la perception. Des travaux pionniers ont montré que dans les régions occipito-pariétales pendant l'état de repos, les oscillations corticales alpha spontanées sont modulées par le rythme lent (~ 0,05 Hz) produit par l'estomac. Ce rythme peut être mesuré de manière non invasive à l'aide de l'électrogastrogramme. Cela nous a conduit à formuler l'hypothèse que lors d'une tâche perceptive, le rythme gastrique est couplé aux oscillations alpha cérébrales et contribue aux fluctuations de la perception. Pour pouvoir tester cette hypothèse, un premier but était d'améliorer et de standardiser les méthodes d'acquisition et d'analyse de l'électrogastrogramme. Nous avons mis en place un protocole d'enregistrement, de prétraitement et d'analyse de l'électrogastrogramme, pour en extraire un rythme gastrique régulier. Le deuxième volet méthodologique concernait les outils statistiques pour détecter au mieux les différents profils de couplage entre la phase du rythme gastrique et le comportement. J'ai systématiquement comparé les performances de différents tests et stratégies statistiques circulaires, en faisant varier les paramètres expérimentaux et les propriétés de l'effet de phase sous-jacent. Dans la troisième partie de ma thèse, nous avons ensuite testé expérimentalement l'hypothèse selon laquelle le rythme gastrique a une influence sur les fluctuations de la perception visuelle. Cependant, aucune preuve que la phase gastrique modulait la probabilité que les cibles soient perçues n'a été trouvée. Toutefois, les oscillations corticales alpha étaient significativement couplées au rythme gastrique dans un vaste cluster incluant les capteurs pariéto-occipitaux jusqu'aux capteurs médians et frontaux. Le degré de couplage individuel ne montrait pas de corrélat fonctionnel dans les performances. En résumé, cette étude a pour la première fois identifié un couplage entre le rythme gastrique et les oscillations alpha alors que les participants sont engagés dans une tâche, mais nous n'avons pas pu identifier de corrélat comportemental des interactions estomac-cerveau, laissant la question du rôle fonctionnelle du couplage estomac-rythme alpha ouverte.

MOTS CLÉS

estomach rhythme gastrique, electrogastrographie, oscillations, perception, statistique circulaire

ABSTRACT

The brain's ongoing activity plays an important role for perception and cognition. In particular, alpha oscillations index arousal and have been linked to fluctuations in perception. Pioneering work has shown that in occipito-parietal brain regions during resting state, alpha oscillations are modulated by the slow rhythm (~0.05 Hz) generated by the stomach, measured non-invasively using the Electrogastrogram. This led us to ask whether the gastric rhythm is coupled to brain alpha oscillations during perceptual tasks and might thereby induce fluctuations in perception. To test this hypothesis, a first aim was to improve and standardize methods to record and analyze the gastric rhythm in healthy participants. We therefore designed and tested a protocol for the recording, preprocessing and analysis of the Electrogastrogram, to extract a regular gastric rhythm. Our second methodological aim was to determine which statistical methodology was sensitive to different profiles of coupling between gastric phase and behavior. I systematically compared the performance of different circular statistical tests and strategies, with respect to experimental parameters and properties of the underlying phase effect. In the third part of my PhD, we then experimentally tested the hypothesis that the gastric rhythm has an influence on fluctuations in visual perception. We found no evidence that gastric phase modulated the probability of target detection. Cortical alpha oscillations were significantly coupled to the gastric rhythm in a large cluster spanning parieto-occipital to mid/frontal sensors. However, individual brain-alpha coupling strength appeared to have no behavioral correlate, since it did not covary with individual hit rate or mean reaction time. In sum, this study for the first time identified gastric-alpha coupling while participants are engaged in a task, but could not identify the behavioral correlate of such coupling, leaving open the question of the functional role of gastric-alpha coupling.

KEYWORDS

stomach, gastric rhythm, electrogastrography, oscillations, perception, circular statistics